

UNIVERSITY OF NEW ENGLAND

**Mapping Soil Salinity and Its Impact on Agricultural
Production in Al Hassa Oasis in Saudi Arabia**

Submitted by

Amal Allbed

BGeog. University of Dammam
MGISc. University of New England

A thesis submitted in fulfilment of the requirements for the degree of

DOCTOR OF PHILOSOPHY

June 2018

Abstract

Soil salinity is considered as one of the major environmental issues globally that restricts agricultural growth and productivity, especially in arid and semi-arid regions. One such region is Al Hassa Oasis in the eastern province of Saudi Arabia, which is one of the most productive date palm (*Phoenix dactylifera* L.) farming regions in Saudi Arabia and is seriously threatened by soil salinity. Development of remote sensing techniques and modelling approaches that can assess and map soil salinity and the associated agricultural impacts accurately and its likely future distribution should be useful in formulating more effective, long-term management plans. The main objective of this study was to detect, assess and map soil salinity and its impact on agricultural production in the Al Hassa Oasis.

The presented research first started by reviewing the related literature that have utilized the use of remote sensing data and techniques to map and monitor soil salinity. This review started by discussing soil salinity indicators that are commonly used to detect soil salinity. Soil salinity can be detected either directly from the spectral reflectance patterns of salt features visible at the soil surface, or indirectly using the vegetation reflectance since it impacts vegetation. Also, it investigated the most commonly used remote sensors and techniques for monitoring and mapping soil salinity in previous studies. Both spectral vegetation and salinity indices that have been developed and proposed for soil salinity detection and mapping have been reviewed. Finally, issues limiting the use of remote sensing for soil salinity mapping, particularly in arid and semi-arid regions have been highlighted.

In the second study, broadband vegetation and soil salinity indices derived from IKONOS images along with ground data in the form of soil samples from three sites across the Al Hassa Oasis were used to assess soil salinity in the Al-Hassa Oasis. The effectiveness of these indices to assess soil salinity over a dominant date palm region was examined statistically. The results

showed that very strongly saline soils with different salinity level ranges are spread across the three sites in the study area. Among the investigated indices, the Soil Adjusted Vegetation Index (SAVI), Normalized Differential Salinity Index (NDSI) and Salinity Index (SI-T) yielded the best results for assessing the soil salinity in densely vegetated area, while NDSI and SI-T revealed the highest significant correlation with salinity for less densely vegetated lands and bare soils.

In the third study, combined spectral-based statistical regression models were developed using IKONOS images to model and map the spatial variation of the soil salinity in the Al Hassa Oasis. Statistical correlation between Electrical Conductivity (EC), spectral indices and IKONOS original bands showed that the Salinity Index (SI) and red band (band 3) had the highest correlation with EC. Integrating SI and band 3 into one model produced the best fit with $R^2 = 0.65$. The high performance of this combined model is attributed to: (i) the spatial resolution of the images; (ii) the great potential of SI in enhancing and delineating the spatial variation of soil salinity; and (iii) the superiority of band 3 in retrieving soil salinity features and patterns. Soil salinity maps generated using the selected model showed that strongly saline soils (>16 dS/m) with variable spatial distribution were the dominant class over the study area. The spatial variability of this class over the investigated areas was attributed to a variety factors, including soil factors, management related factors and climate factors.

In the fourth study, Landsat time series data of years 1985, 2000 and 2013 were used to detect the temporal change in soil salinity and vegetation cover in the Al Hassa Oasis and investigate whether there is any linkage of vegetation cover change to the change in soil salinity over a 28-year period. Normalized Difference Vegetation Index (NDVI) and Soil Salinity Index (SI) differencing images were used to identify vegetation and salinity change/no-change for the two periods. The results revealed that soil salinity during 2000-2013 exhibited much higher increase

compared to 1985-2000, while the vegetation cover declined for the same period. Highly significant ($p < 0.0001$) negative relationships between the NDVI and SI differencing images were detected, confirming the potential long-term linkage between the changes in soil salinity and vegetation cover in the Oasis.

In the fifth study, the effects of physical and proximity factors, including elevation, slope, soil salinity, distance to water, distance to built-up areas, distance to roads, distance to drainage and distance to irrigation factors on agricultural expansion in the Al Hassa Oasis were investigated. A logistic regression model was used for two time periods of agricultural change in 1985 and 2015. The probable agricultural expansion maps based on agricultural changes in 1985 was used to test the performance of the model to predict the probable agricultural expansion after 2015. This was achieved by comparing the probable maps of 1985 and the actual agricultural land of 2015 model. The Relative Operating Characteristic (ROC) method was also used and together these two methods were used to validate the developed model. The results showed that the prediction model of 2015 provides a reliable and consistent prediction based on the performance of 1985. The logistic regression results revealed that among the investigated factors, distance to water, distance to built-up areas and soil salinity were the major factors having a significant influence on agricultural expansion.

In the last study, the potential distribution of date palm was assessed under current and future climate scenarios of 2050 and 2100. Here, CLIMEX (an ecological niche model) and two different Global Climate Models (GCMs), CSIRO-Mk3.0 (CS) and MIROC-H (MR), were employed with the A2 emission scenario to model the potential date palm distribution under current and future climates in Saudi Arabia. A sensitivity analysis was conducted to identify the CLIMEX model parameters that had the most influence on date palm distribution. The model was also run with the incorporation of six non-climatic parameters, which are soil taxonomy, soil texture, soil salinity, land use, landform and slopes, to further refine the

distributions. The results from both GCMs showed a significant reduction in climatic suitability for date palm cultivation in Saudi Arabia by 2100 due to increment of heat stress. The lower optimal soil moisture, cold stress temperature threshold and wet stress threshold parameters had the greatest impact on sensitivity, while other parameters were moderately sensitive or insensitive to change. A more restricted distribution was projected with the inclusion of non-climatic parameters.

Overall, the research demonstrated the potential of remote sensing and modeling techniques for assessing and mapping soil salinity and providing the essential information of its impacts on date palm plantation. The findings provide useful information for land managers, environmental decision makers and governments, which may help them in implementing more suitable adaptation measures, such as the use of new technologies, management practices and new varieties, to overcome the issue of soil salinity and its impact on this important economic crop so that long-term sustainable production of date palm in this region can be achieved. Additionally, the information derived from this research could be considered as a useful starting point for public policy to promote the resilience of agricultural systems, especially for smallholder farmers who might face more challenges, if not total loss, not only due to soil salinity but also due to climate change.

Declaration

I certify that the substance of this thesis has not been submitted for any degree and is not currently being submitted for any other degree or qualification. I certify that, to the best of my knowledge, any assistance received in preparing this thesis, and all sources used, have been acknowledged.



Amal Allbed

Dedication

This work is dedicated to my late mother Zahra Alsafar for her love and support from the Heaven. I am sorry that she has not lived to see me graduate. She was a strong and gentle soul who taught me to trust in God (Allah), believe in hard work and that so much could be earned. I will cherish her memory with warm thoughts, laughter and tears as I reminisce of all the wonderful times that we have shared together.

Acknowledgments

First and foremost, I thank God (Allah) Almighty for giving me the strength, knowledge, ability and opportunity to undertake and finish this thesis. Without his blessings, this achievement would not have been possible. Second, I want to thank my supervisor Professor Lalit Kumar who gave me the opportunity to continue with my studies. Also, many thanks to Dr. Yousef Al-Dakhil for his encouragement and support. A very special thank you to Cate MacGregor, not only for providing technical support, but also being a wonderful source of emotional support and friendship along the rough road that finally became this thesis.

Thanks to all the postgrads who provided help and encouragement during my time here and in particular I will forever be grateful to my dearest friend Hanieh Saremi for believing in me and being always there with a helping hand from the very beginning of my PhD journey.

I finish with the people who shaped me into who I am. I thank with deep gratitude my husband, Zaki Almokhtar, I could never have accomplished this thesis without his support. He always encourages as a best friend and shares my passions in times and difficulties. I appreciate from my heart, I would like to thank for your love and encouragement. Also, a special thank you to my beloved sons, Mohammed and Hassan, who were always forgiving if mum seemed a bit preoccupied at times, will have much more time with me in the future. I would also like to thank my father, Essia and all my dearest brothers and sisters, especially my sister Maryam, for their unstinting support and prayers.

Note to Examiners

This thesis has been written in journal-article format. I have attempted to minimize the duplication of material between chapters. However, some repetition remains, particularly in the methodology sections of certain articles. This is due to the requirements of the journals and the need for each of the papers to stand alone.

Although effort has been made to ensure consistency in the format for the purposes of this thesis, I acknowledge that some inconsistencies remain due to the requirements of each of the journals to which the separate papers were submitted.

Publications from this Thesis during Candidature

Allbed, A., Kumar, L. (2013). Soil salinity mapping and monitoring in arid and semi-arid regions using remote sensing technology: A review. *Advances in Remote Sensing*, 2: 373-385. doi: 10.4236/ars.2013.24040. **Chapter 2**

Allbed, A., Kumar, L., Aldakheel, Y.Y. (2014). Assessing soil salinity using soil salinity and vegetation indices derived from IKONOS high-spatial resolution imageries: Applications in a date palm dominated region. *Geoderma*, 230-231: 1-8. doi: 10.1016/j.geoderma.2014.03.025. **Chapter 3**

Allbed, A., Kumar, L., Sinha, P. (2014). Mapping and modelling spatial variation in soil salinity in the Al Hassa Oasis based on remote sensing indicators and regression techniques. *Remote Sensing*, 6: 1137-1157; doi: 10.3390/rs6021137. **Chapter 4**

Allbed, A., Kumar, L., Sinha, P (2017). Soil salinity and vegetation cover change detection from multi-temporal remotely sensed imagery in Al Hassa Oasis in Saudi Arabia. *Geocarto International*. doi: 10.1080/10106049.2017.1303090. **Chapter 5**

Allbed, A., Kumar, L., & Shabani, F. (2017). Climate change impacts on date palm cultivation in Saudi Arabia. *The Journal of Agricultural Science*, 1-16. doi: 10.1017/S0021859617000260. **Chapter 7**

In addition, the following paper has been submitted to the journal for review and publication.

Allbed, A., Kumar, L., & Alqurashi, A. Spatio-temporal modelling of agricultural expansion based on driving force factors using logistic regression: a case study in the Al Hassa Oasis. Submitted to *ISPRS International Journal of Geo-Information* for review and publication. **Chapter 6**



Please be advised that this thesis contains chapters which have been either published or submitted for publication.

The submitted version(s) of the following chapter(s) have been retained:

Chapter 2:

Allbed, A., Kumar, L. (2013). Soil salinity mapping and monitoring in arid and semi-arid regions using remote sensing technology: A review. *Advances in Remote Sensing*, 2: 373-385. <https://doi.org/10.4236/ars.2013.24040>

Chapter 3:

Allbed, A., Kumar, L., Aldakheel, Y.Y. (2014). Assessing soil salinity using soil salinity and vegetation indices derived from IKONOS high-spatial resolution imageries: Applications in a date palm dominated region. *Geoderma*, 230-231: 1-8. <https://doi.org/10.1016/j.geoderma.2014.03.025>

Chapter 4:

Allbed, A., Kumar, L., Sinha, P. (2014). Mapping and modelling spatial variation in soil salinity in the Al Hassa Oasis based on remote sensing indicators and regression techniques. *Remote Sensing*, 6: 1137-1157; <https://doi.org/10.3390/rs6021137>

Chapter 5:

Allbed, A., Kumar, L., Sinha, P (2017). Soil salinity and vegetation cover change detection from multi-temporal remotely sensed imagery in Al Hassa Oasis in Saudi Arabia. Geocarto International. <https://doi.org/10.1080/10106049.2017.1303090>

Chapter 6:

Downloaded from <https://rune.une.edu.au>, the institutional research repository of the University of New England at Armidale, NSW Australia.



Allbed, A., Kumar, L., & Alqurashi, A. *Spatio-temporal modelling of agricultural expansion based on driving force factors using logistic regression: a case study in the Al Hassa Oasis*. Manuscript submitted for publication.

Chapter 7:

Allbed, A., Kumar, L., & Shabani, F. (2017). Climate change impacts on date palm cultivation in Saudi Arabia. *The Journal of Agricultural Science*, 1-16.
<https://doi.org/10.1017/S0021859617000260>

No Proof of publication could be located for the following chapters:

Chapters 1 and 8

Table of Contents

Abstract.....	i
Declaration.....	v
Dedication	vi
Acknowledgments	vii
Note to Examiners.....	viii
Publications from this Thesis during Candidature.....	ix
List of Tables	xiii
List of Figures.....	xiv
Chapter 1 Introduction and Background	1
1.1 Introduction.....	2
1.2 Aims and Objectives	8
1.3 Thesis Structure.....	8
Chapter 2 Soil Salinity Mapping and Monitoring In Arid and Semi-Arid Regions Using Remote Sensing Technology: A review	11
2.1 Abstract.....	12
2.2 Introduction.....	12
2.3 Soil Salinity and Remote Sensing	15
2.3.1 Soil Salinity Symptoms.....	15
2.4 Mapping and Monitoring Soil Salinity Using Remote Sensing Data.....	18
2.4.1 Multispectral Satellite Sensors for Mapping and Monitoring Soil Salinity.....	18
2.4.2 Limitations of Multispectral Satellite Sensors in Soil Salinity Mapping and Monitoring.....	22
2.4.3 Hyperspectral Remote Sensing Data.....	23
2.5 Using Vegetation and Soil Indices in Soil Salinity Studies	25
2.5.1 Vegetation and Soil Indices	25
2.6 Issues in Mapping Soil Salinity in Arid and Semi-Arid Regions Using Remote Sensing.....	30
2.7 Conclusion.....	32
Chapter 3 Assessing Soil Salinity Using Soil Salinity and Vegetation Indices Derived from IKONOS High-Spatial Resolution Imageries: Applications in a Date Palm Dominated Region	36
3.1 Abstract.....	37
3.2 Introduction.....	37
3.3 Materials and Methods.....	40
3.3.1 Study Area.....	40
3.3.2 Site Selection.....	41
3.3.3 Soil Sampling	41
3.3.4 Satellite Image Data	42
3.3.5 Broadband Indices Selection.....	44
3.3.6 Calculation and Extraction of the Index Values	45
3.4 Results.....	45
3.4.1 EC Ground Measurements	45
3.4.2 Soil spectral reflectance	46
3.4.3 The Broadband Indices	47
3.5 Discussion.....	50
3.5.1 Soil Salinity Analyses	50
3.5.2 Soil Spectral Reflectance	51

3.5.3	Relationships between Soil Salinity and Broadband Indices	52
3.6	<i>Conclusions</i>	54
Chapter 4	Mapping and Modelling Spatial Variation in Soil Salinity in the Al Hassa Oasis Based on Remote Sensing Indicators and Regression Techniques	58
4.1	<i>Abstract</i>	59
4.2	<i>Introduction</i>	60
4.3	<i>Materials and Methods</i>	63
4.3.1	Study Area.....	63
4.3.2	Field Sampling	64
4.3.3	Satellite Data Acquisition and Processing	65
4.3.4	Data Analysis, Model Generation and Selection	66
4.3.5	Model Validation	67
4.4	<i>Results</i>	68
4.4.1	Data Analysis	68
4.4.2	Models Development and Valuations	69
4.4.3	Spatial Variation in Soil Salinity Maps.....	70
4.5	<i>Discussion</i>	75
4.5.1	The Developed Regressions Models	75
4.5.2	Mapping Spatial Variation in Soil Salinity	78
4.6	<i>Conclusion</i>	81
Chapter 5	Soil Salinity and Vegetation Cover Change Detection from Multi-Temporal Remotely Sensed Imagery in Al Hassa Oasis in Saudi Arabia.....	85
5.1	<i>Abstract</i>	86
5.2	<i>Introduction</i>	87
5.3	<i>Materials and Methods</i>	90
5.3.1	Study Area.....	90
5.3.2	Image Acquisition and Pre-processing.....	91
5.3.3	Image Processing	93
5.3.4	Reference Data	95
5.3.5	Threshold Determination of the Differencing Images and Accuracy Evaluation	97
5.3.6	Soil salinity–Vegetation Cover Change Linkage	98
5.4	<i>Results</i>	99
5.4.1	Vegetation Cover and Soil Salinity Change Detection	99
5.4.2	Change Detection Accuracy Assessment.....	100
5.4.3	Soil Salinity-Vegetation Cover Change Relationship.....	100
5.5	<i>Discussion</i>	105
5.6	<i>Conclusion</i>	109
Chapter 6	Spatio-Temporal Modelling of Agricultural Expansion Based on Driving Force Factors Using Logistic Regression: A Case Study in the Al Hassa Oasis	113
6.1	<i>Abstract</i>	114
6.2	<i>Introduction</i>	115
6.3	<i>Materials and Methods</i>	117
6.3.1	Study Area.....	117
6.3.2	Image Acquisition and Pre-processing.....	118
6.3.3	Image Classification and Accuracy Assessment.....	119
6.3.4	Potential Driving Factors of Agricultural Expansion.....	120
6.4	<i>Statistical Analysis</i>	123
6.4.1	Agriculture and Non-Agriculture Data Sampling	123
6.4.2	Logistic Regression.....	123
6.4.3	Prediction of Spatial Patterns of Agricultural Distribution.....	124
6.4.4	Model Validation	125

6.5	<i>Results</i>	126
6.5.1	Agricultural Expansion Probability.....	127
6.6	<i>Discussion</i>	129
6.7	<i>Conclusions</i>	133
Chapter 7	Climate Change Impacts on Date Palm Cultivation in Saudi Arabia	137
7.1	<i>Summary</i>	138
7.2	<i>Introduction</i>	139
7.3	<i>Materials and Methods</i>	143
7.3.1	Current Distribution of Date Palm (<i>Phoenix dactylifera</i> L.).....	143
7.3.2	CLIMEX Software.....	144
7.3.3	Climate Data, Global Climate Models and Climate Change Scenarios.....	146
7.3.4	Fitting CLIMEX Parameters.....	147
7.3.5	Non-Climatic Parameters.....	148
7.3.6	Refining the CLIMEX Outputs.....	150
7.3.7	Climate Sensitivity Analysis.....	151
7.4	<i>Results</i>	151
7.4.1	Current Climate.....	151
7.4.2	Non-Climate Parameters.....	152
7.4.3	Future Climate Projections Based on Climate.....	153
7.4.4	Refined Result.....	154
7.4.5	Sensitivity to Model Parameters.....	157
7.5	<i>Discussion</i>	158
7.6	<i>Conclusions</i>	163
Chapter 8	Synthesis and General Conclusions	167
8.1	<i>Summary of Main Findings</i>	168
8.2	<i>Contribution to Science and Knowledge</i>	175
8.3	<i>Recommendations and Direction of Future Research</i>	177
References	179

List of Tables

Table 2.1 Vegetation and soil salinity Indices that have been proposed and used for soil salinity monitoring and mapping.....	28
Table 3.1 Summary of the most widely used vegetation and soil salinity indices for soil salinity assessments.....	44
Table 3.2 Descriptive statistics of the actual EC and the broadband indices.....	48
Table 3.3 Correlation coefficients between the actual EC values and the broadband indices..	48
Table 4.1 Statistical criteria for evaluating the regression model.....	68
Table 4.2 Descriptive statistics of EC.....	68
Table 4.3 Correlation coefficient between EC and remotely sensed data.....	68
Table 4.4 Developed regression models to predict EC based on remotely sensed data.....	72
Table 5.1 Interpretation of the RGB–NDVI images.....	97
Table 5.2 NDVI and SI change area for the two different change periods.....	104
Table 5.3 Change no-change classification accuracy of Δ NDVI and Δ SI for the two changes.....	104
Table 6.1 Summary results of the logistic regression model.....	127
Table 7.1 Suitable and unsuitable area for <i>P. dactylifera</i> cultivation in Saudi Arabia based on non-climatic parameters.....	153
Table 7.2 Results of CS and MR GCMs and the refined outputs using all suitable non-climate parameters for <i>P. dactylifera</i> cultivation for 2050 and 2100.....	156
Table 7.3 Sensitivity analysis of CLIMEX parameters of <i>P. dactylifera</i> model as change of eco-climatic index (EI).....	157

List of Figures

Figure 3.1 Location of the study area.....	43
Figure 3.2 Study sites, (a) site A, (b) site B and (c) site C.....	43
Figure 3.3 Distribution of soil salinity classes in the three study sites.....	46
Figure 3.4 Spectral reflectance of different soil salinity classes selected randomly from the data sets.....	46
Figure 3.5 Outputs of selected indices.....	49
Figure 3.6 Influence of moisture content, salt quantity, colour and surface roughness on the reflectance of saline.....	52
Figure 4.1 Study area with the location of the study sites.....	64
Figure 4.2 Scatter plots of predicted versus measured EC using the developed regression models.....	71
Figure 4.3 Validation of the developed regression models; a) scatterplots of predicted versus measured EC; b) histogram of residuals; c) normal plot of residuals.....	73
Figure 4.4 Soil salinity maps for different sites in the study region; (a) site one; (b) site two and (c) site three.....	74
Figure 4.5 Spectral reflectance of saline soils differs due to surface roughness, crusting and colour.....	78
Figure 5.1 Standard False Color Composite (RGB: 432) of the year 2013 and location of Al Hassa Oasis in Saudi Arabia.....	91
Figure 5.2 Multi-spectral satellite remote sensing data for Al Hassa Oasis: (a) Landsat 5 TM, January 1985, (b) Landsat 7 ETM+, January 2000, and (c) Landsat 8 OLI, December 2013.....	93
Figure 5.3 The difference images of: (a) the NDVI (Δ NDVI) for the change periods 1985–2000 and 2000-2013, and (b) SI (Δ SI) for the change periods 1985-2000 and 2000-2013.....	101
Figure 5.4 Change/no-change thresholds based on Mean \pm C*SD at different C-values for 1985-2000 and 2000-2013 change periods. The optimal threshold values were determined by highest Kappa value or OA. The figure shows that an optimal C-value for Δ NDVI image for 1985-2000 and 2000-2013 periods can be at 1.8 and 2.00, respectively, and the optimal C-value for Δ SI image in both change periods can be at 1.6.....	102
Figure 5.5 Change/no-change maps of: (a) Δ NDVI for the change periods 1985-2000 and 2000-2013, and (b) Δ SI between for the change periods 1985-2000 and 2000-2013.....	103
Figure 5.6 The relationship between soil salinity and vegetation cover changes in: (a) 1985-2000 change period, and (b) 2000-2013 change period.....	104
Figure 6.1 Location of the Al Hassa Oasis in Saudi Arabia.....	118
Figure 6.2 Selected driving forces of agricultural growth in the Al Hassa Oasis.....	122
Figure 6.3 ROC curve for the selected period.....	127

Figure 6.4 Probability maps of agricultural expansion: a) a comparison of agricultural expansion probability in 1985 and agricultural lands in 2015; b) predict agricultural expansion after 2015.....	128
Figure 7.1 Current and modelled potential distribution of <i>P. dactylifera</i> in Saudi Arabia. EI, eco-climatic index; <i>P. dactylifera</i> , <i>Phoenix dactylifera</i>	144
Figure 7.2 The EI for <i>P. dactylifera</i> for 2050 and 2100 under CS and MR GCMs running with the A2 emission scenario.....	155
Figure 7.3 Changes in heat stress from current time to 2100.....	156
Figure 7.4 Agreement in the CLIMEX projection of suitable areas for <i>P. dactylifera</i> under CS and MR GCMs running with the A2 emission scenario for 2050 and 2100. CS, CSIRO-Mk3.0; EI, eco-climatic index; GCM, global climate model; MR, MIROC-H; <i>P. dactylifera</i> , <i>Phoenix dactylifera</i>	156

Chapter 1 Introduction and Background

1.1 Introduction.

Soil salinity refers to the accumulation of soluble salts in the plant zone or at the surface or near-surface of soil horizon (Tanji, 2004). Soil salinity is a serious environmental issue on a global scale, however, it is most common in the arid and semi-arid regions. According to a report published by FAO in 2000, it is estimated that approximately 397 million hectares in the world are saline soils (Crouch, 2000). In arid and semi-arid regions, there is insufficient rainfall to flush the soluble salts from the soil via leaching, thus the soluble salt accumulates, causing soil salinity. In addition, the buildup of salts in the soil profile is driven by the high evaporation rate which removes water from the soil profile while leaving salts behind. Unfortunately, it has been reported that water shortages and droughts in arid and semi-arid areas are likely to become more frequent and severe in the future (Seager et al., 2007; Cayan et al., 2010), thus increasing soil salinity threats. In arid and semi-arid regions, the quality of irrigation water in irrigated lands is an important contributor to soil salinity. Therefore, excessive irrigation with water containing high levels of soluble salts coupled with poor drainage leads to a rise of the water-table, which enhances salt movement through the soil profile, and consequently increases salt accumulation within the root zone and soil surface. It has been reported that approximately 50% of all existing irrigated lands in the arid and semi-arid regions are adversely affected by soil salinity (Abrol et al., 1988).

Soil salinity is among the leading global environmental hazards, affecting irrigated agriculture and causing billions of dollars in crop damages every year. As an example, it has been reported that in Uzbekistan, up to 53% of irrigated lands are exposed to varying degrees of soil salinity, which ultimately have led to low or no annual crop profits (Djanibekov et al., 2012). In addition, regardless of the physiological cause (ion toxicity, water deficit, and/or nutritional imbalance), high salinity in the root zone severely inhibits plant growth and development, resulting in reduced crop productivity or total crop failure. It has been estimated that globally,

each year 10 million ha of agricultural irrigated lands are abandoned due to the adverse impacts of soil salinity (Szabolcs, 1987). Increased salinization of arable land is expected to cause 30% land loss within the next 25 years and up to 50% by 2050, as reported by Wang et al. (2003).

Crops vary greatly in their tolerance to soil salinity, yet excessive salt can cause significant reductions in the growth, yield and fruit quality even in the high salt tolerant crops such as date palm (*Phoenix dactylifera* L.). For example, Al-Abdoulhadi et al. (2011) found that an increase in soil salinity levels caused leaf injury and adversely impacted on growth and biomass of date palm. Additionally, a study conducted by Alrasbi et al. (2010) indicated that at electrical conductivity (EC) of 18 dS/m, date palm trunk height, number of fronds, leaf length and trunk girth decreased by 53, 48, 39 and 46%, respectively. Ayers and Westcot (1985) reported that the minimum EC for maximum date palm yield is 4.0 dS/m, while at EC of 32 dS/m no yield is achieved. Hence, it is clear that the growth and productivity of date palm plants are negatively affected when soil salinity extends beyond its tolerance potential. Therefore, to better manage the threat soil salinity poses to the agricultural sector, producers, agricultural land users and managers, and policy makers need reliable and up-to-date information about soil salinity.

It is difficult to secure up-to-date knowledge of soil salinity extent, spatial distribution, nature and magnitude by using the traditional point sampling techniques because these techniques are very costly, time consuming and also limited with respect to the temporal and spatial variability, meaning that frequent field studies would be required. To this end, remote sensing has a great potential to identify, map, monitor and assess different dynamic processes including soil salinity and its impact on land cover, in particular, vegetation cover, as it has the ability to provide a broad and repetitive view of the earth objects without making physical contact. A range of different satellite borne sensors have been developed and used to collect information about the earth's surface in the last four decades, each of which has unique spatial, spectral and temporal resolution coverage characteristics (Gardi, 2017). Different types of satellite data

have been used to detect and monitor soil salinity, including coarse spatial resolution data such as that from Moderate Resolution Imaging Spectroradiometer (MODIS), medium spatial resolution data such as that provided by Landsat images and high spatial resolution data such as that from the IKONOS satellite.

In general, all objects (including soil) have unique spectral features (reflectance or emission regions), and they can be identified from remote sensing imagery according to their unique spectral characteristics. Accordingly, soil salinity can be assessed directly from the spectral reflectance patterns of salt features visible at the soil surface, or indirectly using the vegetation reflectance since it impacts vegetation. Increased reflectance in visible (VIS) bands and reduced reflectance in near-infrared (NIR) bands is indicative of unhealthy vegetation and as such could provide an indirect measure of soil salinity levels. For example, Peñuelas et al. (1997) found that the reflectance of barley was lower in the NIR and higher in the VIS regions as a result of increasing salinity. Both approaches have been applied in a number of studies by using different spectral salinity indices that relate reflectance characteristics to saline soil and vegetation indices (VIs) that relate reflectance characteristics to vegetation state and composition, with mixed success in arid and semi-arid areas across the world (Ivushkin et al., 2017). On the basis of the saline soil or stressed vegetation-related spectral features, some researchers have employed remote sensing and modelling techniques to develop quantitative model for predicting the variability of soil salinity and mapping its spatial distribution (Meng et al., 2016; Morshed et al., 2016). Usually a quantitative model relates soil salinity to remote sensing data reflectance in the form of a single spectral band, multi-band or spectral enhancements (e.g., Normalized Difference Vegetation Index (NDVI), Principal Components Analysis (PCA)), or a combination of both. For example, Luleva (2007) used Advanced Spaceborne Thermal Emission and Reflection Radiometer (ASTER) spectra coupled with the Partial Least Squares Regression (PLSR) method for mapping different soil properties,

including soil salinity and organic matter, in southeast Tunisia. Bouaziz et al. (2011b) found that incorporating salinity index with NIR derived from MODIS into a multiple linear regression allowed researchers to gain great insight into the spatial detection of the spread of soil salinity. Other researchers have taken the advantages of the long record and free of charge satellite data such as Landsat datasets (i.e 40 years' coverage) to detect and track the spatio-temporal changes in soil salinity over large-areas on a long-term basis using a series of multi-temporal data (Wu et al., 2008; Matinfar et al., 2013; El Harti et al., 2016; Afrasinei et al., 2017).

The degradation of agricultural soil in the Al Hassa Oasis, one of the Saudi's most important date palm agricultural areas, is a good example of such phenomenon (soil salinity). Date palm is one of the most important cash crops that contributes significantly to agro-ecosystems in Saudi Arabia and plays a major role in the national economy and agricultural sector, through its contribution to economic growth, and meeting local market needs. Saudi Arabia is considered one of the top three date producing countries in the world. In 2013, date production in Saudi Arabia reached 1 065 032 tonnes from 3.7 million trees (FAOSTAT, 2013). In the Al Hassa Oasis, where there is no native vegetation in this region, due to the arid climate with low rainfall, high temperatures and evaporation rates, date palm cultivations are heavily dependent on salty underground water for irrigation. The harsh arid climate and combination of irrigation practices and the absence of adequate drainage systems have affected in inducing soil salinity which have led to a decrease in land productivity in this region. Therefore, soil salinity has become a serious problem across this region. In this regard, it is an important concern to detect soil salinity, assess and monitor the degree of its severity and extent in time, spatial distribution, and determine its impacts on vegetation cover regularly. Proper and timely decisions can implement or support effective soil reclamation programs that minimize or prevent future increases in soil salinity that can protect date palm outputs, sustain agricultural lands and

natural ecosystems and avoid further adverse environmental, social and economic effects in such regions. Accordingly, this thesis reports on investigations into using geographic information system and remote sensing technologies to assess and map soil salinity and its impact on vegetation cover in Al Hassa Oasis.

This study is important because it adds positively to the areas of soil salinity, agriculture, geographic information systems (GIS) and remote sensing. Based on the known research, while progress has been made in detecting and mapping soil salinity in agricultural lands across a wide range of plant species using different spectral indices derived from multispectral satellite images, none has investigated whether vegetation and salinity indices from high spatial resolution images could assess soil salinity in agricultural areas which are covered mainly by date palm. Hence, this study is the first to assess soil salinity using soil salinity and vegetation indices extracted from IKONOS high-spatial resolution imageries in Al Hassa Oasis, which is a date palm dominated region. Also, based on the known research, this study is the first to use high spatial resolution multispectral images to develop combined spectral-based statistical models to predict and map spatial variation in soil salinity of community vegetated mostly with date palm. To date, despite the fact that soil salinity poses a negative threat on vegetation cover, most published studies have looked at either vegetation cover change or soil salinity change in isolation, and few attempts have been made to link vegetation cover change to soil salinity change, especially in date palm-dominated arid and semi-arid regions. This study will fill some of these gaps and attempts to detect the temporal change in vegetation cover and soil salinity in the Al Hassa Oasis and determines whether the change in vegetation cover is a case of soil salinity change over a given period. In addition, agricultural expansion is a spatio-temporal dynamic process controlled by various driving forces including soil salinity during which both the spatial expansion and the drivers vary over time and space. Thus, in a saline environment, like Al Hassa Oasis, understanding the past, current and future spatial distribution of

agricultural expansion and its underlying drivers along with their relationships is a crucial prerequisite, as information on existing agriculture expansion patterns and changes over time plays an important role in the decision-making process to mitigate the negative effects and promote desired outcomes. Added to this, climate change represents a massive threat to plant and crop distribution globally. Saudi Arabia is one of those countries that is highly vulnerable to the adverse effects of climate change, and it has been reported that yield of different types of field fruit trees and crops will experience losses as a consequence of climate change. Thus, information on the potential distribution of date palm as an important cash crop in Saudi Arabia and the relative abundance under projected future climate scenarios is essential as it will enable environmental managers to prepare appropriate strategies to manage the changes and achieve long-term sustainable production of this crop. For Saudi Arabia, to date, there have been no published studies to determine the potential distributions of date palm under future climates and non-climatic parameters.

1.2 Aims and Objectives

The principle aim of this research was to detect, assess and map soil salinity and its impact on agricultural production in the Al Hassa Oasis in the eastern province of Saudi Arabia.

Specifically, the objectives of the research were:

1. To document the use of remote sensing technology in mapping and monitoring soil salinity in arid and semi-arid regions;
2. To assess soil salinity in a date palm dominated region using soil salinity and vegetation indices derived from high-spatial resolution imageries;
3. To map and model spatial variation in soil salinity in the Al Hassa Oasis based on remote sensing indicators and regression techniques;
4. To detect soil salinity and vegetation cover changes from multi-temporal remotely sensed imagery in the Al Hassa Oasis;
5. To examine the effect of physical and proximity factors on the direction of the agricultural expansion in 1985 and 2015 in the Al Hassa Oasis; and
6. To model the potential future spatial distribution of date palm in Saudi Arabia using climate and non-climatic variables.

1.3 Thesis Structure

The thesis is structured in a manuscript style (as a series of journal papers) in which each chapter is treated individually. The thesis starts with a review of literature related to the use of remote sensing techniques to monitor and map soil salinity (Chapter Two). It explores the most-used data and methods from previous studies on the subject and highlights the most important issues limiting the use of remote sensing for soil salinity mapping, particularly in arid and semi-arid regions. This chapter has been published in *Advances in Remote Sensing*.

Chapter Three assesses the soil salinity levels in the Al-Hassa Oasis and investigates the effectiveness of some existing vegetation and soil salinity indices that derived from broadband satellite images for assessing soil salinity over an area vegetated mainly by date palms. The result of this chapter provides basic information which may help decision makers and land planners decide where to implement salinity action plans at a regional level to avoid further adverse environmental effects in the future. In addition, the outcome of this chapter emphasized that since study sites vary in terms of levels of salinity, vegetation cover and density, study sites should be assessed according to the strengths and weaknesses of the proposed indices before appropriate remote sensing-based indices are used for soil salinity mapping and assessing. This chapter has been published in *Geoderma*.

Chapter Four develops statistical regression models based on different spectral indices which were calculated from original bands of IKONOS images to predict and map spatial variation in soil salinity in Al Hassa Oasis, a region dominated by date palms. The simplicity of the developed combined model in this chapter offers a quick method which can contribute greatly to soil salinity prediction and mapping, at lower costs than conventional approaches, which will help farmer and other decision makers to manage soil salinity problems in early stages to prevent soil salinity from becoming prevalent, sustaining agricultural lands and natural ecosystems. This chapter has been published in *Remote Sensing*.

Chapter Five determines the changes in soil salinity and vegetation cover in Al Hassa Oasis over the past 28 years using Landsat time series data and investigates whether there is any linkage between vegetation cover change and change in soil salinity. The findings reported in this study provide an information base for better management practices to control and mitigate salinity to protect the date palm outputs and avoid further adverse environmental, social and economic effects. The outcomes of this chapter are relevant for agricultural workers, scientists and policy makers. This chapter has been published in *Geocarto International*.

Chapter Six investigates the effect of physical and proximity factors, including elevation, slope, soil quality, distance to water, distance to built-up areas, distance to roads, distance to drainage and distance to irrigation on agricultural expansion in Al Hassa Oasis using a logistic regression model for two time periods of agricultural change in 1985 and 2015. This chapter has been submitted to *ISPRS International Journal of Geo-Information* for review and publication.

Chapter Seven develops a niche model to estimate the potential spatial distribution for current and future date palm cultivation in Saudi Arabia using climate and non-climatic variables. The information in this chapter have addressed the importance of incorporating climatic and non-climatic parameters to achieve better accuracy and more robust results when assessing the impact of climate change on predicting the future distribution and fate of economically important crops, such as date palm, since the results must satisfy more extensive requirements. The results of this chapter provide early warning scenarios for how environmental managers should respond to changes in the distribution of the date palm in Saudi Arabia. This chapter has been published in *The Journal of Agricultural Science*.

The final chapter, Chapter Eight, presents the general conclusions of the thesis and describes the main findings of each chapter. Research implications are described and future research needs are highlighted.

Chapter 2 Soil Salinity Mapping and Monitoring In Arid and Semi-Arid Regions Using Remote Sensing Technology: A review

This chapter has been published as:

Allbed, A., Kumar, L. (2013). Soil salinity mapping and monitoring in arid and semi-arid regions using remote sensing technology: A review. *Advances in Remote Sensing*, 2: 373-385. doi: 10.4236/ars.2013.24040.

2.1 Abstract

Soil salinity is a serious environmental problem especially in arid and semiarid areas. It either occurs naturally or is human-induced. High levels of soil salinity negatively affect crop growth and productivity leading land degradation ultimately. Thus, it is important to monitor and map soil salinity at an early stage to enact effective soil reclamation program that help lessen or prevent future increase in soil salinity. Remote sensing has outperformed the traditional method for assessing soil salinity offering more informative and professional rapid assessment techniques for monitoring and mapping soil salinity. Soil salinity can be identified from remote sensing data obtained by different sensors by way of direct indicators that refer to salt features that are visible at the soil surface as well as indirect indicators such as the presence of halophytic plant and assessing the performance level of salt-tolerant crops. The purpose of this paper is to 1) discuss some soil salinity indicators; 2) review the satellite sensors and methods used for remote monitoring, detecting and mapping of soil salinity, particularly in arid and semi-arid regions; 3) review various spectral vegetation and salinity indices that have been developed and proposed for soil salinity detection and mapping, with an emphasis on soil salinity mapping and assessment in arid and semi-arid regions; and 4) highlight the most important issues limiting the use of remote sensing for soil salinity mapping, particularly in arid and semi-arid regions.

Keywords: Soil Salinity, Remote Sensing, Halophytic Plant, Salinity Index.

2.2 Introduction

According to the U.S. Salinity Staff Laboratory, soils with conductivity of the saturation extract (EC) > 4 deciSiemens per meter (dS/m) at 25°C, Exchangeable Sodium Percentage (ESP) < 15 and pH (soil reaction) < 8.5 are referred to saline soils (Richards, 1954b). Salt in the soil mostly derives from the weathering of rocks and primary minerals, which formed *in situ* or transported

by water or wind (Shrestha and Farshad, 2008). Other causes of soil salinity are topography, irrigation and dryland salinity, which occur due to forest clearance, overgrazing, and cutting bushes that cause water-tables to rise and bring saline groundwater close to the land surface. Thus, soil salinity categories are either primary salinity which is naturally occurring or secondary salinity which is human-induced.

Soil salinity is a prevalent environmental hazard in arid and semiarid regions around the world (Hillel, 2000). The United Nations Food and Agriculture Organization (FAO) has estimated that saline soil cover 397 million hectares of the total land area of the world (Koochafkan, 2012). Africa, Asia, Australia, Europe, Latin America, Near East and North America are the most affected areas (Koochafkan, 2012). According to the most recent estimates from a survey of farmers, about 2 million hectares and 20000 farms across Australia alone showed some signs of salinity (Statistics, 2002). A recent study conducted by McFarlane et al. (2004) has estimated that, in Western Australia alone, secondary salinity covers about 10% of the land, and could reach 23% if action is not taken to stop its spread.

Soil salinity adversely affects plant growth, crop production, soil and water quality, and eventually results in soil erosion and land degradation (Rhoades and Loveday, 1990; Zhu, 2001; Corwin and Lesch, 2003). Soil salinity impacts are not limited only to the environment but extend to the economy. For instance, the economic losses due to secondary salinization in Batinah region in Oman have been estimated at US\$ 1,604 ha⁻¹ (28%) when the salinity increases from low to medium level and US\$ 4,352 ha⁻¹ (76%) if it jumps from low to high level (Naifer et al., 2011).

Basically, soil salinity is a dynamic process with severe consequences for the soil, hydrological, climatic, geochemical, agricultural, social, and economic aspects. Therefore, for greater development and implementation of sufficient soil reclamation programs and preventing any

further salinization to sustain agricultural lands and natural ecosystems, information on the spatial extent, nature and distribution of soil salinity is becoming very essential. Thus, timely detection of soil salinity, monitoring and assessment of its severity level and extent become very important in its beginning at local and regional scales.

Conventionally, soil salinity has been measured by collecting *in situ* soil samples and analyzing those samples in the laboratory to determine their solute concentrations or electrical conductivity. However, these methods are time-consuming and costly since dense sampling is required to adequately characterize the spatial variability of an area (Dent and Young, 1981; Dehaan and Taylor, 2002; Nanni, 2006; Brunner et al., 2007). Ghabour and Daels (1993) agreed that detection soil salinity traditionally is time consuming, but remote sensing data and techniques offer more efficiently and economically rapid tools and techniques for monitoring and mapping soil salinity.

Remote sensing data and techniques have been progressively applied to monitor and map soil salinity since 1960s when black- and-white and color aerial photographs used to delineate salt-affected soils (Dale et al., 1986). Multispectral data such as Landsat, Satellite Pour l'Observation de la Terre (SPOT), IKONOS, QuickBird and the Indian Remote Sensing (IRS) series of satellites, as well as hyperspectral data such as EO-1 Hyperion and HyMap have been found to be useful in detecting, mapping, and monitoring soil salinity (Farifteh, 2007; Dwivedi et al., 2008; Weng et al., 2008b; Setia et al., 2011; Dehni and Lounis, 2012; Koshal, 2012; Teggi et al., 2012). Generally, remote sensing uses the electromagnetic energy reflected from targets to obtain information about the Earth's surface with different levels of detail. So, based on this concept, the spectral reflectance of the salt features at the soil surface has been widely studied using remote sensing and used as a direct indicator for soil salinity detection and mapping. However, when the soil moisture is high or the crust salt is invisible on the soil surface or mixed with other soil constituents this direct approach becomes complicated and

may yield unreliable results since these factors influence the soil spectral reflectance. But, the present scattered vegetation or halophytes on the soil surfaces can serve as a sign of the salinity problem, making it possible to indirectly detect and map areas that are affected by soil salinity using the reflectance from vegetation. Normally, unhealthy vegetation has a lower photosynthetic activity, causing increased visible reflectance and the reduced near-infrared reflectance (NIR) from the vegetation (Weiss et al., 2001). This pattern has been found in various plants subjected to salinity stress (Tilley et al., 2007). Therefore, based on this finding, several vegetation indices (VIs) such as Normalized Differential Vegetation Index (NDVI) and Soil Adjusted Vegetation Index (SAVI) have been used as indirect indicators assess and map soil salinity. Similarly, a number of researchers have developed different salinity indices to detect and map soil salinity such as Normalized Difference Salinity Index (NDSI) and Salinity Index (SI).

This review concentrates on the problem of soil salinity and discusses some soil salinity indicators and how remote sensing data and technologies are used for monitoring and mapping soil salinity. Additionally, it will discuss the most current vegetation and salinity indices used for soil salinity detecting and mapping and highlights some of the limitations and problems of using remote sensing for monitoring and mapping this hazard with an emphasis on soil salinity mapping and monitoring techniques for arid and semi-arid regions.

2.3 Soil Salinity and Remote Sensing

2.3.1 Soil Salinity Symptoms

Soil salinity can be detected directly from remotely sensed data through salt features that are visible at the soil surface, such as bare soil with white salt crusts on the surface (Teggi et al., 2012; Matinfar et al., 2013) or indirectly from indicators such as the presence of halophytic

plant, the performance level of salt-tolerant crops (Alhammadi and Glenn, 2008; Aldakheel, 2011; Iqbal, 2011; Zhang et al., 2011).

2.3.1.1 Salt Features at the Soil Surface

The dynamic processes at the surface of saline soil limit the monitoring and assessment of the salinization process because they influence the spectral, spatial and temporal behavior of the salt features (Metternicht and Zinck, 2008a). Via the physico-chemical properties of soil such as soil moisture content, organic matter, soil texture, types of clay color and surface roughness soil spectral reflectance is determined (Baumgardner et al., 1985; De Jong, 1992; Demattê et al., 2004; Shrestha et al., 2005; Brown et al., 2006). Due to salinity these soil properties change which affect the spectral reflectance of features that occur at the soil surface, including salt crusts and efflorescence besides variations in surface texture and structure (Schmid et al., 2008; Thomas, 2011). For example, Schmid et al. (2008) found that crusted saline soil reflects strongly in the visible and near-infrared (NIR) bands; moreover, Rao Singh and Sirohi (1994) noted that a crusted saline soil surface is generally smoother than a non-saline surface and exhibits high reflectance in the visible and NIR bands, which has been confirmed by Rao et al. (1995). On the other hand, Metternicht and Zinck (1997) found that the reflectance in the visible and NIR bands is highly affected by both the crust color and surface roughness factors. Despite the effects of salt features on the soil surface on the spectral reflectance, they have been considered good direct indicators of soil salinity. For example, Fernandez-Buces et al. (2006) used surface features to predict soil salinity. They found that the correlation coefficient between surface colors, EC and the sodium adsorption ratio (SAR) were statistically significant, which suggested that efflorescence color is a promising surface indicator with which to estimate soil salinity.

2.3.1.2 Presence of Halophytic Plants

Halophytic plants (salt-tolerant plants) are plants that tolerate high salt concentrations of the soil and can be grown on a salt affected land (Glenn et al., 1999). Although halophytic plants are common in saline areas, not all have been found to be good remote sensing indicators of soil salinity. For instance, Metternicht (1998) found the spectral reflectance curve with high absorption in the visible range and high reflectance in the NIR range of halophyte Chenopodiaceae in Bolivia, to be equivalent to that of chlorophyll-rich vegetation. In contrast, due to lower chlorophyll content the spectral reflectance curve of date palm (*Phoenix dactylifera* L.), also a halophyte, increased continuously in the visible and NIR bands. This study concluded that halophytic plants were promise indicator to distinguish saline areas from non-affected ones.

2.3.1.3 Crop Performance

The performance of some crops that can be grown on saline soils, such as alfalfa, barley, and cotton, reflect the severity of soil salinity. Cotton is largely cultivated on irrigated land, is therefore considered an ideal indirect indicator for soil salinity, so it has been used as salinity indicators in a variety of studies (Metternicht and Zinck, 2008a). For example, based on the high correlations between the Normalized Difference Vegetation Index (NDVI) values of cotton, sugarcane crops and the EC, Wiegand et al. (1994; 1996) successfully assessed the severity and extent of soil salinity in terms of the economic impact on crop production and also distinguished saline soils from non-affected soils. This strong relationship most likely exists only where salinity is the major factor that causes crop yield variability; lands that suffer from soil salinity are likely to have other factors that affect yields as much or more than salinity, such as high or low temperatures, topography and land management. Therefore, deduction of the relationship between a number of saline fields and an entire landscape is likely to result

in large errors, so the possible use of this indicator for determining the level of soil salinity must be checked carefully. To overcome this issue, some researchers have proposed using average crop production over a series of years to mask out the noise from non-soil factors that differ from year to year. For example, Lobell et al. (2007) warn of the use of inter-annual changes on crop yield as an indirect indicator of soil salinity at regional scales because yield mapping that is limited to only one year does not always give a reliable estimator of soil salinity, particularly when strongly saline soils are scarce. Thus, through the use of a 6-year temporal series of satellite images of yield, they obtained a strong correlation between yield losses and soil salinity; they highlighted that yield loss in agricultural regions could be primarily due to several factors, including soil salinity.

2.4 Mapping and Monitoring Soil Salinity Using Remote Sensing Data

Advantages of using remote sensing technology include saving time, wide coverage (satellite remote sensing provides the only source when data is required over large areas or regions), are faster than ground methods, and facilitate long term monitoring. These techniques provide multispectral image with resolutions that can be ranged from medium to high, as well as hyperspectral image. These remotely sensed data have been successfully used for monitoring and mapping soil salinity for decades with mixed results. Many researchers have used different techniques to monitor and map soil salinity using remote sensing data, as discussed below.

2.4.1 Multispectral Satellite Sensors for Mapping and Monitoring Soil Salinity

Extensive research using satellite imagery for mapping and monitoring soil salinity has been conducted over the last three decades, mostly with multispectral sensors. These include Landsat Thematic Mapper (TM), Landsat Multispectral Scanner System (MSS), Landsat Enhanced

Thematic Mapper Plus (ETM+), SPOT, Advanced Spaceborne Thermal Emission and Reflection Radiometer (Terra-ASTER), Linear imaging self-scanning sensor (LISS-III) and IKONOS (Verma et al., 1994; Dwivedi, 2001; Dwivedi et al., 2008). For example, in the United States of America (USA), Elnaggar and Noller (2010) used Landsat TM imagery integrated with decision-tree analysis (DTA) to map soil salinity in central Malheur County. They found that there was a significant relationship between EC values and reflectance in Landsat bands 1, 2, 3 and 4 as well as the Brightness (BI) and Wetness (WI) indices. Maximum likelihood supervised classification was used to classify the image into non-saline soils ($EC < 4$ dS/m) and saline soils, with accuracies of 97% and 60% respectively, whereas DTA predicted five classes of soil salinity with an overall accuracy of approximately 99%. Their results indicated that the use of Landsat TM imagery effectively identified bare soils that were characterized by high spectral reflectance due to a high salt content on the surface, and the approach of integrating DTA with remote sensing data was more accurate and effective compared to using remote sensing analysis alone.

Many researchers, including Katawatin and Kotrapat (2004), Mehrjardi (2008) and Yu et al. (2010b) have investigated the utility and effectiveness of ETM+ data for soil salinity mapping and monitoring. For example, in Thailand, Katawatin and Kotrapat (2004) investigated the use of Landsat-7 ETM+ with different combinations of three sources of ancillary data (topography, geology, and underground water quality) for soil salinity mapping. A maximum likelihood classification method was employed in this study. Their results showed that the use of Landsat ETM+ data bands 4, 5 and 7 in combination with all three types of ancillary data yielded the most accurate soil salinity map, with 83.6% overall accuracy. Additionally, Douaoui et al. (2006), Farifteh et al. (2006) and Eldeiry and Garcia (2008) agreed that an integrated approach using remote sensing techniques in addition to ancillary data such as field data, topography and

spatial models geophysical surveys can improve the development of high quality soil salinity maps.

Using multispectral sensors for soil salinity research has also been studied by Goossens et al. (1993). Their study examined and compared the accuracy of Landsat TM, MSS, and SPOT XS imagery for soil salinity mapping. They found that Landsat TM was optimal for soil salinity mapping. Another comparative assessment of the suitability of multisensor data for soil salinity studies was conducted in Pakistan by Ahmed and Andrianasolo (1997). They compared the performance of Landsat TM and SPOT XS in mapping salinity at a semi-detailed level. Their results were completely opposite to that of Goossens et al. (1993). They found that the SPOT XS data were more helpful than Landsat TM as it provided finer details of various thematic variables.

Thermal band has proven to be a useful tool in soil salinity studies. It has a key role in differentiating saline soils, especially in areas of bare soil or sparse and similar vegetation. For example, Verma et al. (1994) demonstrated that the addition of the thermal band of Landsat TM to the visible–NIR bands helped overcome spectral similarity issues with saline soils. Furthermore, thermal band was used to discriminate salt and sodium-affected soils by Metternicht and Zinck (1997). They found that the incorporation of the thermal band allowed for better salt and sodium detection. Furthermore, in a case study in Iran, Alavi Panah and Goossens (2001) found that the addition of the thermal band to the best Landsat TM visible–NIR band combination had great potential for separating saline soil from gypsiferous soil. This study confirmed the result obtained by Goossens et al. (1999), who reported the key role of the TM thermal band in separating gypsiferous soil from saline soils. In China, Huang et al. (2005) used Terra ASTER imagery to identified saline areas dominated by sodium chlorides and sodium sulfates. Their results showed a good correlation between surface salt concentrations and band 1 of the ASTER sensor, followed by bands 2 and 3.

It cannot be denied that medium or low spatial resolution of the satellite images can limit the mapping and detection of saline regions, particularly when the affected areas are smaller than the pixel size. Thus, high resolution multispectral sensors with pixel size of less than 5 m are becoming an essential for soil salinity studies (Dwivedi et al., 2008). However, only limited attempts have been made to identify and map soil salinity problems using fine spatial resolution (0.6 m – 4 m) images that are available from IKONOS (4 bands) and Quickbird (4 bands) satellites, as well as WorldView-2, which has 8 multispectral bands at 1.84 m spatial resolution and one panchromatic band at 0.5 m spatial resolution (Navulur, 2006). This is most likely due to the higher cost of this higher-resolution imagery and these sensors being more recently developed systems. Elhaddad and Garcia (2005) have used IKONOS satellite imagery and crop reflectance to identify the severity level of soil salinity and its effect on crop yield in Arkansas River Basin, Colorado. Image enhancement was used to separate the crop condition into several classes, and supervised classification was applied to delineate the different levels of soil salinity. They concluded that the superior effectiveness of their approach was primarily due to the use of high spatial resolution imagery. On the other hand, Dwivedi et al. (2008) conducted a comparative study on the performance of IKONOS imagery and imagery from the IRS-ID LISS-III sensor for mapping salt-affected soils. Different image classification and transformation techniques were used in their study, and an overall accuracy of 92.4% was gained when using IKONOS data compared to an overall accuracy of 78.4% and 84.3% obtained when using the IRS-ID LISS-III multispectral sensor, which indicates the great potential of high spatial resolution IKONOS images for soil salinity mapping and detection. In South Australia, Setia et al. (2011) detected and mapped soil salinity in an agricultural area using QuickBird imagery. They found that 99% of the variation in spectral values occurred in bands 2 and 4. Furthermore, they found that by dividing the image into hundreds of paddocks (small fields) and performing an unsupervised classification using a paddock-by-paddock

approach, which is a procedure where each individual paddock is classified and mapped separately, they were able to map soil salinity severity levels more accurately. Thus, they concluded that a paddock-by-paddock classification approach for QuickBird imagery is a promising method for detecting degrees of salinity severity at a farm level. However, in spite of these promising results, it should be noted that it would be extremely difficult to assess the validity and reliability of this approach at regional scales because it is a time-consuming and labor-intensive procedure. Thus, further investigations will help to elucidate whether and how a paddock-by-paddock classification approach will work at regional scales.

2.4.2 Limitations of Multispectral Satellite Sensors in Soil Salinity Mapping and Monitoring

Multispectral satellite sensors have been and still are the preferred method for mapping and monitoring soil salinity. This is primarily due to the low cost of the imagery (e.g., Landsat, SPOT) and the ability to map extreme surface expressions of salinity. Nevertheless, multispectral data has limited diagnostic capability because of its coarse spatial and spectral resolutions (Spies and Woodgate, 2005). For example, Furby et al. (1995) and Howari (2003) reported that direct mapping of soil salinity with multispectral imagery had major limitations that arise, especially where there are no salt features on the soil surface and where saline soils are dominated by halophyte plants. Additionally, Furby et al. (1995) stated that multispectral satellite sensors caused confusing reflectance, as they found that non-saline soils were confused with bare, extremely saline areas. In the case of Landsat imagery, Fraser and Joseph (1998) reported that the spectral resolution of Landsat was insufficient due to the difference between the spectra of saline land and waterlogged land not being sufficient to allow spectral separation, as well as the variable spectral response of saline soil. Additionally, Hick & Russell (1987) state that the ability of discriminating plant species and plant health conditions is challenging

with Landsat imagery due to the absence of narrow bands in the range of 700-730 nm, 730-760 nm and 900-1100 nm.

2.4.3 Hyperspectral Remote Sensing Data

Most of the studies discussed above have attempted to map and monitor soil salinity using different multispectral satellite sensors. However, the use of such sensors is restrictive, as their spectral resolution influences the quality and quantity of the information they provide. The development of airborne and satellite-based hyperspectral sensors has overcome some of the spatial and spectral limitations of multispectral satellite imagery for monitoring and mapping soil salinity, both regionally and locally. Hyperspectral sensors offer a large number of spectral bands with high spatial resolution that allow the discrimination of halophyte plants from non-halophyte plants as well as the identification of surface salt features in more detail than the multispectral sensors (Gupta, 2003; Dutkiewicz, 2006). Taylor et al. (1994) demonstrated the possibility of using airborne hyperspectral data to map salinity in the soil. They described the use of visible–NIR and shortwave infrared (SWIR) hyperspectral data that were collected with airborne Geoscan sensor to map soil salinity at Pyramid Hill, Victoria, Australia. They found that differentiation of salt-affected soils based on the mapping of halophytic plants simply achieved via the employing of the principal component analysis of Geoscan imagery. The potential of the HyMap airborne hyperspectral sensor, which captures images within a spectral range of 450–2500 nm in 128 bands, for soil salinity studies has been tested by Dehaan and Taylor (2002; 2003). They concluded that HyMap has considerable potential for mapping saline areas that characterize the variety of salinity levels and scattered halophyte plants. Likewise, Farifteh et al. (2007) measured reflectance spectra from multiple sources (experimental, field, and airborne datasets) to predict salt concentrations with Partial Least Squares Regression (PLSR) and Artificial Neural Networks (ANN) and mapped soil salinity

using airborne hyperspectral data acquired with HyMap. Their results indicated that both PLSR and ANN enabled good mapping of soil salinity.

After the year 2000, two experimental hyperspectral sensors were launched, CHRIS and Hyperion (Metternicht and Zinck, 2008b). Compared to airborne hyperspectral remote sensing, very limited numbers of studies on soil salinity have been conducted with these space-borne hyperspectral data. In Turkey, soil salinity was assessed by Satir et al. (2000) using CHRIS PROBA sensor imagery and the spectral characteristics of indicator crops. Their study showed a strong correlation between the spectral wavebands of CHRIS PROBA and the reflected signals of cotton and wheat for detecting soil salinity, which confirmed that the condition of cotton and wheat crops is a good indirect indicator of soil salinity. On the other hand, a study by Dutkiewicz (2006) evaluated the performance of Hyperion imagery for mapping surface symptoms of dryland salinity using mixture-tuned matched filtering in southern Australia. She found that the hyperspectral imagery was unable to distinguish halophytic samphire vegetation at slight or moderate levels of salinity; however, it could be used to map high to very high and extremely high salinity. In China, Weng et al. (2008b) have investigated the potential of data from the spaceborne Earth Observing 1 (EO-1) Hyperion sensor for the prediction of soil salinity. Partial Least-Squares Regression (PLSR) and Stepwise Linear Regression (SWR) were used as prediction models. Their results indicated that the PLSR model produced more accurate estimations of soil salt content than SWR and could overcome the difficulties that were caused by high dimensionality and strong correlation among input variables as well as noisy data. Thus, they concluded that PLSR was a promising approach for the quantitative mapping of soil salinity with Hyperion data over a large area. These results suggest that further studies need to be conducted to examine prediction models based on nonlinear regression methods, and the spectral noise of hyperspectral data should be taken into consideration to increase the accuracy of soil salinity mapping. In addition, a more recent study was conducted

in Iran by Hamzeh et al. (2012b) to investigate the ability of Hyperion spaceborne hyperspectral data for mapping salinity stress in sugarcane fields. Different classifications such as Support Vector Machine (SVM), Spectral Angle Mapper (SAM), Minimum Distance (MD) and Maximum Likelihood (ML) were used with different band combinations to classify soil salinity into three classes (low, moderate and high salinity). Their results indicated that SVM classification using all bands as input data yielded a salinity map with good accuracy, with an overall accuracy and kappa coefficient of 78.7% and 0.68, respectively.

2.5 Using Vegetation and Soil Indices in Soil Salinity Studies

2.5.1 Vegetation and Soil Indices

As mentioned previously, halophytic plants grow naturally in saline soil, and can be adapted to high soil salinity. Therefore, vegetation has been used as an indirect indicator to predict and map soil salinity. Accordingly, numerous researchers have conducted studies on the mapping and delineation of soil salinity using different Spectral Vegetation Indices (SVI). Among the vegetation indices, NDVI, SAVI, Ratio Vegetation Index (RVI) and Tasseled Cap Transformation that consisted of the Soil Brightness Index (SBI), the Green Vegetation Index (GVI), and the Wetness Index (WI) have been used in soil salinity studies (Wang et al., 2002a; Eldeiry and Garcia, 2008; Jabbar and Chen, 2008; Lobell et al., 2010; Aldakheel, 2011; Zhang et al., 2011; Matinfar et al., 2013).

Due to absorption in the visible range and high reflectance in the NIR range of the electromagnetic spectrum, the NDVI (Table 2.1) has been widely used to map soil salinity by monitoring halophytic plants (Fernandez-Buces et al., 2006; Jabbar and Chen, 2008; Elnaggar and Noller, 2010). The difference in reflectance between the visible and NIR bands is divided by the sum of the two bands' reflectance (Table 2.1). This normalizes differences in the amount

of incoming light and produces a number from -1 to 1; the range of actual values is approximately 0.1 for bare soils to 0.9 for healthy vegetation (Deering and Rouse, 1975). In Mexico, Fernandez-Buces et al. (2006) found a significant correlation between NDVI, EC and SAR. Moreover, Pérez González et al. (2006) have correlated the NDVI of halophytic vegetation with the spatial variability of the chemical and physical properties of a transect to identify saline hydromorphic soils. Their results showed the NDVI to be very proper in detecting halophytic plant and relating it to saline soils. Additionally, Bannari et al. (2008) have stated that because plant growth declines due to soil salinity, salt stress could be predicted using the NDVI. However, researchers such as Metternicht and Zinck (2008b) and Zhang, et al. (2011) argue that detecting soil salinity using the NDVI is challenging because the presence of vegetation could cause spectral confusion with the reflectance properties of salt and also because the NDVI is considered an unreliable indicator, as it is also correlated to other yield variables such as chlorophyll content, biomass and leaf area. Liu and Huete (1995) have developed a modification of the NDVI to reduce the atmospheric and canopy background noise, the enhanced soil and atmosphere resistant vegetation index (EVI) (Table 2.1). A comparison study of the efficiency of the EVI and NDVI calculated from Multi-year Moderate Resolution Imaging Spectroradiometer (MODIS) imagery for assessing soil salinity in the Red River Valley, United States has been conducted by Lobell et al. (2010). They found that the EVI is a more reliable indicator of salinity than the NDVI. The use of the RVI (Table 2.1) to measure the spectral reflectance of soybean canopy and elephant grass under different salinity and irrigation treatments was investigated by Wang et al. (2002a) and Wang et al. (2002b). In both studies, the results showed that the canopy spectral reflectance in the NIR region was reduced as salinity level increase.

Furthermore, SAVI (Table 2.1) was developed by Huete (1988) to eliminate soil-induced variation and for use in areas where soil backgrounds differed, and the low canopy cover was

present. Depending on the crop density, the L factor generally ranges from 0 for higher densities and 1 for lower densities (Huete, 1988). The resulting SAVI values in the classified image are either positive, negative or zero. A positive SAVI value indicates that there is a decrease in the vegetation, while a negative value indicates an increase in vegetation. A zero value indicates no change in vegetation. The effectiveness of this index for soil salinity detection and mapping has been studied by several researchers, including Zhang et al. (2011), Alhammadi (2010), Koshal (2010), Elnaggar and Noller (2010) and Masoud and Koike (2006). For example, in the United Arab Emirates (UAE) Alhammadi and Glenn (2008) used the SAVI index for detecting date palm health under soil salinity. They found that the SAVI values decreased with increasing soil salinity; for instance, the SAVI value was 0.155 at the lowest salinity level of 6900 parts per million (ppm), whereas the value decreased to 0.104 at the very high salinity of 41000 ppm. These results showed the potential of using the date palm, which is a halophytic plant, as an indirect indicator of soil salinity as well as the effectiveness of the SAVI in detecting plant stress related to severe salinity and thus permitting the identification and mapping of saline areas indirectly. Recently, Zhang et al. (2011) have proposed four Soil-adjusted Salinity Indices (SASIs) through the most sensitive bands in a SAVI form. For halophyte plants, SASIs produced better results compared to other selected vegetation indices such as the NDVI and SAVI. These results indicate that in highly saline areas that are covered mainly by halophyte plants, SASIs would give superior results, whereas VIs such as NDVI and SAVI would only be proper to assess salinity in low saline areas covered by salt-sensitive plants.

Table 2.1 Vegetation and soil salinity Indices that have been proposed and used for soil salinity monitoring and mapping

	Indices	Equation	References
1	Normalized Differential Vegetation Index	$NDVI = (NIR - R)/(NIR + R)$	(Deering and Rouse, 1975)
2	Enhanced Vegetation Index	$EVI = 2.5 (NIR - R)/(NIR + 6R - 7.5BLUE + 1)$	(Liu and Huete, 1995)
3	Soil Adjusted Vegetation Index	$SAVI = ((NIR - R)/(NIR + R + L)) \times (1 + L)$	(Huete, 1988)
4	Ratio Vegetation Index	$RVI = NIR/R$	(Major et al., 1990)
5	Normalized Differential Salinity Index	$NDSI = (R - NIR)/(R + NIR)$	
6	Brightness Index	$BI = \sqrt{R^2 + NIR^2}$	(Khan et al., 2005)
7	Salinity Index	$SI = \sqrt{BLUE \times R}$	
8	Salinity Index	$SI1 = \sqrt{G \times R}$	
9	Salinity Index	$SI2 = \sqrt{G^2 + R^2 + NIR^2}$	(Douaoui et al., 2006)
10	Salinity Index	$SI3 = \sqrt{G^2 + R^2}$	
11	Salinity Index	$SI-1 = ALI9/ALI10$	
12	Salinity Index	$SI-2 = (ALI6 - ALI9)/(ALI6 + ALI9)$	
13	Salinity Index	$SI-3 = ((ALI9 - ALI10))/(ALI9 + ALI10)$	(Bannari et al., 2008)
14	Soil Salinity and Sodidity Indices	$SSSI-1 = (ALI9 - ALI10)$	
15	Soil Salinity and Sodidity Indices	$SSSI-2 = ((ALI9 \times ALI10 - ALI10 \times ALI10))/ALI9$	
16	Salinity Index	$S_1 = Blue/R$	
17	Salinity Index	$S_2 = (Blue - R)/(Blue + R)$	
19	Salinity Index	$S_3 = (G \times R)/Blue$	
20	Salinity Index	$S_4 = \sqrt{Blue \times R}$	(Abbas and Khan, 2007)
21	Salinity Index	$S_5 = (Blue \times R)/G$	
22	Salinity Index	$S_6 = (R \times NIR)/G$	

Similarly, various spectral salinity indices have been developed for salt mineral detection and mapping. Douaoui et al. (2006) have proposed three salinity indices (Table 2.1) produced from SPOT XS imagery to detect and map soil salinity hazards in a semi-arid environment in Algeria. They found that those indices were strongly correlated with measured values, but considerably underestimated the salinity of areas with high levels of surface salt. Besides, Khan et al. (2005) have proposed three spectral salinity indices: the Brightness index (BI), Normalized Difference Salinity Index (NDSI) and Salinity Index (SI) (Table 2.1) from the LISS-II sensor of the IRS-1B satellite to assess hydrosalinized land degradation in Pakistan. Among these indices, they found that NDSI yielded the most acceptable results in identifying different salt classes. Another study conducted by Vidal et al. (1996) and Vincent et al. (1996) looked at salinity by differentiating vegetated from non-vegetated areas using NDVI; then the BI was computed to identify the moisture and salinity status of fallow land and deserted fields. Furthermore, three different salinity indices, SI-1, SI-2 and SI-3 (Table 2.1) from the EO-1 ALI spectral bands, have been proposed by Bannari et al. (2008) to discriminate slight and moderate soil salinity and sodicity in Morocco. Although the results showed that SI-3 had the highest correlation (46.9%), the result from this index was not adequate to provide precise information. Therefore, they devised another two Soils Salinity and Sodicity Indices (SSSI) (Table 2.1). Their results indicated that these SSSI indices were likely to increase the identification accuracy in areas with low and medium salinity because they offered the most significant correlation (52.9%) with the ground EC measurement. In Pakistan, Abbas and Khan (2007) have suggested an integrated approach based on the spatial analysis of both ground and satellite data to assess soil salinity. Remotely sensed data-based salinity indices and a Principal Components Analysis (PCA) were developed to detect soil salinity. Their result showed that out of the six salinity indices (Table 2.1) S3 produced the most promising result compared to

ground measurements. Moreover, they concluded that PCA and salinity indices are promising techniques for soil salinity prediction based on satellite images.

Looking at these vegetation and soil salinity indices in the literature, a number of results stand out. Utilizing vegetation indices in the assessment and mapping of soil salinity in areas of densely vegetated soils will yield promising results, whereas on bare soils, the identification of salt based on vegetation indices will not work. Thus, soil salinity indices will be the appropriate method in the case of bare soils or soils with very low scattered vegetation cover, providing superior results. These observations are in agreement with Bouaziz et al. (2011b) and Fan et al. (2012). Bouaziz et al. (2011b) found that vegetation indices such as SAVI, NDVI and EVI had a low correlation with EC due to an insufficient density of vegetation cover, whereas soil salinity indices exhibited higher correlations with EC. Additionally, Fan et al. (2012) found that NDVI values had a significant negative relationship with soil salinity in soils covered by vegetation, whereas this relationship was not clear on bare soil.

2.6 Issues in Mapping Soil Salinity in Arid and Semi-Arid Regions Using Remote Sensing

The spatial, temporal and vertical variability in the soil profile are the limiting factors in the assessment and mapping of soil salinity using remote sensing data because the spectral reflectance is unable to provide information on the whole soil profile, as it only observes the soil surface (Schmugge et al., 2002; Sethi et al., 2010). Moreover, the surface characteristics in many cases may not be representative of the deeper soil profile (Dewitte et al., 2012). However, combining remote sensing data with geophysical surveys and simulation models can be an alternative option (Farifteh et al., 2006).

The direct detection of soil salinity becomes applicable and much easier for bare soils and/or whenever salt-related symptoms (e.g., crusts) and scattered vegetation are visible on the

surface; in these cases, information such as salt types and quantity as well as the crust thickness can be provided based on the soil surface spectral signatures (Howari, 2003; Ghrefat et al., 2007). Yet, the direct deduction of soil salinity in arid and semi-arid regions that are characterized by dense vegetation cover would be difficult, as the vegetation will cause spectral mixing (Kaleita et al., 2005; Ding et al., 2011).

On the other hand, different studies such as Tashi et al. (2010), Fernandez-Buces et al. (2006) have successfully used indirect indicator to map soil salinity through monitoring the vegetation condition by using NDVI. Generally, these methods assume that soil salinity is the only stressor decreasing and damaging the crop condition, whereas other factors such as inappropriate soil management and water quality are neglected. Moreover, reductions in vegetation growth and vigor could be related to a lack of necessary nutrients rather than the occurrence of salt. Additionally, different plants generally grow in different levels of salinity, so that the NDVI is considered an uncertain indicator for soil salinity monitoring and mapping. Besides, the existence of halophytic plants may confuse soil salinity detection based on the NDVI due to mixing with the spectral signature of salt, which then will lead to classification errors (Sethi et al., 2010). Hence, to overcome this issue and remove classification errors to some degree, the SAVI index and other indices and enhancement models have helped to separate soil and vegetation signals (Mulder et al., 2011).

Additionally, low spectral resolution satellite images limit the direct detection and mapping of soil salinity, primarily due to their inability to detect particular absorption bands of some salt types and the frequent occurrence of problems with mixed spectral signatures that come from a variety of surface components (Mougenot et al., 1993; Dehaan and Taylor, 2003). Nevertheless, the advance of hyperspectral sensors has enabled spectral features associated to the characteristic absorption bands of salt minerals to be mapped with more detail (Cloutis, 1996). The above shortcomings indicate that detecting and mapping soil salinity in arid and

semi-arid regions using remote sensing is challenging. This is primarily attributed to the weakness of the spectral signals from saline soils compared to the noise caused by other factors. Obviously, there is no agreed-on best approach to this technology for monitoring and mapping soil salinity, as many researchers have used and applied different tools and techniques to map and monitor saline soils with varying degrees of success. For example, in the case of vegetation indices, some researchers like Elnaggar and Noller (2010) have found that vegetation indices (NDVI, SAVI, and GVI) had a weak correlation with the EC measurements, which suggests that halophytes could not be used to identify salt-affected soils under vegetation cover. Sethi et al. (2006) in a study in India, found the same, whereas Pérez González et al. (2006) found the NDVI to be very useful in detecting halophytic plants and relating it to saline soils. Despite these varying results of using halophytic plants as indirect indicators for soil salinity detection and mapping, it is ineffective to monitor and map soil salinity through non-halophyte plants, as they cannot live in highly saline areas. Thus, taking into consideration the spectral reflectance of halophytic plants is necessary for soil salinity detection and mapping, particularly in highly saline areas.

2.7 Conclusion

Soil salinity, either naturally occurring or human-induced is a serious global environmental problem, especially in arid and semi-arid regions. This is a complex dynamic process with serious consequences for the soil environment as well as, geochemical, hydrological, climatic, agricultural, and economic impacts. Being a severe environmental hazard, the frequent detection of soil salinity and assessment of its extent and severity at an early stage become very important at both local and regional scales. Traditionally, soil salinity was assessed via collecting *in situ* soil samples and analyzing those samples in the laboratory. Undertaking this

method, especially over a large area, is expensive and time consuming. Remote sensing represents a good alternative for monitoring and mapping changes in soil salinity.

Remote sensing data have been used extensively to identify and map saline areas, and the potential of remote sensing for assessing and mapping soil salinity is enormous. Multispectral satellite sensors are the preferred method for mapping and monitoring soil salinity, largely due to the low cost of such imagery and the ability to map extreme surface expressions of salinity. However, multispectral data have limited capabilities due to their spatial and spectral resolution. Hyperspectral imagery, with its fine spatial and spectral resolutions, allows soil salinity mapping in greater detail and represents another alternative.

Surface reflectance is highly affected by soil's moisture content, salt content, color, and surface roughness. High salt concentrations can be identified through the existence of characteristic vegetation types and growth patterns or by the salt efflorescence and crust that are present on bare soils. Similar to vegetation indices, researchers have developed different salinity indices to detect and map soil salinity. As discussed, these indices have been applied with varying degree of success. Field sites differ in terms of levels of salinity and the amount of vegetation cover; hence, a single selected index may not perform best in all cases. Each site needs to be assessed regarding the strengths and weaknesses of the proposed indices before appropriate remote sensing-based indices are used for soil salinity mapping and assessing.

**Higher Degree Research Thesis by Publication
University of New England**

STATEMENT OF ORIGINALITY

We, the Research Master/PhD candidate and the candidate's Principal Supervisor, certify that the following text, figures and diagrams are the candidate's original work.

Type of work	Page number/s

Name of Candidate: Amal Allbed

Name/title of Principal Supervisor: Professor Lalit Kumar



Candidate

20 June 2018

Date



Principal Supervisor

20 June 2018

Date

**Higher Degree Research Thesis by Publication
University of New England**

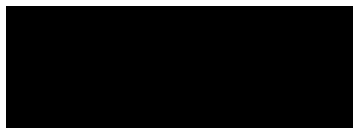
STATEMENT OF AUTHORS' CONTRIBUTION

We, the Research Master/PhD candidate and the candidate's Principal Supervisor, certify that all co-authors have consented to their work being included in the thesis and they have accepted the candidate's contribution as indicated in the *Statement of Originality*.

	Author's Name (please print clearly)	% of contribution
Candidate	Amal Allbed	80
Other Authors	Lalit Kumar	20

Name of Candidate: Amal Allbed

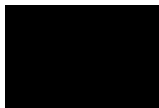
Name/title of Principal Supervisor: Professor Lalit Kumar



Candidate

20 June 2018

Date



Principal Supervisor

20 June 2018

Date

Chapter 3 Assessing Soil Salinity Using Soil Salinity and Vegetation Indices Derived from IKONOS High-Spatial Resolution Imageries: Applications in a Date Palm Dominated Region

This chapter has been published as:

Allbed, A., Kumar, L., Aldakheel, Y.Y. (2014). Assessing soil salinity using soil salinity and vegetation indices derived from IKONOS high-spatial resolution imageries: Applications in a date palm dominated region. *Geoderma*, 230-231: 1-8. doi: 10.1016/j.geoderma.2014.03.025.

3.1 Abstract

In saline soils, the spectral reflectance of either salt features at the surface or of vegetation that was negatively affected by salt varies with different salinity levels. Thus, several indices for vegetation and soil salinity have been developed. This study was conducted to assess the soil salinity levels in the Al-Hassa Oasis, which is dominated by date palm vegetation, in the eastern province of Saudi Arabia. Ground and remote sensing data were used to determine if any existing vegetation and soil salinity indices could be used to assess the soil salinity of communities vegetated with date palm. A systematic regular grid-sampling approach was used to collect a total of 149 composite soil samples from the study area. Thirteen broadband indices, which encompassed vegetation and soil salinity indices, were extracted from IKONOS satellite images. The predictive power of these indices for soil salinity was examined. The study area was dominated by areas of high salinity. Among the investigated indices, the Soil-Adjusted Vegetation Index (SAVI), Normalized Differential Salinity Index (NDSI) and Salinity Index (SI-T) yielded the best results for assessing the soil salinity of cultivated lands with dense and uniform vegetation. In contrast, the NDSI and SI-T exhibited the highest significant correlation with salinity for less densely vegetated lands and bare soils. Generally, the soil salinity in the areas that were dominated by date palms was successfully assessed by broadband vegetation and soil salinity indices that were extracted from the IKONOS satellite images.

Keywords: Soil salinity, Vegetation indices, Soil salinity indices, Date palm

3.2 Introduction

The buildup of soluble salts at or near the soil surface is referred to as soil salinity. Generally, salt accumulation is measured by determining the Electrical Conductivity (EC) of a solution extracted from a water saturated soil paste (Richards, 1954b). Saline soils are characterized by an EC of > 4 deciSiemens per meter (dS/m), an Exchangeable Sodium Percentage (ESP) of $<$

15% and a pH (soil reaction) of < 8.5 (Richards, 1954b). Soil salinity is a severe environmental hazard in most arid and semi-arid regions, including Saudi Arabia (Tripathi, 2009).

In the Al-Hassa Oasis (situated in the eastern province of Saudi Arabia) soil salinity is a serious problem that threatens sustainable agriculture (Al-Taher, 1999). The Al-Hassa Oasis is dominated by date palms (*Phoenix dactylifera* L.) and is considered one of the most productive date palm production regions in Saudi Arabia (Al-Abdoulhadi et al., 2012). This region provides a significant source of income for farmers and the government (Jain et al., 2011). The date palm is highly tolerant of salinity (Zaid and Arias Jiménez, 1999). Nevertheless, the growth and productivity of date palms in this Oasis are negatively impacted by increasing soil salinity. Therefore, it is important to assess the severity of soil salinity in this Oasis to implement effective soil reclamation programs that minimize or prevent future increases in soil salinity. The remote sensing technique is one rapid assessment technique that can be used for this purpose.

Remote sensing uses the electromagnetic energy that is reflected from targets to obtain information about the Earth's surface (Khorram et al., 2012). Because soil salinity impacts vegetation, remotely sensed vegetation reflectance can be used as an indirect indicator of soil salinity (Metternicht and Zinck, 2008a; Zhang et al., 2011). Healthy vegetation has a low reflectance in the visible region due to absorption by chlorophyll, which is used for photosynthesis, and a high reflectance in the Near infrared (NIR) region due to the cellular structure of plant leaves (Kumar et al., 2002). In contrast, unhealthy vegetation has less chlorophyll and thus shows an increased reflectance in the visible region and reduced reflectance in NIR region. These reflectance changes were observed for various plants during salinity stress (Peñuelas et al., 1997; Wang et al., 2002b; Fernandez-Buces et al., 2006; Tilley et al., 2007; Elmetwalli et al., 2012). Consequently, several studies have assessed soil salinity with vegetation reflectance using a variety of vegetation indices. In addition, a number of

spectral soil salinity indices were developed to detect and map mineral salt deposits. Table 3.1 contains some of the most commonly used spectral indices that were found in the literature. The relationships between the actual soil salinity and the different vegetation and salinity indices derived from broadband satellite images have been found to vary considerably.

The spatial resolution of the satellite imagery is an important factor should be considered when mapping and assessing soil salinity (Ben-Dor et al., 2008b; Schmid et al., 2008). Manchanda (1984) has used Landsat Multispectral Scanner System (MSS), for soil salinity mapping and observed that Landsat-MSS was of limited use to identify saline areas due to its low spatial resolution. Additionally, Bouaziz et al. (2011b) declared that the low spatial resolution of the Moderate-resolution Imaging Spectroradiometer (MODIS) data is one of the main reasons for the weak correlation between soil salinity data and MODIS data. The efficiency of different medium spatial resolution imageries (Landsat and Indian Remote Sensing Satellite (IRS-ID LISS-III)) and high spatial resolution (IKONOS and SPOT) in soil salinity mapping and detection has been conducted by several researchers. For example, Ahmed and Andrianasolo (1997) compared the performance of Landsat Thematic Mapper (TM), and SPOT XS in mapping salinity at a semi-detailed level, and found that the SPOT XS data were more helpful than Landsat TM as it provided finer details of various thematic variables. Beside, Dwivedi et al. (2008) found that delineation of soil salinity based on IKONOS high spatial resolution data scored better results than the IRS-ID LISS-III, due to increasing spatial resolution. Moreover, a comparative study on the performance of two spatial models using the IKONOS and Landsat images for detecting soil salinity in agricultural areas was conducted by Eldeiry and Garcia (2008). Their results revealed that satellite image spatial resolution plays a key role in soil salinity detection. They found that results derived from IKONOS images were better than those obtained from Landsat images for detecting soil salinity. Thus, these studies confirmed that high spatial resolution images outperform medium spatial resolution in mapping and detecting

soil salinity due to their high spatial resolution which has a significant effect on the capacity to identify soil salinity.

Although significant progress was made for assessing soil salinity using vegetation and soil salinity indices that were derived from different broadband satellite images, however, to date, no research has assessed the soil salinity in the date palm dominated Al-Hassa Oasis based on such methods. Furthermore, no studies have investigated the effectiveness of vegetation and soil salinity indices that derived from broadband satellite images for assessing soil salinity in areas that are dominated by date palms. Therefore, this research was conducted to assess soil salinity in the Al-Hassa Oasis, which is situated in the eastern province of Saudi Arabia. In addition, this research evaluated the efficiency of some existing vegetation and salinity indices by using IKONOS satellite images to assess soil salinity over an area that was vegetated mainly by date palms.

3.3 Materials and Methods

3.3.1 Study Area

Al-Hassa Oasis is one of the largest and oldest oases in the Arabian Peninsula (Al-Dakheel and Massoud, 2006). Al-Hassa Oasis is situated approximately 70 km inland of the Gulf coast between a latitude of 25° 05' and 25° 40' N and a longitude of 49° 10' and 49° 55' E (Figure 3.1). This Oasis covers an area of approximately 20,000 ha and is at an altitude of approximately 130 to 160 m above sea level (Al-Dakheel and Massoud, 2006; Al-Zarah, 2011). The Al-Hassa Oasis is L-shaped and is actually composed of two separate oases. Both of these oases are slightly sloped to the north and east (Hussain, 1982; Al-Barrak and Al-Badawi, 1988; Citino, 2012).

Currently, the total cultivated land area within the Oasis is approximately 8,000 ha, of which 92% is planted in date palm (Al-Zarah, 2008). The main Oasis water sources include the

Neogene groundwater aquifer and several free flowing springs that are distributed across the area (Al Sayari et al., 1984). Of the springs, only 32 are useable and productive. Since 1971, these springs were managed by the Al-Hassa Irrigation and Drainage Authority (HIDA) for the Al-Hassa Irrigation and Drainage Project (IDP) (Hussain and Sadiq, 1991; Al-Zarah, 2008). The Oasis groundwater is primarily used for domestic, irrigational and industrial purposes. The main drainage direction follows the natural eastward slope in the eastern part of the Oasis and the natural northern slope in the northern part of the Oasis (Al-Barrak and Al-Badawi, 1988; Shaltout and El-Halawany, 1992).

This area is characterized by an arid climate with a high potential evaporation rate that exceeds the annual average precipitation of approximately 488 mm. The absolute ambient temperature exceeds 45 °C during the summer season (from June to August). During the winter, (December, January and February) the temperature is between 2 and 22 °C.

3.3.2 Site Selection

Based on visual interpretation of a false color composite from a satellite image, ground truthing and the division of the oasis, the three following sites were selected: site "A" in the northern Oasis at Al-Uyoun city, site "B" in the middle of the Oasis at Al-Bataliah village, and site "C" at the town of Al-Umran in the eastern Oasis (Figure 3.2).

3.3.3 Soil Sampling

Soil sampling was conducted during the dry season (January and February) of 2012 with a systematic regular grid-sampling scheme that was generated with the ESRI® ArcGIS 9.3® software. This procedure was designed to collect composite soil samples in the field. Prior to sampling, the coordinates of each composite soil sample in the three sites were recorded with the Global Positioning System (GPS). Each composite soil sample consists of four core sub-samples were collected at a distance of 20 m north, south, east and west of the center sampling

point. The sub-samples were collected at a depth of 0 to 20 cm with a hand auger and were crushed and mixed together to form one sample. Each composite sample was placed into a plastic bag, sufficiently dried and labeled for examination in the laboratory. A total of 149 composite soil samples were collected from the three defined sites. Soil salinity was determined by measuring the EC from the soil saturation extracts in the laboratory, as described by Richards (1954a).

3.3.4 Satellite Image Data

High spatial resolution cloud-free IKONOS satellite images were used in this study and were acquired near the actual soil sampling date on April 20th, 2012. These data were obtained from the King Abdul-Aziz City of Science and Technology in Saudi Arabia. These IKONOS satellite images have a dynamic range of 8 bits per pixel and a pixel size of 1 m. The IKONOS images contain 4 bands that record the reflected or emitted radiation from the Earth's surface in the B, G, R and NIR ranges of the electromagnetic spectrum (Dial, 2003). The spectral ranges of these bands are as follows: band 1 (B) 0.40 - 0.52 μm , band 2 (G) 0.52 - 0.60 μm , band 3 (R) 0.63 - 0.69 μm and band 4 (NIR) 0.76 - 0.90 μm . The images were geo-rectified to the Universal Transverse Mercatore (UTM) coordinate system with the datum World Geodetic System (WGS) 1984 and zone 39 north. Atmospheric correction was performed using Dark-Object Subtraction (DOS) technique (Chavez, 1996).

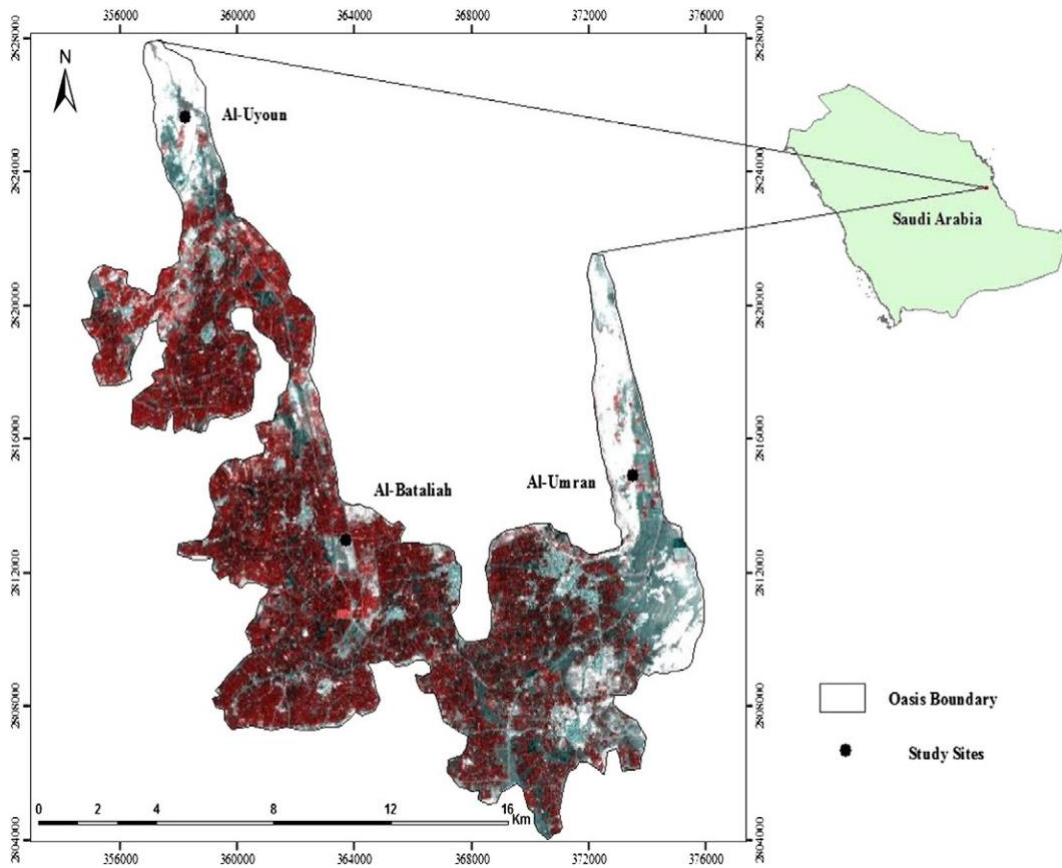


Figure 3.1 Location of the study area

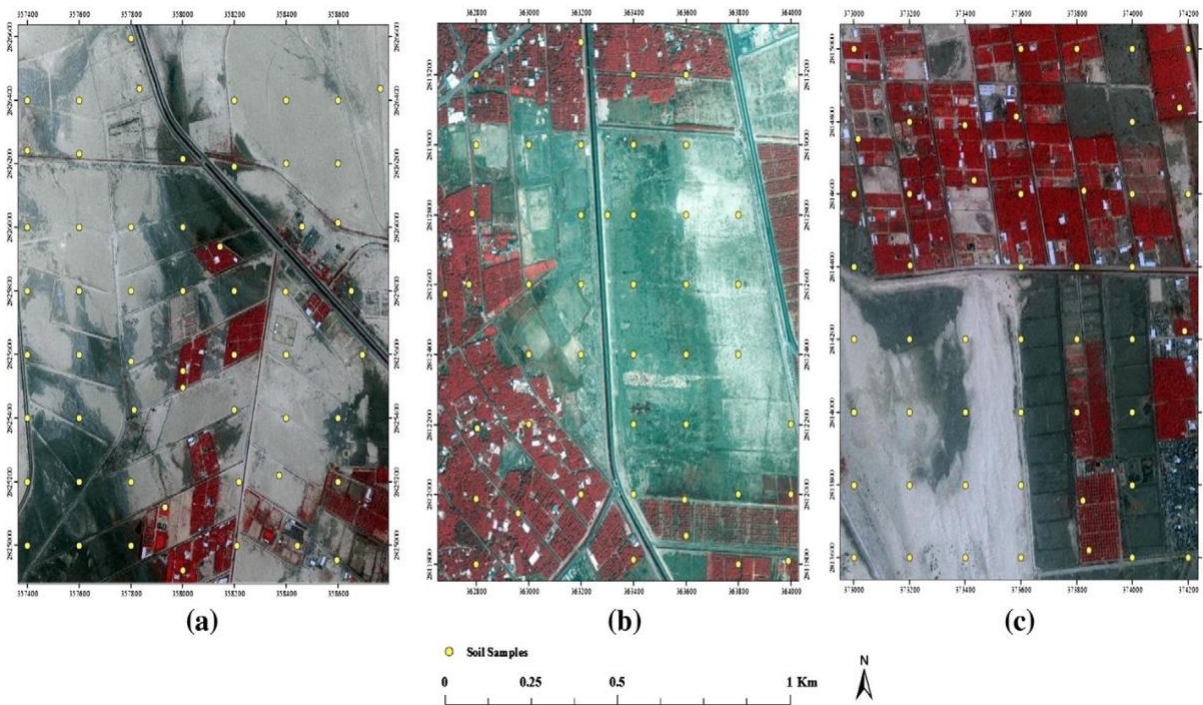


Figure 3.2 Study sites, (a) site A, (b) site B and (c) site C

3.3.5 Broadband Indices Selection

One vegetation and 12 soil salinity broadband indices that were derived from the IKONOS images were examined based on their potential for assessing soil salinity. These broadband indices were selected according to their relative importance for determining soil salinity. The vegetation index SAVI was chosen because it minimizes the spectral variation that is caused by the soil background (Huete, 1988). A soil adjustment factor (L) of 0.5 was used to account for soil background variation of vegetation with an intermediate density (Huete, 1988). A positive SAVI value indicates that the vegetation decreased with time and a negative SAVI value indicates that the vegetation increased with time. A SAVI value of zero indicates that no change in vegetation occurred. The soil salinity indices included NDSI, BI, SI, SI1, SI2, SI3, S1, S2, S3, S5, S6, and SI-T (see Table 3.1 for details).

Table 3.1 Summary of the most widely used vegetation and soil salinity indices for soil salinity assessments

Index	Formulation	Reference
Soil-Adjusted Vegetation Index (SAVI)	$(NIR - R)/(NIR + R + L) (1 + L)$	(Huete, 1988)
Salinity index (SI-T)	$(R/NIR) \times 100$	(Tripathi et al., 1997)
Brightness Index (BI)	$\sqrt{R^2 + NIR^2}$	
Normalized Differential Salinity Index (NDSI)	$(R - NIR)/(R + NIR)$	(Khan et al., 2005)
Salinity Index (SI)	$\sqrt{B \times R}$	
Salinity Index 1 (SI1)	$\sqrt{G \times R}$	
Salinity Index 2 (SI2)	$\sqrt{G^2 + R^2 + NIR^2}$	(Douaoui et al., 2006)
Salinity Index 3 (SI3)	$\sqrt{G^2 + R^2}$	
Salinity Index (S1)	B/R	
Salinity Index (S2)	$(B - R)/(B + R)$	
Salinity Index (S3)	$(G \times R)/B$	(Abbas and Khan, 2007)
Salinity Index (S5)	$(B \times R)/G$	
Salinity Index (S6)	$(R \times NIR)/G$	

B: Blue band, G: green band, R: red band, NIR: Near infrared band.

L is a soil adjustment factor; and a, b and γ are the soil line parameters.

3.3.6 Calculation and Extraction of the Index Values

The Band Math function of the Environment for Visualizing Images (ENVI) 4.8 was used to compute the selected broadband indices. Separate enhanced images were obtained for each selected index. The spectral range of these estimated indices is summarized in Table 3.2.

Due to the spatial uncertainty that is associated with the accuracy of the images geo-referencing and the GPS, the sample points were not represented by a single pixel image. Therefore, a convolution low pass filter with a kernel size of 5×5 was applied to each classified image. This filter, known as a smoothing filter, removes high spatial frequency details and preserves the low frequency components (Lasaponara and Masini, 2012). This filter contains the same weights in each kernel and replaces the center pixel value with an average of the surrounding values.

Next, the spectral average values for the 4 sub-sample points were extracted from all of the enhanced images and the overall average values for the composite soil samples were computed. Finally, a Pearson correlation coefficient (R) was calculated between the EC estimated values using broadband indices and the actual EC ground measurement values in the R® software.

3.4 Results

3.4.1 EC Ground Measurements

Five salinity classes were established using the EC values based on the Food and Agriculture Organization (FAO) soil salinity classification system as follows: 1) very strongly saline, >16 dS/m; (2) strongly saline, 8-16 dS/m; (3) moderately saline, 4-8 dS/m; (4) slightly saline, 4-2 dS/m; and (5) non-saline, 0-2 dS/m (Abrol et al., 1988). Table 3.2 contains the EC ground measurement summary statistics of the total composite samples from the three sites. The EC values ranged from very strongly saline to non-saline. Overall, the very strongly saline class

(EC >16 dS/m) was dominant at all three sites and accounted for approximately 87.50, 60 and 67.35% of the total samples at sites "A", "B" and "C" respectively (Figure 3.3).

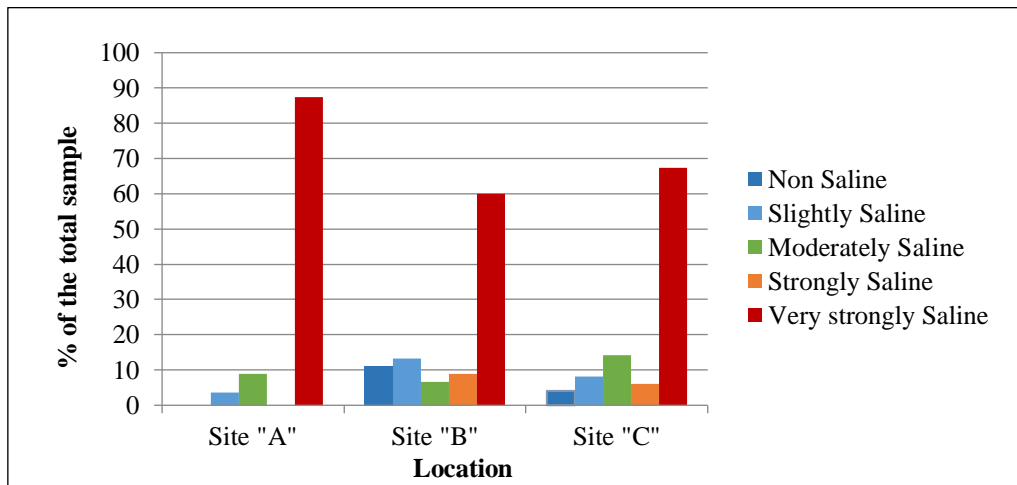


Figure 3.3 Distribution of soil salinity classes in the three study sites

3.4.2 Soil spectral reflectance

The spectral reflectance of soil samples were examined over the visible and NIR wavelength ranges. Spectral reflectance is increased as soil salinity increased. Figure 3.4 illustrates that moderately saline soil shows higher reflectance than non-saline soil, whereas strongly saline soil presents higher spectral response than moderately saline soil. Overall, the strongly saline soil reflects the highest amount of radiation as compared to the other soil salinity levels.

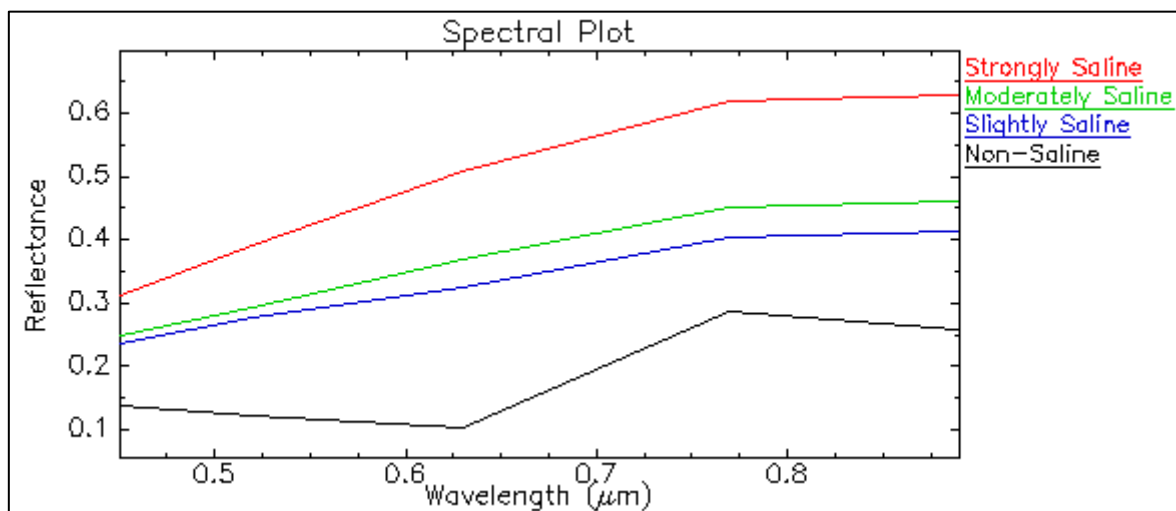


Figure 3.4 Spectral reflectance of different soil salinity classes selected randomly from the data sets

3.4.3 The Broadband Indices

Table 3.3 shows the relationships between the selected broadband indices and the EC. For site "A", the correlation analyses showed that a significant positive relationship occurred between EC and the NDSI and SI-T indices ($p < 0.001$). However, all other indices were not significant. For site "B", the correlations between EC and SAVI, NDSI and SI-T were slightly higher. In addition, a significant negative correlation ($p < 0.001$) occurred between EC and the S_1 and S_2 salinity indices. Moreover, the analyses for site "C" revealed that a significant negative correlation ($p < 0.001$) occurred between the SAVI, S_1 and S_2 indices, and a highly significant positive correlation ($p < 0.001$) occurred between the SI-TN, NDSI and EC. Generally, the correlation coefficients for site "C" were greater than those for sites "A" and "B". Among all of the assessed indices, S_6 was the poorest predictor of salinity at all sites. Figure 3.5 illustrates some of the studied indices.

Table 3.2 Descriptive statistics of the actual EC and the broadband indices

Site		EC (dS/m)	SAVI	NDSI	BI	SI	SI1	SI2	SI3	S1	S2	S3	S5	S6	SI-T
A (Al-Uyoun) (N=56)	Mean	75.26	-0.03	0.02	189.14	115.93	137.35	234.23	194.24	0.72	-0.16	191.77	97.3	129.24	104.39
	SD	54.61	0.04	0.02	15.54	9.12	11.93	18.97	16.85	0.02	0.02	21.17	7.53	11.32	4.67
	Min.	3.4	-0.06	-0.08	159.69	96.03	111.55	198.73	157.91	0.69	-0.18	146	80.19	106.57	85.3
	Max.	190.4	0.12	0.04	212.25	129.22	154.74	262.41	218.84	0.79	-0.12	222.55	108.22	145.64	108.46
B (Al-Bataliah) (N=44)	Mean	51.84	0.09	-0.06	148.97	89.6	103.1	184.26	146.32	0.82	-0.1	131.96	74.71	102.13	89.54
	SD	49.75	0.07	0.05	9.41	7.36	9.77	13.14	13.42	0.05	0.03	17.22	6.51	6.34	8.4
	Min.	1.43	0.01	-0.15	135.59	77.53	87.71	165.8	124.76	0.75	-0.14	104.1	63.54	93.26	73.75
	Max.	154.2	0.23	0	172.3	104.9	125.15	213.4	174.41	0.91	-0.05	167.02	87.87	118.35	99.33
C (Al-Umran) (N=49)	Mean	90.53	0.03	-0.02	180.99	107.79	126.95	221.94	179.6	0.74	-0.15	174.71	90.3	126.9	96.61
	SD	75.74	0.07	0.05	17.39	11.64	15.15	21.92	21.38	0.03	0.02	26.93	9.87	12.12	9.13
	Min.	1.62	-0.04	-0.12	157.94	92.5	107.11	196.98	151.69	0.68	-0.19	138.55	77.05	105.25	81.13
	Max.	202	0.16	0.03	217.41	130.9	157.1	267.98	222.18	0.8	-0.11	226.95	109.37	150.66	105.98

Table 3.3 Correlation coefficients between the actual EC values and the broadband indices

	Site	EC (dS/m)	Variables											
			SAVI	NDSI	BI	SI	SI1	SI2	SI3	S ₁	S ₂	S ₃	S ₅	S ₆
A (Al-Uyoun)	EC (dS/m)	-0.51 ^{ns}	0.51 ^{***}	0.10 ^{n_s}	0.21 ^{ns}	0.20 ^{ns}	0.14 ^{ns}	0.20 ^{ns}	-0.23 ^{ns}	-0.23 ^{ns}	0.20 ^{ns}	0.22 ^{ns}	0.02 ^{n_s}	0.51 ^{***}
B (Al-Bataliah)	EC (dS/m)	-0.67 ^{***}	0.67 ^{***}	0.24 ^{n_s}	0.44 ^{**}	0.45 ^{**}	0.26 ^{ns}	0.44 ^{**}	-0.59 ^{***}	-0.58 ^{***}	0.46 ^{**}	0.47 ^{**}	0.14 ^{n_s}	0.67 ^{***}
C (Al-Umran)	EC (dS/m)	-0.78 ^{***}	0.77 ^{***}	0.28 [*]	0.50 ^{***}	0.49 ^{***}	0.35 ^{**}	0.49 ^{***}	-0.59 ^{***}	-0.58 ^{***}	0.50 ^{***}	0.51 ^{***}	0.09 ^{n_s}	0.78 ^{***}

Significant: * $p < 0.05$; ** $p < 0.01$; *** $p < 0.001$; ns = not

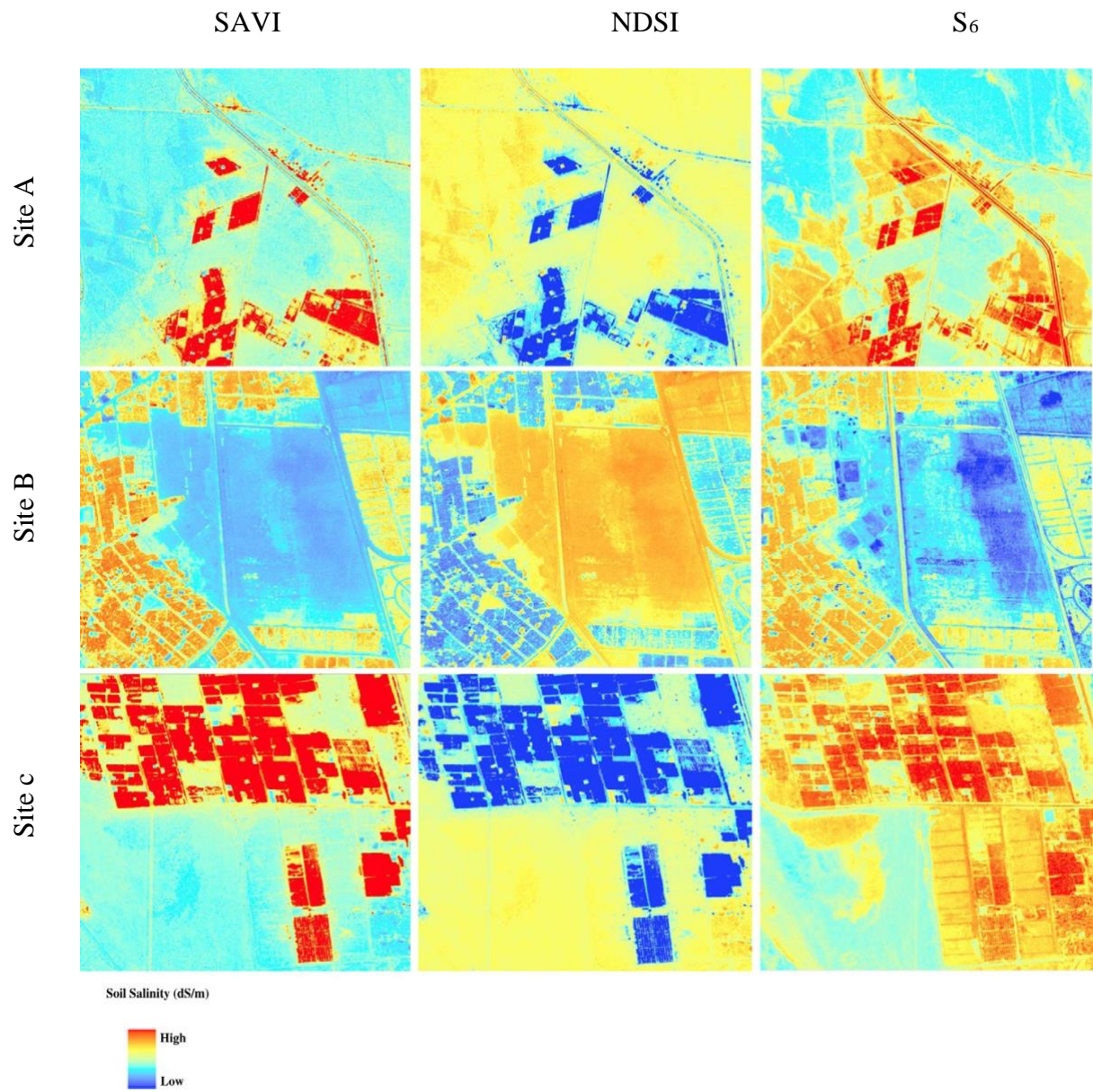


Figure 3.5 Outputs of selected indices

3.5 Discussion

3.5.1 Soil Salinity Analyses

Strongly saline soils with an EC value of more than 16 dS/m generally dominated the three selected Oasis sites. These soils mainly occurred on uncultivated or abandoned stretches of land that were locally referred to as sabkhas or (more precisely) inland sabkhas. "Sabkha" is an Arabic term for describing a saline and flat area that is subjected to high evaporation. These areas are often crusted with salts and occur on sand, silt or clay soils (Al-Amoudi, 1995). When flooded by rain or rising groundwater, these sites may temporarily turn into salt lakes. When these salt lakes dry, they produce the sabkha saline soil. Some sabkha surfaces in these study sites were covered by a thin crust or by puffy soils with a crust. Other surfaces consisted of gravel, which was associated with fine-grained sediments, dead plant matter and snail shells. These results suggest that swamps were previously present. These swamps dried up, which resulted in the death of the plants and snails. In addition, salt tolerant plants were scattered across some of these inland sabkhas. Thus, this finding indicates that the extensive very strongly saline soils that occupy these three sites were attributed to the abundance of inland saline sabkha soils on these uncultivated lands in combination with the high evaporation rates and the low rainfall in the area.

The lower observed salinity on cultivated lands may occur because the cultivated lands are subjected to leaching. Nevertheless, there were pronounced salinity differences occurred between the three sites on cultivated lands. These differences were potentially caused by terrain topography diversity, soil type and structure, poor drainage and irrigation water quality.

3.5.2 Soil Spectral Reflectance

Within the visible and NIR range, the samples represented in Figure 3.6 show a good distinction between the different salinity classes from the IKONOS data. In general, as shown in Figure 3.6 and as Rao et al. (1995), Karavanova et al. (2001), Schmid et al. (2008) and Bouaziz et al. (2011b) revealed, reflectance in the visible and NIR regions of the spectrum increases with increasing quantity of salts at the terrain surface. According to the investigated samples in this study, strongly saline soil shows a higher spectral response in the visible and NIR range compared to the other salinity levels. The amount of salt crystal formation on the surface of the strongly saline soil contributes directly to this high surface spectral reflectance. This finding is consistent with those of Everitt (1988), Abdel-Hamid and Shrestha (1992), and Setia et al. (2011) who found that well developed saline efflorescence and crusts are associated with high reflectance in the visible and NIR spectra. On the other hand, the good structure and high organic matter are most likely to account for the decrease of the spectral reflectance of the non-saline soil; therefore, this result is supported by those of Bannari et al. (2008).

Besides, in this study, saline soil of a dry, smooth and light salt crust surface showed higher spectral reflectance in the visible region of the spectral (especially red) band, in contrast to saline soil characterized by wet, coarse and dark puffy salt crust exhibiting a decrease in spectral reflectance in this band (Figure 3.6). These findings are in agreement with those of Schmid et al. (2008) and Fallah Shamsi et al. (2012) and confirm the fact that saline soil reflectance results from spectral properties such as presence of salt crust, roughness, color and moisture content, which have a combined effect on the amount of reflectance.

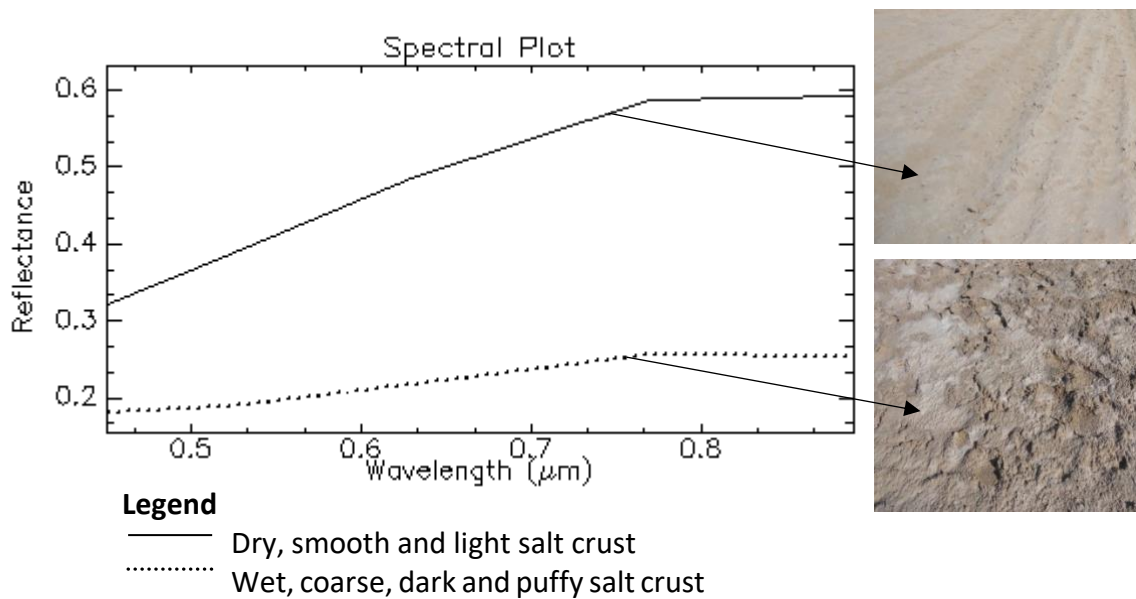


Figure 3.6 Influence of moisture content, salt quantity, colour and surface roughness on the reflectance of saline

3.5.3 Relationships between Soil Salinity and Broadband Indices

The correlation analysis indicated that the relationships between soil salinity and the selected broadband indices were different between the three sites. At site "A", NDSI and SI-T were the only useful soil indices. However, in some studies, significant correlations between soil salinity and other soil salinity indices were observed (Douaoui et al., 2006; Abbas and Khan, 2007; Bouaziz et al., 2011b; Noroozi et al., 2012). The good performance of the NDSI and SI-T indices most likely resulted from the red and NIR bands that were used to retrieve the soil salinity patterns and features, such as the surface crust (Howari et al., 2002; Metternicht and Zinck, 2008a). The red and NIR spectral regions have been found to be relevant for the identification of soil minerals that are formed during salt stress and in crusts (Clark et al., 1990; Ben-Dor et al., 1999; Ben-Dor et al., 2002; Zhang et al., 2011). In addition, satisfactory results for assessing soil salinity at sites "B" and "C" could be achieved by using the NDSI and SI-T indices. These findings are supported by those of Tripathi et al. (1997) and Khan et al. (2005), who found that the NDSI and SI-T indices provided satisfactory results for determining

different salt concentrations on soil surfaces. However, the results of Bannari et al. (2008) indicated that the NDSI index was a poor indicator for salt concentrations.

In contrast, the SAVI vegetation index yielded poor results for assessing soil salinity at site "A". This finding suggested that the density of vegetation cover was insufficient for assessing soil salinity. This result agrees with the results obtained by Bouaziz et al. (2011b) and Fan et al. (2012), who found that SAVI, NDVI and EVI vegetation indices were poorly correlated with EC values due to insufficient density of vegetation cover, while the soil salinity indices were more strongly correlated with the EC values. However, the SAVI index performed very well and yielded good results for assessing soil salinity at sites "B" and "C". This result likely occurred due to the lower sensitivity of the SAVI index to external factors, such as soil background, and the dense uniform vegetation cover that occurred at those sites. In most cases, the SAVI values at sites "B" and "C" decreased as the soil salinity increased. Similarly, Alhammadi and Glenn (2008) found that the SAVI values for date palm were high for low salinity levels and decreasing for areas of high salinity. These differences permitted the identification of salinity. Thus, these findings verify that SAVI is a promising vegetation index for assessing soil salinity in strongly saline areas that are dominated by halophytic plants with an open canopy structure (such as date palm). In addition, these results are supported by those of Alhammadi and Glenn (2008), but not by those of Zhang et al. (2011). Zhang et al. (2011) stated that SAVI is only suitable for assessing the salinity of low saline areas that are dominated by salt sensitive plants.

Accordingly, based on this study and on previous studies that assessed soil salinity with vegetation and soil salinity indices, it is clear that these indices are applied with varying degrees of success. Hence, it should be noted that, although vegetation and salinity indices are helpful for assessing soil salinity, no particular vegetation or soil salinity index could be used across

all environmental conditions with satisfactory results. These indices vary with different environmental conditions, soil types, and vegetation cover and density.

3.6 Conclusions

Very strongly saline soils are spread across the study area. The salinity of these soils varies significantly throughout the area. This variation is likely caused by several environmental and human-induced factors, including topography, poor drainage, poor irrigation water quality and mismanaged agricultural practices. Hence, additional research is needed to investigate the factors that enhance and cause soil salinity in this Oasis. This basic information may help decision-makers and land planners determine where to implement salinity action plans at a regional level to avoid further adverse environmental effects.

Overall, the SAVI, NDSI and SI-T indices that were extracted from the IKONOS satellite images were the most useful for assessing the soil salinity in the areas that were dominated by date palm. However, using these indices at other sites may produce variable results because their performance varies with different environmental conditions, soil, vegetation cover and density. Generally, this study indicated that it would be better to use the NDSI and SI-T indices in arid areas with low vegetation cover to assess soil salinity. In addition, vegetation indices, such as the SAVI index, would yield better results for assessing soil salinity in densely vegetated areas. Thus, before appropriate remote sensing-based indices are used for soil salinity assessment, the study site should be assessed to determine which index should be used. The amount of vegetation cover will impact which index will work best at a given site.

Although this study contains promising results for assessing soil salinity in this Oasis with broadband indices that were extracted from the IKONOS high-spatial resolution imageries, additional research is needed. For example, narrow-band indices derived from hyperspectral images should be investigated because they may yield a greater degree of accuracy. Besides,

modeling the variability of soil salinity and mapping its spatial distribution are becoming increasingly important in order to implement or support effective soil reclamation programs that minimize or prevent future increase in soil salinity. Thus, this study can be extended in the future by developing predictive models for soil salinity based on remote sensing indicators and regression techniques.

Acknowledgements

The authors would like to thank the Space Research Institute at the King Abdul-Aziz City for Sciences and Technology for providing the IKONOS satellite images.

**Higher Degree Research Thesis by Publication
University of New England**

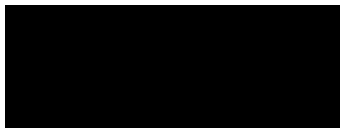
STATEMENT OF ORIGINALITY

We, the Research Master/PhD candidate and the candidate's Principal Supervisor, certify that the following text, figures and diagrams are the candidate's original work.

Type of work	Page number/s
Figure 3.1	43
Figure 3.2	43
Figure 3.3	46
Figure 3.4	46
Figure 3.5	49
Figure 3.6	52

Name of Candidate: Amal Allbed

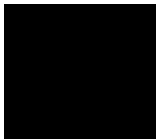
Name/title of Principal Supervisor: Professor Lalit Kumar



Candidate

20 June 2018

Date



Principal Supervisor

20 June 2018

Date

**Higher Degree Research Thesis by Publication
University of New England**

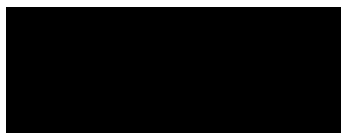
STATEMENT OF AUTHORS' CONTRIBUTION

We, the Research Master/PhD candidate and the candidate's Principal Supervisor, certify that all co-authors have consented to their work being included in the thesis and they have accepted the candidate's contribution as indicated in the *Statement of Originality*.

	Author's Name (please print clearly)	% of contribution
Candidate	Amal Allbed	80
Other Authors	Lalit Kumar	15
	Yousef Y. Aldakheel	5

Name of Candidate: Amal Allbed

Name/title of Principal Supervisor: Professor Lalit Kumar



Candidate

20 June 2018

Date



Principal Supervisor

20 June 2018

Date

Chapter 4 Mapping and Modelling Spatial Variation in Soil Salinity in the Al Hassa Oasis Based on Remote Sensing Indicators and Regression Techniques

This chapter has been published as:

Allbed, A., Kumar, L., Sinha, P. (2014). Mapping and modelling spatial variation in soil salinity in the Al Hassa Oasis based on remote sensing indicators and regression techniques. *Remote Sensing*, 6: 1137-1157; doi: 10.3390/rs6021137.

4.1 Abstract

Soil salinity is one of the most damaging environmental problems worldwide, especially in arid and semi-arid regions. An integrated approach using remote sensing in addition to various statistical methods has shown success for developing soil salinity prediction models. The aim of this study was to develop statistical regression models based on remotely sensed indicators to predict and map spatial variation in soil salinity in the Al Hassa Oasis. Different spectral indices were calculated from original bands of IKONOS images. Statistical correlation between field measurements of Electrical Conductivity (EC), spectral indices and IKONOS original bands showed that the Salinity Index (SI) and red band (band 3) had the highest correlation with EC. Combining these two remotely sensed variables into one model yielded the best fit with $R^2 = 0.65$. The results revealed that the high performance of this combined model is attributed to: i) the spatial resolution of the images; ii) the great potential of the enhanced images, derived from SI, by enhancing and delineating the spatial variation of soil salinity; and iii) the superiority of band 3 in retrieving soil salinity features and patterns, which was explained by the high reflectance of the smooth and bright surface crust, and the low reflectance of the coarse dark puffy crust. Soil salinity maps generated using the selected model showed that strongly saline soils (>16 dS/m) with variable spatial distribution were the dominant class over the study area. The spatial variability of this class over the investigated areas was attributed to a variety of factors, including soil factors, management related factors and climate factors. The results demonstrate that modelling and mapping spatial variation in soil salinity based on regression analysis and remote sensing data is a promising approach as it facilitates timely detection with a low-cost procedure, and allows decision makers to decide what necessary action should be taken in the early stages to prevent soil salinity from becoming prevalent, sustaining agricultural lands and natural ecosystems.

Keywords: Soil salinity, Electrical conductivity, Remote sensing, Salinity index, Regression analysis.

4.2 Introduction

Soil salinity refers to surface or near-surface accumulation of salts (Tanji, 2004). It is a worldwide environmental problem that mainly occurs in arid and semiarid regions and causes soil degradation (Jordán et al., 2004). The spatial variability of soil salinity over the landscape is highly sensitive and controlled by a variety of factors. These factors include soil factors (parent material, permeability, water table depth, groundwater quality and topography), management factors (irrigation and drainage) and climatic factors (rainfall and humidity) (Douaik et al., 2008). The characterization of soil salinity is generally done by measuring the electric conductivity (EC) in a saturated soil paste or in aqueous extracts with different soil/water ratios and using a spectrometer (Ben-Dor et al., 2008a; Goldshleger et al., 2013). To elaborate detailed maps, density of soil samples using the previous technique is required, through an extensive design, which makes mapping time consuming and expensive.

In recent decades, there has been a widespread application of remote sensing data to map soil salinity either directly from bare soil or indirectly from vegetation in a real time and cost effective manner at various scales (Metternicht and Zinck, 2008a). Besides, assessing soil salinity spatial modelling, which is the utilization of numerical equations to simulate and predict real phenomena and processes, has followed several approaches. The approaches used range from artificial neural network (Patel et al., 2002; Farifteh et al., 2007; Fethi et al., 2010; Akramkhanov and Vlek, 2012), to classification and regression tree (Tóth et al., 2002; Taghizadeh-Mehrjardi et al., 2014), to fuzzy logic (Malins and Metternicht, 2006), to generalized bayesian analysis (Douaik et al., 2004), to geostatistics (e.g., Kriging, CoKriging and regression kriging) (Triantafylis et al., 2001; Douaoui et al., 2006; Tajgardan et al., 2010;

Eldeiry and García, 2011) and statistical analysis (e.g. regression, ordinary least squares) (Douaoui et al., 2006; Eldeiry and Garcia, 2008; Fethi et al., 2010; Fan et al., 2012; Judkins and Myint, 2012). An overview of these techniques and how they provide optimal results under certain circumstances is given in the review papers of McBratney et al. (2003) and Scull et al. (2003).

An integrated approach using remote sensing in addition to various statistical methods has great potential for developing soil prediction models. In the case of soil salinity, statistical analysis, in particular linear regression, has created a tremendous potential among other techniques for improvement in the way that soil salinity is modelled, because of its rapid, practical and cost-effective manner (Lesch et al., 1995; McBratney et al., 2003). A variety of statistical models based on remote sensing data has been developed and has revealed reasonable predictors of soil salinity in the literature (Eldeiry and Garcia, 2004; Douaoui et al., 2006; Fernandez-Buces et al., 2006; Shrestha, 2006; Wang et al., 2007; Mehrjardi et al., 2008; Weng et al., 2008a; Yonghua et al., 2008; Afework, 2009; Tajgardan et al., 2010; Judkins and Myint, 2012; Noroozi et al., 2012; Pakparvar et al., 2012; Shamsi et al., 2013). In Thailand, Shrestha (2006) developed several salinity prediction models containing spectral variables including Normalized Difference Vegetation Index (NDVI), Normalized Difference Salinity Index (NDSI), the eight original bands of Landsat Enhanced Thematic Mapper plus (Landsat ETM+) and soil properties. The results indicated that mid-infrared (band 7) and near-infrared (band 4) had the highest association with the measured EC. Combining these variables yielded salinity prediction models to infer soil salinity over a large area. In contrast, Mehrjardi et al. (2008) found that among the Landsat ETM+ bands 1, 2,3,4,5 and 7, band 3 (red band) had the highest correlation with EC, and based on that result, a regression model fitted to relate EC to band 3 and the exponential relation was found to be the best type of model.

A regression model based on image enhancement techniques (spectral indices, Principal Components Analysis (PCA) and Tasseled Cap Transformation (TCT)) have also been extensively used to predict soil salinity and to improve the characterized variability of salinity. For example, Tajgardan et al. (2007) combined Principal Components Analysis (PCA) techniques and regression analysis to predict and map soil salinity from data collected by the Advanced Spaceborne Thermal Emission and Reflection Radiometer (ASTER) at the north of the Aq-Qala Region in northern Iran. From this study, a suitable regression model was developed with electrical conductivity (EC) to predict and map soil salinity. Similarly, Afework (2009) built a reliable model to predict soil salinity in the Metehara sugarcane farms in Ethiopia by relating EC to the Normalized Difference Salinity Index (NDSI) using linear regression.

Other researchers found that incorporating satellite images spectral bands with enhanced images has great promise for soil salinity modeling and mapping. Bouaziz et al. (2011b) conducted a study to detect soil salinity based on the Moderate Resolution Imaging Spectroradiometer (MODIS) and a multiple linear regression. They found that incorporating Salinity Index SI2 with near-infrared (NIR) (band 3) into a statistical model allowed researchers to gain great insight into the spatial detection of the spread of soil salinity. Recently, Judkins and Myint (2012) found that Landsat band 7, Transformed Normalized Vegetation Index (TNDVI) and Tasseled Cap 3 and 5, derived from TCT, provided high correlation to the variation in soil salinity. Combining these spectral variables into a multiple linear regression model enabled them to predict and map soil salinity surface variation levels efficiently.

Most of the reviewed studies and others found in the literature modelled soil salinity using statistical analysis and multispectral images with moderate spatial resolution (e.g. Landsat, MODIS, etc.), while only in limited studies multispectral high spatial resolution images such as IKONOS were used (Eldeiry and Garcia, 2008). Moreover, several studies have been

undertaken for mapping and modelling soil salinity over vegetation species other than date palms and so far a limited study has been undertaken to map soil salinity in a primarily date palm region. One such region is Al Hassa Oasis in the eastern province of Saudi Arabia which is the most productive date palm (*Phoenix dactylifera* L.) farming regions in Saudi Arabia and is seriously threatened by soil salinity. Although the date palm is highly tolerant of soil salinity, the growth and productivity of date palms in this Oasis are being negatively impacted by an increasing soil salinity problem (Al-Abdoulhadi et al., 2011). Thus, predicting the variability of soil salinity and mapping its spatial distribution are becoming increasingly important in order to implement or support effective soil reclamation programs that minimize or prevent future increases in soil salinity.

The overall aim of this study was to develop effective combined spectral-based statistical regression models using IKONOS high-resolution images to predict and map spatial variation in soil salinity in the Al Hassa Oasis, a region dominated by date palms.

4.3 Materials and Methods

4.3.1 Study Area

The Al Hassa Oasis is situated approximately 70 km inland of the gulf coast between a latitude of 25° 05' and 25° 40' N and a longitude of 49° 10' and 49° 55' E (Figure 4 1). This Oasis covers an area of approximately 20,000 ha and is at an altitude of approximately 130 to 160 m above sea level (Al-Dakheel and Massoud, 2006; Hussain et al., 2012). The Al Hassa Oasis is L-shaped and is actually composed of two separate oases (Al-Naeem, 2011). The main water sources include the Neogene groundwater aquifer and some free flowing springs that are distributed across the area (Al Tokhais and Rausch, 2008). The Oasis groundwater is primarily used for domestic, irrigation and industrial purposes. The Oasis is characterized by an arid climate with a high potential evaporation rate that goes above the annual average precipitation

of approximately 488 mm. The absolute ambient temperature exceeds 45 °C during the summer season (from June to August). During the winter (December to February), the temperature is between 2 and 22 °C. The study area covers six different soil types, which are Torripsamments, Torriorthents, Calciorthids, Salorthids, Gypsiorthids and Haplaquepts (Elprince, 1985; Al-Barrak, 1990). The particle size distribution reveals that soils are sandy loam in texture.

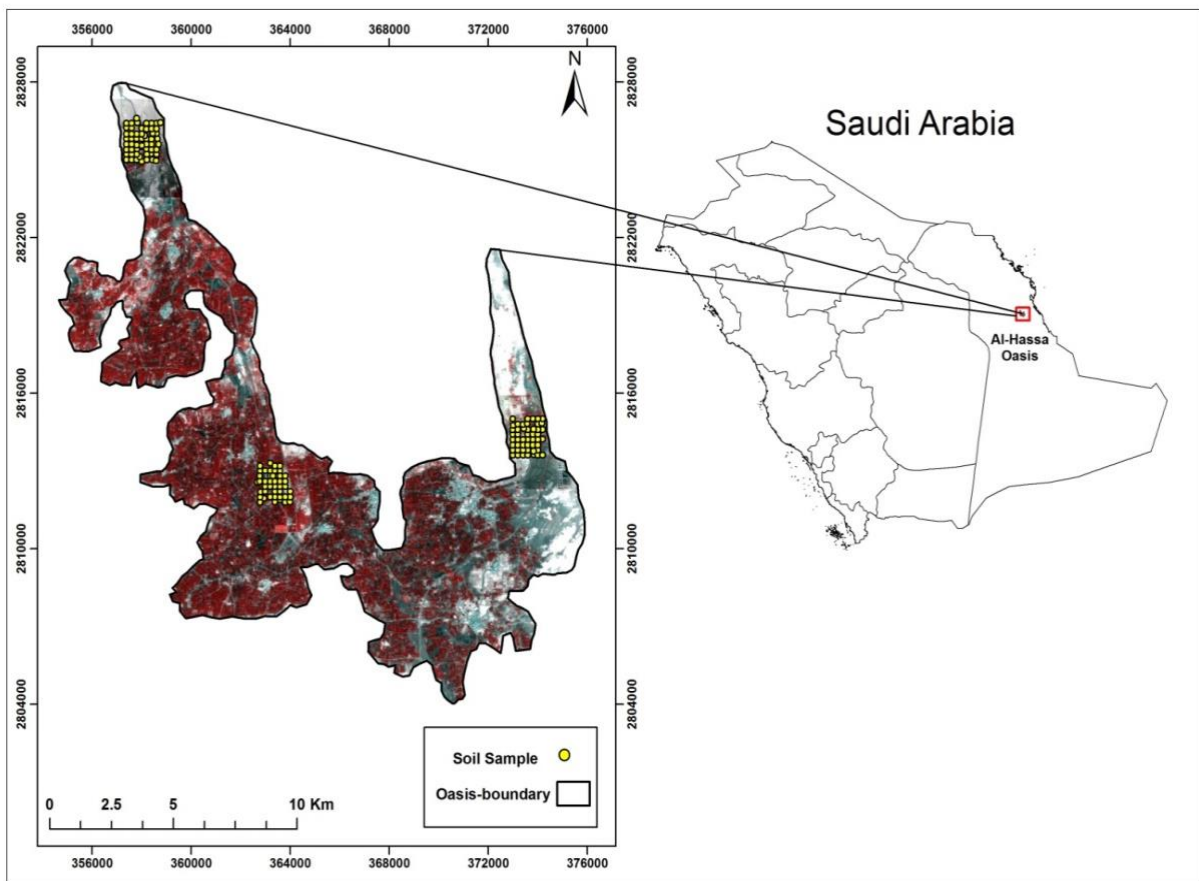


Figure 4.1 Study area with the location of the study sites

4.3.2 Field Sampling

Three sampling sites were selected based on the division of the Oasis and different amounts of vegetation. The first site was located in the northern part of the Oasis at Al-Uyoun city, which is characterised by low vegetation cover. The second site, in the middle of the Oasis at Al-Bataliah village, had high vegetation cover. The last set of samples was collected under

medium vegetation cover in the eastern Oasis, which is located in the town of Al-Umran (Figure 4.1).

Composite soil sampling was performed during January and February (the dry season) of 2012 following the sampling procedures of Bouaziz et al. (2011a). The exact coordinates of each composite sample were registered using a global positioning system (GPS) with an accuracy of ± 5 m. Each composite soil sample was comprised four core sub-samples that were collected at a distance of 20 m north, south, east and west of the centre sampling point. The sub-samples were collected from the surface horizon (0-20 cm) with a hand auger (10 cm diameter) and were crushed and mixed together to form one sample. A total of 149 composite soil samples were collected from the three defined sites. Soil salinity can be measured directly by measuring the EC in the field and remotely including the lab measurement. However, since the aim of this study is to establish a relationship between EC and satellite spectral band and extrapolate point information to generate a soil salinity map of study area, soil salinity direct measurement was performed by measuring the EC in the soil saturation extracts in the laboratory, as described by Richards (1954a).

4.3.3 Satellite Data Acquisition and Processing

High spatial resolution cloud-free IKONOS satellite images were used in this study and were acquired near the actual soil sampling date on April 20th, 2012. The IKONOS images include multispectral bands (blue, 0.40 - 0.52 μm ; green, 0.52 - 0.60 μm ; red, 0.63 - 0.69 μm ; near-infrared (NIR), 0.76 - 0.90 μm) and record the reflected or emitted radiation from the Earth's surface (Dial et al., 2003). The images were geo-rectified to a Universal Transverse Mercator (UTM) coordinate system using World Geodetic System (WGS) 1984 datum assigned to north UTM zone 39. Atmospheric correction was performed using the Dark-Object Subtraction

(DOS) technique (Chavez, 1996). All the remote sensing data processing was performed using the Environment for Visualizing Images (ENVI) version 4.8 software.

4.3.4 Data Analysis, Model Generation and Selection

Initially, the EC data was tested to establish whether it conformed to a normal distribution. The normality test exhibited that EC data had positive-skewed frequency distributions, thus Box-Cox transformation was carried out to improve sample symmetry and to stabilise the spread. As part of the model generation process, various spectral soil salinity indices were tested for assessing and enhancing the variations in surface soil salinity. Out of all indices tested, the Salinity Index (SI) (Equation (4.1)), which has been proposed by Tripathi et al. (1997), was used to create enhanced images for soil salinity in this study due to its very highly significant correlation with EC. To ascertain the spatial location of the soil samples, a convolution low pass filter with a kernel size of 5×5 was applied to the enhanced images, then digital values were extracted at the location of sample points over those enhanced images.

$$\text{Salinity Index (SI)} = \frac{R}{\text{NIR}} \times 100 \quad (4.1)$$

where R is the red band and NIR is the near-infrared band of the IKONOS image.

Subsequently, Pearson Correlation analysis between the four bands (blue, green, red and near-infrared) and SI with EC were conducted to reveal the relationship between these variables and assess their efficiency in predicting soil salinity. The explanatory variables chosen were those showing the highest significant correlations with EC.

To build the regression model, samples were randomly split into two subsets. One subset was used for training (n=98), the other for testing purposes (n=51). Deciding which explanatory variables to include in the regression model is not always easy, and increasing the number of variables in a model may lead to an over-fit and provide poor prediction when used with a different data set (Royston and Sauerbrei, 2008). To overcome these issues, stepwise regression was used to determine the variables that best explained most of the variability of the dependent variable, which was EC. Once all the developed regression models were tested, models with i) a high R^2 , signifying a strongly linear relationship; ii) low standard errors of the model's variables; and iii) few variables with a p-value of < 0.05 , were selected for evaluation using the testing data. Consequently, the best performed regression model that met all the model selection and validation criteria was chosen and used to predict and map the spatial variation in soil salinity. All statistical analyses were undertaken in JMP[®]10 (JMP statistical discovery software from SAS), and significance levels set to $p < 0.05$.

4.3.5 Model Validation

The performance of the developed regression models that met the model selection criteria was quantified using the testing subset to ensure that they not only worked on one particular data set but also yielded an accurate result on different data sets. Two quantitative criteria between measured and predicted values were calculated (Table 4 1). R^2 values indicate the strength of the statistical linear relationship between measured and predicted soil salinity values, and Root Mean Square Error (RMSE) indicates absolute estimation errors (Moriassi et al., 2007). In addition to these criteria, histograms, normal probability plots and Shapiro–Wilk tests (W) were employed to assess whether or not the residuals present a normal distribution. If the W test is significant ($p < 0.05$) or highly significant ($p < 0.001$) then the distribution is non-normal (Field et al., 2012a).

Table 4.1 Statistical criteria for evaluating the regression model

Function name	Equation	Equation number
Coefficient of determination	$R^2 = \left[\frac{\sum_{i=1}^n (\chi_i - \bar{\chi})(\gamma_i - \bar{\gamma})}{\sqrt{\sum_{i=1}^n (\chi_i - \bar{\chi})^2 + \sum_{i=1}^n (\gamma_i - \bar{\gamma})^2}} \right]^2$	(2)
Root Mean Square Error	$RMSE = \sqrt{\frac{\sum_{i=1}^n (\chi_i - \gamma_i)^2}{n}}$	(3)

* χ_i and γ_i are measured and predicted values, respectively; $\bar{\chi}$ and $\bar{\gamma}$ represent the means of the measured and predicted values, respectively; n is the number of samples

4.4 Results

4.4.1 Data Analysis

The main statistical parameters for EC data are given in Table 4.2. According to the soil salinity classification of the Food and Agriculture Organization (FAO), EC values of the study area vary from very strongly saline (>16 dS/m) to non-saline (0-2 dS/m). The high Co-efficient of Variation (CV) of 85.39% confirms the variations of the EC values over the study area. About 73% of the total samples were classified as very strongly saline soil, signifying that this is the dominant soil salinity class. Correlation analysis showed a significant positive correlation ($p < 0.001$) between EC and remotely sensed data of the blue (B1), green (B2), red (B3) and SI respectively, but not with near-infrared (B4) (Table 4.3).

Table 4.2 Descriptive statistics of EC

	Mean	Max	Min	SD	CV (%)
EC	73.37	202	1.43	62.65	85.39

Max: Maximum; Min: Minimum; SD: Standard deviation; CV: Coefficient of variation

Table 4.3 Correlation coefficient between EC and remotely sensed data

Variables	B1	B2	B3	B4	SI
EC	0.41***	0.42***	0.45***	0.06 ^{ns}	0.70***

Significant: * $p < 0.05$; ** $p < 0.01$; *** $p < 0.001$; ns = not

4.4.2 Models Development and Valuations

Remotely sensed data with a significant correlation to EC were considered for developing the regression models. The developed regression models are shown in Figure 4.2 and their statistical results are summarized in Table 4.4, showing how well spatial variation in soil salinity can be predicted by applying the different developed regression models. All the developed regression models were highly significant; however, models 1, 2, 3, 4 and 9 were best able to predict soil salinity spatial variation as they met all the model selection criteria. Among these models, model 4, which combines SI with B3, provided the best fit overall. It had the highest R^2 , signifying a strongly linear relationship between estimated and predicted EC and indicated that 65% of the variance in the EC values could be explained by this model with relatively low standard errors for its variables at 29.99, 0.52 and 0.26 respectively. Each of these variables had significant p -values indicating a strong correlation with EC.

The validation results for the best regression models (1, 2, 3, 4 and 9) are shown in Figure 4.3. The results show that model 4 was most accurate whereas model 2 was the worst. Model 4 outperformed the other regression models with regard to the normality test of the residuals. Furthermore, the W test for model 4 upgraded to 0.98 with a non-significant p -value ($p < 0.05$), and the bell-shaped histogram indicates the normal distribution of the residuals. Furthermore, values of R^2 equaling 0.34 and RMSE of 39 dS/m indicate that this regression model had the best fit compared to the others. Values of R^2 of 0.28 and RMSE values of 42 dS/m for regression model 9 indicate that this model would not predict soil salinity with high accuracy using remotely sensed data. Thus, these statistical results reveal that regression model 4 met both the model selection and model evaluation criteria.

4.4.3 Spatial Variation in Soil Salinity Maps

Maps of the study areas generated using the selected model (model 4) are presented in Figure 4.4. In general, these maps show that most of the areas with very strongly saline soil (>16 dS/m) are non-vegetated, and areas with vegetation have soils with lower salinity levels, although still in the >16 dS/m class.

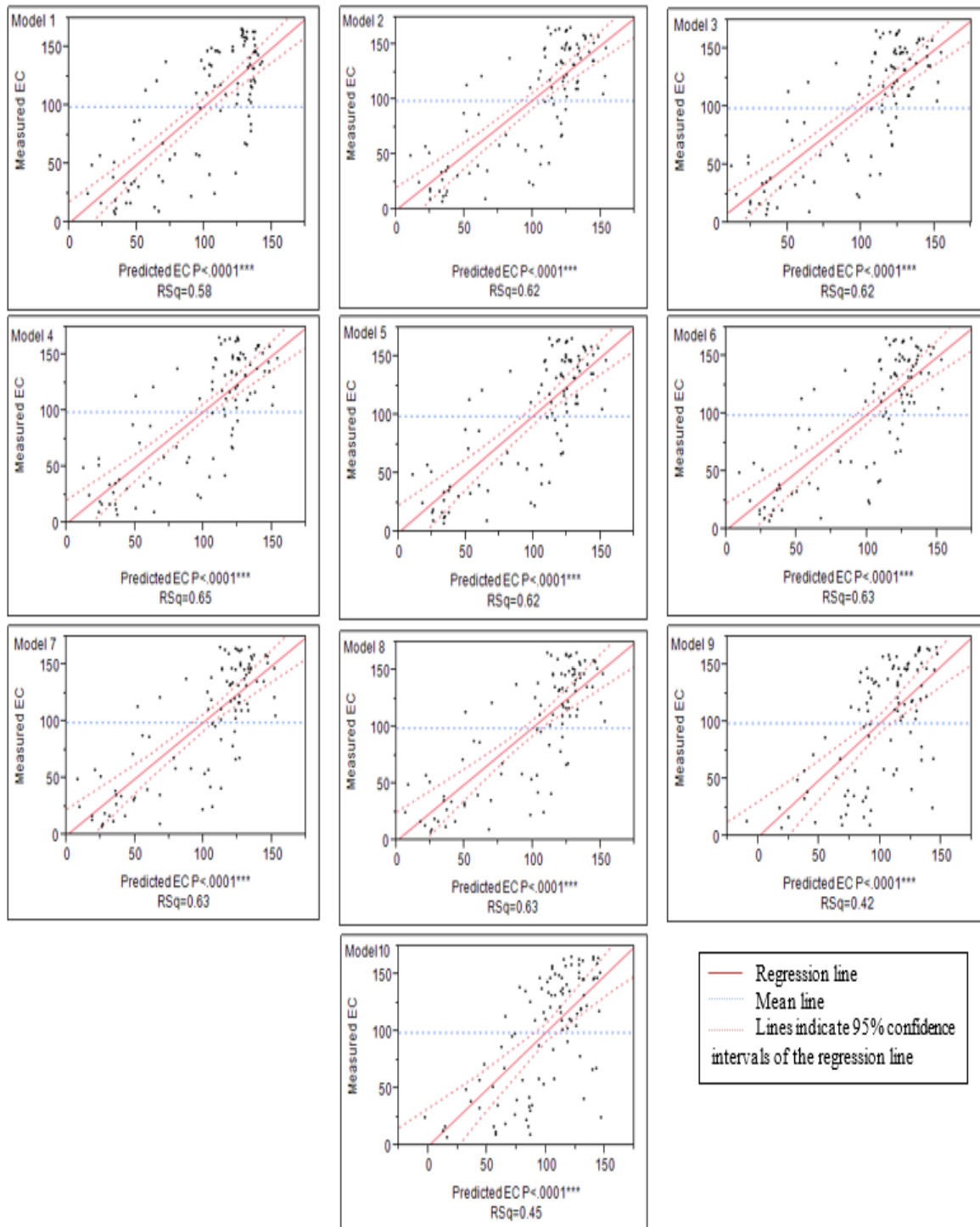


Figure 4.2 Scatter plots of predicted versus measured EC using the developed regression models

Table 4.4 Developed regression models to predict EC based on remotely sensed data

	Model Variable	Regression coefficient	Standard Error	p-value
1	Intercept	-239.49	29.82	<0.0001***
	SI	3.52	0.31	<0.0001***
		R = 0.76***	R ² = 0.58***	
2	Intercept	-205.25	29.95	<0.0001***
	SI	-1.77	0.511	0.0008***
	B1	4.83	0.48	<0.0001***
		R = 0.79***	R ² = 0.62***	
3	Intercept	-239.60	28.31	<0.0001***
	SI	4.83	0.48	<0.0001***
	B2	-1.011254	0.30	0.001**
		R = 0.79***	R ² = 0.62***	
4	Intercept	-269.13	29.99	<0.0001***
	SI	4.87	0.52	<0.0001***
	B3	-0.83	0.26	0.002**
		R = 0.81***	R ² = 0.65***	
5	Intercept	-193.18	83.48	0.02*
	SI	4.81	0.49	<0.0001***
	B1	-2.39	4.04	0.5559
	B2	0.36	2.35	0.8771
		R = 0.79***	R ² = 0.62***	
6	Intercept	-136.12	93.24	0.1476
	SI	4.64	0.54	<0.0001***
	B1	-3.59	2.38	0.1356
	B3	0.95	1.21	0.4355
		R = 0.79***	R ² = 0.63***	
7	Intercept	-115.70	84.33	0.1734
	SI	4.31	0.59	<0.0001***
	B2	-4.97	2.56	0.0551
	B3	3.49	2.24	0.1226
		R = 0.79***	R ² = 0.63***	
8	Intercept	-130.65	93.04	0.1636
	SI	4.23	0.62	<0.0001***
	B1	1.93	4.95	0.6983
	B2	-6.80	5.36	0.2077
	B3	4.12	2.78	0.1412
		R = 0.79***	R ² = 0.63***	
9	Intercept	320.95	74.94	<0.0001***
	B2	-14.25	2.78	<0.0001***
	B3	12.914	2.3	<0.0001***
		R = 0.65***	R ² = 0.42***	
10	Intercept	165.52	100.03	0.1013
	B1	13	5.69	0.02*
	B2	-25.44	5.61	<0.0001***
	B3	16.02	2.62	<0.0001***
		R = 0.67***	R ² = 0.45***	

Significant: *p < 0.05; **p < 0.01; ***p < 0.001; ns = not

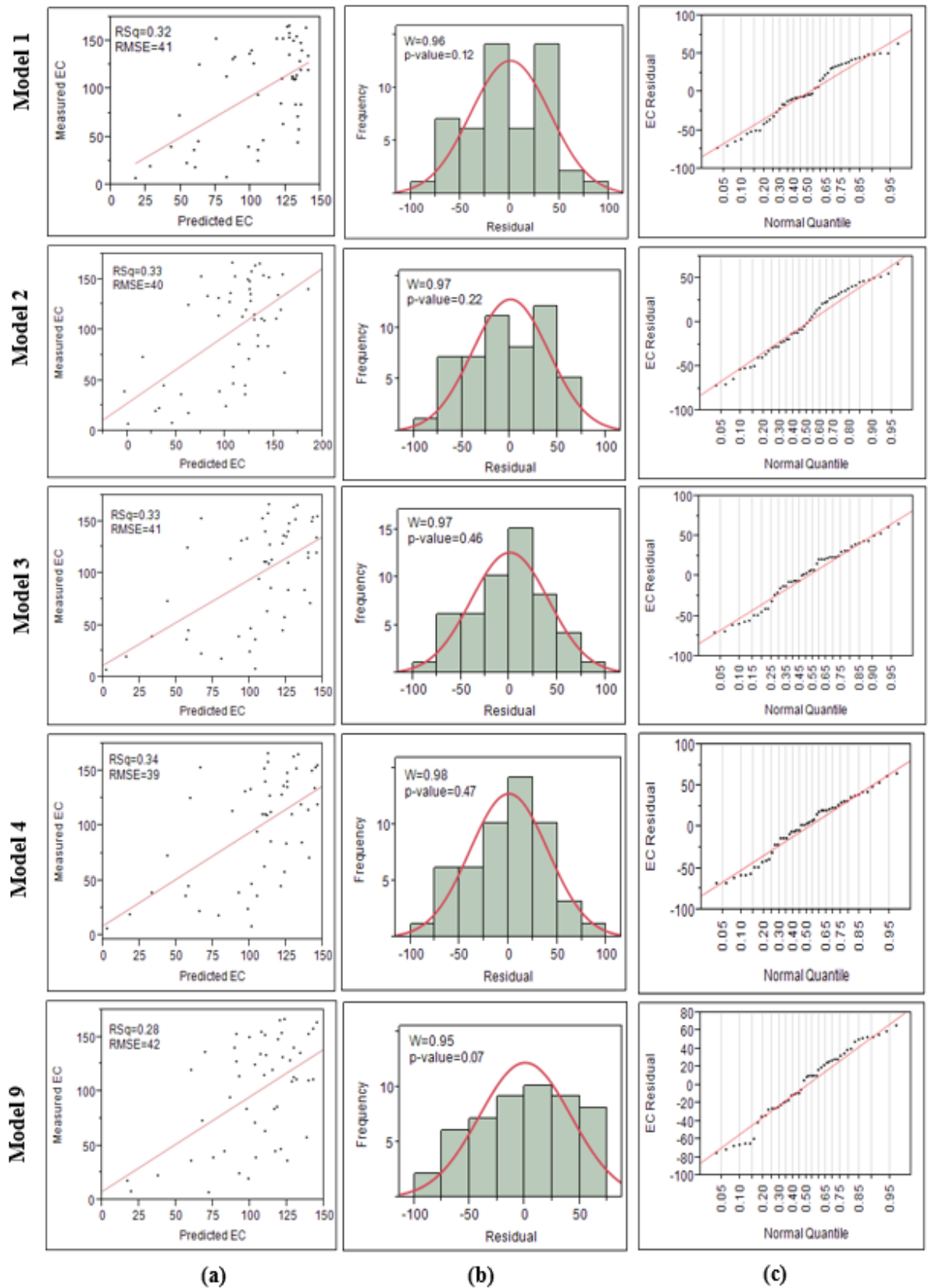


Figure 4.3 Validation of the developed regression models; a) scatterplots of predicted versus measured EC; b) histogram of residuals; c) normal plot of residuals

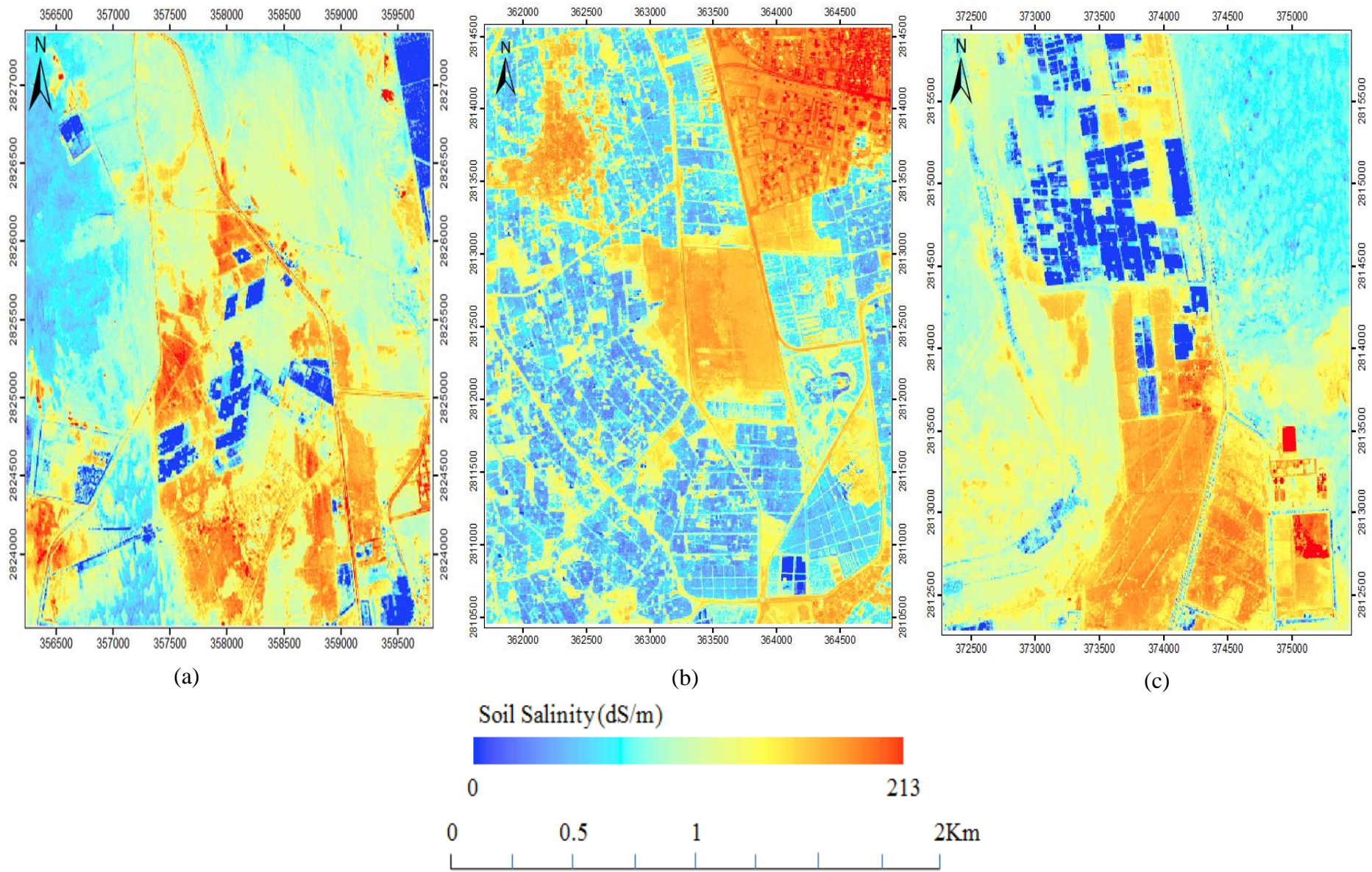


Figure 4.4 Soil salinity maps for different sites in the study region; (a) site one; (b) site two and (c) site three

4.5 Discussion

4.5.1 The Developed Regressions Models

The efficiency of the selected regression model to predict and map the spatial variation in soil salinity is shown by the good relationship ($R^2=0.65$) at the 99% probability level, RMSE of 39 dS/m and the normality of the residuals. This is in part due to the high spatial resolution of the IKONOS images. The selected model in this study showed superiority in the prediction power ($R^2=0.65$) of soil salinity over those reported by Shrestha (2006) ($R^2=0.23$) and recently by Shamsi et al. (2013) ($R^2=0.39$), which have been developed using different moderate spatial resolution satellite images. Moderate spatial resolution images, such as the Advanced Spaceborne Thermal Emission and Reflection Radiometer (ASTER), Moderate Resolution Imaging Spectroradiometer (MODIS) and Landsat, are economically priced or free, more accessible, and typically offer broader spatial coverage than more expensive high spatial resolution imagery. Nonetheless, differences in spatial resolution can have a high impact on predicting soil salinity. Our finding that the prediction of soil salinity based on IKONOS images yields better results than those based on moderate resolution images is in agreement with Eldeiry and Garcia (2008). Given this concern, it is important to take into account spatial resolution as one of the key factors to consider when using satellite imagery to infer soil salinity.

Moreover, the good performance of the selected model in this study is due to the enhanced images efficacy in highlighting information from soil salinity and suppressing the other details. Image enhancement is data processing that aims to increase the overall visual quality of an image or to enhance the visibility and interpretability of certain features of interest in it (Gao, 2008). Several studies have shown that image enhancement techniques consisting of spectral indices (e.g. NDVI, SI, NDSI, TNDVI) have a great potential in enhancing and delineating soil

salinity detail in an image (Khan et al., 2005; Fernandez-Buces et al., 2006; Odeh and Onus, 2008; Naumann et al., 2009; Lobell et al., 2010; Iqbal, 2011; Hamzeh et al., 2012a; Noroozi et al., 2012). For example, Tripathi et al. (1997) found and emphasized that identifying salt-affected soils based on the image enhancement method, represented by the salinity index, yields better results than individual bands due to its ability to enhance the saline patches by suppressing the vegetation. Recently, Shamsi et al. (2013) conducted a study to characterise soil salinity in the south-east of Fars Province, Iran, using remote sensing and statistical analysis, and found that using an image enhancement method (Salinity Index (SI)) reduced estimation errors and increased the model's efficiency.

Beside this, the superiority of the visible red band over the other bands in retrieving soil salinity has contributed to improving the regression model. This result is supported by those of Arasteh (2010) and Mariappan (2010) who found that the visible red band performs best among the Landsat ETM+ bands at characterizing the pattern and features of soil salinity due to its high correlation with EC ground measurements. Soil salinity spectral reflectance is affected by the physical–chemical properties of soil: quality and mineralogy of salt, together with soil moisture, colour and surface roughness (Metternicht and Zinck, 2008b). Salts influenced surface features are crusts without or with only a little evidence of salt; thick salt crusts and puffy structures. Salt causes variations in the surface roughness which induces variation in the soil spectral reflectance (Ben-Dor et al., 2008a; Goldshleger et al., 2012; Goldshleger et al., 2013). Most salt-affected soils can be identified by a white salt crust that will form on the soil surface; thus, these soils tend to increase spectral reflectance (Ben-Dor et al., 2003; Panah et al., 2008; De Jong et al., 2011). Crusted soil, which affects soil structure and reduces the soil infiltration rate (Agassi et al., 1985) is characterized with significant spectral changes due to the structural crust formation and colour (Ben-Dor et al., 2003). Salt crust at its inception (high infiltration rate) presents low spectral reflectance, whereas in intense salt crust soil the spectral

reflectance will be significantly higher (Ben-Dor et al., 2003). Besides, smooth crust surfaces have higher spectral reflectance than rougher crust surfaces (Ben-Dor et al., 2003; Metternicht and Zinck, 2003; Goldshleger et al., 2004; Elnaggar and Noller, 2010).

According to the investigated samples in this study, saline soils with a smooth and light salty crust surface show high spectral reflectance in the red band, in contrast saline soils characterized by coarse dark puffy surface crust exhibit a decrease in spectral reflectance (Figure 4.5). These findings are in agreement with the those of Metternicht and Zinck (1997), Schmid et al. (2008) and Shamsi et al. (2013), and confirm the fact that saline soil reflectance results from spectral properties such as the presence of salt crust, soil colour and moisture content, which have a combined effect on the amount of reflectance.

Thus, it is clear that a combination of spectral bands and image enhancement yield a better result than the actual band used for modelling and mapping soil salinity alone. This finding is consistent with those of Tajgardan et al. (2007), Eldeiry and Garcia (2008), Bouaziz et al. (2011b), Judkins and Myint (2012) and Noroozi et al. (2012), who found that this method of combining spectral bands with enhanced images in a single model is a promising tool for soil salinity detection and mapping. That is to say, the combination is the key, giving better results than either spectral band alone or image enhancement alone.

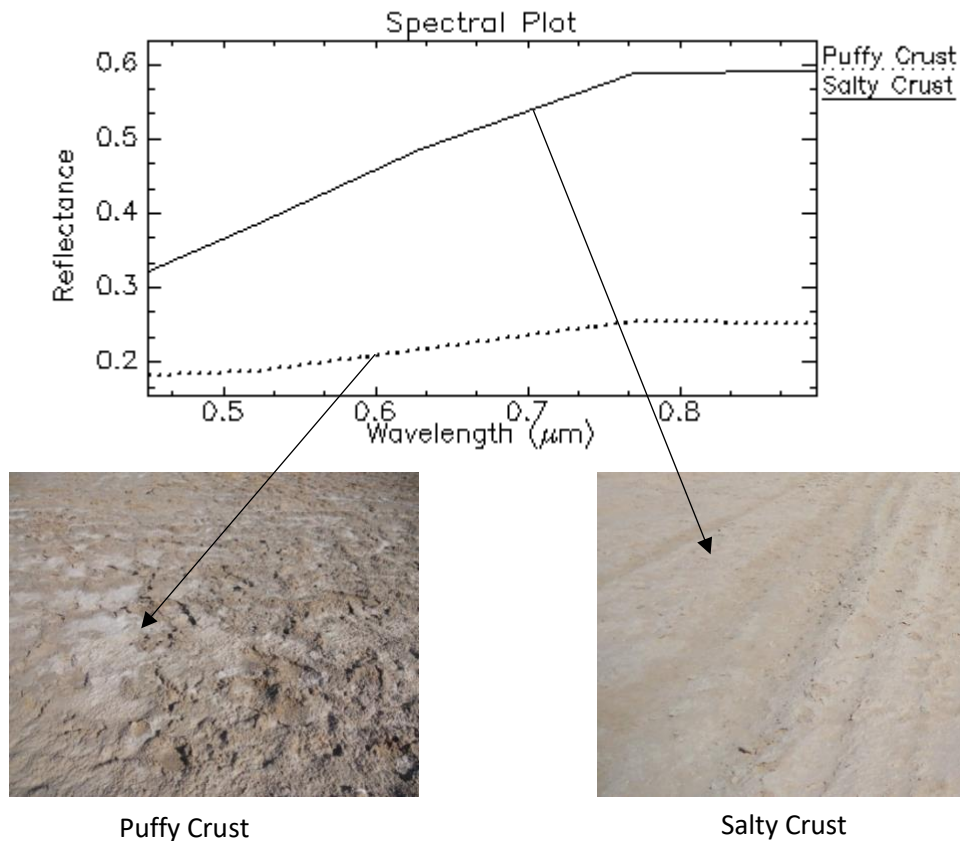


Figure 4.5 Spectral reflectance of saline soils differs due to surface roughness, crusting and colour

4.5.2 Mapping Spatial Variation in Soil Salinity

Factors causing soil salinity include inappropriate and excessive irrigation without an adequate drainage system, irrigation water quality, a rising water table, climate, rainfall history, local topography, soil composition and farming practices (Chhabra, 1996; Hillel, 1998; Sparks, 2003; Shi et al., 2007; Braimoh and Vlek, 2008). Therefore, increasing soil salinity at the surface is most likely to vary according to the distribution of these different factors across the landscape. For example, Bilgili (2013) found that the spatial distribution of saline soils in the Harran Plain, southeast Turkey, is likely due to inappropriate irrigation coupled with high evaporation and topographical factors.

In this study, soil salinity maps that were generated using the selected model showed large surface areas with very strongly saline soil (>16 dS/m). The spatial distribution in this soil

salinity class was variable over the investigated areas. Patches with strongly saline soil along the three sites were most pronounced in non-vegetated wet and dry areas. Wet areas, shown in red and orange colours in the maps (Figure 4), form due to a rising water table and are characterized by a moisture-filled soil (Keddy, 2010). The rising water table brings salt from deep in the soil up to the surface causing salt accumulation (Ashraf et al., 2009). On the other hand, dry lands, which are shown in a colour graduation from yellow to light blue, occurs when a saline water table comes close to the ground level and a high evaporation rate leaves salts at the soil surface (Jardine et al., 2007). Thus, these findings suggested that a rising water table and salt accumulation at the surface combined with a high evaporation rate are one of the most likely factors that have resulted in the spatial variation in soil salinity over these lands. Similar results in an arid region, Sultanate Oman, were found by Hussain et al. (2006).

On the other hand, vegetated areas occupy strongly saline soil but within lower salinity levels compared to the non-vegetated areas. The lower observed salinity levels on the vegetated areas may occur because vegetated areas are subjected to a leaching process which reduces salinity levels. In spite of this, there were pronounced salinity differences between the three sites over the vegetated areas. These differences were potentially caused by variation in topography, soil type and structure, poor drainage and irrigation water quality. All of these parameters are known to affect soil salinity distribution across the landscape (Thiruchelvam and Pathmarajah, 1999; Cetin and Kirda, 2003; Hussain et al., 2006; Zheng et al., 2009; Sakadevan and Nguyen, 2010). However, while irrigation water quality can be problematic, this can be overcome by proper irrigation management. Therefore, the observed salinity differences in the salinity levels on vegetated areas could be caused by different irrigation management practices, including irrigation scheduling. For example, instruments that measure and monitor soil moisture were not used for irrigation scheduling at any of the three study sites as farmers were not aware of them and/or lacked the required skills for use. In addition, many farmers cannot afford these

instruments and no extension services are available to encourage their use. Consequently, excessive water applications and poor timing result in various levels of salt build-up in these soils which adversely affect date palm. Several studies have found that soil salinity can cause significant effects on date palm growth and productivity, even though date palm is a high salt-tolerant crop (Hussein et al., 1993; Ramoliya and Pandey, 2003; Alhammadi and Glenn, 2008; Alhammadi and Edward, 2009). Recently, Al-Abdoulhadi et al. (2011) conducted a study to describe the effects of soil salinity on date palms. The results of their study revealed that salinity depressed plant growth and the biomass of date palms, and as the salinity increased the leaf length of the fronds was significantly reduced.

This study shows how regression analysis, coupled with high spatial resolution remote sensing images, could successfully predict and map spatial variation in soil salinity over an area vegetated mainly with date palms. Thus, the information presented here can help agricultural workers, scientists and engineers to manage soil salinity problems affecting the ecosystem. Additionally, the simplicity of this approach, with its satisfactory accuracy, can contribute greatly to soil salinity prediction and mapping, at lower costs than conventional approaches.

While, this study focuses on mapping and modelling soil salinity on a spatial variation basis at one point in time, further research requires investigating the temporal variation of soil salinity in this Oasis in order to assess the pattern of soil salinity change over time as soil salinity is a space-time variation phenomena. This timely detection of soil salinity, prediction and mapping of its severity and extent, will enable decision makers to decide what necessary actions should be taken, especially in areas of strongly saline soils, to protect the date palm outputs, sustain agricultural lands and natural ecosystems.

Besides, although this study contains promising results for modelling and mapping soil salinity based on regression analysis and IKONOS high spatial resolution images, the absence of the

thermal band, which has been found a useful tool in several soil salinity studies (Verma et al., 1994; Metternicht and Zinck, 1997; Alavipanah and Goossens, 2001), and the poor spectral resolution of the images, most likely limit the model capability. Thus, this study can be extended in the future by using hyperspectral images and investigating how this can increase the accuracy of spatial variation in similar modelling and mapping environments. Different studies have reported that hyperspectral images have a promising potential in the assessment and mapping of soil salinity (Ben-Dor et al., 2002; Lu et al., 2005; Farifteh et al., 2007; Weng et al., 2008b; Yonghua et al., 2008; Zhang et al., 2011; Hamzeh et al., 2012b). For example, Weng et al. (2008b) found that soil salinity can be predicted and mapped successfully based on Partial Least Squares Regression (PLSR) techniques with Hyperion hyperspectral data in a large area. More recently, in the Jezre'el Valley, northern Israel, Goldshleger et al. (2013), based on PLSR techniques, assessed the relationships between salinity in tomato plants and soil spectral reflectance obtained using a hyperspectral radiometer and found that the results promising. They concluded that a hyperspectral radiometer is useful for characterizing salinity in growing vegetation and assessing its salt quality. To the best of our knowledge, hyperspectral remote sensing data have never been used to model and map soil salinity in communities vegetated mainly with date palms in the remote sensing domain. Therefore, further research is needed to investigate the capability of hyperspectral remote sensing data in mapping and modelling soil salinity under such conditions.

4.6 Conclusion

The present study demonstrates that combining the IKONOS red band and the salinity index into a regression model offers a potentially quick and inexpensive method to map and model the spatial variation in soil salinity of communities vegetated mostly with date palm. The combination of these remotely sensed variables into one model were able to explain 65% of

the spatial variation in the soil salinity of the study area. The great capacity of this combined model over the other developed models is attributed to the enhanced images and the red band efficacy in highlighting information from soil salinity. The developed model's simplicity and acceptable degree of accuracy makes it a promising tool for continued use in soil salinity prediction. Thus, this model can be used by the decision makers in Al Hassa Oasis municipality and similar regions to implement or support effective soil reclamation programs that minimize or prevent future increases in soil salinity.

Although this study demonstrates that soil salinity mapping and modelling can be undertaken with good accuracy based on high spatial resolution multispectral images, further research is needed to focus on investigating the possibility of hyperspectral data in mapping and modelling soil salinity over areas dominated by date palm and investigating whether it can increase the accuracy of modelling and mapping process.

Acknowledgements

The authors would like to thank the Space Research Institute at the King Abdul-Aziz City for Sciences and Technology for providing the IKONOS satellite images.

**Higher Degree Research Thesis by Publication
University of New England**

STATEMENT OF ORIGINALITY

We, the Research Master/PhD candidate and the candidate's Principal Supervisor, certify that the following text, figures and diagrams are the candidate's original work.

Type of work	Page number/s
Figure 4.1	64
Figure 4.2	71
Figure 4.3	73
Figure 4.4	74
Figure 4.5	78

Name of Candidate: Amal Allbed


Name/title of Principal Supervisor: Professor Lalit Kumar



Candidate

20 June 2018

Date



Principal Supervisor

20 June 2018

Date

**Higher Degree Research Thesis by Publication
University of New England**

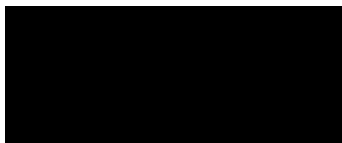
STATEMENT OF AUTHORS' CONTRIBUTION

We, the Research Master/PhD candidate and the candidate's Principal Supervisor, certify that all co-authors have consented to their work being included in the thesis and they have accepted the candidate's contribution as indicated in the *Statement of Originality*.

	Author's Name (please print clearly)	% of contribution
Candidate	Amal Allbed	80
Other Authors	Lalit Kumar	10
	Priyakant Sinha	10

Name of Candidate: Amal Allbed

Name/title of Principal Supervisor: Professor Lalit Kumar



Candidate

20 June 2018

Date



Principal Supervisor

20 June 2018

Date

Chapter 5 Soil Salinity and Vegetation Cover Change Detection from Multi-Temporal Remotely Sensed Imagery in Al Hassa Oasis in Saudi Arabia

This chapter has been published as:

Allbed, A., Kumar, L., Sinha, P (2017). Soil salinity and vegetation cover change detection from multi-temporal remotely sensed imagery in Al Hassa Oasis in Saudi Arabia. *Geocarto International*. doi: 10.1080/10106049.2017.1303090

5.1 Abstract

Detecting soil salinity changes and its impact on vegetation cover are necessary to understand the relationships between these changes in vegetation cover. This study aims to determine the changes in soil salinity and vegetation cover in Al Hassa Oasis over the past 28 years and investigates whether the salinity change causing the change in vegetation cover. Landsat time series data of years 1985, 2000 and 2013 were used to generate Normalized Difference Vegetation Index (NDVI) and Soil Salinity Index (SI) images, which were then used in image differencing to identify vegetation and salinity change/no-change for two periods. Soil salinity during 2000-2013 exhibits much higher increase compared to 1985-2000, while the vegetation cover declined to 6.31% for the same period. Additionally, highly significant ($p < 0.0001$) negative relationships found between the NDVI and SI differencing images, confirmed the potential long term linkage between the changes in soil salinity and vegetation cover.

Keywords: Soil salinity. Vegetation cover. Differencing image. Change detection. Al Hassa Oasis.

5.2 Introduction

Soil salinity represents a major threat in arid and semiarid regions (Valipour, 2014), and this has serious negative impacts on several aspects of agriculture and environmental sustainability. Likewise elsewhere, it inhibits plant growth and subsequent agricultural output, it also has similar impact in the Al Hassa Oasis in the eastern part of Saudi Arabia (Al-Taher, 1999; Pitman and Läuchli, 2002). This Oasis is a primarily date palm (*Phoenix dactylifera* L.) region and is regarded as one of the leading date palm producing regions in Saudi Arabia, providing an important source of income for the government and farmers (Jain et al., 2011; Al-Abdoulhadi et al., 2012). Although date palm is considered a fairly salt tolerant tree (some date palm varieties can adapt to very high levels of soil salinity (up to 12.8 dS/m, and in few cases up to 34 dS/m) (Ramoliya and Pandey, 2003; Alhammadi and Kurup, 2012), their growth and yield get impacted (Erskine et al., 2004). Long term experiments showed significant fruit yield reduction in the saline soil of 4.7 dS/m, and accumulation of salts over long periods can reduce the production and extinction rate of new leaves by 50% day and 30% day, respectively (Jaradat, 2016). This caused a substantial reduction in productivity growth, delayed ripening of fruit, and ultimately led to loss of salt-sensitive or vulnerable cultivars (Jaradat, 2016). In Al Hassa Oasis, the growth and productivity of date palm have negatively impacted by the dynamic process of soil salinity, which changes in space and time because of the effects of biological and physical, chemical processes operating at various scales and adversities (Metternicht and Zinck, 2008a). In this context, detecting and tracking the temporal change in soil salinity, especially on long-term basis, and determining its impacts on vegetation cover seems useful for understanding this process in the study area, which can aid management in preventing further salinization in order to maintain sustainable agriculture.

Detecting long term environmental changes required repeatable and consistent data which are available over many years. Multi-temporal Landsat data from different sensors (Multispectral

Scanner (MSS), Thematic Mapper (TM), Enhanced Thematic Mapper plus (ETM+), Operational Land Imager (OLI) with a spatial resolution of 30×30 m have become a major source of data for such applications, and have been widely applied in the soil salinity and vegetation cover change studies using different change detection techniques (e.g., Wang and Jia, 2012; Matinfar et al., 2013; Rahimi et al., 2015). The effective use of Landsat individual bands for soil salinity studies have been investigated by several researchers. Landsat's single bands, especially visible and Shortwave Infrared (SWIR) bands, have been widely acknowledged as a powerful tool in soil salinity detection. For example, TM bands 1-5, 7 was found good for identifying salt minerals by Menenti et al. (1986), while Madani (2005) found a robust relationship between the difference of TM SWIR band and near-infrared (NIR) band with soil salinity. Shrestha (2006) found SWIR of ETM+ to be superior in terms of closest correlation with soil salinity compared to the other bands. Bannari et al. (2008) also found SWIR has varying degrees of sensitivity to slight and moderate levels of soil salinity. In addition, a number of researchers have shown the potential of the image enhancement techniques to develop spectral indices for soil salinity studies (e.g., Fernandez-Buces et al., 2006; Lobell et al., 2010; Allbed et al., 2014a; Allbed et al., 2014b), and their findings justified the usefulness of indices in yielding improved results compared to original bands. For example, Al-Mulla and Al-Adawi (2009) applied different image enhancements to determine temporal change in soil salinity in Al-Rumais region of Oman. Tripathi et al. (1997) reported that using salinity index to detect salt-affected soils leads to better results compared to a single band because of its capability in enhancing the saline soils through repressing the vegetation. Al-Khaier (2003) found that salinity index composed of two SWIR bands allowed the detection and mapping of soil salinity effectively. Similarly, the application of the normalized difference ratio of SWIR bands enabled Nield et al. (2007) to map salt-affected soils efficiently. All these

studies implied that the spectral region between 1.5 and 2.5 nm is suitable to show the presence of salts in the soils on remote sensing data.

For vegetation cover, various studies have shown the usefulness of the Normalized Difference Vegetation Index (NDVI) for detecting changes in vegetation cover (e.g., Lunetta et al., 2006; Wang et al., 2009; Lhermitte et al., 2011). Among these techniques, NDVI image differencing has been one of the most popular change detection methods and proven to be a valuable approach for the detection of change in vegetation cover (e.g., Sinha and Kumar, 2012, 2013; Mancino et al., 2014). For example, Lyon et al. (1998) compared different vegetation indices in vegetation change detection with Landsat images. They established that the NDVI differencing techniques achieved the best results for vegetation change detection purposes. Besides, since saline soil is usually characterized by poorly vegetated areas, the potential of NDVI to demonstrate the inhibitory effects of soil salinity on vegetation cover has been recognized in many studies (e.g., Turhan et al., 2010; Platonov et al., 2013). Recently, Goto et al. (2015) found that area where vegetation is affected by salinization, a reduction in NDVI is observed. Also, Brunner et al. (2007) stated that NDVI has a potential to reveal salt stress as plant growth is inhibited by soil salinity.

The above studies represent a body of evidence that shows remote sensing techniques to be an important tool for change detection, particularly in soil salinity and vegetation cover applications. However, despite the fact that soil salinity has a negative threat on vegetation cover, most recent studies have looked at either vegetation cover change or soil salinity change in isolation, and limited studies have attempted to link vegetation cover change to soil salinity change especially in date palm dominated arid and semi-arid regions. The current study attempts to fill some of these gaps and aims to detect the temporal change in vegetation cover and soil salinity in the Al Hassa Oasis and determines whether there is any linkage of vegetation cover change to the change in soil salinity over a 28-year period. The study is important in

investigating the implications of these changes in agricultural output in the future in this Oasis. The results from this work can help farmers, scientists, agricultural workers and engineers in various decision making processes such as: (a) identifying priority areas for implementation of soil salinity plans to protect the vegetation cover, particularly date palm outputs; and (b) sustaining agricultural lands and avoiding further adverse environmental, social and economic effects.

5.3 Materials and Methods

5.3.1 Study Area

The Al Hassa Oasis is L-shaped area located between a latitude of 25° 05' and 25° 40' N and a longitude of 49° 10' and 49° 55' E (Figure 5.1), at an altitude of approximately 130 to 160 m above sea level (Hussain et al., 2012). The overall area is composed of two separate oases that are somewhat sloped to the north and east (Abderrahman, 1988; Citino, 2012). The Oasis is considered one of the important agricultural regions in Saudi Arabia covering an area of approximately 20,000 ha. The total cultivated area in this Oasis is approximately 7000 ha, where about 92% date palms of 40 different varieties are grown (Elprince et al., 1982; Al-Barrak, 1986). In the northern Oasis the date palms plantation covers an area of 1800 ha, whereas in the eastern Oasis (5200 ha) (Elprince et al., 1982). The climate in this area is typically arid with an ambient temperature exceeding 45°C during the summer and a high evaporation rate that exceeds the annual average precipitation of approximately 488 mm. The soil is sandy loam in texture and covers six taxonomic classes such as Gypsiorthids, Haplaquepts, Calciorthids, Torripsamments, Salorthids and Torriorthents (Al-Barrak, 1990).

The Neogene aquifer is the primary water source of agricultural and other uses. The Al Hassa Irrigation and Drainage Project (IDP) of about 1482 km comprises networks of concrete canals and drainage (Abderrahman, 1988) is the sources of irrigation water in the study area. The Al

Hassa Oasis is considered the largest and most important natural agricultural date palm Oasis in Saudi Arabia because of its contribution to the economic growth and fulfilling the local market's needs. However, date palms growth and productivity in this Oasis are being negatively impacted as many farms have been abandoned due to soil salinity problem.

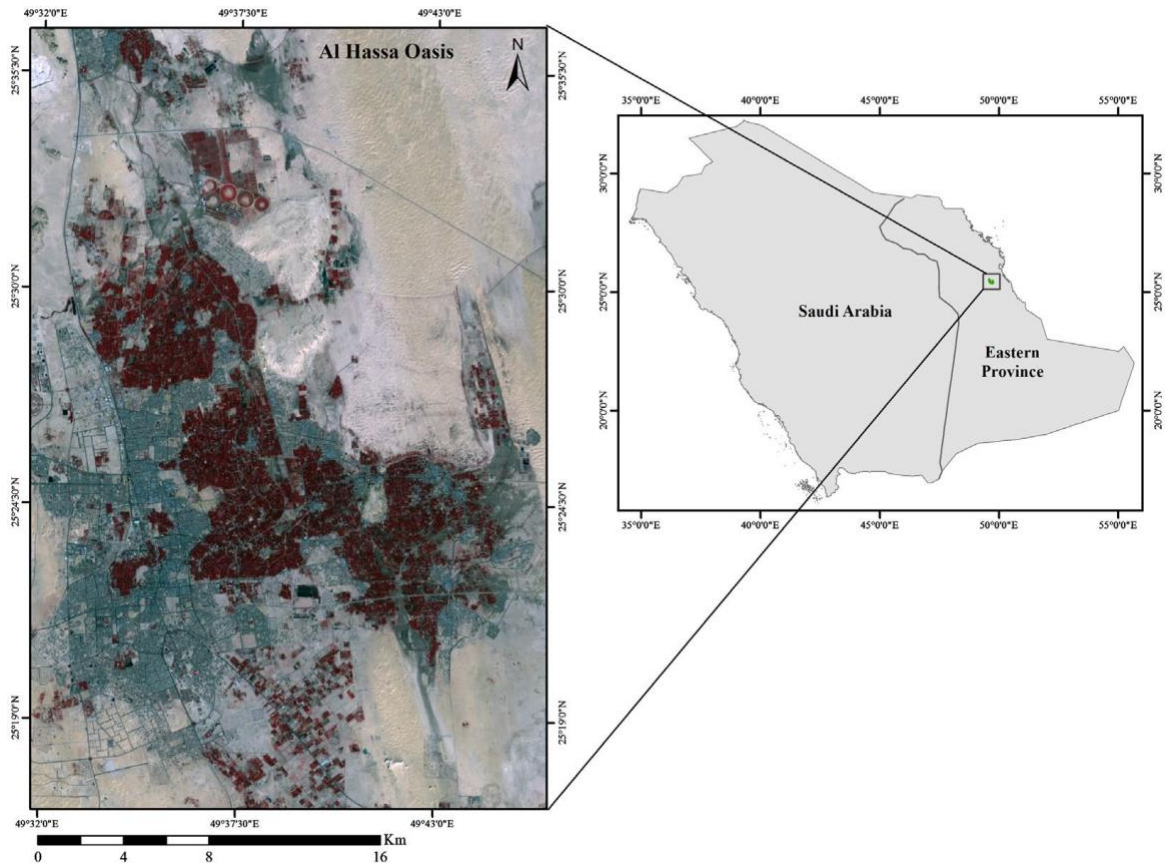


Figure 5.1 Standard False Color Composite (RGB: 432) of the year 2013 and location of Al Hassa Oasis in Saudi Arabia

5.3.2 Image Acquisition and Pre-processing

Three multi-temporal Landsat images in winter season were acquired for the study area (Figure 5.2). The 1985 (TM) and 2000 (ETM+) images were of January months, while Landsat 8 (OLI) of 2013 image was acquired in the December. Care was taken to acquire images of the same time period, and a month difference in the image acquisition dates was considered not posing much impact on this study results since the change detection was performed mainly for perennial vegetation. All remote sensing data pre-processing and digital image analysis were

performed by using environment for visualizing images (ENVI) version 4.8 software. Image pre-processing was carried out to make images from different dates as similar as possible so that they can be considered taken under the same environmental conditions (Hall et al., 1991). The images were georeferenced to a Universal Transverse Mercator (UTM) coordinate system using World Geodetic System (WGS) 1984 datum assigned to north UTM zone 39. A relative radiometric normalization was undertaken in order to make the temporal images acquired on different dates radiometrically similar by normalizing the difference in atmospheric conditions, solar irradiance condition and other properties (Yuan and Elvidge, 1996). Yang and Lo (2000) used a linear regression method to normalize two images captured on different dates by assuming image pixel values on date 1 to be a linear function of the values of the same pixel on date 2. For this purpose Landsat 8 OLI image was selected as the base image because of its highest sun angle. To develop accurate regression models normalization targets were selected from a varied range of dark and bright pixels. Then, a linear regression equation was applied to TM and ETM+ images to match a given pixel's DN with the corresponding pixel's DN on the base image. Finally, through the equation suggested by Chander et al. (2009) all the three multispectral image Digital Number (DN) values were converted to Top of Atmosphere (TOA) reflectance values. Dark-Object Subtraction (DOS) was also carried out for radiometric and atmospheric normalization (Canty et al., 2004; Vicente-Serrano et al., 2008). While the radiometric normalization process does not account for atmospheric interference, it provides a standardized measure directly comparable between images (Price, 1987).

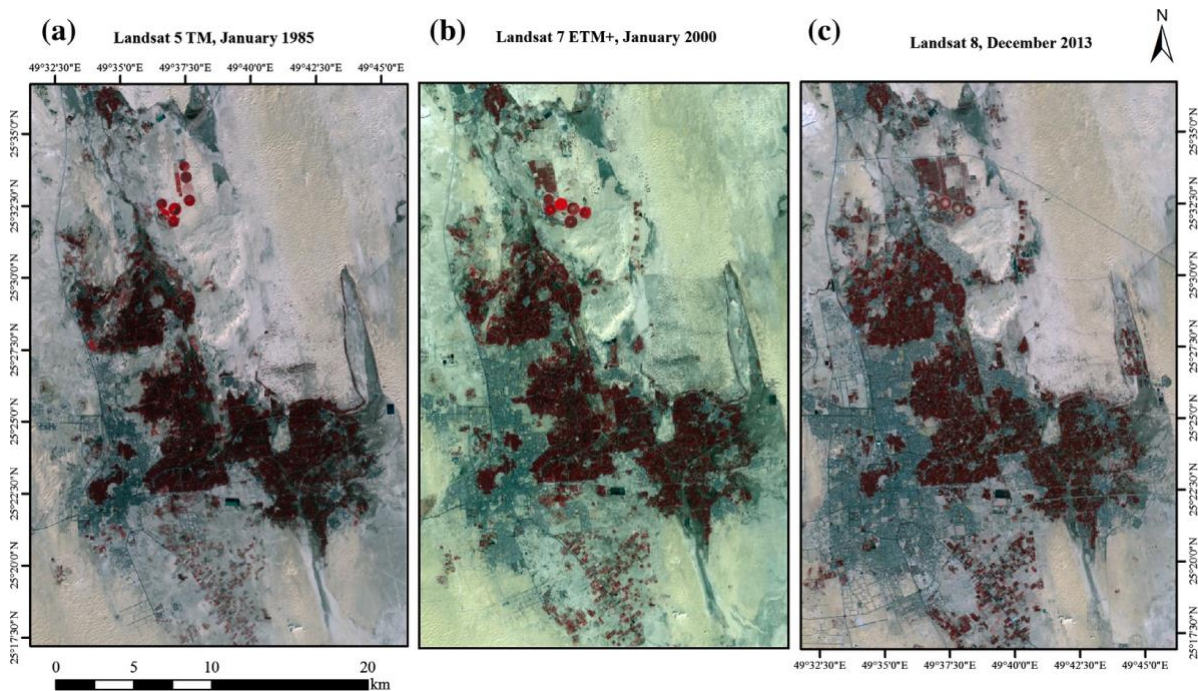


Figure 5.2 Multi-spectral satellite remote sensing data for Al Hassa Oasis: (a) Landsat 5 TM, January 1985, (b) Landsat 7 ETM+, January 2000, and (c) Landsat 8 OLI, December 2013

5.3.3 Image Processing

5.3.3.1 NDVI Difference Image

The Vegetation Index (VI), which is defined as the arithmetic combination of two or more bands related to the spectral characteristics of vegetation (Pallé and Rodríguez, 2010), has been widely used for detecting vegetation cover condition. Among existing VIs, NDVI is the most commonly used index because of its ratio properties that compensates large proportion of the noise caused by changing topography, sun angles and other atmospheric conditions. In this study, NDVIs for three change years (1985, 2000 and 2013) were computed as a normalized ratio of the reflectance in the red and NIR bands of the electromagnetic spectrum as $NDVI = (NIR - Red)/(NIR + Red)$. During photosynthesis, red light is absorbed by the green vegetation while NIR light is scattered due to the internal structure of the leaves, making these two spectral regions ideal for NDVI calculation (Tucker, 1979). Also, in these two spectral bands, the contrast among vegetation and soil is at a maximum. NDVI values range from -1 to $+1$. NDVI of healthy vegetation is normally tend to high positive values (0.3 to 0.9), depending upon the

vegetation greenness. Soils generally exhibit a NIR reflectance somewhat higher than the red, therefore tend to generate slightly small positive NDVI values (0.1 to 0.2) (Adams and Gillespie, 2006).

Image differencing technique, which is a process of pixel-by-pixel subtraction of different images bands in a time-series, is often used in research as an efficient method for land-cover change detection (Kleynhans et al., 2011; İlsever and Ünsalan, 2012; Sinha and Kumar, 2012, 2013). The brightness values of the difference images are approximately Gaussian, where no-change pixel brightness's are distributed around the mean, and change pixels are found in the two tails of the distribution (Wolter et al., 1995). The method is relatively simple and the resultant image is easy to interpret; however, defining appropriate threshold values is critical to distinguishing change areas from no-change areas. In this study, NDVI difference image (Δ NDVI) was created for the two change periods (1984-2000) and (2000-2013) by subtracting one date of NDVI value from those of the previous date as Δ NDVI = NDVI (t1) – NDVI (t2). The resulting image will have positive values indicating increasing proportions of green vegetation (change increase), whereas negative values indicate decreasing proportions of green vegetation (change decrease) and near zero values representing no change in vegetation (Coppin et al., 2004) between the two change periods.

5.3.3.2 Salinity Index (SI) Differencing Images

The usefulness of the spectral index for soil salinity assessment and mapping is widely highlighted in the literature as mentioned earlier (e.g., Abbas and Khan, 2007; Lobell et al., 2010; Allbed and Kumar, 2013; Allbed et al., 2014a; Elhag, 2016). The efficiency of different soil salinity indices derived from IKONOS high-spatial resolution imageries (1×1 m) for detecting and mapping soil salinity for a subsection of this study area has been reported in earlier work by the authors Allbed, Kumar and Aldakheel (2014a). The result showed that the Soil Adjusted Vegetation Index (SAVI), Normalized Differential Salinity Index (NDSI) and Salinity Index (SI) provided optimum results compared to the other indices investigated. In the absence of the IKONOS imageries for entire study area for selected change period, the SI based on the two SWIR Landsat bands was used in this study. These two bands have been found highly suited for soil salinity determination (e.g., Al-Khaier, 2003; Bannari et al., 2008; Meng et al., 2016). The SI generally attempts to enhance the spectral contribution of saline soils by minimizing and suppressing the spectra related to the vegetation. The SI for the 1985, 2000 and 2013 change years were calculated using the equation: $SI = (SWIR_1 - SWIR_2) / (SWIR_1 + SWIR_2)$. Soil salinity difference image (ΔSI) for the two change periods was created by subtracting one date of SI value from those of the previous date as: $\Delta SI = SI(t_1) - SI(t_2)$. On the resulting ΔSI image the positive values indicated increasing proportions of salinity, whereas negative values indicated decreasing proportions of salinity and near zero values represented no change in salinity between the two change periods.

5.3.4 Reference Data

In absence of historical reference data for changes in the study area, a visual interpretation method based on combination of primary colours (RGB) of similar brightness was used to develop reference data for change evaluation in this study (Cohen et al., 1998). The method is

based on the fact that any combination of primary colours of similar brightness makes a complementary colour as a change (Sader and Winne, 1992; Lillesand et al., 2014). Therefore, if NDVI images of three different dates are displayed in sequence as R, G and B, then an area with no-vegetation (cleared) on dates 1 and 2, but with vegetation (regrow) before date 3, can be seen as blue colour and so on. Thus, to develop the reference data for change pixels, NDVI of years 1985, 2000 and 2013 was displayed as red (R), green (G) and blue (B), respectively as RGB composite. The combination of three primary colours allowed to establish a three-date (1985–2000–2013) classification system (Table 5.1) to highlight changes. On this classification system, ‘Y’ represents presence of vegetation cover in a given area and ‘N’ for no-vegetation area. Therefore, on three date change system, the NYN code represents clearing of vegetation cover on or before 1985 (i.e., ‘N’), regrow between 1985 and 2000 (i.e., ‘Y’) and again cleared between 2000 and 2013 (i.e., ‘N’). Finally, the entire change and no-change data were grouped into the overall change and no-change classes. A total of 800 sample points were finalized as reference data for vegetation cover change/no-change classes for 1985-2000-2013 period. To determine the reference samples between two change periods (i.e., 1985-2000 and 2000-2013), the three-date reference points were re-grouped into two parts by merging similar classes on two successive dates into one. For example, code NNY was split as NN (i.e., no change between date 1 and date 2 as ‘no change’) and NY (i.e., no-vegetation cover to vegetation cover to as ‘positive change’ between dates 2 and 3). The details of this change detection classification system are explained in Table 5.1. Merged reference pixels were used for the evaluation of changes between 1985 and 2000 and also between 2000 and 2013, separately. Similar procedure was followed for soil salinity change identification error evaluations by generating separate 800 sample points from SI for 1985, 2000 and 2013, each displayed on RGB composite to create three-date change systems, and similar interpretations were made for identification of soil salinity changes between dates.

Table 5.1 Interpretation of the RGB–NDVI images

Additive colour	1985 (R)	2000 (G)	2013 (B)	Code	Interpretation of change	Change classes	
						1985-2000	2000-2013
Red	Y	N	N	YNN	Decrease between dates 1 and 2, no change between dates 2 and 3	negative change	no change
Green	N	Y	N	NYN	Increase between dates 1 and 2, decrease between dates 2 and 3	positive change	negative change
Blue	N	N	Y	NNY	No change between dates 1 and 2, increase between dates 2 and 3	no change	positive change
Yellow	Y	Y	N	YYN	No change between dates 1 and 2, decrease between dates 2 and 3	no change	negative change
Magenta	Y	N	Y	YNY	Decrease between dates 1 and 2, increase between dates 2 and 3	negative change	positive change
Cyan	N	Y	Y	NYY	Increase between dates 1 and 2, no change between dates 2 and 3	positive change	no change
Black	N	N	N	NNN	No change in no vegetation	no change	no change
Gray/white	Y	Y	Y	YYY	No change in high vegetation	no change	no change

5.3.5 Threshold Determination of the Differencing Images and Accuracy Evaluation

Ideally, the differences between feature brightness values are the places highlighting the changes, however, to quantify and separate change from no-change areas, a threshold value is required (Fung and LeDrew, 1988). The selection of an optimal threshold value is a key procedure to distinguish the change and no-change areas, as it affects the binary image classification accuracy and robustness of the final change detection accuracy. Several methods to determine the optimal threshold value have been proposed to separate changed from unchanged areas (e.g., Mas, 1999; Bruzzone and Prieto, 2000). The methods were found subjective and based on a trial-and-error process to select appropriate thresholds values. In this study, the mean and the standard deviation (SD) for each differencing image were computed and used in formula $\text{Mean} \pm C \times \text{SD}$ to determine the threshold values. Different thresholds (C -values) were tested, ranging from 0.2 to 3 with interval of 0.2 using reference data for change and no-change classes. At each threshold (C -value), a binary (change/no-change) classified image was generated which was then evaluated with respect to change/no-change accuracy using reference data collected for positive, negatives and no-change areas. For each

classified image an error matrix in terms of producer's error, user's error and overall accuracy was produced for the change/no-change classification accuracies assessment. A coefficient of agreement between classified images and reference data was also calculated using Kappa coefficient. It takes into account non-diagonal elements and has been recognized as a powerful method for analyzing a single error matrix and comparing different error matrices (Congalton, 1991; Smits et al., 1999). The Kappa coefficient (K) was computed as follows:

$$k = \frac{\sum_{i=1}^r x_{ii} - \sum_{i=1}^r (x_i + x + i)}{N^2 - \sum_{i=1}^r (x_i + x + i)} \quad (5.1)$$

where r is the number of rows in the matrix, x_{ii} is the number of observations in row i and column i , x_{i+} and x_{+i} are the marginal totals of row i and column i , respectively, and N is the total number of observations. Finally, the optimal threshold for differentiating change/no-change areas was determined based on highest kappa value or overall accuracy (OA) (e.g., Fung and LeDrew, 1988; Sinha and Kumar, 2012, 2013).

5.3.6 Soil salinity–Vegetation Cover Change Linkage

To understand the soil salinity-vegetation cover changes relationship, a Pearson correlation analysis was performed on random points ($n = 220$) selected from Δ NDVI and Δ SI images across the study area. The statistical analysis was performed using JMP[®]10 (JMP statistical discovery software from SAS), and the level of significance was set to $p < 0.05$.

5.4 Results

5.4.1 Vegetation Cover and Soil Salinity Change Detection

The difference images of the NDVI (Δ NDVI) and SI (Δ SI) is shown in Figure 5.3(a) and (b) for the change periods 1985-2000 and 2000-2013. The brighter pixels indicating positive change between the change period (i.e., increase in vegetation cover or salinity), while darker pixels representing negative change for the same period. Grey pixels represent no-change area.

Figure 5.4 shows the process of optimal threshold identification for the Δ NDVI and the Δ SI images for the change period 1985-2000 and 2000-2013, respectively using $\text{Mean} \pm C \times \text{SD}$. The optimal threshold value was determined by highest kappa value or OA determined at different C-values. The optimal C-value for Δ NDVI image of 1985-2000 and 2000-2013 periods, can be set to 1.8 and 2.0 respectively, as kappa or OA was the highest in the series at these values. The bi-directional change/no-change maps for Δ NDVI image of the two change periods based on optimal threshold values is presented in Figure 5.5(a). The figure demonstrates a noticeable change in vegetation cover over the 28 years mostly in the northern and southern regions of the study area between the two change periods. For 1985-2000 period, a decrease in vegetation cover was observed more towards the northern part of the study area, however, for 2000-2013 period, the vegetation decrease was more spread out with change concentration situated in north and central part of the study area. The increase in vegetation cover occurred throughout the study area for 1985-2000 period, while it was mostly towards northern and southern portion between 2000 and 2013 periods. Table 5.2 summarizes the area (ha) and percentage change in the NDVI values between years 1985-2000 and 2000-2013. Over 7% of the total study area experienced positive change (increasing vegetation cover) between 1985 and 2000, whereas nearly 3% of showed negative change, that is decline in vegetation cover for the same period. However, between the 2000 and 2013 period, the positive changes

decreased to 6.98%, while the negative changes increased to 6.30%, indicating much vegetation loss during this period in the study area.

The optimal C-value for ΔSI image of both 1985-2000 and 2000-2013 periods can be set at 1.6, as kappa or OA were the highest in the series at these values (Figure 5.4). The change/no-change maps for ΔSI image of the two change periods, based on the optimal threshold values are presented in Figure 5.5(b). The change detection results for soil salinity areas are presented in Table 5.2. Between 1985 and 2000 soil salinity increased by 3.76%, while for 2000-2013 period there was a much higher increase of soil salinity by 15.11% of the total area. On the other hand, the decline in soil salinity between 1985 and 2000 was 5.74% of the study area, which was further down to about 3.89% between 2000 and 2013. Thus, overall there was much increase in salinity in the study area than reduction over the change period (1985-2013).

5.4.2 Change Detection Accuracy Assessment

Change/no-change classification accuracies of $\Delta NDVI$ and ΔSI for the two change periods are summarized in Table 5.3. The highest overall accuracy was achieved of $\Delta NDVI$ for 2000-2013 with (94.24%, Kappa 0.91), while it was a bit lower in the case of $\Delta NDVI$ in 1985-2000 with overall accuracy of 94.09 (Kappa 0.90). High accuracies were also obtained with all change periods for the ΔSI . In general, the user's and producer's accuracies of $\Delta NDVI$ and ΔSI change classes were high in the two change periods. Overall, the positive change class for $\Delta NDVI$ and ΔSI in both change periods showed the highest user's and producer's accuracies.

5.4.3 Soil Salinity-Vegetation Cover Change Relationship

Figure 6 illustrates the correlations between soil salinity and vegetation cover change detected in the two change periods, 1985-2000 and 2000-2013. The analysis reveals highly significant correlation ($p < 0.0001$) with a strong negative linear relationship between the soil salinity-vegetation cover changes (R^2 Adj of 0.83 and 0.80, respectively) in the two change periods.

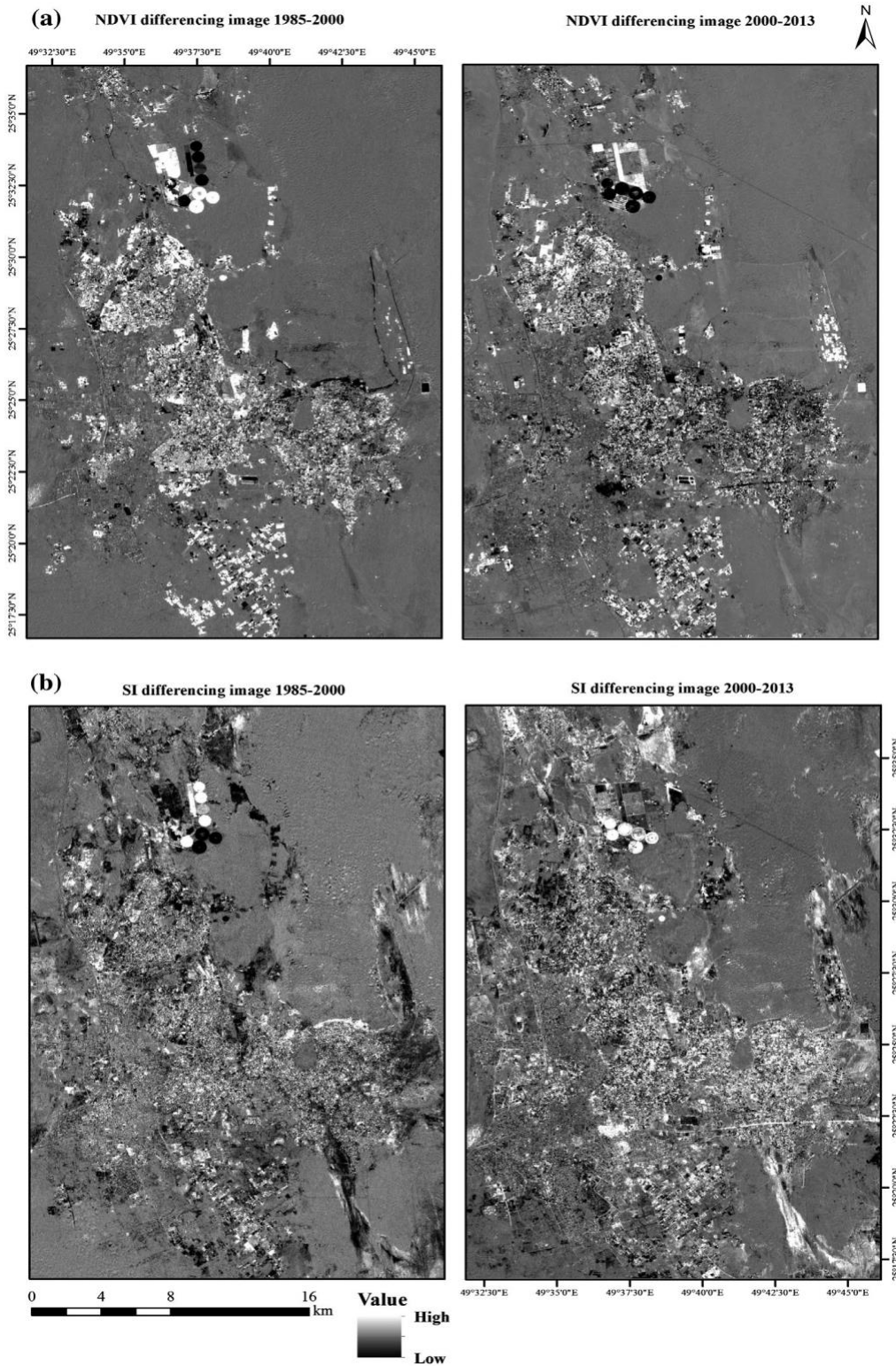


Figure 5.3 The difference images of: (a) the NDVI (Δ NDVI) for the change periods 1985–2000 and 2000-2013, and (b) SI (Δ SI) for the change periods 1985-2000 and 2000-2013

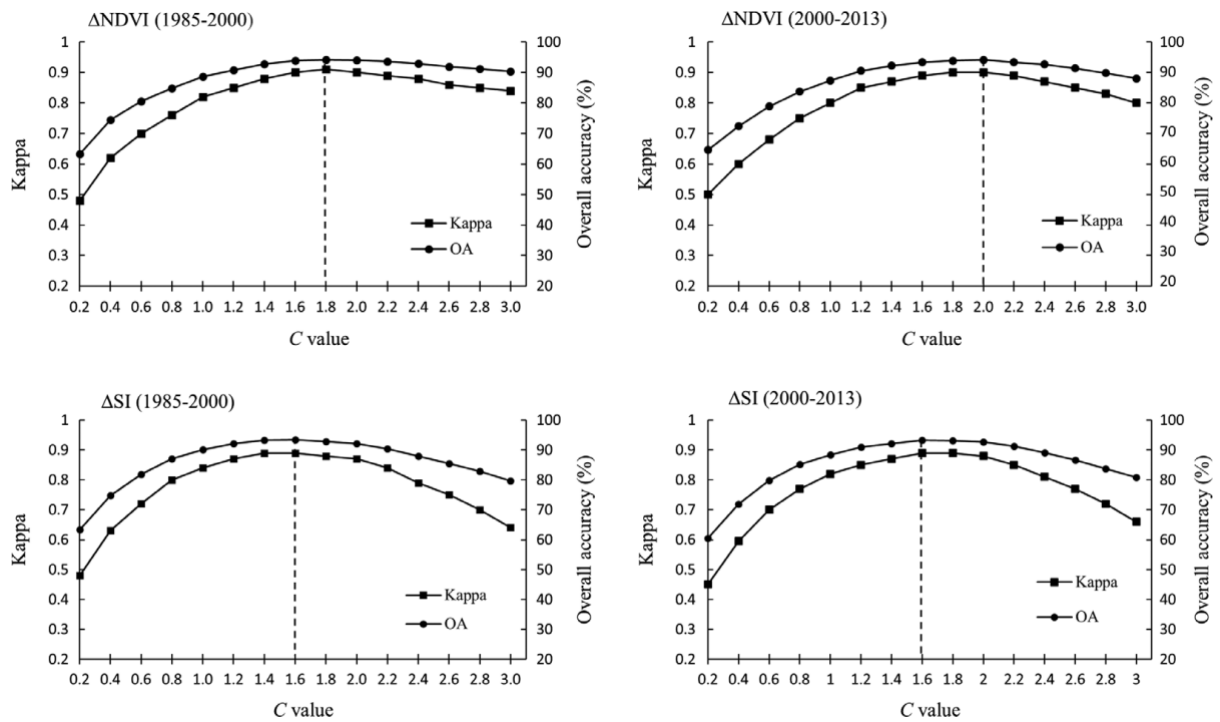


Figure 5.4 Change/no-change thresholds based on Mean \pm C*SD at different C-values for 1985-2000 and 2000-2013 change periods. The optimal threshold values were determined by highest Kappa value or OA. The figure shows that an optimal C-value for Δ NDVI image for 1985-2000 and 2000-2013 periods can be at 1.8 and 2.00, respectively, and the optimal C-value for Δ SI image in both change periods can be at 1.6

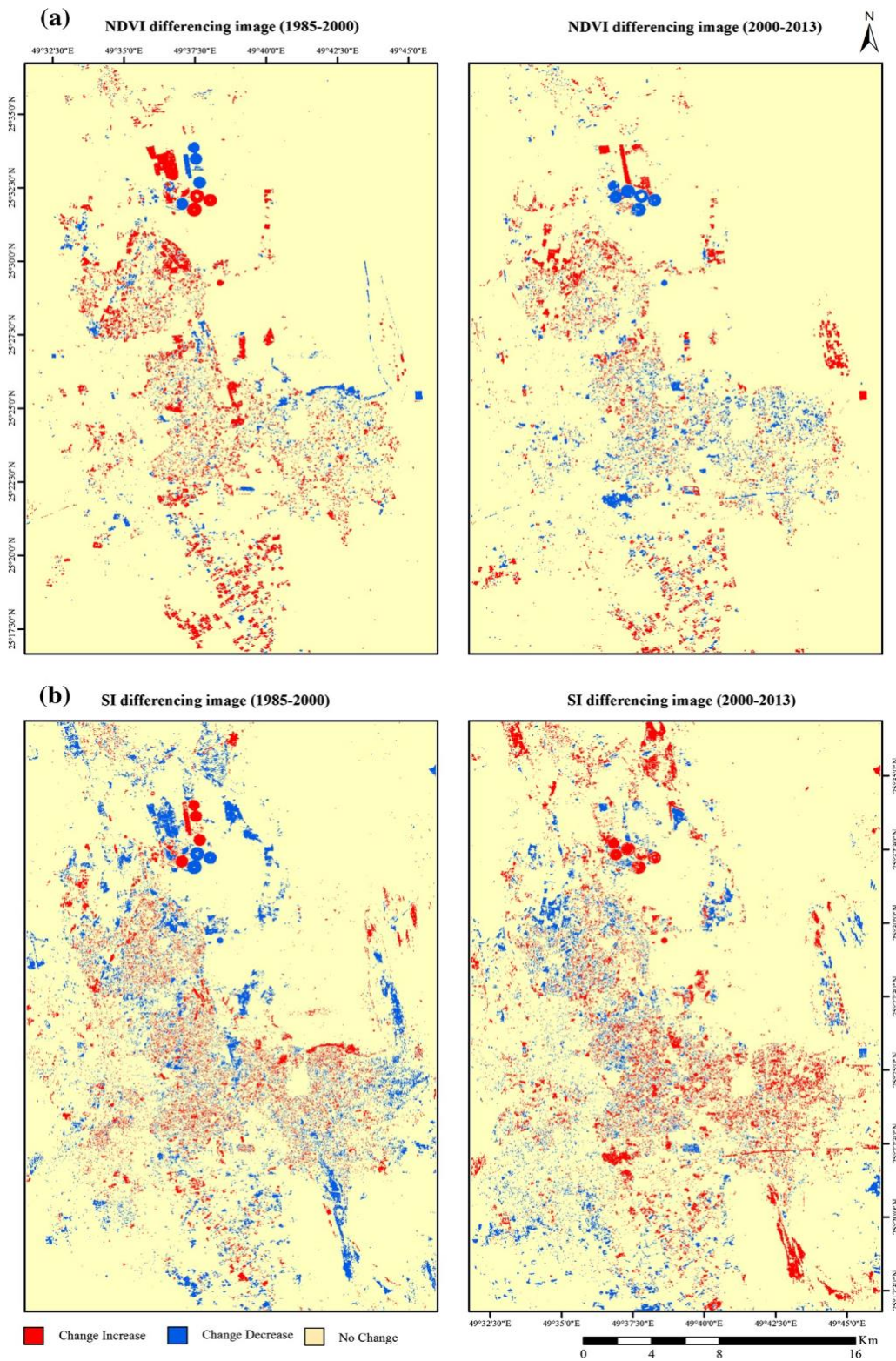


Figure 5.5 Change/no-change maps of: (a) Δ NDVI for the change periods 1985-2000 and 2000-2013, and (b) Δ SI between for the change periods 1985-2000 and 2000-2013

Table 5.2 NDVI and SI change area for the two different change periods

Change class	NDVI				SI			
	1985-2000		2000-2013		1985-2000		2000-2013	
	(ha)	(%)	(ha)	(%)	(ha)	(%)	(ha)	(%)
Change decrease	3318.03	3.73	5605.38	6.31	5101.83	5.74	3457.62	3.89
No change	78599.43	88.45	77041.26	86.71	80410.77	90.50	71972.1	81.00
Change increase	6936.12	7.81	6206.94	6.98	3340.89	3.76	13423.86	15.11

Table 5.3 Change no-change classification accuracy of Δ NDVI and Δ SI for the two changes

Change class	1985-2000				2000-2013			
	Δ NDVI		Δ SI		Δ NDVI		Δ SI	
	PA%	AU%	PA%	UA%	PA%	UA%	PA%	UA%
Change decrease	84.38	95.07	95.38	91.16	86.75	94.42	95.18	97.32
No change	96.68	91.90	93.56	93.21	95.68	93.00	92.19	94.13
Change increase	98.63	97.77	91.00	96.17	98.88	96.58	93.13	87.75
OA	94.09		93.38		94.24		93.22	
Kappa Coefficient	0.90		0.89		0.91		0.89	

PA= producer's accuracy; UA= user's accuracy; OA= overall accuracy.

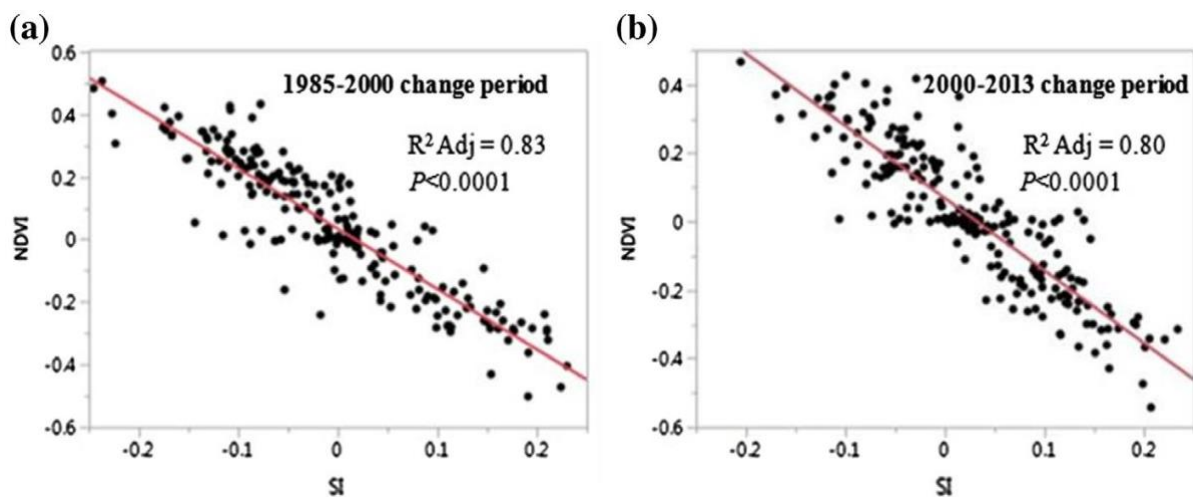


Figure 5.6 The relationship between soil salinity and vegetation cover changes in: (a) 1985-2000 change period, and (b) 2000-2013 change period

5.5 Discussion

This study has attempted to detect soil salinity and vegetation cover changes, and to determine whether the vegetation cover change is associated with soil salinity change in Al Hassa Oasis. Vegetation cover and soil salinity change detection was carried out based on temporal image differencing of three Landsat images spanning 15 and 13 years acquired from 1985 to 2013. Based on prior understanding and previous study (e.g., Allbed and Kumar, 2013) on absorption in the visible range and high reflectance in the NIR range of the electromagnetic spectrum, this study used the NDVI to map soil salinity by monitoring halophytic plants (e.g., date palm) conditions for different time periods. The salinity index (SI) computed using the two SWIR bands in this study was found capable of enhancing the spectral contribution of saline soils by minimizing and suppressing the spectra related to the vegetation. The results were found in accordance with other similar studies which showed the usefulness of the two SWIR Landsat bands for soil salinity determination (e.g., Al-Khaier, 2003; Bannari et al., 2008; Nawar et al., 2014; Meng et al., 2016). For example, Nawar, et al. (2014) found the two SWIR Landsat bands, particularly SWIR1 (Band 5) band had highest contribution to the assessment of soil salinity. They found a high correlation between the Landsat spectral bands and resampled spectra reflectance values ($R^2 > 0.93$) indicating that the reflectance values derived from Landsat have great potential for predicting and mapping soil salinity. In another study, Fourati et al. (2015) used Landsat 8 OLI data to model soil salinity within a semi-arid region using spectral analysis and found the highest correlations correspond to band 6 (1600 nm) and band 7 (2200 nm) confirming the usefulness of mid-infrared (SWIR) bands for detection of salt features. Bannari, et al. (2008) studied the potential of OLI spectral bands to discriminate soil salinity levels in Morocco and noticed that SI derived from the two SWIRs provided the best correlation. In this study, the soil salinity change identified for 1985-2000 and 2000-2013

periods highlighted area undergone increase or decrease in salinity level and also for no-change area.

The main necessities here are to highlight the areas where soil salinity brightness values have decreased or increased (mostly due to changes in soil salinity concentration) or remained unchanged during the change period. However, determination of suitable thresholds to identify change/no-change areas is a critical factor that effects change detection result accuracy. The use of image differencing and determination of optimal thresholding in both directions (positive and negative changes) in this study were found very effective and useful for identification of change/no-change areas based on a simple concept and easy computation technique. The method has advantage in terms of selection of threshold values that produce highest accuracy in change/no-change identification and also provided details on the directional change through quantification of spectrally increased and decreased areas along with no change areas. In addition, the study used a method of selection of historical reference data for changes in the study area through visual interpretation of RGB composite based on combination of primary colours of similar brightness where complementary colour reflected as a change. The three-date classification system further allowed to determine the reference samples between two change periods by re-grouping the three-date reference points into two parts by merging similar classes on two successive dates into one. The method was found very effective and useful for change evaluations from historical data in absence of reference data related to changes.

The analysis results showed a remarkable change in vegetation cover as well as soil salinity accrued. The soil salinity has undergone variable change over the two change periods and can be attributed to different factors, including poor irrigation water quality (Sparks, 2003; Hussain et al., 2006). This study area is primarily dominated by date palm plantations, irrigated mainly with ground water. Several studies from Al-Zarah (2008); Al-Naeem (2011) and Hussain, et

al. (2012) conducted to investigate the irrigation water quality in the Al Hassa Oasis. They found that the EC of the ground water ranged between 1.46 and 16.17 dS/m, which is classified as high (C3) to very high salinity (C4), according to Regional Salinity Laboratory, U.S., water classification scheme, leading to serious effects on soil. Further, the harsh arid climate (high temperatures, low rainfall and high evaporation rates) probably also has effects in inducing soil salinity in the study area. For example, Howari and Goodell (2008) found that the combined effect of high temperature and infrequent rainfall results in significant evaporation and contributes to high soil salinity. Wu et al. (2014) reported similar results in an arid region of Iraq recently.

Significantly high relationships between vegetation cover change and soil salinity were detected for the two change periods (Figure 5.6). Overall, the vegetation cover change increased as soil salinity decreased and vice versa in the study area. These findings suggest that the noticeable change of vegetation cover may be likely due to soil salinity change, which have negatively impacted the vegetation cover. Studies have shown the *negative* impacts of soil salinity on agriculture include decreased plant growth, yield and nutrition (Bernstein, 1975). Raes et al. (2002) reported that excess watering in saline soils can cause loss of essential plant nutrients out of the root zone and soil salinization, which results in limited growth and yield reductions. The side effects of the observed increase in soil salinity in this study area were pronounced in the decrease in the vegetation cover, which is covered mostly by date palm. Though date palm can adapt to high levels of soil salinity, several studies have shown that soil salinity has considerable negative impacts on date palm productivity and growth (e.g., Alhammadi and Edward, 2009; El-Khawaga, 2013; Sperling et al., 2014). A detailed survey in Algeria showed that date palm potential yield was far below expected when it was grown under saline soil conditions (Daddi Bouhoun et al., 2011). Recently, Al-Abdoulhadi, et al. (2012) investigated the impacts of soil salinity on date palms, their results showed that the fronds and

leaf length were significantly reduced as the salinity increased and that the reduction in growth was related to soil salinity. Also, Tripler et al. (2007) and Darwesh (2013) found that soil salinity stress reduced water uptake and growth of date palm in terms of plant height.

In some parts of the study area, there was an apparent decrease in soil salinity over the change period which had possibly led to an increase in the vegetation cover. There might be different factors that have contributed to this change such as leaching application to the soil surface, use of modern irrigation system and management practices, etc. For example, Mostafazadeh-Fard et al. (2008) found that leaching utilization had a significant effect on improving soil salinity via decreasing the salt stress, which caused significant improvement in yield. In addition, use of modern irrigation systems (e.g., drip, sprinkler, flood and bubble) as suggested by similar studies (e.g., Bustan et al., 2004; Malash et al., 2005; Ali et al., 2007) may have controlled soil salinity to some extent resulting in improved vegetation cover conditions.

Overall, there was more increase in soil salinity level and decline in vegetation cover, particularly during 2000-2013 period, than decrease in soil salinity level. The observed changes in this area will have significant implications on agricultural output in the future if these processes continue as increase in soil salinity level was found one of the reasons contributing to the decline in vegetation cover change. Consequently, the loss of vegetation cover will enhance evaporation and promote more salinity. The two mutually inclusive effects will result in reduction of suitable land for future agricultural use and will have economic and social impacts as these regions are important source of income for the government and local farmers (Jain et al., 2011). For example, in Oman it was estimated that annual losses due to soil salinity and abandoned date palm farms ranges between 7.3 and 14.0 million Omani rials per annum (Ahmed et al., 2013). Thus, the finding reported in this study can be considered a useful starting point to help agricultural workers, scientists and engineers understanding the effects of vegetation cover and soil salinity changes in order to protect the vegetation cover, especially

date palm outputs, sustain agricultural lands and avoid further adverse environmental, social and economic effects.

5.6 Conclusion

Soil salinity is a dynamic process that changes over time and has harmful impacts on agriculture. Thus, knowledge of the change in soil salinity dynamics over time and its impacts on vegetation cover is required in order to support decision makers to work on different actions needed to control soil salinity and sustain the vegetation cover. From this viewpoint, this study was conducted to detect soil salinity and vegetation cover changes in Al Hassa Oasis; and to investigate whether the change in vegetation cover is a case of soil salinity change based on multi-temporal Landsat imagery. With NDVI and SI difference images, changes in the vegetation cover and soil salinity were detected. A strong inverse relationship was found between the NDVI and SI values, indicating that there is a potentially strong linkage between the vegetation cover change and soil salinity change over the study area. Overall, the soil salinity level has experienced remarkable changes in Al Hassa Oasis in the past 28 years probably due to improper land use and poor management practices (e.g., poor irrigation system, fertilizer application, etc.). The increased soil salinity will have long consequences in terms of decline in the vegetation cover and date farm production causing serious environmental, economic and social impacts. Thus, better management practices are required to mitigate these changes and to improve soil conditions.

The medium resolution remote sensing data and the analysis techniques used in this study to investigate vegetation and soil salinity changes showed satisfactory results. However, the results can be improved with higher spatial/spectral resolution remote sensing images and a subsequent study has been proposed to use of such data for the study area. Nevertheless, the study showed the usefulness of time-series remote sensing data for soil salinity and vegetation

change detection. The results will help the managers in identifying problem areas and in taking appropriate actions to control and mitigate salinity to protect the date palm outputs and avoid further adverse environmental, social and economic effects.

Acknowledgments

The authors would like to gratefully acknowledge the data analysis support and assistance kindly provided by Catherine MacGregor from School of Environmental and Rural Science, University of New England. We would like to express our deep gratitude to the editors and the two anonymous reviewers for their constructive comments and suggestions to improve the quality of the paper.

**Higher Degree Research Thesis by Publication
University of New England**

STATEMENT OF ORIGINALITY

We, the Research Master/PhD candidate and the candidate's Principal Supervisor, certify that the following text, figures and diagrams are the candidate's original work.

Type of work	Page number/s
Figure 5.1	91
Figure 5.2	93
Figure 5.3	101
Figure 5.4	102
Figure 5.5	103
Figure 5.6	104

Name of Candidate: Amal Allbed

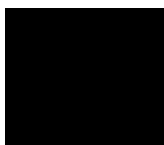
Name/title of Principal Supervisor: Professor Lalit Kumar



Candidate

20 June 2018

Date



Principal Supervisor

20 June 2018

Date

Higher Degree Research Thesis by Publication
University of New England

STATEMENT OF AUTHORS' CONTRIBUTION

We, the Research Master/PhD candidate and the candidate's Principal Supervisor, certify that all co-authors have consented to their work being included in the thesis and they have accepted the candidate's contribution as indicated in the *Statement of Originality*.

	Author's Name (please print clearly)	% of contribution
Candidate	Amal Allbed	80
Other Authors	Lalit Kumar	10
	Priyakant Sinha	10

Name of Candidate: Amal Allbed

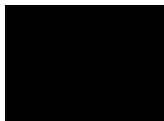
Name/title of Principal Supervisor: Professor Lalit Kumar



Candidate

20 June 2018

Date



Principal Supervisor

20 June 2018

Date

Chapter 6 Spatio-Temporal Modelling of Agricultural Expansion Based on Driving Force Factors Using Logistic Regression: A Case Study in the Al Hassa Oasis

This chapter has been submitted to the journal for review and publication.

Allbed, A., Kumar, L., & Alqurashi, A. Spatio-temporal modelling of agricultural expansion based on driving force factors using logistic regression: a case study in the Al Hassa Oasis. Submitted to *ISPRS International Journal of Geo-Information* for review and publication

6.1 Abstract

The agricultural industry is vital not only for providing food but also through its contribution to economic growth and environmental sustainability. Understanding agriculture's underlying driving factors, as well as how agricultural areas have expanded and where the growth will occur in the future, are important for sustainable development plans. In the current study, the effects of the following factors on agricultural expansion in the Al Hassa Oasis were investigated: physical and proximity factors, including elevation, slope, soil salinity, distance to water, distance to built-up areas, distance to roads, distance to drainage and distance to irrigation. A logistic regression model was used for two time periods of agricultural change- in 1985 and 2015. The probable agricultural growth maps based on agricultural changes in 1985, was used to test the performance of the model to predict the probable agricultural expansion after 2015. This was achieved by comparing the probable maps of 1985 and the actual agricultural land of 2015. The Relative Operating Characteristic (ROC) method was also used and together these two methods were used to validate the developed model. The results showed that the prediction model of 2015 provides a reliable and consistent prediction based on the performance of 1985. The logistic regression results revealed that among the investigated factors, distance to water, distance to built-up areas and soil salinity were the major factors having a significant influence on agricultural expansion. Such results will contribute to a deeper understanding of the process of agricultural expansion and provide a scientific basis for future forecasting and decision-making processes regarding sustainability.

Keywords: agricultural growth; driving forces; logistic regression; GIS; remote sensing

6.2 Introduction

In most countries of the world, whether underdeveloped, developing or even developed, agriculture plays a vital role not only in regard to food security and rural sustainable development, but also in making contributions to economic growth (Diao et al., 2010; Izuchukwu, 2011; Raza et al., 2012). It has been reported that the most direct contribution of agricultural growth is through generating higher incomes for farmers (Irz et al., 2001), expansion of marketable surplus, as well as the development of material (e.g., industry), and in the non-material production sectors, which contribute substantially to the overall economic development of the country. Agricultural expansion, which is considered as one of the main dynamics of land cover change, is a spatio-temporal dynamic process controlled by various driving forces (socio-economic, physical and proximate), their interactions and processes, during which both the spatial expansion and the drivers vary over time and space (Mitsuda and Ito, 2011). Like elsewhere, Al Hassa Oasis in the eastern part of Saudi Arabia is regarded as one of the main agricultural regions in Saudi Arabia providing a significant source of income for farmers and the government (Jain et al., 2011; Al-Abdoulhadi et al., 2012). However, with the change in land use it has been reported that agricultural distribution in this Oasis has experienced remarkable alteration (Al-Jabr, 1984; Akkad, 1990), yet the physical and proximate driving forces behind this change in agricultural expansion have not been studied. Hence, understanding the past and current spatial distribution of agriculture and its underlying drivers along with their relationships, is a crucial prerequisite, as information on existing agriculture patterns and changes over time play an important role in the decision-making process to mitigate the negative effects and promote desired outcomes.

Remote sensing in conjunction with the advancement of geographic information systems (GIS) and the increasing quality and spatial coverage of global resource databases have enabled modelling of the changes in land use/land cover (LULC) at a variety of spatial scales (Aspinall,

2004; Tayyebi et al., 2014; Paudel et al., 2016). A range of empirical models which use statistical analysis to compute LULC changes probabilities, indicating the likelihood of occurrence of a specific LULC type at a location (Almeida et al., 2008), have been developed and have been used to uncover the interaction between the dynamic changes and the driving factors based on historical data. Amongst these approaches, a logistic regression model has been the most popular for empirically predicting probabilities of events in multiple applications due to its efficiency in handling binary dependent variables. In the case of LULC, change in the influence of independent variables can readily be identified, and its results can be directly used to predict the locations of future change (Cheng and Masser, 2003; Dubovyk et al., 2011; Li et al., 2013). For example, Li, et al. (2013) examined the effects of physical, socioeconomic, and neighborhood factors on urban expansion in Beijing using binary logistic regression. Similarly, Newman, et al. (2014) adopted a logistic modelling technique to investigate the driving forces of both deforestation and reforestation in the Cockpit Country, Jamaica. In many cases, this model fits spatial processes and LULC change outcomes reasonably well.

In comparison to the extensive studies using binary logistic regression models (Cheng and Masser, 2003; Hu and Lo, 2007; Tayyebi et al., 2010; Nong and Du, 2011; Achmad et al., 2015; Alqurashi et al., 2016), studies that have been conducted all around the world to understand the spatial patterns and the driving factors of land use change, in particular urban expansion, agricultural expansion as a form of land cover change has received relatively little attention. Even less research has sought to use agricultural expansion modelling by developing a logistic regression model based on physical and proximate driving factors. Accordingly, this paper aims to conduct, using a logistic regression model, the first known spatio-temporal modelling of agricultural expansion in the Al Hassa Oasis in 1985 and 2015 to: (1) identify drivers of past and present spatial distribution of agricultural land cover, with a goal of

identifying the key drivers' factors that have shaped the expansion of the agricultural land cover at two years, and (2) predict agricultural expansion after 2015.

6.3 Materials and Methods

6.3.1 Study Area

Al-Hassa Oasis is located between a latitude of 25° 05' and 25° 40' N and a longitude of 49° 10' and 49° 55' E in the eastern province of Saudi Arabia (Figure 6.1), at an elevation range of about 130 to 160 m above sea level. This Oasis covers an area of approximately 20,000 ha that are made up of two separate oases that are somewhat sloped to the north and east. It is an agricultural land, mainly dominated by date palms (*Phoenix dactylifera* L.); while alfalfa, rice and other vegetables are also cultivated. The ground water is the main water source for agricultural and other uses in this Oasis and comes from the Neogene groundwater aquifer and several free flowing springs that are distributed across the area (Al Sayari et al., 1984). The main drainage direction follows the natural northern and eastward slope in the eastern and northern Oasis (Al-Barrak and Al-Badawi, 1988; Shaltout and El-Halawany, 1992). The Al-Hassa Oasis is characterized by an arid climate with an ambient temperature that exceeds 45°C during the summer and has a high evaporation rate that exceeds the annual average precipitation by approximately 488 mm. During the winter the temperature is between 2 and 22 °C.

The Al Hassa Oasis is considered one of the largest and most productive agricultural regions in Saudi Arabia. It is dominated by date palm farming, providing a significant source of income for farmers and the government. The key issue that influences the agricultural growth and productivity in this Oasis is soil salinity, due to the local weather conditions, along with improper land use and poor management practices. These include poor irrigation water quality, poor irrigation systems and fertilizer application.

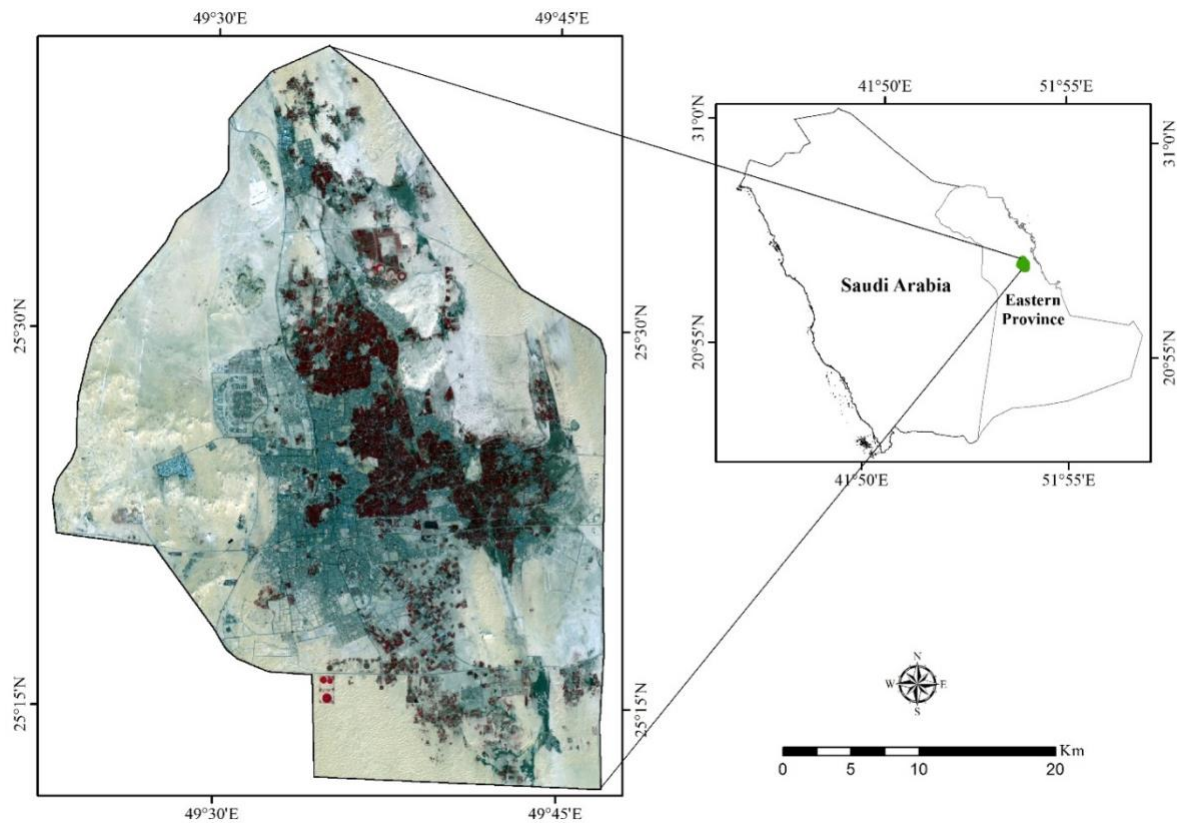


Figure 6.1 Location of the Al Hassa Oasis in Saudi Arabia

6.3.2 Image Acquisition and Pre-processing

Landsat Thematic Mapper (TM) image for January 1985 and Operational Land Imager (OLI) image for December 2015, obtained from the United States Geological Survey (USGS), were used to quantify the rate of agricultural change in the study area. Ideally, the images should have been taken during the same time period; however, this was not possible due to unavailability of data. It is considered that such a small difference in the image acquisition dates should not significantly affect results. These data sets are located on satellite path 164 and row 42. The images were geo-referenced to a Universal Transverse Mercator (UTM) coordinate system using World Geodetic System (WGS) 1984 datum assigned to north UTM zone 39. A relative radiometric normalization was conducted to remove radiometric distortions and make the images comparable. For this purpose, Dark-Object Subtraction (DOS) was carried out for radiometric and atmospheric normalization (Canty et al., 2004; Vicente-Serrano

et al., 2008). The multispectral image Digital Number (DN) values were converted to Top of Atmosphere (TOA) reflectance values through the equation suggested by Canty, et al. (2004). Finally, image subsets were extracted for the study area. The entire data pre-processing and digital image analysis were carried out using Environment for Visualizing Images (ENVI) version 5.3 software.

6.3.3 Image Classification and Accuracy Assessment

To derive land cover information from remotely sensed images, image classification was carried out to obtain the thematic maps of the two time periods. Several classification techniques, such as maximum likelihood, decision tree and neural network classifiers, have been developed since the first Landsat image was acquired. In this study, the classification process was performed using spectral indices and the Support Vector Machines (SVM) classifier, both of which were derived from statistical theories and are commonly used in land cover classification studies. Normalized Difference Vegetation Index (NDVI), and Normalized Difference Water Index (NDWI) were used to extract the agricultural lands and waterbodies from the images.

SVM has often been found to provide higher classification accuracies than other widely used techniques (Akbari et al., 2004). In brief, SVM is a supervised non-parametric statistical learning technique (Mountrakis et al., 2011) in which the optimization algorithms are employed to specify the optimal boundaries between classes (Huang et al., 2002). Built-up areas and bare soil are not linearly separable in the study area. Thus, misclassification errors are an inherent problem when using traditional classification algorithms such as maximum likelihood classifiers. However, SVM increases the margin width between classes and consequently minimizes the quantity of proportional to the number of misclassification errors (Pal and Mather, 2005). Zakeri, et al. (2017) have applied SVM and maximum likelihood classifiers to

detect built-up areas and bare soil in Tehran city in Iran, and they found that SVM produced a higher accuracy than the maximum likelihood classification. Therefore, the SVM approach was selected to classify built-up areas and bare soil for 1985 and 2015. Since the aim of this paper was to analyze agricultural growth, the other three classes - water, built-up and bare soil were reclassified as non-agriculture areas. Thus, the final results presented two categories, agriculture and non-agriculture areas, which were then used in the statistical analysis.

Accuracy assessment is an important component of image classification. In this study, stratified random sampling methods were applied to evaluate the classified images. The results indicated a high overall accuracy (average overall accuracies were 88.09% and 90.56% in 1985 and 2015 respectively) and kappa coefficient (average kappa coefficients were 0.82 and 0.87 in 1985 and 2015 respectively), which show good agreement between the referenced and classified images.

6.3.4 Potential Driving Factors of Agricultural Expansion

To determine the potential driving factors of agricultural expansion, a total of eight factors within two main categories, physical and proximity, were selected. The physical factors considered were elevation, slope and soil salinity, while the proximity factors comprised the distance to water, distance to built-up areas, distance to roads, distance to drainage and distance to irrigation. These factors were selected based on their effects as described in previous studies (Akkad, 1990; Mitsuda and Ito, 2011). Figure 6.2 shows the variables used as potential driving factors in binary logistic regression models.

Topography-related factors, elevation and slope, play a vital role in agricultural expansion as they determine the extent of soil erosion, transport facilities and cultivation methods (Somashekar, 2003). Generally, an increase in elevation and slope make agricultural practices quite difficult, or even impossible, with related costs becoming higher. However, in flat areas there is no such problem, with these areas more suitable for agricultural development (Scherr

et al., 1997). The role of soil salinity is also important (Kersten et al., 2000; Somashekar, 2003) as agricultural production depends on soil health. Usually high levels of soluble salts in soil inhibit plant growth and subsequent agricultural development. Accordingly, elevation, slope and soil salinity, which is a major problem in this region as mentioned previously, were selected as the physical factors. Both elevation and slope were derived from the 30-m resolution digital elevation model (DEM) that was obtained from the USGS site for the study area. The slope was calculated as a percentage, dividing the rise by the run and multiplying by 100. Soil salinity maps were obtained from the Ministry of Agriculture.

Since agricultural production is a biological process, its growth is not possible without water. The distance to sufficient water resources is considered a fundamental determinant of the extent, the spatial distribution, and the spatial expansion of agricultural land. Greater distance to water resources is expected to have a negative impact on agricultural expansion. Thus, in the study area the distance to water bodies' locations was calculated using the Euclidean distance algorithm in ArcGIS 9.2.

From an environmental perspective, built-up areas and roads that penetrate into agricultural land are the biggest peril, since they often promote large-scale agricultural loss (Laurance et al., 2014). Therefore, the greater the proximity to the built-up areas or the roads, the less the probability of lands being attractive to farmers to expand or establish new plantations. However, high quality roads that connect existing agricultural areas with markets may reduce degradation, and such roads can act as magnets that attract farmers to areas that are already dominated by human beings, and away from vulnerable frontier areas (Weinhold and Reis, 2008). These roads could promote greater agricultural productivity while enhancing farmers economically. For each year in this study, the distance to built-up areas was generated by extracting the urban class from the classified images and running the Euclidean distance algorithm on the output. As roads are usually temporally dynamic, road layers were delineated

using heads-up digitizing from the time-series Landsat images for each year then the distance from roads was calculated using the Euclidean distance algorithm.

While irrigation is a key factor for increasing agricultural production, excessive irrigation with poor quality water in places without proper drainage systems poses many hazards to agricultural production. Scientists agree that one of the biggest threats to irrigated agriculture, such as in this study area, is salinity (Hoffman et al., 2007). In light of this, where irrigation and drainage canal systems with appropriate management exist, the lower the likely salinity intensity would be and higher agricultural growth is to be expected. In this study, the layers for both irrigation and drainage canals were obtained from Al Hassa Irrigation and Drainage Authority (HIDA), then the distance from the irrigation and drainage canals was calculated using the Euclidean distance algorithm.

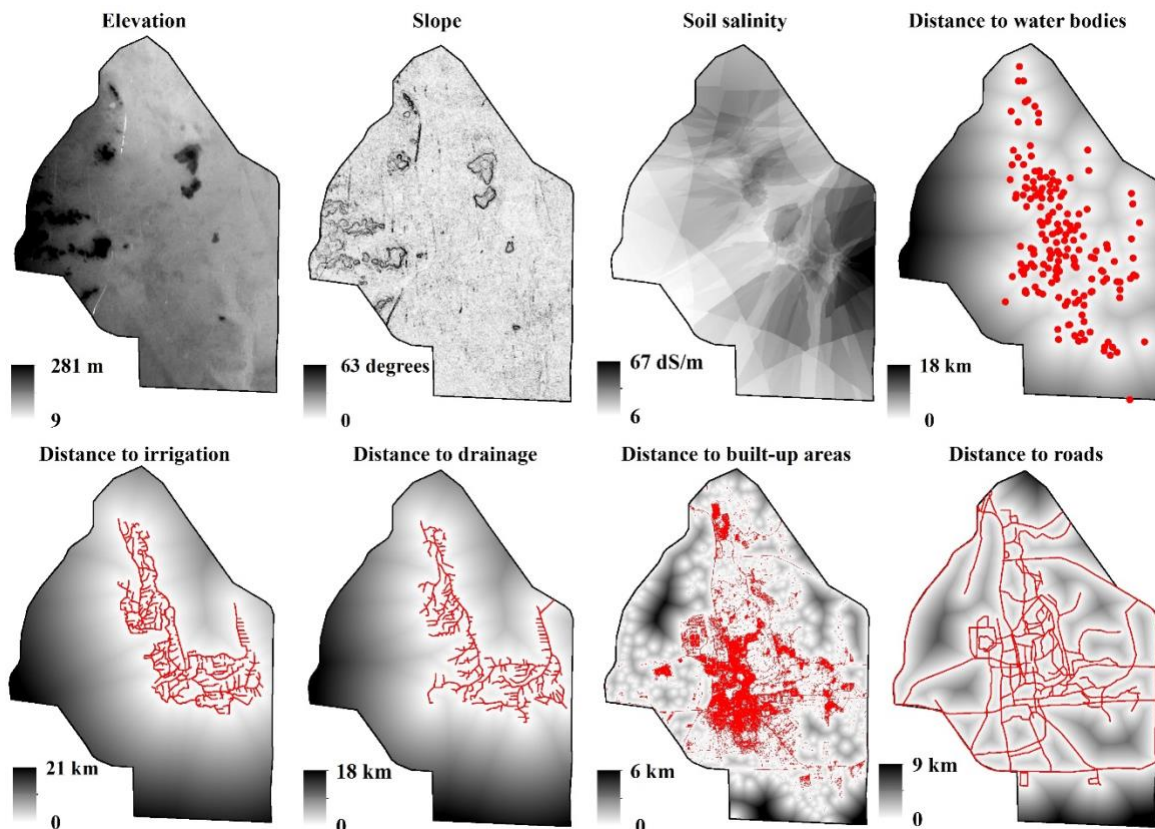


Figure 6.2 Selected driving forces of agricultural growth in the Al Hassa Oasis

6.4 Statistical Analysis

6.4.1 Agriculture and Non-Agriculture Data Sampling

In this study, the derived layers for the dependent and independent variables were very large (1352 × 1819) with a 30-m resolution. In the later investigative statistical analysis, dealing with such a large data set is computationally difficult, tedious and extremely time consuming (Dong et al., 2015; Alqurashi et al., 2016). Besides, both dependent and independent variables may have spatial autocorrelation, and this has several implications that may yield biased results in the later logistical regression analysis. To avoid these previously mentioned issues, attention was paid to selecting an appropriate data sampling method. Thus, systematic random sampling was applied for both agricultural and non-agricultural features to extract cell values of dependent and independent variables on which the logistic regression model was fitted. The sample points were selected with a relatively large distance of greater than 300-m between each point in order to minimize spatial autocorrelation. The points that were agricultural were coded as 1 (presence) while non-agricultural points were coded as 0 (absence). Consequently, the numbers of sample points used in the later logistical regression with an equal quantity of points coded as 0 and 1 were 412 and 442 for 1985 and 2015, respectively.

6.4.2 Logistic Regression

Logistic regression is a non-linear statistical model that is used to model and discover the empirical relationships between a dependent variable (Y) and several independent categorical and continuous variables (Xs) (Kleinbaum and Klein, 2010). In logistic regression, the dependent variable is usually dichotomous, which means that the value of 1 is assigned when the areas are likely being converted to, for example, agriculture, or 0 when there is no transition. This type of variable is called a binary variable.

Compared with other regression models, the logistic regression model has the ability to estimate the agriculture probability of the occurrence of a discrete response factor (Rienow and Goetzke, 2015). Also, it can empirically identify the influence of independent variables on the dependent variable, and thus can provide a degree of confidence regarding their contribution (Hu and Lo, 2007). In this study, the binary logistic regression model in agricultural growth was calculated using the following equation:

$$\log \text{it}(y) - \log\left(\frac{y}{1-y}\right) = \beta_0 + \beta_1\chi_1 + \dots + \beta_\eta\chi_\eta + \varepsilon \quad (6.1)$$

where y is the probability of conversion identifying agriculture land as 1, χ_η is an independent variable or driving force, β_0 is the intercept, β_η is the estimated coefficients of variable χ_η , ε is a randomly distributed residual error.

Binary logistic regression was used to investigate the driver factors that are associated with agricultural growth, and to develop an agricultural growth probability map. For this purpose, binary logistic regression was used first in 1985 to quantify and compare the agricultural growth probability with the agricultural map of 2015 that was generated from satellite data, then it was applied to the agricultural growth in 2015 using equation (6.1).

6.4.3 Prediction of Spatial Patterns of Agricultural Distribution

After generating the probability maps using equation (6.1), the coefficient values of the selected driving factors and the intercept values were calculated in ArcGIS 10.2. The odds ratio of value 1 was used individually for each map of 1985 and 2015. The calculation was first applied to the 1985 data in order to validate the probability maps of 2015. A visual comparison was performed by overlaying the probability map of 1985 and the agricultural area map of 2015

that was produced from the image classification of the 2015 image. The logistic regression model was then applied to the 2015 map.

6.4.4 Model Validation

To evaluate the performance of the binary logistic regression model, robust statistical methods are needed. Relative operating characteristics (ROC) is the most widely used method for predicting accuracy when evaluating and comparing models (Martínez et al., 2011). Besides, ROC has been previously used in LULC change modelling to measure the relationship between simulated change and real/observed change (Newman et al., 2014; Alqurashi et al., 2016). Basically, ROC is used to evaluate the validity of a model that predicts the occurrence of an event and assesses how well the pair of maps agrees in terms of the location of cells being changed into agriculture, by comparing a probability image depicting the probability of that event occurring, and a binary image showing where that class actually exists when the simulated and observed maps are compared. The ROC analysis is based on a rate curve of true positive rates versus false positive rates over all possible cut-off points. Generally, the higher the true positive rates relative to the false positive rates, the greater is the area under the ROC curve (AUC). Simply, the ROC statistic is the area under the curve (AUC) that connects the plotted points. The value of AUC ranges from 0.5 for a model that assigns at random the probability of a particular land cover change to 1 for a model that perfectly assigns this probability, and the larger the AUC, the more accurate the model (Pontius and Parmentier, 2014). In addition, assessing the goodness-of-fit of binary logistic regression based on the Percent Correct Predictions (PCP) is common in this type of modelling (Li et al., 2013). Moreover, it has been reported that the combination of both approaches, ROC and PCP, for logistic regression evaluation, can be more efficient providing more objective details on the models' performance (Dubovyk et al., 2011). Therefore, the AUC of ROC and PCP through

cross-tabulate prediction, along with observation, were calculated in this study. All analyses were undertaken in R version 3.3.2 and IDRISI TerrSet 18.31 software.

6.5 Results

The statistical analysis results of eight independent variables used in the logistic regression model are summarized in Table 6.1. Both the variables of physical and proximity factors significantly affected the agricultural growth in the Al Hassa Oasis; however, their effects varied with period (Table 6.1). Distance to built-up areas, distance to water bodies and soil salinity were decisive determinants on agricultural expansion for both 1985 and 2015. Elevation and slope negatively affected agricultural expansion in 1985 but showed less influence in 2015. The distance to irrigation, distance to drainage and distance to roads had no effect for the selected time period. Overall, the effect of distance to built-up areas, distance to water and soil salinity in the agricultural distribution in this Oasis were less important in the past whilst in recent years these factors have had greater impact. This indicates that the possibility of agricultural expansion will be smaller in the future.

The good fit of the logistic regression model, indicated by the PCP values with the cut-off point of 0.5 were 85.68 and 76.92% respectively for 1985 and 2015, along with the driving variables, could effectively interpret the process of agricultural growth. The ROC curve presented in figure 6.3 illustrates how well the logistic regression model, together with the driving factors, predicted agricultural growth. Since the ROC curves rise quickly, the fitted models have a high predictive accuracy indicating a high degree of spatial consistency between the model predictions and actual agricultural growth. This accuracy is confirmed by the large area under the ROC curve. The AUC values were 0.95, and 0.90 AUC for the respective study periods. From this result, we can say that the respective prediction accuracy is 95 and 90% for 1985 and 2015 respectively.

Table 6.1 Summary results of the logistic regression model

Variable	1985			2015		
	β	S.E	p (> z)	β	S.E	p (> z)
Intercept	8.5420	2.2850	0.000185 ***	5.5250	1.3910	7.10e-05 ***
Elevation	-0.0192	0.0108	0.0744	-0.0208	0.0088	0.018450 *
Slope	-0.0320	0.1155	0.7815	-0.2346	0.0975	0.016169 *
Distance to irrigation	-0.0003	0.0002	0.0766	-0.0001	0.0002	0.3950
Distance to drainage	0.0001	0.0003	0.8273	0.0002	0.0002	0.3357
Distance to roads	0.0001	0.0002	0.5432	0.0001	0.0002	0.5227
Distance to built-up areas	-0.0008	0.0003	0.004937 **	-0.0025	0.0007	0.000108 ***
Distance to water bodies	-0.0003	0.0001	0.020331 *	-0.0005	0.0001	1.73e-06 ***
Soil Salinity	-0.9875	0.3896	0.011249 *	-0.0314	0.0140	0.024927 *
PCP (%)	85.68			76.92		

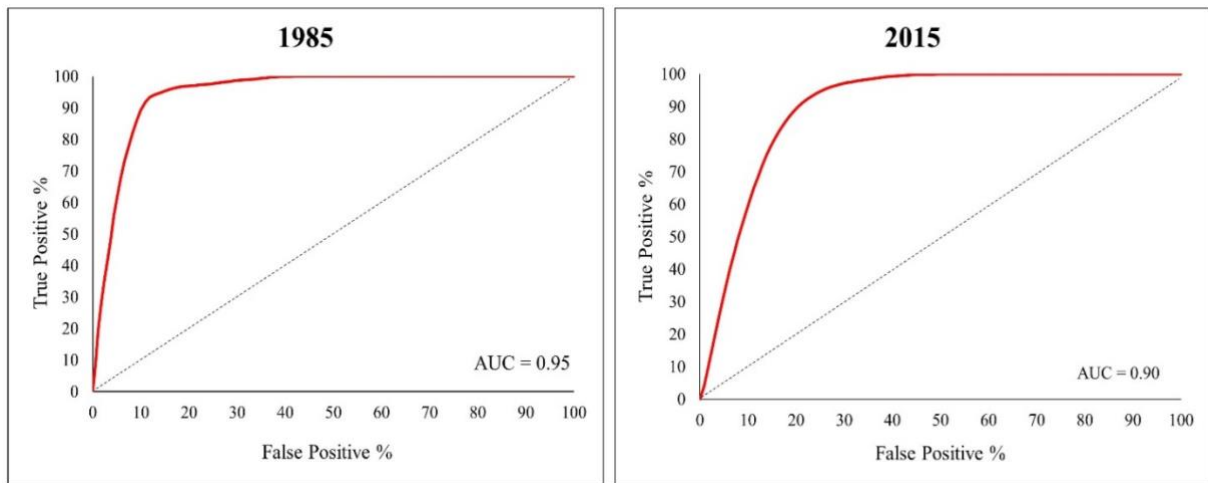


Figure 6.3 ROC curve for the selected period

6.5.1 Agricultural Expansion Probability

In order to test the effectiveness of the logistic regression model for predicting agricultural expansion probability in 2015, the model was run using 1985 data and compared with the result produced from the satellite image for the agricultural land of 2015. Figure 6.4 shows a visual comparison of the result of agricultural expansion probability in 1985 and agricultural cover in 2015. The brighter pixels represent higher probabilities of agricultural growth, while darker pixels indicate lower probabilities of agricultural growth.

The relatively flat, low elevation structure and gentle surface slope gradients of the Al Hassa Oasis located in the central, northern, eastern, north-eastern and southern portions of the Oasis, showed the most noticeable probable areas of agricultural growth due to the effect of physical factors. While the probability areas tend to be located in the above locations, the growth of agriculture is likely controlled by non-saline soil. The probabilities of agricultural growth in these parts of the study area are also reflected in the strong influence that the proximity factors, particularly distance to built-up areas and distance to water bodies, have on the location of agriculture areas, i.e., a location adjacent to water resources will be more attractive to farmers to establish or expand their farming area. Likewise, the distance to built-up areas seems to determine significantly the agricultural growth toward the southern and south-eastern parts; meaning that regions far from built-up areas have a higher likelihood of being faced with agricultural expansion.

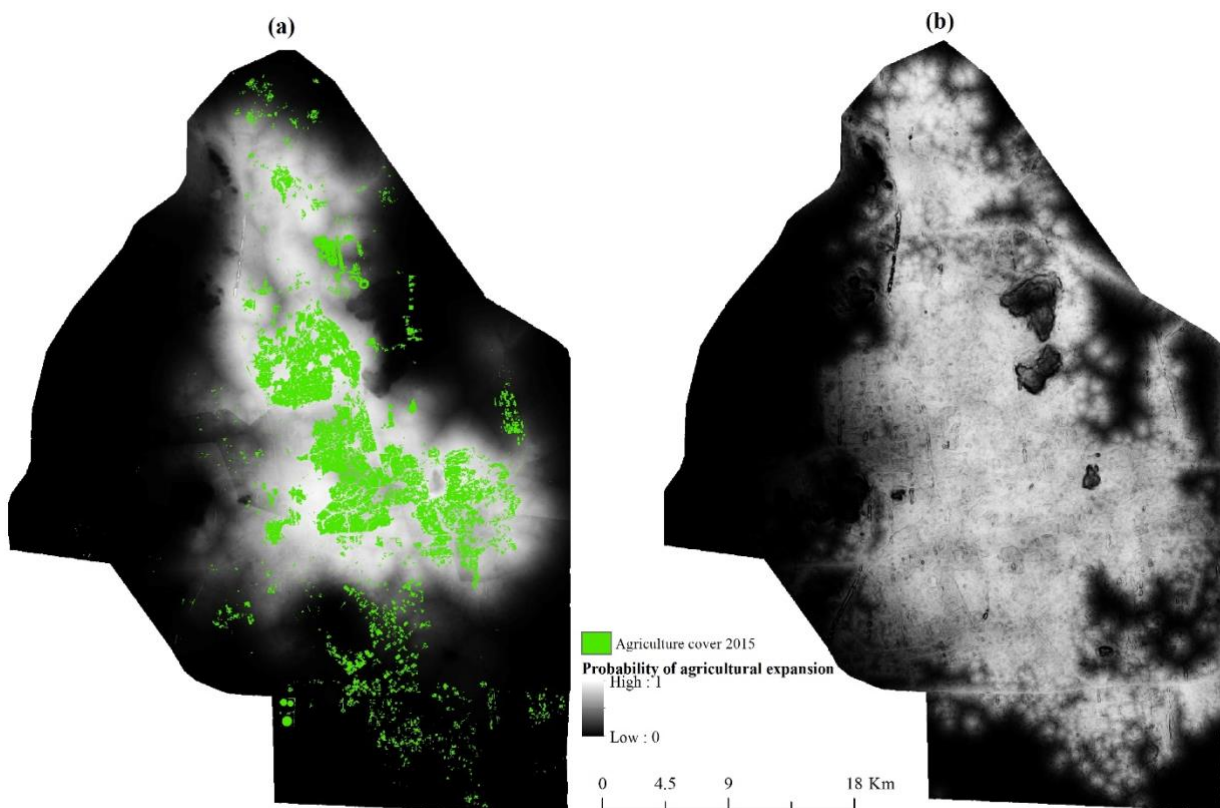


Figure 6.4 Probability maps of agricultural expansion: a) a comparison of agricultural expansion probability in 1985 and agricultural lands in 2015; b) predict agricultural expansion after 2015

6.6 Discussion

In this study, logistic regression models based on a set of physical and proximity variables were used to quantify the spatio-temporal patterns and underlying drivers of agricultural expansion in the Al Hassa Oasis in 1985 and 2015. The results from both 1985 and 2015 showed that among proximity variables, distance to water bodies has the strongest effect on agricultural expansion, followed by distance to built-up areas. Water resources are inextricably linked to climate, so in arid climatic regions such as the Al Hassa Oasis the high temperatures, high evaporation rate and low rainfall rates limit conventional water resources. This region is dependent mainly on groundwater as the main water source for agricultural irrigation. This is not enough to satisfy water demands, and due to improper planning and excessive pumping, the groundwater is very much reduced (Alsharhan et al., 2001; Mohamed, 2006). The scarcity of water resources in this region has significantly impacted on agricultural growth (Al-Jabr, 1984) and will likely have serious implications for agricultural growth in the future if no remedial action is taken, as water scarcity is considered one of the limiting constraints for crop production (Kang et al., 2009). That is to say, the significant effects of distance to water bodies indicates that the probability of agricultural growth is tied to being close to water resources. Thus, locations close to water bodies are likely to be developed more than locations that are far from the available water sources, because proximity to water bodies is vital to the establishment of agricultural activities. Moreover, farmland quality near water bodies is usually high because of excellent irrigation conditions, and farmers prefer to expand or establish new plantations along water bodies. This result is in agreement with the results presented by Maeda, et al. (2010) and Serneels and Lambin (2001), who reported the relationship between the distance to water bodies and the probability of agricultural expansion.

It is widely recognized that rapid urbanization, resulting from urban population growth and internal and external migration, is accelerating the loss of agricultural land. The rate at which

agricultural land in areas adjacent to built-up areas is lost is expected to continue to increase as a function of urban expansion (d'Amour et al., 2016). In this sense, significant negative relationships between the probability of agricultural expansion and the distance to built-up areas were found in this study, suggesting that the closer the area is to built-up areas, the lower the likelihood of agricultural development. In line with this finding, Krannich (2006) reported that America's most productive agricultural land, which was situated in close proximity to large urban centers, was replaced with urban expansion. More recently, in China, Song, et al. (2015) found that agricultural lands close to urban areas have been encroached upon by urban expansion. This finding may be attributed to the fact that agricultural land close to urban areas is particularly attractive for urban development because it is flat, well-drained and usually has a long farming history with a better soil profile. Therefore, agricultural land can be easily converted for commercial, industrial, or residential purposes. Thus, to avoid the anticipation of future conversion to urban use, either because of land speculation or spillover effects generated by urbanization, agriculture should expand preferentially in areas far from built-up areas.

It is firmly believed that irrigation and drainage are key components for agriculture and water management, and these have been identified as gateways to increased agricultural growth, especially for irrigated agricultural areas with growing water scarcity. Although agriculture is a significant user of water sources, in the Al Hassa Oasis distance to irrigation and drainage canals do not seem to have a significant impact as they showed the least effects on agricultural growth. This result may have been found because of the fact that only 32% of the Al Hassa irrigation and drainage network is served by HIDA, while the majority of agricultural lands are irrigated with water from individual private wells (Bastiaanssen et al., 2011). Also, this result may have been found as irrigation canals were built a long time ago and the soils around these canals have become very saline. Areas around these irrigation networks showed less

agricultural growth. Thus, the new plantations have been established away from these canals in order to avoid the soil salinity problem.

In addition, our results showed that the effects of the two physical factors (i.e., slope and elevation) on agricultural growth, varied over time. Elevation and slope showed low negative effects on agricultural expansion in the past forty-five years, indicating that these factors limited the distribution of agricultural expansion. However, the effects of these variables became greater in 2015. This change in the magnitude of the effects of these physical factors on agricultural expansion reflects the fact that agricultural lands in areas with rugged terrain are often abandoned since they experience higher cultivation costs. However, the influence of elevation and slope may decrease in the future due to the advancement of technology which with low relative cost can simplify construction on locations with high elevations and steep slopes, and therefore increase the probability of agricultural expansion in such areas, as well as reducing the availability of low-slope land.

Undoubtedly, in agricultural markets, distance to roads is an important factor because it relates to the mobility cost of agricultural input and output markets. However, from an environmental perspective, while some research found nearest road distance has an effect on agriculture (e.g., loss of agricultural land to human settlements) (De Espindola et al., 2012), our result contradicted this. This result may be because most of the growth in the past has been in areas around road access points as those areas were virgin land. Therefore, the soil nutrients were still good and soil was not saline. This can be an attractive draw card for the land to be reclaimed close to roads. Also, this finding may be due to the land tenure security or conservation easements placed on these agricultural lands. These contributions restrict and prevent the converting of agricultural land adjacent to roads to other uses (e.g., residential uses). However, the probability of agricultural growth is unlikely to happen close to roads in future because most of those areas closer to roads have been used in the past, and the

soil quality near roads has changed significantly over time as soil organic matter, the contents of clay particle, and other nutrient contents declined. Therefore, areas close to roads will not be attractive for agricultural reclamation in the future. Thus, in the study area, the future direction of agricultural lands is likely to be away from roads.

The analysis also indicates that soil salinity had a significant negative effect on agricultural growth. This is logical because a high level of salts in the soil decreases plant growth due to the water-deficit effect, specific-ion toxicities and nutritional imbalances or a combination of these factors. Although there is a great variation in salt tolerance of plants and crops, most normal crops and plants cannot tolerate high levels of salinity and will eventually die under saline conditions. Thus, the probability for agricultural growth to occur in such conditions is much lower. In order to ensure long term agricultural growth and stability, farmers prefer to crop on non-saline soils, as good soil is considered the first essential step to growing healthy plants.

In this study the logistic regression model had the ability to predict agricultural growth. However, it has been reported that the ideal way to test the reliability of the prediction model is to develop a model based on the change over a one-time period and to apply the model to predict the probabilities of the change after the second time period. Then the model is tested by comparing the predicted change with the observed change at the second time (Aspinall, 2004). In this study applying the model to predict agricultural growth in 1985 offered the researchers an opportunity to test the ability of the model to predict agricultural probabilities based on 2015 agricultural growth. The results of agriculture probability maps based on 1985 agricultural change and the selected driving forces showed higher predictors compared with the actual agricultural growth in 2015. This result means that the model that was applied to predict the probable areas of agriculture after 2015 provides consistent and accurate

probabilities of agricultural growth. Consequently, multi-temporal datasets offer a technique to compare actual and simulated agricultural growth.

Overall, logistic regression showed that distance to water, distance to built-up areas and soil salinity are the main factors controlling agricultural growth. These factors will probably continue to have significant implications on agricultural growth in the future if no action is taken to overcome these problems. Consequently, the loss of agricultural land due to residential use or the abandoning of agricultural land, both due to water security or soil salinity, will enhance evaporation and promote more salinity. These mutually inclusive effects, along with the lack of awareness and education about the loss of agricultural land, will result in the reduction of suitable land for future agricultural growth and will have economic and social impacts as this Oasis is an important source of income for the government as well as local farmers. Thus, the finding reported in this study provides a useful starting point to understanding the past and present spatial dimensions of agricultural areas, the driving forces behind agricultural growth and the likely future occurrences of farming, so that the government and agricultural organizations can formulate sustainable future planning strategies and policies, which in turn can effectively lead to the conservation and development of the agricultural sector.

6.7 Conclusions

It is increasingly important to have a spatially explicit understanding of the agricultural growth process, along with knowledge of its underlying drivers in order to achieve long-term sustainable agriculture. Agricultural organizations and environmental managers need a definitive answer to the question as to what factors have an impact on the expansion of agricultural growth. Misunderstanding the spatial distribution of agricultural land and its underlying driving factors in the past and the present will result in unpredictable expansion and

economic growth in the future. This study tried to address this question by examining the effect of the physical and proximity factors on agricultural expansion in the Al Hassa Oasis in 1985 and 2015 using satellite data and a logistic regression model.

This study highlighted that integration of satellite images and regression statistical analysis (e.g., logistic regression) is an efficient and effective tool in enhancing our understanding of the trend and distribution of future agricultural expansion. It also provides vital information on the variables that most affected agricultural expansion in the past and will most affect it in the future. The results revealed that among the investigated factors, distance to water, distance to built-up areas and soil salinity were the major factors that had effects on agricultural growth. The current results suggest that agriculture in the Al Hassa Oasis is likely to develop on non-saline soil near to water resources but far from built-up areas.

Although the logistic regression model in this study showed promising results for modelling agricultural area, it does not have the ability to indicate when agricultural expansion will occur. In addition, the potential productivity of agricultural land is usually indicated by natural conditions and climatic variables such as temperature. However, climatic variables were not included in this study due to limitations in the availability of these data. Thus, further research is needed to develop a potential distribution model for agricultural expansion in the future based on the incorporation of climatic and non-climatic variables.

**Higher Degree Research Thesis by Publication
University of New England**

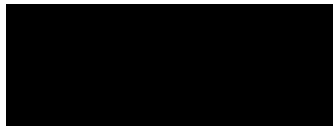
STATEMENT OF ORIGINALITY

We, the Research Master/PhD candidate and the candidate's Principal Supervisor, certify that the following text, figures and diagrams are the candidate's original work.

Type of work	Page number/s
Figure 6.1	118
Figure 6.2	122
Figure 6.3	127
Figure 6.4	128

Name of Candidate: Amal Allbed

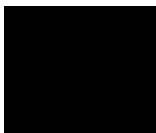
Name/title of Principal Supervisor: Professor Lalit Kumar



Candidate

20 June 2018

Date



Principal Supervisor

20 June 2018

Date

**Higher Degree Research Thesis by Publication
University of New England**

STATEMENT OF AUTHORS' CONTRIBUTION

We, the Research Master/PhD candidate and the candidate's Principal Supervisor, certify that all co-authors have consented to their work being included in the thesis and they have accepted the candidate's contribution as indicated in the *Statement of Originality*.

	Author's Name (please print clearly)	% of contribution
Candidate	Amal Allbed	80
Other Authors	Lalit Kumar	10
	Abdullah Alqurashi	10

Name of Candidate: Amal Allbed

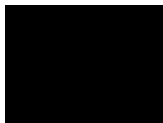
Name/title of Principal Supervisor: Professor Lalit Kumar



Candidate

20 June 2018

Date



Principal Supervisor

20 June 2018

Date

Chapter 7 Climate Change Impacts on Date Palm Cultivation in Saudi Arabia

This chapter has been published as:

Allbed, A., Kumar, L., & Shabani, F. (2017). Climate change impacts on date palm cultivation in Saudi Arabia. *The Journal of Agricultural Science*, 1-16. doi: 10.1017/S0021859617000260.

7.1 Summary

Date palm (*Phoenix dactylifera* L.) is an important cash crop in many countries, including Saudi Arabia. Understanding the likely potential distribution of this crop under current and future climate scenarios will enable environmental managers to prepare appropriate strategies to manage the changes. In the current study, the simulation model CLIMEX was used to develop a niche model to estimate the impacts of climate change on the current and future potential distribution of date palm. Two Global Climate Models (GCMs), CSIRO-Mk3.0 and MIROC-H under the A2 emission scenario for 2050 and 2100, were used to assess the impacts of climate change. A sensitivity analysis was conducted to identify which model parameters had the most effect on date palm distribution. Further refinements of the potential distributions were performed through the integration of six non-climatic parameters in a Geographic Information System (GIS). Areas containing suitable soil taxonomy, soil texture, soil salinity, land use, landform and slopes of less than 7° for date palm were selected as suitable refining variables in order to achieve more realistic models. The results from both GCMs exhibited a significant reduction in climatic suitability for date palm cultivation in Saudi Arabia by 2100. Climate sensitivity analysis indicates that the Lower optimal soil moisture (SM1), Cold Stress Temperature Threshold (TTCS) and Wet stress threshold (SMWS) parameters had the most effect on sensitivity, while other parameters were moderately sensitive or insensitive to change. The study also demonstrated that the inclusion of non-climatic parameters with CLIMEX outputs increased the explanatory power of the models. Such models can provide early warning scenarios for how environmental managers should respond to changes in the distribution of the date palm in Saudi Arabia.

7.2 Introduction

Date palm (*Phoenix dactylifera* L.) is an important fruit crop in the palm family (Arecaceae) grown in the arid and semi-arid regions of the world, including Saudi Arabia. Date palm is one of the most important cash crops that contributes significantly to agroecosystems in Saudi Arabia and plays a major role in the national economy and agricultural sector through its contribution to economic growth, and meeting local market needs. There are more than 400 date palm cultivars in Saudi Arabia and each region is characterized by certain cultivars, but only approximately 50–60 cultivars are used commercially (Mikki, 1998). Saudi Arabia is considered one of the top three date producing countries in the world. In 2013, date production in Saudi Arabia reached 1 065 032 tonnes, from 3.7 million trees (FAOSTAT, 2013). However, despite great government support and attention to date palm cultivation in Saudi Arabia, the level of date productivity remains low compared to other date-producing countries, and exports of dates have not reached the expected level (Aleid et al., 2015). A number of factors could be behind this reduction, such as plant diseases, insect pests as well as environmental stress factors including salinity, drought and temperature extremes as a result of climate change.

Changes in climate have serious implications in the agricultural sector due to direct exposure to and dependence on weather conditions, both of agriculture and other natural resources (Yu et al., 2010a). A substantial number of studies have been conducted on the impacts of climate change on agricultural productivity. As an example, it has been reported that climate change could lower agricultural productivity in four agricultural sectors (paddy rice, wheat, other grains and other crops) in Southeast Asia, specifically by 15–26% in Thailand, 2–15% in Vietnam, 12–23% in the Philippines and 6–18% in Indonesia (Zhai and Zhuang, 2012). In some countries, it has been projected that reductions in yields from rain-fed agriculture could reach as high as 50% by 2020 (Field et al., 2012b). In addition, a 40% decline in agricultural

productivity by the 2080 is expected in India as a result of climate change has been documented by IPCC (2007).

Saudi Arabia is one of those countries that are highly vulnerable to the adverse effects of climate change, due to its arid climate. It has been predicted that the average temperatures in Saudi Arabia would increase by as much as 6.0°C by 2100 as a consequence of climate change, and the crop irrigation water demands would rise by about 602 and 3122 million cubic meter (MCM) at 1°C and 5°C increases, respectively, and the expected yield of different types of field fruit trees and crops will experience losses that range from 5% to > 25% (Zatari, 2011). This means that climate change is expected to impact heavily on agriculture and food production in Saudi Arabia, especially through reducing water availability and direct effects on crop yields. For example, during the 2010 season many farmers noticed unusual early blooming of date palm as a direct consequence of climate change (Assiri and Darfaoui, 2009). To deal with such change, optimizing the cropping pattern in Saudi Arabia according to the regional competitive advantage was considered as one of the actions to adapt to the adverse effects of climate change. Alabdulkader et al. (2016) applied a mathematical sector model to optimize the date palm cropping pattern using limited water resources and cultivated lands. The results showed great potential for Saudi Arabia to adapt to the adverse effects of climate change by optimizing date palm cropping in accordance with its scarce water resources and limited cultivated lands.

Climate change may also impact an economy directly by affecting its agricultural outputs. For instance, it has been reported that maize production in Africa and South America could decline by 10% by 2055, causing a loss of \$2 billion per year due to climate change (Jones and Thornton, 2003). Moreover, the total annual income from date palms in Middle Eastern countries has declined from 1990 to 2000 due to plant diseases and water shortages resulting from climate change (Zaid and Arias Jiménez, 1999). Currently, at a global scale, 0.20–0.25 of harvested crops are lost due to harvest disease and these losses are expected to rise with climate

change (Dixon, 2012). Consequently, food security will be affected and the global and regional agricultural productivity will be negatively impacted. Added to this, climate change is very likely to have significant impacts on the distribution, quantity and quality of global agricultural production (Thung and Rao, 1999; Wheeler and Von Braun, 2013).

Decision makers should prepare management strategies that address climate change impacts on agriculture to achieve long-term sustainable production of cash crops such as date palm. Thus, information on the potential distribution of the species and the relative abundance under projected future climate scenarios is essential. A variety of distribution models have been used to study the effect of climate change on species distribution, including bioclimate envelope models (e.g. Spatial Evaluator of Climate Impacts on the Envelope of Species (SPECIES)) (Hampe, 2004), global climate models (GCMs) (e.g. UKMO-HadCM3, GFDL-CM2.0 and MIROC3.2) (Porfirio et al., 2014), ecological niche models (ENMs) (e.g. Generalized Linear Model (GLM)) (Silva et al., 2014), MaxEnt (Nazeri et al., 2012), Random Forest (RF) (Vincenzi et al., 2011), Boosted Regression Tree (BRT) (Radinger et al., 2015) and CLIMEX (Aljaryian et al., 2016; Shabani et al., 2016). CLIMEX, a mechanistic model, is a well-known climate modelling software for predicting species' responses to climate change due to its extensive phenological observations and geographic range (Sutherst et al., 2007). With CLIMEX, users can detect areas where selected species can be established and maintained or developed based on predicted climate changes. CLIMEX has been extensively used in multiple applications; some examples include projecting crop diseases such as *Fusarium oxysporum* f. spp. (Shabani et al., 2014a), determining the impact of climate change on invasive weeds such as *Lantana camara* L. (Taylor et al., 2012b) and illustrating the potential distribution of the common bean (Ramirez-Cabral et al., 2016), among other applications.

Most studies examining climate change effects on species using CLIMEX often use climate variables alone and exclude non-climatic parameters such as soil type, land use and topography.

Hence, it is possible that some projected suitable regions for specifically studied species may be inaccurate, and may be unsuitable with regard to non-climatic parameters. Therefore, to overcome this limitation, incorporation of climatic and non-climatic parameters has been suggested to achieve greater accuracy and more robust results, since the results must satisfy more extensive requirements (Sutherst et al., 2007; Beaumont et al., 2008). As an example, Cheng et al. (2006) found that the combination of biotic and non-biotic factors led to a significant improvement in the prediction of potential distribution of *F. occidentalis* in China compared to prediction by climate variables alone. Additionally, Shabani et al. (2014b) projected date palm distribution at the national level for Iran by including non-climatic parameters such as land use, topography and soil taxonomy, only 220 000 km² would be suitable for date palm cultivation, compared to 610 000 km² based on climatic suitability. In other words, the incorporation of climatic and non-climatic factors is the key, and provides better results than models based purely on climatic factors when assessing the impact of climate change on predicting the future distribution and fate of economically important crops, such as date palm.

The above-mentioned studies provide evidence that climate change represents a massive threat to plant and crop distribution. It is highly likely that the productivity potential of some regions will increase while others will decrease as a result of climate change and unsuitability due to abiotic factors (e.g. slope, soil texture, soil taxonomy, soil salinity and land use). Therefore, it is vital to consider the impact of both climatic and non-climatic parameters when predicting the potential future distribution of the species. The main objectives of the current study were to (i) develop climatic models of date palm in Saudi Arabia for the current time, 2050 and 2100; (ii) find the main climatic stresses that may drastically affect date palm in Saudi Arabia by 2050 and 2100; (iii) refine the projection based on suitability of soil taxonomy, soil texture, soil salinity, slope and land use to find areas that are practical, accurate and possible to cultivate

date palm; and (iv) identify the most sensitive climatic parameters through a sensitivity analysis. The models will be used to investigate how these changes will impact the potential future distribution of date palm in Saudi Arabia. It is assumed that climate change will alter the agricultural areas that currently produce date palm. Model results from the current study will benefit governments and decision makers by preparing for the circumstances ahead, and along this line increase economic advantages that can help enhance local economies. Even more importantly, those managing areas that could become unfavourable can be made aware of the circumstances and the likely change to their economies, providing a chance to plan for other sources of income.

7.3 Materials and Methods

7.3.1 Current Distribution of Date Palm (*Phoenix dactylifera* L.)

Information on the current geographical distribution and locations of *P. dactylifera* are essential for modelling the future distribution of this crop. Based on *P. dactylifera* literature in the CAB Abstracts databases (e.g., Al Hammadi, 2006; Bokhary, 2010; Al-Senaïdy and Ismael, 2011; Shabani et al., 2012; Shabani and Kumar, 2013; Shabani et al., 2014b, 2014c) and the Global Biodiversity Information Facility (GBIF), date palm can be found worldwide in large parts of northern and central Algeria; south-eastern Spain; Sudan; Australia; south-western USA; Greece; north-western Libya; north-eastern Egypt; south-western, southern and south-eastern Iran; Yemen; India; Oman; and in central, northern, eastern, southern, western and south-western Saudi Arabia.

In the present study, an attempt has been made to maximize the number of occurrences in Saudi Arabia to improve the accuracy of model predictions. Model predictions were based on satellite images available from the United States Geological Survey (USGS) database and GBIF along with data acquired from the Center of Palms and Dates Research, the National Center for Palms

and Dates (NCPD) and the Ministry of Agriculture in Saudi Arabia. A total of 930 records were collected, only 460 of which were used after excluding duplicate points and records with no geographic coordinates. This step is an important part of data quality control, as only verified location points with geographic coordinates can be used in the parameter fitting procedure. Thus, 460 records were used in parameter fitting (Figure 7.1).

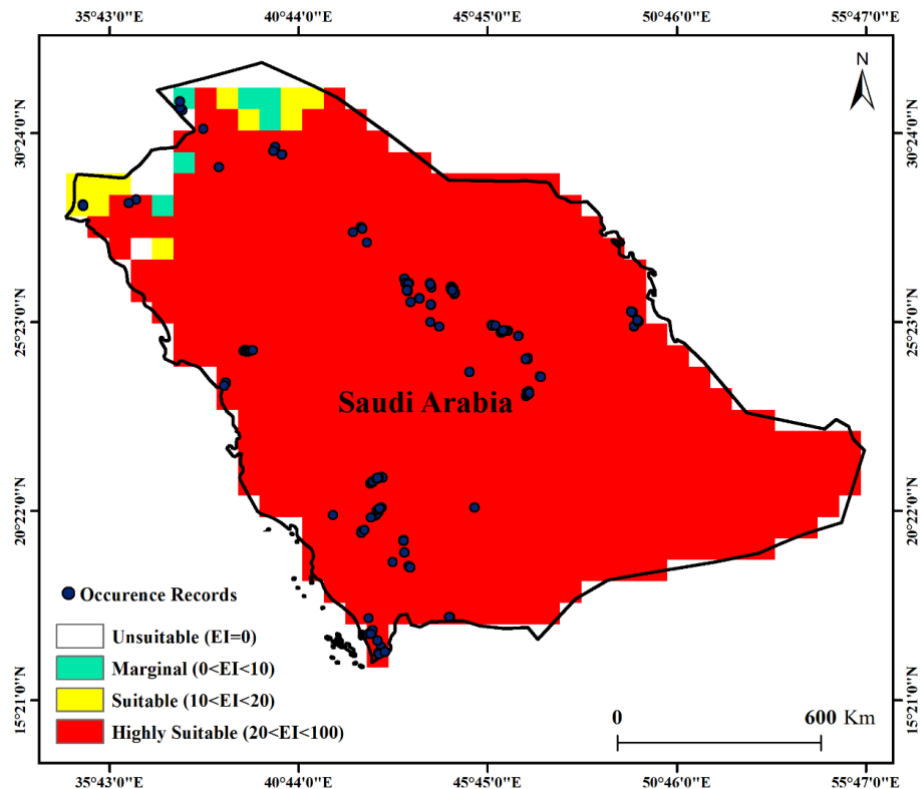


Figure 7.1 Current and modelled potential distribution of *P. dactylifera* in Saudi Arabia. EI, eco-climatic index; *P. dactylifera*, *Phoenix dactylifera*

7.3.2 CLIMEX Software

CLIMEX is an eco-climatic modelling package used to describe the relationship between the current and projected niche of any species (Wharton and Kriticos, 2004; Kriticos et al., 2005). Basically, it predicts the potential distribution and relative abundance of a species in a new region using climatic information, biological data and the known geographic distribution of that species. Climate predictions can be made at regional and world scales (Sutherst et al., 2007). This method assumes that species populations increase during suitable climate seasons

and decrease during unsuitable seasons. CLIMEX uses different indices that are grouped into growth-related and stress-related indices to predict the potential growth and survival of a species at a given location. The potential population growth during favourable seasons is described by an annual growth index (GI_A), while four stress indices (SI) (Cold, Hot, Wet and Dry Stresses) describe the population survival possibility during unfavourable seasons (Sutherst et al., 2007). The GI_A is determined from different growth indices, including the temperature index (TI) and the moisture index (MI) that describe the species' temperature and soil moisture requirements for population growth. The four climatic parameters used to describe the suitable temperature for population growth are DV0 and DV3 (limiting low and high temperatures, respectively) and DV1 and DV2 (lower and upper optimal temperatures, respectively). Similarly, the MI comprises four climatic parameters, which are SM0 and SM3 (limiting low and high soil moisture, respectively), and SM1 and SM2 (lower and upper optimal soil moisture, respectively). These indices, TI and MI, are multiplied to provide a weekly growth index and the yearly average of this gives the GI_A . The stress indices, Cold, Hot, Wet and Dry Stresses, are combinations of the two parameters, the threshold value, and the stress accumulation rate. Stress accumulation during the year is exponential and once this value equals 1, the species will be unable to survive in that geographic region (Sutherst et al., 2007).

The model combines these growth and stress indices into an overall eco-climatic index (EI) that represents the suitability of the location for the species under various climate change scenarios as a number between 0 and 100. If the EI value is close to 0, it indicates that a site is unsuitable for the species, values from 0 to 10 indicate marginal habitats, values from 10 to 20 indicate a suitable climate area, and EI values > 20 indicate optimal conditions for the species (Sutherst and Maywald, 2005). The outcome models provided by CLIMEX will predict almost

all climatically suitable areas for date palm and provide early risk assessments to decision makers about the potential effects of climate change on this essential crop.

7.3.3 Climate Data, Global Climate Models and Climate Change Scenarios

CLIMEX for Windows, version 5 was used to develop potential distribution models for date palm under two future climate scenarios, 2050 and 2100, chosen to provide snapshots of climate change projections for the near and further future, respectively. The CliMond 10' gridded climate data (http://www.hearne.com.au/Software/CLIMEX/Edits#version_CLIMEX_3.0.2) were used to model the potential distribution of date palm. To project potential future climate in 2050 and 2100, overall minimum and maximum monthly temperatures (T_{\min} and T_{\max} , respectively), overall monthly precipitation (P_{total}) and the relative humidity at 09:00 h ($RH_{9:00}$) and 15:00 h ($RH_{15:00}$) were used. The potential distribution of date palms under future climate was based on two different Global Climate Models (GCMs), namely, CSIRO-Mk3.0 (CS) and MIROC-H (MR) (Center for Climate Research, Japan), available as part of the CliMond datasets.

These two models were selected from 23 GCMs because of the availability of temperature, precipitation, mean sea level (MSL) pressure and specific humidity, which are required for CLIMEX (Nakicenovic et al., 2000). Moreover, the models contain relatively small horizontal grid spacing and performed well compared to other GCMs in representing the core aspects of the observed climate at a regional scale, according to Taylor et al. (2012b) and Kriticos et al. (2012). The A2 emission scenario was selected in the current study because it includes different variables such as financial, demography and technological forces driving greenhouse gas (GHG) emissions. The A2 emission scenario considers a world with higher population growth but slower economic growth and technological changes, and assumes moderate global GHG

emissions compared to the other emissions scenarios such as A1F1, A1B, B2, A1T and B1 by 2100 (Suppiah et al., 2007; Kriticos et al., 2012; Taylor et al., 2012b).

7.3.4 Fitting CLIMEX Parameters

The basic CLIMEX parameter values for date palm modelling were taken from Shabani et al. (2012). For a detailed description of these CLIMEX parameters and the procedure by which they were selected, refer to Shabani et al. (2012). In the current study, to ensure all date palm occurrences were within the suitable groups of climate in Saudi Arabia, 6 out of 14 parameters were slightly modified based on current date palm occurrence, including SM0, SM1, SM2, the cold stress temperature threshold (TTCS), the cold stress temperature rate (THCS) and the wet stress rate (HWS). Temperature and moisture response parameter values were then transformed into CLIMEX compatible Temperature and Moisture Index parameters and Cold, Heat, Dry and Wet stress threshold values.

The CLIMEX parameter values that were used for *P. dactylifera* were set as follows: DV0 at 14°C, DV1 at 20°C, DV2 at 39°C, DV3 at 46°C, SM0 at 0.007, SM1 at 0.014, SM2 at 0.82, SM3 at 0.9, the cold stress temperature threshold (TTCS) at 4°C, the cold stress temperature rate (THCS) at -0.011/week, the heat stress parameter threshold (TTHS) at 46°C, the heat stress accumulation rate (THHS) at 0.9/week, the wet stress threshold (SMWS) at 0.9, and the wet stress rate at 0.024/week. The fitted parameters were then used to project the date palm's potential distribution in Saudi Arabia under two future climate scenarios in 2050 and 2100. The data sets were output from CLIMEX and imported into GIS software (ArcGIS Software Version 10.2) for further processing and mapping. All locations were classified into two classes of suitability for date palm using EI values. Locations with EI = 0 were classified as unsuitable while EI > 0 were classified as suitable.

7.3.5 Non-Climatic Parameters

7.3.5.1 Soil Taxonomy

To define the current extent of date palm cultivation in Saudi Arabia, Landsat satellite images with 30 m spatial resolution were used. The general soil map of Saudi Arabia (1:4 000 000) obtained from the Ministry of Agriculture, which represents soil taxonomy, was used to extract all soil types that are suitable for date palm cultivation by overlaying the date palm observation layer onto the soil map. The results identified 9 out of 12 suitable soil types, namely: Calciorthids, Camborthids, Gypsiorthids-Calciorthids, Haplaquepts-Eutrochrepts, Torriorthents, Salorthids, Torrifuvents-Torripsamments-Calciorthids, Torriorthents-Calciorthids, and Torripsamments-Torriorthents. The details of all the soil types can be found in Soil Survey Staff (2010).

7.3.5.2 Soil Texture

The soil texture map of Saudi Arabia (1:4,000,000) was obtained from the Ministry of Agriculture. To determine which soil textures are suitable for date palm growth and cultivation, the locations of date palm observations were considered, and the date palm occurrences were overlaid onto the soil texture map. The results revealed that the soil textures suitable for date palm cultivation in Saudi Arabia are sand; sandy loam comprising 60% sand, 10% clay and 30% silt; loam soil comprising 40% sand, 40% silt, and 20% clay; and clay loam comprising 40% sand, 30% silt and 30% clay. This is supported by the fact that date palm is not sensitive to soil types and can grow in a range of diverse types of soil from sand, sandy loam, and clays to heavy alluvial soils (Morton and Dowling, 1987; Lim, 2012).

7.3.5.3 Soil Salinity

Date palm is considered to have the highest salt tolerance of all fruit crops: some date palm varieties can adapt to levels of soil salinity up to 12.8 dS/m (Ramoliya and Pandey, 2003) while

others can tolerate much higher levels, up to 34 dS/m (Abbas et al., 2015). Nevertheless, excessive salt can cause significant reductions in the growth, yield and fruit quality of date palm (Erskine et al., 2004). Ayers and Westcot (1985) reported that the minimum electrical conductivity (EC) to have maximum yield for date palm is 4.0 dS/m, while the plant produced no yield at the EC of 32 dS/m. Additionally, a study conducted by Alrasbi et al. (2010) indicated that decreases of 53, 48, 39 and 46% occurred in date palm trunk height, number of fronds, leaf length and trunk girth, respectively, at an EC of 18 dS/m. Thus, it is clear that date palm plants will be affected negatively when soil salinity extends beyond its tolerance potential. In the current study, a soil salinity map of Saudi Arabia obtained from the Harmonized World Soil Database (HWSD) was used to extract all soil salinity levels suitable for date palm. Thus, areas with soil salinity of 4–16 dS/m were considered as suitable while areas with soil salinity > 16 dS/m were considered unsuitable.

7.3.5.4 Land Use

The most suitable land uses were targeted based on the current land use map of the country, obtained from the Food and Agriculture Organization (FAO) geo-network, and the current distribution of date palm. Agricultural land including cropland, sparsely vegetated areas, irrigated lands and managed bare area were considered suitable for date palm cultivation. The remaining land use types, such as urban areas, mountains, wetland, road and commercial sites were considered unsuitable land use types.

7.3.5.5 Landform

Date palm is characterized by a deep root system that reaches horizontally up to 25 m away from the trunk, and vertically more than 6 m deep, which helps to hold down the soil and take up water and nutrients stored deep underground (Zaid and Arias Jiménez, 1999). In the current study, based on the current landform map of the country, obtained from the Ministry of

Agriculture, and the current distribution of date palm, attempts were made to find possible land forms that enable date palm to establish its deep network of roots. Thus, pediplain, gypseous pediplain, degraded pediplain, sand sheet, sand dunes, alluvial fans, alluvial plain and wadi were identified as potentially suitable for date palm growth and its root establishment and distribution.

7.3.5.6 Slope

The Advanced Spaceborne Thermal Emission and Reflection Radiometer (ASTER) digital elevation model (DEM) of Saudi Arabia at 30 m spatial resolution, obtained from the King Abdul-Aziz City of Science and Technology in Saudi Arabia, was used to generate a slope surface map. By considering the location of each date palm farm, 0.90 of the locations were found on slopes $< 7^\circ$. These areas were considered as suitable for date palm growth while areas with slopes $> 7^\circ$ were considered unsuitable. This is supported by the fact that steeply sloped areas will affect date palm growth by affecting run-off, insolation, temperature, moisture and depth of the soil. The steeper the slope, the greater the run-off and soil erosion. Further, the intensity of insolation, temperature, moisture of the soil surface, and depth of soil varies with increasing slope (Dash, 2001). Additionally, various studies report that lands with slopes $> 10^\circ$ are unsuitable for a date palm plantation (Salah et al., 2001; Chao and Krueger, 2007; Jain, 2011). Subsequently, the classified slope data in raster format were converted to polygon shape files and queries were designed using attributes and date palm locations to extract those areas demonstrating suitable slope.

7.3.6 Refining the CLIMEX Outputs

CLIMEX outputs from both the CS and MR GCMs for 2050 and 2100 were overlaid on the location of areas comprising suitable soil taxonomy, soil texture, soil salinity, land use, landform and slope for the whole country. Locations that satisfied the condition of $EI > 0$ and

all the above environmental conditions were selected and extracted, using ArcGIS software, as areas suitable for date palm cultivation, while areas with $EI = 0$ were classified as unsuitable.

7.3.7 Climate Sensitivity Analysis

Sensitivity analysis is an effective tool to identify the input parameters that are most influential to model predictions. The latest version of CLIMEX software (Version 5) has a newly developed climate sensitivity analysis function. This function adjusts the fitted parameter values upward and then downward by a certain amount, then the impact on the species range and a set of selected state variables is determined. Most of the variables (e.g. TI Change, CS Change and HS Change) describe the mean sum square change of the index value (e.g. EI) at all given locations and are included in the sensitivity analysis. CLIMEX presents the results of the sensitivity analysis to users in a table that shows all the parameters, the amount by which they have been adjusted on both sides, and the effect of this adjustment on those particular variables. Parameters found to have significant influence on model results when they are adjusted are those that are considered sensitive.

In the current study, by using the newly developed function, a sensitivity analysis was performed to quantify the response of date palm to the 14 parameters used in the model. From the baseline model, different incremental models were developed to reflect the possible range of these variables that might occur in Saudi Arabia. During this procedure, only one parameter was adjusted at a time, while all other parameters were held constant as in the baseline model.

7.4 Results

7.4.1 Current Climate







The current and potential distribution of *P. dactylifera* in Saudi Arabia is shown in Figure 7.1. The map illustrates that current distribution is consistent with the EI values of the CLIMEX

model. The modelled result indicated that the majority (0.95) of the *P. dactylifera* records fall within the highly suitable category, which confirms that the selected values for the different parameters in CLIMEX were optimum. Further, the CLIMEX projection shows only 1.95 million ha in the northern and north-western parts of the country as having marginal climatic conditions with EI values between 1 and 10.

7.4.2 Non-Climate Parameters

Table 7.1 shows the suitable and unsuitable areas for date palm cultivation in Saudi Arabia based on non-climatic parameters. Considering the suitability of soil taxonomy in Saudi Arabia, results showed that approximately 0.75 of the area is suitable for date palm cultivation. Only portions of the western part of the country are unsuitable in terms of soil taxonomy. Additionally, a large area of approximately 167.40 million ha is suitable for date palm cultivation in terms of soil texture and spans the country, and only approximately 0.22 of the area was defined as unsuitable. Furthermore, the current results highlight that portions of eastern, western and northern Saudi Arabia have soils with salinities > 16 dS/m, which indicates that the soil in these parts is unsuitable for date palm growth. The area of suitable land use indicates that the majority of the northern, eastern and southern sectors of Saudi Arabia have suitable land use classes that are conducive to date palm growth. Only some areas in the western part of the country are not suitable. The results identified approximately 125.59 million ha in Saudi Arabia with suitable landforms that are conducive for date palm growth. Suitable landform areas were mainly located in the southern to the north-eastern part, while those areas in the western region do not meet the landform date palm cultivation requirements. Moreover, almost the whole country has a suitable slope, which is $< 7^\circ$, excluding only the mountainous regions.

Table 7.1 Suitable and unsuitable area for *P. dactylifera* cultivation in Saudi Arabia based on non-climatic parameters

Non-climatic parameters	Suitable area		Unsuitable area		Location
	(million ha)	(%)	(million ha)	(%)	
Soil Taxonomy	162.27	0.75	52.73	0.25	
Soil Texture	167.40	0.78	47.60	0.22	
Soil Salinity	153.57	0.71	61.43	0.29	
Land Use	172.82	0.80	42.18	0.20	
Landform	125.59	0.58	89.41	0.42	
Slope	170.93	0.80	44.07	0.21	

 Suitable  Unsuitable

P. dactylifera, *Phoenix dactylifera*.

7.4.3 Future Climate Projections Based on Climate

The modelling results of the CS and MR GCMs under the A2 emission scenario forecasting the optimal distribution of *P. dactylifera* for 2050 and 2100 are illustrated in Figure 7.2. A quick comparison of the modelled maps for 2050 and the current time shows that there are no significant differences between the currently suitable areas for date palm cultivation and the result of CS and MR GCMs for 2050 based on climate alone. Both models agree that almost 0.95 of Saudi Arabia will remain climatically suitable for date palm cultivation by 2050.

However, both CS and MR GCMs project that large parts (0.70–0.75) of Saudi Arabia will become climatically unsuitable for date palm cultivation by 2100. The results of the CS GCM indicates that the total area conducive for date palm cultivation will decline to approximately 62.05 million ha by 2100 (Table 7.2). The same trend is also observed using MR GCM, which estimates a reduction of suitable areas to 79.16 million ha by 2100 (Table 7.2).

7.4.4 Refined Result

The potential distribution of date palm generated using both climate and non-climatic data with CS and MR GCMs demonstrates a general reduction of suitable area (Figure 7.2). Based on climate alone, the output of the CS and MR GCMs predicts that almost 0.95 of Saudi Arabia is projected to remain suitable for date palm growth by 2050. However, only 0.75 of this area is suitable for growth of date palm after considering non-climatic parameters. The refined CS and MR results show that approximately 80.17 and 80.46 million ha, respectively, will be highly conducive for this species to grow by 2050 (Table 7.2). By 2100, the situation is markedly less favourable when refining the CS and MR GCMs using the six non-climatic parameters. The refined results indicate that only approximately 0.15 of Saudi Arabia will be highly suitable for date palm cultivation by 2100. Changes in heat stress from current time to 2100 is shown in Figure 7.3. Figure 7.4 indicates the extent of agreement in the CLIMEX projection of suitable areas for *P. dactylifera* under CS and MR GCMs running the with A2 emission scenario for 2050 and 2100.

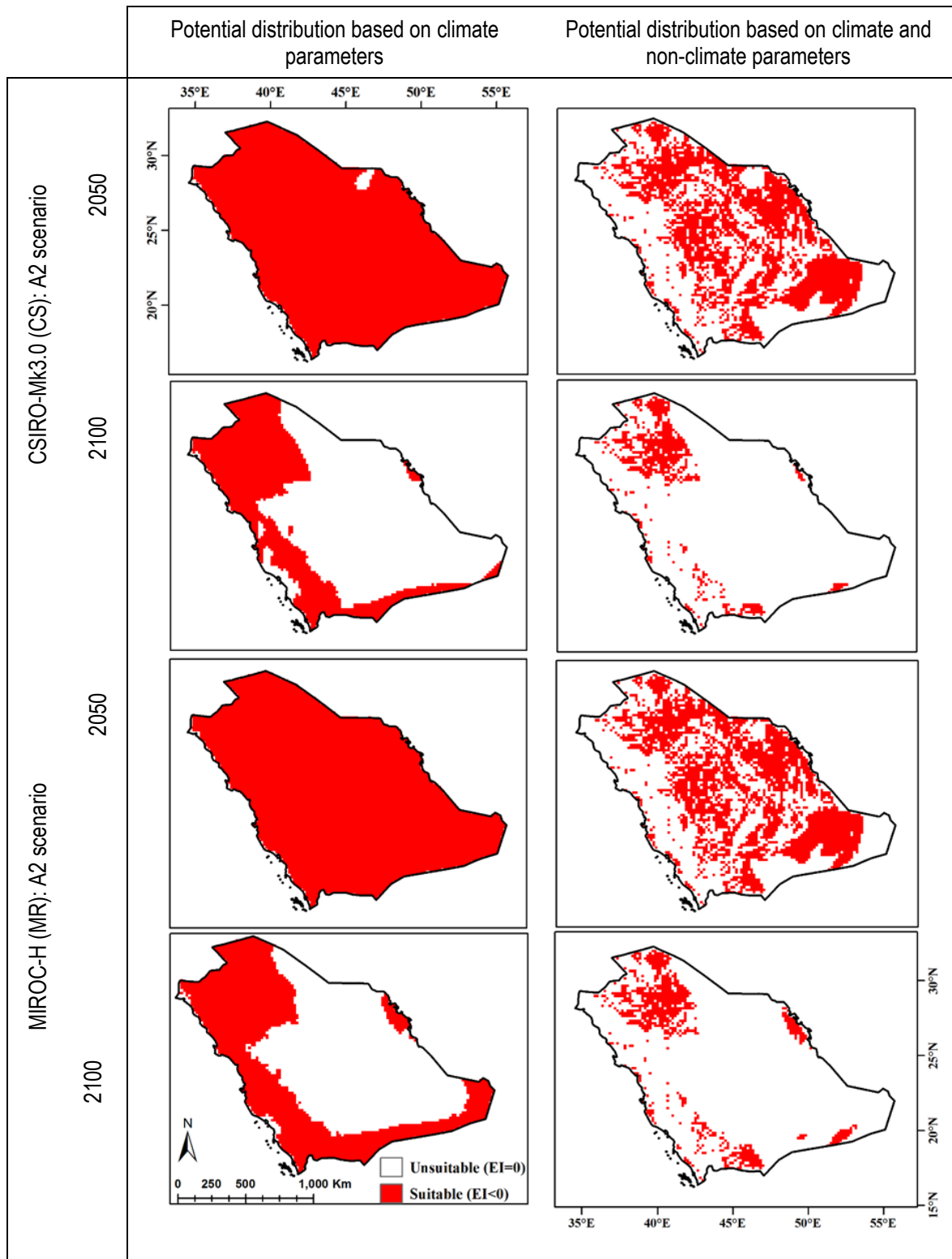


Figure 7.2 The EI for *P. dactylifera* for 2050 and 2100 under CS and MR GCMs running with the A2 emission scenario

Table 7.2 Results of CS and MR GCMs and the refined outputs using all suitable non-climate parameters for *P. dactylifera* cultivation for 2050 and 2100

Years	CS (million ha)	MR (million ha)	CS + Suitable non-climate parameters (million ha)	MR + Suitable non-climate Parameters (million ha)
2050	177.04	178.19	80.17	80.46
2100	62.05	79.16	17.95	22.77

CS, CSIRO-Mk3.0; MR, MIROC-H; *P. dactylifera*, *Phoenix dactylifera*

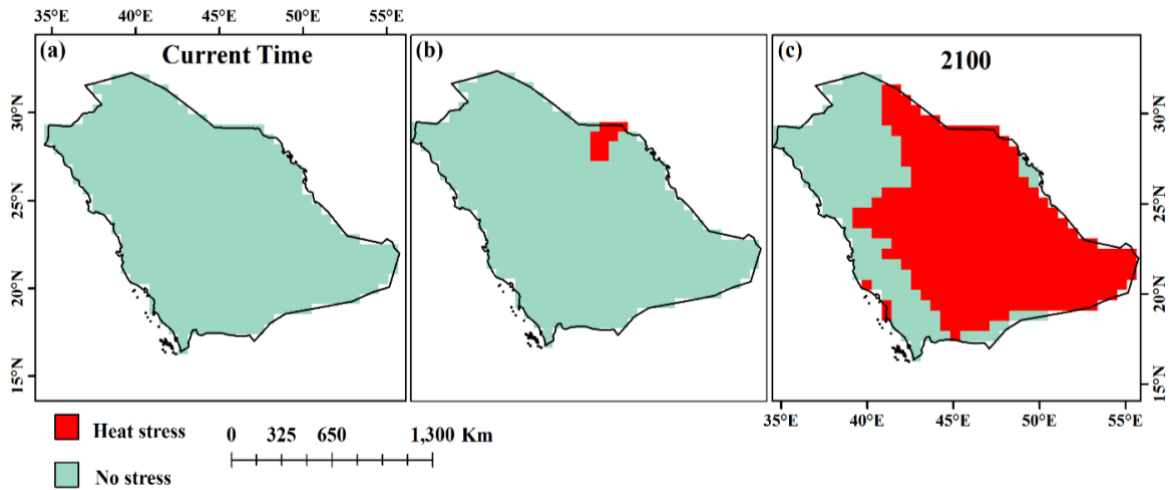


Figure 7.3 Changes in heat stress from current time to 2100

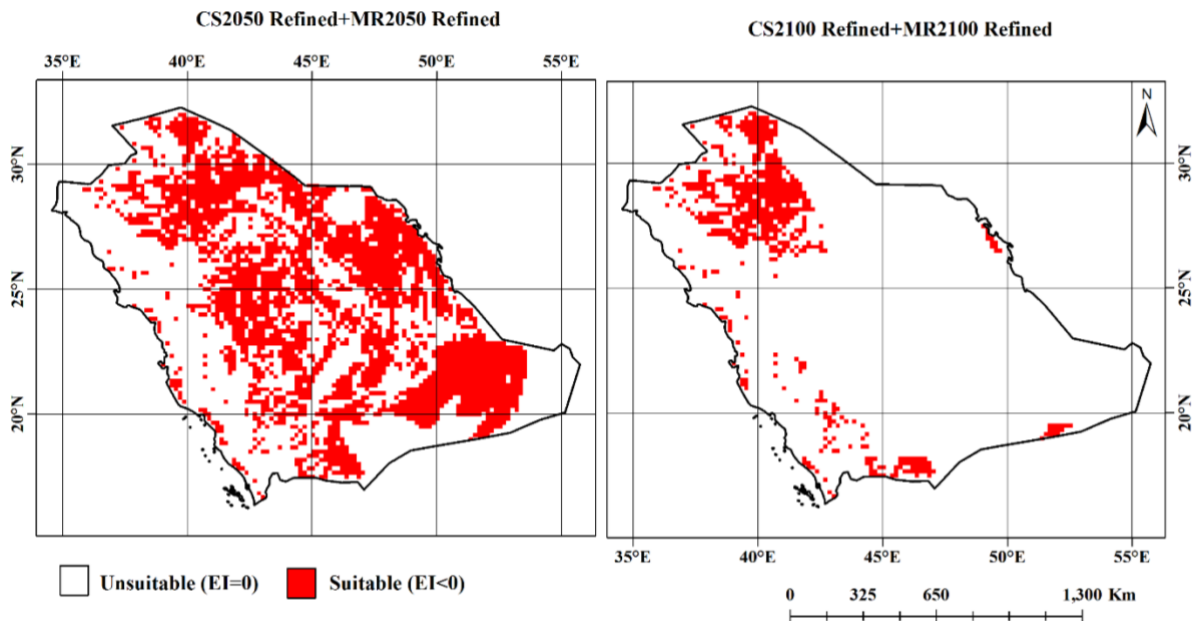


Figure 7.4 Agreement in the CLIMEX projection of suitable areas for *P. dactylifera* under CS and MR GCMs running with the A2 emission scenario for 2050 and 2100. CS, CSIRO-Mk3.0; EI, eco-climatic index; GCM, global climate model; MR, MIROC-H; *P. dactylifera*, *Phoenix dactylifera*

7.4.5 Sensitivity to Model Parameters

Table 7.3 shows that SM1, TTCS and SMWS are the most sensitive parameters influencing the modelled distributions of date palm in Saudi Arabia. Increasing the SM1, TTCS and SMWS to 0.0014%, 5°C and 1, respectively, led to the most profound effects on EI values. The EI change values were maximized by changing SM1, TTCS and SMWS parameters, to 13.97, 11.13 and 8% respectively. However, changes in SM0, DV1 and HWS resulted in lower changes in EI. An adjustment in these parameters had only moderate effects on the EI value changes. With changes to SM0, DV1 and HWS, EI values changed by 5.06, 4.02 and 3.64%, respectively. In other words, suitable areas for date palm cultivation changed less rapidly with SM0, DV1 and HWS adjustments from the baseline model. Additionally, alterations to the other parameters SM2, SM3, DV0, DV2, DV3, THCS and TTHS had little effect on the EI value, whereas changes in THHS had no effect on the EI value (Table 7.3).

Table 7.3 Sensitivity analysis of CLIMEX parameters of *P. dactylifera* model as change of eco-climatic index (EI)

Parameter	Code	Low	Default	High	Run	EI change
Limiting low moisture	SM0	0	0.007	0.013	1	5.06
Lower optimal moisture	SM1	0.007	0.014	0.113	2	13.97
Upper optimal moisture	SM2	0.71	0.82	0.9	3	1.28
Limiting high moisture	SM3	0.81	0.9	1	4	1.17
Limiting low temperature	DV0	13	14	15	5	1.12
Lower optimal temperature	DV1	19	20	21	6	4.02
Upper optimal temperature	DV2	38	39	40	7	0.7
Limiting high temperature	DV3	45	46	47	8	0.23
Cold Stress Temperature Threshold	TTCS	3	4	5	9	11.13
Cold Stress Temperature Rate	THCS	-0.012	-0.011	-0.008	10	1.97
Heat Stress Temperature Threshold	TTHS	45	46	47	11	1.01
Heat Stress Temperature Rate	THHS	0.72	0.9	1	12	0
Wet Stress Threshold	SMWS	0.81	0.9	1	13	7.94
Wet Stress Rate	HWS	0.0176	0.024	0.0264	14	3.64

7.5 Discussion

A niche model was developed using CLIMEX species distribution modelling to estimate date palm potential distribution under current and future climate scenarios. The results showed that under the current climate, large parts of Saudi Arabia are highly conducive to date palm growth and cultivation, and this agrees well with the observed distribution. The major reason for this highly suitable climate is because there are no heat, wet, cold or dry stressors in this region under the current climate. In addition, sensitivity analysis results revealed that *P. dactylifera* distribution is highly sensitive to changes in SM1, TTCS and SMWS parameters, and moderately sensitive to changes in SM0, DV1 and HWS parameters. These results contrasted with those of Shabani and Kumar (2014), who conducted a sensitivity analysis of CLIMEX parameters based on the Taguchi method of modelling the potential distribution of date palm in Iran and found that the distribution of date palm was highly sensitive to changes in DV3, DV3, SM2 and SM3, and slightly sensitive to changes in SM1, SM0, and SMWS parameters. These considerable differences between the current results and those of Shabani and Kumar (2014) are probably attributed to the different sensitivity analysis methods used.

Generally, climate change negatively affects plant growth and development via an increase of abiotic stresses (i.e., heat, cold, drought and wet). It has been reported that when global average temperature increases by $> 3.5^{\circ}\text{C}$, a significant extinction of plant species is expected due to lethal heat stress (IPCC, 2007). Extensive agricultural production losses have been attributed to disturbances in growth due to climate change-associated heat stress (Kotak et al., 2007). For example, it has been shown that exposure of *C. arabica* to changes in heat stress affects its growth and yield and raises the stachyose and raffinose levels during abiotic stress events (Drinnan and Menzel, 1995). Similarly, Shabani et al. (2014c) found that there will be a substantial reduction in suitable areas for date palm cultivation in central Iran as a consequence of increased heat stress by 2100. In the current study, when climate alone is considered, the

projection showed that 0.70 of the current date palm cultivation area is located in the central and southwestern parts of Saudi Arabia. These areas will remain climatically suitable for date palm cultivation since both GCMs indicate that date palms will not suffer from any dry, wet or cold stress by 2050. However, both MR and CS GCMs projected that the majority of the central regions will become unsuitable by 2100 as a result of a significant increase in heat stress. These changes will impose serious restrictions on date palm growth and development and eventually have a negative impact on society. Heat stress, similar to other abiotic stress, imposes adverse effects on different physiological processes of date palm such as germination, growth, development, reproduction and yield. At high temperatures, date palm seeds will still germinate but at a lower rate. However, when seedlings develop and are exposed to excessive heat, they may experience heat shock (Hadrami et al., 2011). Additionally, excessive heat over an extended period and during stages of fruit development can influence the quality of date palm (Jarvis et al., 2016). In areas where date palm thrives, high temperatures are responsible for an increase in soil evaporation and transpiration of the plant, which consequently induces low plant-water potentials and high transpiration rates (Hadrami et al., 2011). Heat stress can also cause injuries to the cell wall that can lead to a collapse of cellular organization (Schlesinger, 1990). These injuries eventually result in starvation, production of toxic compounds, reduction in ion flux, an increase of reactive oxygen species (ROS) and inhibition of plant growth (Wahid et al., 2007).

Climate has long been considered the main determinant of species distribution (Woodward, 1987). Nevertheless, different factors unrelated to climate (e.g. topography, land uses, soil types) often play a vital role in determining the patterns of species distribution. For example, species might be missing from sites within their climatic boundaries due to inappropriate resources under suitable climatic conditions (Araújo and Pearson, 2005). Therefore, pure climate models are likely to provide incomplete predictions when species move from

equilibrium with climate owing to a suite of non-climatic factors (Luoto et al., 2006). Modelling performance might be considerably improved by combining abiotic factors in the models, as this allows for the identification of regions with suitable climate but unsuitable local environmental conditions to achieve more realistic estimates of distribution changes (Alahuhta et al., 2011; Shabani et al., 2014b). In respect of slope, for date palm, irrigation should be applied in a controlled manner in order to provide an optimum situation for crop transpiration and for this, flat land or areas with slopes $< 7^\circ$ would be appropriate for date palm cultivation (Kassem, 2007). Furthermore, it has been documented that slope greatly impacts plant root systems (Caviezel et al., 2014) at the expense of depth (Khuder et al., 2006). For young date plantlets, root depth can vary from 25 to 50 cm and the radius from 10 to 30 cm, depending on the size of the plant, and this means that irrigation water must be applied within these boundaries to enable the plant roots to reach it (Manickavasagan et al., 2012). However, it is important to apply water in such a way that it does not reach the deeper soil levels in order to ensure proper root development of date palms (Zaid and Arias Jiménez, 1999). Thus, considering the effects of non-climatic parameters in potential date palm distribution, taking into account slopes where tree roots have a greater positive impact on slope stability should not be neglected, as the slope influences spatial root distribution and areas suitable for date palm establishment (Vergani et al., 2014; Rogers and Benfey, 2015). In line with such expectations, the CLIMEX results were refined in the current study using six non-climatic parameters including soil salinity, soil taxonomy, soil texture, land use, landform and slope. The suitable areas where date palm could be established by 2050 were constrained by non-climatic factors, as the realized distribution of date palm is substantially smaller than the climate envelope projected by both MR and CS GCMs for 2050. For example, both models show that 177.04 and 178.18 million hectares may become conducive by 2050 considering climatic factors alone, while 97 million hectares of these projections are not actually valid due to the unsuitability of

soil salinity, soil taxonomy, soil texture, land use, landform or slope variables. Further, both models indicate only 0.35 of areas located from 25° to 35° N and 35° to 45° E are going to be suitable for date palm cultivation by 2100 based on both climate change and suitability of the six non-climatic factors. Similarly, for the same year, both models showed that the southwestern region, which is projected to be suitable based only on climate, it is not a practical place for date palm cultivation because of the unsuitability of soil salinity, soil taxonomy, soil texture, land use, landform and slope.

Areas projected to be climatically suitable for date palm cultivation by the pure climate models of both MR and CS GCMs for 2100 were much higher than those projected based non-climatic parameters. It was not surprising that models showed differences between pure climate and non-climatic variables. Including non-climatic variables improved model accuracy compared to the pure climate models. These findings are supported by others who found that the inclusion of non-climatic variables increases the prediction accuracy of bioclimatic models (e.g., Sormunen et al., 2011; Hyvönen et al., 2012; Taylor et al., 2012a; Shabani et al., 2014b). Accordingly, based on the current and previous studies, it is clear that climate is not the sole determinant of establishment (Sutherst and Maywald, 1985) and other factors can play a major role in determining species distribution and dynamics of distribution changes.

Both models are relatively consistent in the projections of suitable areas for date palm cultivation and showed a similar trend. However, variations between the results of the CS and MR GCMs can be observed in Figure 7.2 and Table 7.1. For example, areas projected to be climatically suitable for date palm cultivation by MR were somewhat larger compared to the CS GCM. These difference in projected areas conducive to date palm are due to differences between the two models in their temperature and rainfall predictions. The CS model predicts an increase in temperature of 2.11°C, while the MR model assumes that temperature will rise by approximately 4.31°C by 2100 (Kriticos et al., 2012). These two models also differed in

rainfall pattern predictions: the CS model predicts a 14% reduction in future mean annual rainfall, while the MR model predicts only a 1% drop (Kriticos et al., 2012). To decrease the uncertainty of projections and satisfy the non-climatic parameters, once the two modelled outputs were refined using non-climatic parameters, intersection techniques were utilized to extract areas in common between both GCM projections. The modelling output led to better agreement between CS and MR GCMs in projections of suitable areas for date palm. Both MR and CS GCMs project that 80.17 million ha of Saudi Arabia will be climatically suitable for date palm cultivation by 2050. Additionally, analysis from both GCMs showed that only 17.86 million ha of the study area would be suitable for date palm cultivation by 2100. This result confirms that the inclusion of non-climatic variables increases the prediction accuracy of bioclimatic models.

Overall, there will be less area conducive for date palm cultivation in Saudi Arabia by 2100 as a result of heat stress. The country will be unable to cultivate this cash crop at the same level in the future as it has previously, which will lead to significant economic decline. For example, it was reported that the quantity of date palm exports from Saudi Arabia was 77.8 thousand tons (valued at US\$86.3 million) in 2011 (FAOSTAT, 2013). Hence, if date production falls by a large percentage in the future, then Saudi Arabia may become a net importer rather than a net exporter. Thus, the findings reported in the current study can be considered a useful starting point to provide some advanced warning of this situation so that the government and agricultural organizations can prepare management strategies for this situation, and even more importantly become aware of any potential adverse effects on the agricultural sector.

It should be noted that although the current study showed that large areas of Saudi Arabia are climatically suitable for date palm cultivation, and date palm is able to survive under arid climate, it does require sufficient water of acceptable quality to reach its potential yield. Besides, date palm production is labour intensive and requires workers with sufficient

experience; therefore, operating costs are relatively high. This means that the lack of water resources in Saudi Arabia as a result of climate change coupled with the shortage of skilled labourers are the most significant cost and obstacle to expanding date palm cultivation in the future. Furthermore, limitation of arable lands is another key factor in the expansion of date plantation in Saudi Arabia, which will limit future date palm distribution. In addition, the regional comparative advantage between crops is another factor to consider (Alabdulkader et al., 2012). Therefore, the results of the present study could be an initial step and an economical integrated assessment should be undertaken to prioritize which areas will cost less. In other words, an economic feasibility must be estimated based on the assumption that the decision to plant date palms by landholders is motivated by a desire to maximize their return to land.

7.6 Conclusions

This research developed potential distribution models for current and future date palm cultivation in Saudi Arabia. The results from both GCMs showed a significant reduction in climatic suitability for date palm cultivation in Saudi Arabia. The MIROC-H projected a larger area as unsuitable for date palm cultivation in 2100 compared to CSIRO-Mk3.0. The inclusion of six non-climatic parameters, soil taxonomy, soil texture, soil salinity, landform, land use and slope resulted in more realistic estimates of the distribution models. The sensitivity analysis indicated that SM1, TTCS and SMWS parameters were the most sensitive parameters among the other investigated parameters in terms of suitable area for date palm cultivation in this region. The current results suggest that the CLIMEX model can provide a useful first-filter estimate for the identification of potential distributional changes of date palm at regional scales. Such modelling is useful for planning long-term strategies and reducing economic effects in areas that might be adversely impacted and for preparing to take advantage of new opportunities in areas that might be positively impacted. This type of long-term planning is

mainly applicable to date palm production, as this species needs a prolonged period to establish and become productive.

**Higher Degree Research Thesis by Publication
University of New England**

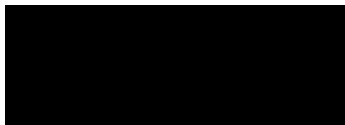
STATEMENT OF ORIGINALITY

We, the Research Master/PhD candidate and the candidate's Principal Supervisor, certify that the following text, figures and diagrams are the candidate's original work.

Type of work	Page number/s
Figure 7.1	144
Figure 7.2	155
Figure 7.3	156
Figure 7.4	156

Name of Candidate: Amal Allbed

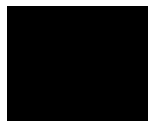
Name/title of Principal Supervisor: Professor Lalit Kumar



Candidate

20 June 2018

Date



Principal Supervisor

20 June 2018

Date

**Higher Degree Research Thesis by Publication
University of New England**

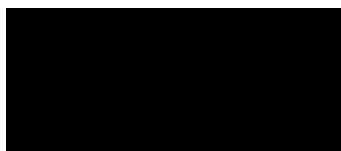
STATEMENT OF AUTHORS' CONTRIBUTION

We, the Research Master/PhD candidate and the candidate's Principal Supervisor, certify that all co-authors have consented to their work being included in the thesis and they have accepted the candidate's contribution as indicated in the *Statement of Originality*.

	Author's Name (please print clearly)	% of contribution
Candidate	Amal Allbed	80
Other Authors	Lalit Kumar	10
	Farzin Shabani	10

Name of Candidate: Amal Allbed

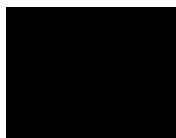
Name/title of Principal Supervisor: Professor Lalit Kumar



Candidate

20 June 2018

Date



Principal Supervisor

20 June 2018

Date

Chapter 8 Synthesis and General Conclusions

8.1 Summary of Main Findings

As soil and agriculture are one of the fundamental components for supporting life on the planet, the protection and the sustainable management of soil in any region such as Al Hassa Oasis is of paramount importance, particularly in the context of the sustainability of agriculture. Various reports have indicated that soil salinity is the major problem facing the development of irrigated agriculture that is dominated by date palm (*Phoenix dactylifera* L.), in this Oasis, which is largely due to the high concentration of soluble salts in the irrigation water, over irrigation, poor drainage facilities, low rainfall and high evaporation rates. From the perspective of a policy-maker interested in topics such as soil salinity and irrigated agriculture in Al Hassa Oasis, this situation requires up-to-date and relevant soil salinity and agricultural information. The accurate observation of soil salinity and agricultural conditions can result in potentially great environmental, economic and social benefits. Many remote sensing and modelling techniques can be investigated for assessing and monitoring the changes and providing the essential information for soil salinity and its effects of growth conditions on plant. The utility of quantitative methods, in particular, indices and statistical models with broadband satellite imagers to assess, map and model soil salinity has not been previously investigated in the date palm dominated Al Hassa Oasis. The effects of different physical and proximity factors on the agricultural expansion for two time periods, detecting the long-term temporal change in vegetation cover and soil salinity and investigating whether the salinity change causing the change in vegetation cover in the Al Hassa Oasis are other areas that require exploration, as well as potential date palm distribution under current and future climate conditions. This study has attempted to bridge these research gaps. This concluding chapter summarizes the main findings of the research and proposes recommendations and future research needs.

An assessment of soil salinity level was carried out in three sites across the Al Hassa Oasis by utilizing vegetation and salinity indices obtained from IKONOS images combined with

laboratory analysis to measure EC of soil samples. The analysis of the soil samples showed that strongly saline soils with an EC >16 dS/m generally dominated the three selected Oasis sites. These soils mainly occurred in non-vegetated areas or abandoned stretches of land that were locally referred to as sabkhas which are crusted with salt and some salt tolerant plants scattered around, as well as vegetated areas but with a lower salinity level compared to the non-vegetated areas. Among all the spectral indices used the SAVI, NDSI and SI-T indices were the most useful predictors of soil salinity in the investigated areas. However, their performance varied within the three sites.

Utilizing NDSI and SI-T in the assessment of soil salinity will be the preferred means in the case of bare soils or soils with low scattered vegetation cover, providing better results. The good performance of the NDSI and SI-T indices are likely attributed to the superiority of the red and NIR bands that were used to retrieve the soil salinity patterns and features, such as the surface crust, as these bands have been found to be relevant for the identification of soil minerals that are formed during salt stress and in crusts. While vegetation index SAVI yielded promising results in areas of densely vegetated soils, on bare soils or soils with low scattered vegetation cover, the identification of salt based on SAVI did not work. This result likely occurred due to the lower sensitivity of the SAVI index to external factors, such as soil background, and the dense uniform vegetation cover that occurred at those sites. Thus, care should be taken when applying such indices at other sites, because their performance varies with different environmental conditions, soil, vegetation cover and density.

Investigating the efficiency of vegetation and salinity indices to assess soil salinity provided scope to model and map the spatial variation of the soil salinity in the Al Hassa Oasis. This was done by developing combined spectral-based statistical regression models using IKONOS images. Correlations between reflectance indices, IKONOS original bands and EC measured in the laboratory, showed that salinity index (SI) and red band offer the best correlation. The

combination of these remotely sensed variables (SI and red band) into one model was able to explain 65% of the spatial variation in the soil salinity of the study area with relatively low standard errors for its variables. The great capacity of this combined model is attributed to the spatial resolution of the images, enhanced images and the red band efficacy in highlighting information from soil salinity. Soil salinity maps generated using the selected model revealed patches with strongly saline soil along the three sites were most pronounced in non-vegetated wet and dry areas which are probably due to the rising water table close to the ground level bringing salt accumulation to the surface combined with a high evaporation rate. Salinity in the vegetated areas was relatively low compared to non-vegetated areas which may be accounted for by a leaching process, although still in the >16 dS/m class. Nevertheless, there were pronounced variances of this class between the three sites over the vegetated areas which is likely attributed to a variety of aspects, including soil factors and management related factors, as these parameters are known to affect soil salinity distribution across the landscape.

Spectral reflectance of saline soils can be a result of the salt itself, or indirectly, from other factors such as soil moisture, colour and surface roughness. The analysis results of the soil samples indicated that the curves of the soil spectral reflectance in the visible and NIR regions increased with increasing quantity of salts at the terrain surface and vice versa. The increase of soil moisture on the other hand reduces salt in dilution, so the presence of soil moisture tends to darken the soil, which reduced the overall surface reflectance. Besides, the results showed saline soils with a smooth and light salty crust surface had high spectral reflectance in the red band, in contrast saline soils characterized by coarse dark puffy surface crust exhibited a decrease in spectral reflectance.

Since soil salinity is a dynamic process in time and space and negatively impacts agriculture, the information on overall change/no-change in these land covers can aid management in preventing further salinization in order to maintain sustainable agriculture. Landsat time series

data years 1985, 2000 and 2013 were used to detect the temporal change of soil salinity and vegetation cover in the study region. Also, investigation was carried out to determine whether the change in vegetation cover is a case of soil salinity change. Due to the simplistic nature and relative ease in identifying both negative and positive changes from difference images technique, the SI (based on SWIR bands) and NDVI differencing images were used for salinity and vegetation cover change identification in the study region. Threshold determination for highlighting areas where features brightness values increased or decreased, or remained unchanged were identified.

A highly significant ($p < 0.0001$) inverse relationship was found between the NDVI and SI values, indicating that there is a potential linkage between the vegetation cover change and soil salinity change over the study area. These results suggest that the noticeable change of vegetation cover could be likely due to soil salinity change, which has harmfully impacted the vegetation cover. In some parts of the study area, there was a decrease in soil salinity over the change period which had perhaps led to an increase in the vegetation cover. There might be different factors that have contributed to this change, such as leaching application to the soil surface, use of modern irrigation systems and management practices. In terms of salinity, the soil salinity level has experienced remarkable changes in Al Hassa Oasis in the past 28 years, which is probably due to improper land use, poor management practices (e.g. poor irrigation system, fertilizer application) combined with the climate factors. Overall, there was more increase in soil salinity level and decline in vegetation cover, particularly during the 2000–2013 period, than decrease in soil salinity level. Thus, the observed changes in this area will have significant implications on agricultural output in the future if these two mutually inclusive processes continue as increase in soil salinity level was found to be one of the reasons contributing to the decline in vegetation cover change.

Landsat data were effectively used to identify the change of soil salinity and vegetation cover in the study region, and soil salinity was found to be one of the reasons contributing to the change in vegetation cover. However, meaningful information on the effect of the different factors on the distribution of agricultural expansion across space and time cannot be provided when using such data. Thus, further analysis on the cause underlying the changes in the spatial distribution of agriculture in this area is needed as it is considered one of the main agricultural regions in Saudi Arabia, providing a significant source of income for farmers and the government. Such analysis is important as it enables an understanding of the effect of the different factors that have controlled the agricultural expansion in the past and that might dominate the future agriculture distribution.

To attain this, a logistic regression model was used to investigate the effect of eight driving factors including elevation, slope, soil salinity, distance to water, distance to built-up areas, distance to road, distance to drainage and distance to irrigation in the Al Hassa Oasis. Two sets of Landsat images from 1985 and 2015 were used for this purpose. SVM approach was used to classify built-up areas and bare soil for 1985 and 2015, and spectral indices including NDVI and NDWI were used to extract the agricultural lands and waterbodies. The three classes of water, built-up and bare soil were reclassified as non-agriculture areas. The final results, which presented two categories, including agriculture and non-agriculture areas, were used as input along with the driving factors for the prediction model. The logistic regression model was able to provide an easily discernible prediction of agricultural expansion based on the applied factors. The model validation using the ROC revealed a stable level in 1985 and 2015. Nevertheless, the spatial prediction of agricultural expansion performance could not be tested using ROC as it was used to quantitatively validate the model. Hence, an additional analysis was conducted for this propose by overlaying the probability map of 1985 and the actual agricultural growth of 2015. This analysis offered an opportunity to test the ability of the model

to predict the probabilities of agricultural expansion after 2015 based on the 1985 agricultural expansion prediction. The results showed that the prediction model of 2015 provides a consistent and reliable prediction based on the performance of 1985.

The analysis of the deriving factors showed variable effects over time in the study region. Among the investigated factors, distance to water, distance to built-up areas and soil salinity were the major factors having effect on agricultural expansion. This indicated that agriculture in Al Hassa Oasis is likely to develop on good quality soils near to water resources but far from built-up areas. Distance to irrigation and drainage canals showed the least effects on agricultural expansion. This result may have been found because the majority of farmers prefer to irrigate their agricultural lands from their individual private wells. Elevation and slope exhibited low negative effects on agricultural expansion in the past forty-five years, indicating that these factors limited the distribution of agriculture. However, the effect of these variables became greater in 2015. This change in the magnitude of the effects of these factors on agricultural expansion reflect the fact that agricultural lands in areas with rugged terrain are often abandoned since they experience higher cultivation costs. However, technological advances that enable building on sloping lands combined with the limited area of flat land are likely to reduce the effects of these factors in the future. Such an analysis allowed a better understanding of the process of agricultural expansion and provides a scientific basis for future forecasting and decision-making processes which can effectively lead to the conservation of the agricultural sector.

The potential productivity of species is usually indicated by natural and climatic conditions. Thus, to help decision makers and local authorities preparing management strategies to achieve long-term sustainable production of cash crops, such as date palm, information on the potential distribution of date palm and the relative abundance in the future, based on climate and non-climate parameters, is essential. This study employed CLIMEX to model the distribution of

date palm in Saudi Arabia under current and future climate scenarios. Two global climate models (GCMs), CSIRO-MK3.0 (CS) and MIROC-H (MR), were used to assess the impact of climate change on the potential distribution of date palm at two arbitrarily chosen future time points, i.e. 2050 and 2100. Furthermore, the inclusion of physical factors, specifically soil taxonomy, soil texture, soil salinity, land use, landform and slope, was used to refine potential distributions. Under current climate, a large part of Saudi Arabia was projected to have suitable climatic conditions for date palm growth and cultivation. Under future climate scenarios, both GCMs indicated that date palms will not suffer from any dry, wet or cold stress by 2050, hence the central and southwestern parts of Saudi Arabia will remain climatically suitable for date palm. However, by 2100 the majority of the country will become unsuitable for date palm cultivation due to increment of heat stress in the region; as a result Saudi Arabia will be unable to cultivate this cash crop at the same level in the future as it has previously, which will lead to significant economic decline.

The inclusion of the non-climatic parameters led to a substantial reduction in suitable areas for date palm cultivation by both MR and CS GCMs for 2050 and 2100. Further, the result indicated that the soil factors and landform have a greater effect than land use and slope, in terms of the suitability of locations for the cultivation of date palm. The sensitivity analysis that was performed to identify the parameters of greatest functional importance, in order to enhance the understanding of the climatic factors that most affect date palm projection scenarios in CLIMEX, demonstrated that date palm distribution is highly sensitive to changes in SM1, TTCS and SMWS parameters, and moderately sensitive to changes in SM0, DV1 and HWS parameters.

8.2 Contribution to Science and Knowledge

This study has demonstrated the potential of remote sensing and modelling techniques for assessing, mapping, change identification and modelling soil salinity and its impacts on agricultural production. The capability to remotely assess and map soil salinity using broadband indices extracted from high spatial resolution satellite imagery can provide reliable, up-to-date information on its abundance. This is necessary for the evaluation of control strategies, prevention of spread to unaffected areas, and improved management. Moreover, identifying and mapping soil salinity more accurately can contribute significantly in the design and execution of cost-effective agricultural production methods of the future. A further aspect of the study is that the indices used for assessing soil salinity in this study are not restricted to assessing soil salinity in date palm region. Therefore, other regions can use these indices, but an obvious note of caution needs to be known before appropriate remote sensing-based indices are used for soil salinity mapping and assessing that no particular vegetation or soil salinity index could be used across all environmental conditions with satisfactory results, as these indices vary with different environmental conditions, soil types, and vegetation cover and density.

The great potential of the enhanced images, derived from SI, and the IKONOS red band in highlighting information from soil salinity also provide the option for developing statistical regression models to predict and map spatial variation in soil salinity in a region dominated by date palms. This model offers a quick method which can contribute greatly to soil salinity prediction and mapping as it facilitates timely detection at lower costs than conventional approaches and allows decision makers to decide in early stages what crucial action should be taken to prevent soil salinity from becoming prevalent, protect the date palm outputs, sustaining agricultural lands and natural ecosystems. Therefore, this model can be used by the decision

makers in Al Hassa Oasis municipality and similar regions to support or implement effective soil reclamation programs that minimize or prevent increases in soil salinity in the future.

Agricultural workers, scientists, policy makers and governments need reliable and up-to-date information about the temporal change in soil salinity, especially on long-term basis, and determining its impacts on vegetation cover to formulate effective strategies to manage this issue. This study provides the essential knowledge to support the decision-making processes of soil salinity management planning to sustain date palm production in Al Hassa Oasis. The successful application of mid-resolution Landsat data using image differencing technique for soil salinity and vegetation change detection helps to understand the past changes and to quantify the overall rate of change. Furthermore, it gives confidence in the use of such images and methods in regions that are dominated by date palm and where high spatial resolution imagery is not available or cannot be afforded. With this finding, government agencies such as the Ministry of Environment, non-government organizations and educational and research institutes will have motivation to develop a proper and continuous monitoring system in a simple, time saving, efficient and cost-effective way to overcome the impact of soil salinity on date palm production to ensure that long-term sustainable production of date palm in this region can be achieved. Further, this finding will not only help in opening the avenue of such applicability for other regions having similar issues, but also emphasize the importance of remote sensing in agro-environmental applications.

The investigation of agricultural expansion and responsible physical and proximity forces for this expansion through a logistic regression model provides some scientific understanding of the trend and distribution of the past and future agricultural expansion in the Al Hassa Oasis. The outcome of this study helps to understand the dynamics of the agricultural land in this region and the forces that are responsible for the expansion. National authorities and organizations can consider the outcome of this research to design management strategies to

ensure sustainability of the agricultural production, particularly date palm production, in this Oasis and also provides inputs for further work for researchers within this field.

Another contribution of this research is through how CLIMEX software could be used to provide information on the potential distribution of date palm for the whole Saudi Arabia under current and future climate scenarios. Furthermore, it demonstrates that the inclusion of factors other than climate, such as soil salinity and land use, can significantly refine the potential spatial distribution of date palm. The outcome models provided by CLIMEX provide some advanced warning of the situation, and the distribution maps could be used by the governments and agricultural organizations as an initial guide to prepare management strategies for the circumstances ahead in order to overcome the impact of climate change and the other non-climatic parameters on this important economic crop, and even more importantly become aware of any potential adverse effects on the agricultural sector.

8.3 Recommendations and Direction of Future Research

Ongoing monitoring of soil salinity at Al Hassa Oasis is recommended to provide long-term data on soil salinity variability. This will also ensure that the initial objectives of the rehabilitation and management of saline soils to improve agricultural productivity in this region are being met into the future. Further, frequent monitoring of groundwater level dynamics and quality in Al Hassa Oasis is required to get a complete and temporal overview of the fluctuations of the groundwater and to confirm the role of irrigation in the development of the soil salinity problem and thereby provide a policy background to water and soil management for sustainable agriculture.

The IKONOS high spatial resolution image that was used in this study is hindered by the absence of a thermal band, which has been found to be a useful tool in soil salinity studies. There is a scope to determine whether the development of a salinity index and empirical model

which includes a thermal band would increase the accuracy of soil salinity identification in a date palm dominated area.

Though it was possible to investigate vegetation and soil salinity changes using multispectral Landsat data in this study, airborne and spaceborne hyperspectral imagery may provide better results for this purpose as hyperspectral sensors provide a large number of spectral bands that allow identifying surface features, while airborne hyperspectral sensors provide high spatial resolution imagery that contributes to improved identification of the object in more detail than those visible in the space-borne multispectral images. To the best of our knowledge, no research has been undertaken on the use of hyperspectral imagery for soil salinity detection in a date palm dominated region, probably due to its unaffordable high operational *cost*. In line with this, it is highly recommended to investigate whether using hyperspectral imagery would bring appreciably improved results over multispectral sensors in the detection of soil salinity in communities vegetated mainly with date palms.

In terms of change modelling, integrating the logistic regression model with other models, such as geographically weighted regression (GWR, is a further aspect of future study; as such incorporation could be useful to determine the heterogeneity in the estimated correlation between independent and dependent variables. In addition, this study has utilized one modelling software program, namely CLIMEX, to determine potential future distribution of date palm. It would be worthwhile to conduct a comparative study with other species distribution modelling software. Generally, species distribution modelling methods use gridded climate datasets of moderate spatial resolution. The impact of varying the spatial resolution of climatic datasets on the potential distribution of date palm is another subject that requires further investigation.

References

- Abbas, A., & Khan, S. (2007). *Using remote sensing techniques for appraisal of irrigated soil salinity*. Paper presented at the MODSIM 2007 International Congress on Modelling and Simulation, Modelling and Simulation Society of Australia and New Zealand, New Zealand.
- Abbas, M. F., Jasim, A. M., & Shareef, H. J. (2015). Role of Sulphur in salinity tolerance of Date Palm (*Phoenix dactylifera* L.) offshoots cvs. Berhi and Sayer. *International Journal of Agricultural and Food Science*, 5(3), 92-97.
- Abdel-Hamid, M. A., & Shrestha, D. P. (1992). Soil salinity mapping in the Nile delta, Egypt using remote sensing techniques. *International Society for Photogrammetry and Remote Sensing*, 29(Part 7B, commission VII), 783-787.
- Abderrahman, W. (1988). Water management plan for the Al-Hassa irrigation and drainage project in Saudi Arabia. *Agricultural Water Management*, 13(2), 185-194. doi: 10.1016/0378-3774(88)90153-9
- Abrol, I., Yadav, J. S. P., & Massoud, F. (1988). *Salt-affected soils and their management*: Food & Agriculture Org.
- Achmad, A., Hasyim, S., Dahlan, B., & Aulia, D. N. (2015). Modeling of urban growth in tsunami-prone city using logistic regression: Analysis of Banda Aceh, Indonesia. *Applied Geography*, 62, 237-246.
- Adams, J. B., & Gillespie, A. R. (2006). *Remote Sensing of Landscapes with Spectral Images: A Physical Modeling Approach*: Cambridge University Press.
- Afework, M. (2009). *Analysis and mapping of soil salinity levels in Metehara Sugarcane Estate irrigation farm using different models*. (Master of Science in Remote Sensing and Geographical Information Systems (GIS)), Addis Ababa University Ethiopia, Addis Ababa.
- Afrasinei, G. M., Melis, M. T., Buttau, C., Bradd, J. M., Arras, C., & Ghiglieri, G. (2017). Assessment of remote sensing-based classification methods for change detection of salt-affected areas (Biskra area, Algeria). *Journal of Applied Remote Sensing*, 11(1), 016025-016025.
- Agassi, M., Morin, J., & Shainberg, I. (1985). Effect of raindrop impact energy and water salinity on infiltration rates of sodic soils. *Soil Science Society of America Journal*, 49(1), 186-190.
- Agriculture, U. S. D. O., Service, N. R. C., & Staff, S. S. (2010). *Keys to Soil Taxonomy (Eleventh Edition)*: Books Express Publishing.
- Ahmed, I., & Andrianasolo, H. H. (1997). *Comparative assessment of multisensor data for suitability in study of the soil salinity using remote sensing and GIS in the Fordwah irrigation division, Pakistan*. Paper presented at the Geoscience and Remote Sensing, 1997. IGARSS '97. Remote Sensing - A Scientific Vision for Sustainable Development.
- Ahmed, M., Hussain, N., & Al-Rawahy, S. A. (2013). Management of Saline Lands in Oman: Learning to Live with Salinity. In Shabbir A. Shahid, Mahmoud A. Abdelfattah & F. K. Taha (Eds.), *Developments in Soil Salinity Assessment and Reclamation: Innovative Thinking and Use of Marginal Soil and Water Resources in Irrigated Agriculture* (pp. 265-281): Springer Science & Business Media.
- Al-Barrak, S. A. (1990). Characteristics of some soils under date palm in Al-Hassa eastern oasis, Saudi Arabia. *Journal of King Saud University Agricultural Sciences*, 2(1), 115-130.
- Akbani, R., Kwek, S., & Japkowicz, N. (2004). Applying support vector machines to imbalanced datasets. *Machine learning: ECML 2004*, 39-50.

- Akkad, A. A. (1990). Socio-economic factors affecting agricultural development in Al-Hassa Oasis, Saudi Arabia. *GeoJournal*, 20(3), 259-270.
- Akramkhanov, A., & Vlek, P. (2012). The assessment of spatial distribution of soil salinity risk using neural network. *Environmental monitoring and assessment*, 184(4), 2475-2485.
- Al-Abdoulhadi, I. A., Dinar, H. A., Ebert, G., & Bttner, C. (2011). Effect of salinity on leaf growth, leaf injury and biomass production in date palm (*Phoenix dactylifera* L.) cultivars. *Indian Journal of Science and Technology*, 4(11), 1542-1546.
- Al-Abdoulhadi, I. A., Dinar, H. A., Ebert, G., & Bttner, C. (2012). Influence of salinity levels on nutrient content in leaf, stem and root of major date palm (*Phoenix Dactylifera* L) cultivars. *International Research Journal of Agricultural Science and Soil Science*, 2(8), 341-346.
- Al-Amoudi, O. S. B. (1995). *Soil stabilization and durability of reinforced concrete in sabkha environments*. Paper presented at the Proc., 4th Saudi Engineering Conf.
- Al-Barrak, S. (1986). Properties and classification of some oasis soils of Al-Ahsa, Saudi Arabia. *Arab Gulf journal of scientific research*.
- Al-Barrak, S., & Al-Badawi, M. (1988). Properties of some salt affected soils in Al-Ahsa, Saudi Arabia. *Arid Land Research and Management*, 2(2), 85-95.
- Al-Dakheel, Y. Y., & Massoud, M. A. (2006). *Towards sustainable development for groundwater in Al-Hassa and the role of geographic information systems*. Paper presented at the The 2nd International Conference on Water Resources and Arid Environment, King Saud University, Riyadh
- Al-Jabr, M. A. (1984). *Agriculture in al-hassa oasis, Saudi Arabia: a review of development*. (Master), Durham University.
- Al-Khaier, F. (2003). *Soil salinity detection using satellite remote sensing*. (M.Sc), International Institute for Geo-information Science and Earth Observation, The Netherlands.
- Al-Mulla, Y. A., & Al-Adawi, S. (2009). *Mapping temporal changes of soil salinity in Al-Rumais region of Oman using geographic information system and remotesensing techniques*. Paper presented at the American Society of Agricultural and Biological Engineers (ASABE) Annual International Meeting, Reno, Nevada, USA.
- Al-Naeem, A. A. (2011). Evaluation of groundwater of al-hassa oasis, eastern region Saudi Arabia. *Research Journal of Environmental Sciences*, 5(7), 624-642.
- Al-Senaidy, A. M., & Ismael, M. A. (2011). Purification and characterization of membrane-bound peroxidase from date palm leaves (*Phoenix dactylifera* L.). *Saudi Journal of Biological Sciences*, 18(3), 293-298. doi: 10.1016/j.sjbs.2011.04.005
- Al-Taher, A. A. (1999). *Al-Hassa: A Geographic Study*. Riyadh: Alhsaini Perss.
- Al-Zarah, A. I. (2008). Chemistry of Groundwater of Al-Alisa Oasis Eastern Region Saudi Arabia and Its Predictive Effects on Soil Properties. *Pakistan Journal of Biological Sciences*, 11(3), 332-341.
- Al-Zarah, A. I. (2011). Elemental Composition of Groundwater and Spring Waters in Al-Ahsa Oasis, Eastern Region Saudi Arabia. *Trends in Applied Sciences Research*, 6(1), 1-18.
- Al Hammadi, M. S. (2006). *Salt tolerance and current status of the date palms in the United Arab Emirates*. (Doctor of Philosophy), University of Arizona.
- Al Sayari, S. S., Jado, A. R., & Zötl, J. (1984). *Quaternary period in Saudi Arabia: Sedimentological, hydrogeological, hydrochemical, geomorphological, geochronological and climatological investigations in Western Saudi Arabia* (Vol. 2). Berlin: Springer Verlag.

- Al Tokhais, A. S., & Rausch, R. (2008). *The hydrogeology of Al Hassa springs*. Paper presented at the The 3rd International Conference on Water Resources and Arid Environments and the 1 Arab Water Forum, st Riyadh, Saudi Arabia.
- Alabdulkader, A. M., Al-Amoud, A. I., & Awad, F. S. (2012). Optimization of the cropping pattern in Saudi Arabia using a mathematical programming sector model. *Agricultural Economics / Zemedelska Ekonomika*, 58(2), 56-60.
- Alabdulkader, A. M., Al-Amoud, A. I., & Awad, F. S. (2016). Adaptation of the agricultural sector to the effects of climate change in arid regions: competitive advantage date palm cropping patterns under water scarcity conditions. *Journal of Water and Climate Change*, 7(3), 514-525. doi: 10.2166/wcc.2016.096
- Alahuhta, J., Heino, J., & Luoto, M. (2011). Climate change and the future distributions of aquatic macrophytes across boreal catchments. *Journal of Biogeography*, 38(2), 383-393. doi: 10.1111/j.1365-2699.2010.02412.x
- Alavi Panah, S., & Goossens, R. (2001). Relationship Between the Landsat TM, MSS Data and Soil Salinity. *JOURNAL OF AGRICULTURAL SCIENCE AND TECHNOLOGY (JAST)*, 3(2), 101-111.
- Alavipanah, S. K., & Goossens, R. (2001). Relationship between the Landsat TM, MSS data and soil salinity. *Journal of Agricultural Science and Technology*, 3(2), 101-111.
- Aldakheel, Y. Y. (2011). Assessing NDVI Spatial Pattern as Related to Irrigation and Soil Salinity Management in Al-Hassa Oasis, Saudi Arabia. *Journal of the Indian Society of Remote Sensing*, 39(2), 171-180.
- Alleid, S. M., Al-Khayri, J. M., & Al-Bahrany, A. M. (2015). Date Palm Status and Perspective in Saudi Arabia. In M. J. Al-Khayri, M. S. Jain & V. D. Johnson (Eds.), *Date Palm Genetic Resources and Utilization: Volume 2: Asia and Europe* (pp. 49-95). Dordrecht: Springer Netherlands.
- Alhammadi, M. S. (2010). *Using QuickBird Satellite Images to Study the Salinity Effect on Date Palm Field*. Paper presented at the International Congress Geotunis 2010, Tunis.
- Alhammadi, M. S., & Edward, G. P. (2009). Effect of salinity on growth of twelve cultivars of the United Arab Emirates date palm. *Communications in soil science and plant analysis*, 40(15-16), 2372-2388.
- Alhammadi, M. S., & Glenn, E. P. (2008). Detecting date palm trees health and vegetation greenness change on the eastern coast of the United Arab Emirates using SAVI. *International Journal of Remote Sensing*, 29(6), 1745-1765.
- Alhammadi, M. S., & Kurup, S. S. (2012). Impact of Salinity Stress on Date Palm (*Phoenix Dactylifera* L)-A Review. In P. Sharma (Ed.), *Crop Production Technologies* (pp. 276): InTech
- Ali, M. H., Hoque, M., Hassan, A., & Khair, A. (2007). Effects of deficit irrigation on yield, water productivity, and economic returns of wheat. *Agricultural Water Management*, 92(3), 151-161. doi: 10.1016/j.agwat.2007.05.010
- Aljaryian, R., Kumar, L., & Taylor, S. (2016). Modelling the current and potential future distributions of the sunn pest *Eurygaster integriceps* (Hemiptera: Scutelleridae) using CLIMEX. *Pest Management Science*, 72(10), 1989-2000. doi: 10.1002/ps.4247
- Allbed, A., & Kumar, L. (2013). Soil Salinity Mapping and Monitoring in Arid and Semi-Arid Regions Using Remote Sensing Technology: A Review. *Advances in Remote Sensing*, Vol.02No.04, 13. doi: 10.4236/ars.2013.24040
- Allbed, A., Kumar, L., & Aldakheel, Y. Y. (2014a). Assessing soil salinity using soil salinity and vegetation indices derived from IKONOS high-spatial resolution imageries: Applications in a date palm dominated region. *Geoderma*, 230-231, 1-8. doi: 10.1016/j.geoderma.2014.03.025

- Allbed, A., Kumar, L., & Sinha, P. (2014b). Mapping and Modelling Spatial Variation in Soil Salinity in the Al Hassa Oasis Based on Remote Sensing Indicators and Regression Techniques. *Remote Sensing*, 6(2), 1137.
- Almeida, C., Gleriani, J., Castejon, E. F., & Soares-Filho, B. (2008). Using neural networks and cellular automata for modelling intra-urban land-use dynamics. *International Journal of Geographical Information Science*, 22(9), 943-963.
- Alqurashi, A. F., Kumar, L., & Al-Ghamdi, K. A. (2016). Spatiotemporal modeling of urban growth predictions based on driving force factors in five Saudi Arabian cities. *ISPRS International Journal of Geo-Information*, 5(8), 139.
- Alrasbi, S. A. R., Hussain, N., & Schmeisky, H. (2010). *Evaluation of the growth of date palm seedlings irrigated with saline water in the Sultanate of Oman*. Paper presented at the IV International Date Palm Conference 882.
- Alsharhan, A., Rizk, Z., Nairn, A. E. M., Bakhit, D., & Alhajari, S. (2001). *Hydrogeology of an arid region: the Arabian Gulf and adjoining areas*: Elsevier.
- Arasteh, P. D. (2010). *Soil salinity change detection in irrigated area under Gazvin plain irrigation network using satellite imagery*. Paper presented at the the 9th International Drainage Symposium, Québec, Canada.
- Araújo, M. B., & Pearson, R. G. (2005). Equilibrium of species' distributions with climate. *Ecography*, 28(5), 693-695. doi: 10.1111/j.2005.0906-7590.04253.x
- Ashraf, M., Öztürk, M. A., & Athar, H. R. (2009). *Salinity and water stress: improving crop efficiency*. Dordrecht, Netherlands: Springer
- Aspinall, R. (2004). Modelling land use change with generalized linear models—a multi-model analysis of change between 1860 and 2000 in Gallatin Valley, Montana. *Journal of environmental management*, 72(1), 91-103.
- Assiri, A., & Darfaoui, E. (2009). Response to Climate Change in the Kingdom of Saudi Arabia. *A report prepared for FAO-RNE*, 17.
- Ayers, R. S., & Westcot, D. W. (1985). *Water quality for agriculture*: Food and Agriculture Organization of the United Nations.
- Bannari, A., Guedon, A. M., El-Harti, A., Cherkaoui, F. Z., & El-Ghmari, A. (2008). Characterization of Slightly and Moderately Saline and Sodic Soils in Irrigated Agricultural Land using Simulated Data of Advanced Land Imaging (EO-1) Sensor. *Communications in soil science and plant analysis*, 39(19-20), 2795-2811. doi: 10.1080/00103620802432717
- Bastiaanssen, W., Wilink, S., Obando, E. B., & Leclert, L. (2011). Mapping and assessment by remote sensing of the prevailing agro-hydrological and soil salinity conditions in the Al Hassa Oasis, Saudi Arabia. Wageningen, The Netherlands: WaterWatch.
- Baumgardner, M., Silva, L., Biehl, L., & Stoner, E. (1985). Reflectance properties of soils. *Advances in agronomy*, 38, 2-44.
- Beaumont, L. J., Hughes, L., & Pitman, A. J. (2008). Why is the choice of future climate scenarios for species distribution modelling important? *Ecology Letters*, 11(11), 1135-1146. doi: 10.1111/j.1461-0248.2008.01231.x
- Ben-Dor, E., Goldshleger, N., Benyamini, Y., Agassi, M. R., & Blumberg, D. G. (2003). The spectral reflectance properties of soil structural crusts in the 1.2-to 2.5- μ m spectral region. *Soil Science Society of America Journal*, 67(1), 289-299.
- Ben-Dor, E., Goldshleger, N., & Eshel Mor, V. (2008a). Combined active and passive remote sensing methods for assessing soil salinity: a case study from Jezre'el Valley, Northern Israel. In G. Metternicht & J. A. Zinck (Eds.), *Remote sensing of soil salinization: impact on land management* (pp. 236-253). Boca Raton, United States of America: CRC Press.

- Ben-Dor, E., Irons, J. R., & Epema, G. (1999). Soil reflectance. In A. N. Rencz & R. A. Ryerson (Eds.), *Manual of Remote Sensing, Remote Sensing for the Earth Sciences* (3 ed., Vol. 3, pp. 111–188). New York: John Wiley & Sons.
- Ben-Dor, E., Metternicht, G., Goldshleger, N., Mor, E., Mirlas, V., & Basson, U. (2008b). Review of remote sensing based methods to assess soil salinity. In G. Metternicht & J. A. Zaid (Eds.), *Remote Sensing of Soil Salinization: Impact on Land Management* (pp. 39-56). New York: CRC Press, Taylor and Francis
- Ben-Dor, E., Patkin, K., Banin, A., & Karnieli, A. (2002). Mapping of several soil properties using DAIS-7915 hyperspectral scanner data—a case study over clayey soils in Israel. *International Journal of Remote Sensing*, 23(6), 1043-1062.
- Bernstein, L. (1975). Effects of salinity and sodicity on plant growth. *Annual review of phytopathology*, 13(1), 295-312.
- Bilgili, A. V. (2013). Spatial assessment of soil salinity in the Harran Plain using multiple kriging techniques. *Environmental monitoring and assessment*, 185(1), 777-795.
- Bokhary, H. A. (2010). Seed-borne fungi of date-palm, *Phoenix dactylifera* L. from Saudi Arabia. *Saudi Journal of Biological Sciences*, 17(4), 327-329. doi: 10.1016/j.sjbs.2010.06.005
- Bouaziz, M., Gloaguen, R., & Samirb, B. (2011a). *Remote mapping of susceptible areas to soil salinity, based on hyperspectral data and geochemical, in the southern part of Tunisia*. Paper presented at the Proc. SPIE 8174, Remote Sensing for Agriculture, Ecosystems, and Hydrology XIII, Prague, Czech Republic
- Bouaziz, M., Matschullat, J., & Gloaguen, R. (2011b). Improved remote sensing detection of soil salinity from a semi-arid climate in Northeast Brazil. *Comptes Rendus Geoscience*, 343(11-12), 795–803.
- Braimoh, A. K., & Vlek, P. L. G. (2008). *Land use and soil resources*: Springer
- Brown, D. J., Shepherd, K. D., Walsh, M. G., Dewayne Mays, M., & Reinsch, T. G. (2006). Global soil characterization with VNIR diffuse reflectance spectroscopy. *Geoderma*, 132(3), 273-290.
- Brunner, P., Li, H., Kinzelbach, W., & Li, W. (2007). Generating soil electrical conductivity maps at regional level by integrating measurements on the ground and remote sensing data. *International Journal of Remote Sensing*, 28(15), 3341-3361.
- Bruzzone, L., & Prieto, D. F. (2000). Automatic analysis of the difference image for unsupervised change detection. *Geoscience and Remote Sensing, IEEE Transactions on*, 38(3), 1171-1182. doi: 10.1109/36.843009
- Bustan, A., Sagi, M., De Malach, Y., & Pasternak, D. (2004). Effects of saline irrigation water and heat waves on potato production in an arid environment. *Field crops research*, 90(2), 275-285. doi: 10.1016/j.fcr.2004.03.007
- Canty, M. J., Nielsen, A. A., & Schmidt, M. (2004). Automatic radiometric normalization of multitemporal satellite imagery. *Remote Sensing of Environment*, 91(3), 441-451. doi: 10.1016/j.rse.2003.10.024
- Caviezel, C., Hunziker, M., Schaffner, M., & Kuhn, N. J. (2014). Soil–vegetation interaction on slopes with bush encroachment in the central Alps – adapting slope stability measurements to shifting process domains. *Earth Surface Processes and Landforms*, 39(4), 509-521. doi: 10.1002/esp.3513
- Cayan, D. R., Das, T., Pierce, D. W., Barnett, T. P., Tyree, M., & Gershunov, A. (2010). Future dryness in the southwest US and the hydrology of the early 21st century drought. *Proceedings of the National Academy of Sciences*, 107(50), 21271-21276. doi: 10.1073/pnas.0912391107
- Cetin, M., & Kirda, C. (2003). Spatial and temporal changes of soil salinity in a cotton field irrigated with low-quality water. *Journal of Hydrology*, 272(1), 238-249.

- Chander, G., Markham, B. L., & Helder, D. L. (2009). Summary of current radiometric calibration coefficients for Landsat MSS, TM, ETM+, and EO-1 ALI sensors. *Remote Sensing of Environment*, 113(5), 893-903. doi: 10.1016/j.rse.2009.01.007
- Chao, C. T., & Krueger, R. R. (2007). The date palm (Phoenix dactylifera L.): overview of biology, uses, and cultivation. *HortScience*, 42(5), 1077-1082.
- Chavez, P. S. (1996). Image-based atmospheric corrections-revisited and improved. *Photogrammetric engineering and remote sensing*, 62(9), 1025-1035.
- Cheng, J.-f., Wan, F.-h., & Guo, J.-y. (2006). Potential Distribution of Frankliniella occidentalis (Pergande)(Thysanoptera: Thripidae) in China by Using Combined CLIMEX and GIS Tools [J]. *Scientia Agricultura Sinica*, 3, 013.
- Cheng, J., & Masser, I. (2003). Urban growth pattern modeling: a case study of Wuhan city, PR China. *Landscape and urban planning*, 62(4), 199-217.
- Chhabra, R. (1996). *Soil salinity and water quality*. Brookfield, United States of America: Taylor and Francis.
- Citino, N. J. (2012). Desert Kingdom: How Oil and Water Forged Modern Saudi Arabia. *Technology and Culture*, 53(1), 234-236.
- Clark, R. N., King, T. V. V., Klejwa, M., Swayze, G. A., & Vergo, N. (1990). High spectral resolution reflectance spectroscopy of minerals. *Journal of Geophysical Research*, 95(B8), 12653-12612,12680.
- Cloutis, E. (1996). Review Article Hyperspectral geological remote sensing: evaluation of analytical techniques. *International Journal of Remote Sensing*, 17(12), 2215-2242.
- Cohen, W. B., Fiorella, M., Gray, J., Helmer, E., & Anderson, K. (1998). An efficient and accurate method for mapping forest clearcuts in the Pacific Northwest using Landsat imagery. *Photogrammetric engineering and remote sensing*, 64(4), 293-299.
- Congalton, R. G. (1991). A review of assessing the accuracy of classifications of remotely sensed data. *Remote Sensing of Environment*, 37(1), 35-46. doi: 10.1016/0034-4257(91)90048-B
- Coppin, P., Jonckheere, I., Nackaerts, K., Muys, B., & Lambin, E. (2004). Review Article Digital change detection methods in ecosystem monitoring: a review. *Int J Remote Sens*, 25(9), 1565-1596. doi: 10.1080/0143116031000101675
- Corwin, D., & Lesch, S. (2003). Application of soil electrical conductivity to precision agriculture. *Agronomy Journal*, 95(3), 455-471.
- Crouch, R. (2000). *Rehabilitation and management of salt affected soils with reference to project TCP/THA/8922*. Paper presented at the FAO Regional Workshop on the Impact of Shrimp Farming on Arable Land and Rehabilitation of Resultant Salt Affected Soils, 4, Ayutthaya (Thailand), 20-24 Nov 2000.
- d'Amour, C. B., Reitsma, F., Baiocchi, G., Barthel, S., Güneralp, B., Erb, K.-H., . . . Seto, K. C. (2016). Future urban land expansion and implications for global croplands. *Proceedings of the National Academy of Sciences*, 201606036.
- Daddi Bouhoun, M., Marlet, S., Brinis, L., Saker, M. L., Rabier, J., & Côte, M. (2011). A survey of the combined effects of waterlogging and salinity on fruit yield in the date palm groves of the Wargla basin, Algeria. *Fruits*, 66(01), 11-24. doi: 10.1051/fruits/2010037
- Dale, P., Hulsman, K., & Chandica, A. (1986). Classification of reflectance on colour infrared aerial photographs and sub-tropical salt-marsh vegetation types. *International Journal of Remote Sensing*, 7(12), 1783-1788.
- Darwesh, R. S. (2013). Improving growth of date palm plantlets grown under salt stress with yeast and amino acids applications. *Annals of Agricultural Sciences*, 58(2), 247-256. doi: 10.1016/j.aas.2013.07.014

- Dash, M. C. (2001). *Fundamentals Of Ecology*: Tata McGraw-Hill Education.
- De Espindola, G. M., De Aguiar, A. P. D., Pebesma, E., Câmara, G., & Fonseca, L. (2012). Agricultural land use dynamics in the Brazilian Amazon based on remote sensing and census data. *Applied Geography*, 32(2), 240-252.
- De Jong, S. (1992). The analysis of spectroscopical data to map soil types and soil crusts of Mediterranean eroded soils. *Soil technology*, 5(3), 199-211.
- De Jong, S. M., Addink, E. A., Van Beek, L. P. H., & Duijsings, D. (2011). Physical characterization, spectral response and remotely sensed mapping of Mediterranean soil surface crusts. *Catena*, 86(1), 24-35.
- Deering, D., & Rouse, J. (1975). *Measuring 'forage production' of grazing units from Landsat MSS data*. Paper presented at the 10th International Symposium on Remote Sensing of Environment, Ann Arbor, Michigan.
- Dehaan, R., & Taylor, G. (2003). Image-derived spectral endmembers as indicators of salinisation. *International Journal of Remote Sensing*, 24(4), 775-794.
- Dehaan, R. L., & Taylor, G. R. (2002). Field-derived spectra of salinized soils and vegetation as indicators of irrigation-induced soil salinization. *Remote Sensing of Environment*, 80(3), 406-417. doi: 10.1016/S0034-4257(01)00321-2
- Dehni, A., & Lounis, M. (2012). Remote Sensing Techniques for Salt Affected Soil Mapping: Application to the Oran Region of Algeria. *Procedia Engineering*, 33, 188-198.
- Demattê, J. A. M., Campos, R. C., Alves, M. C., Fiorio, P. R., & Nanni, M. R. (2004). Visible–NIR reflectance: a new approach on soil evaluation. *Geoderma*, 121(1), 95-112.
- Dent, D., & Young, A. (1981). *Soil survey and land evaluation*: George Allen & Unwin.
- Dewitte, O., Jones, A., Elbelrhiti, H., Horion, S., & Montanarella, L. (2012). Satellite remote sensing for soil mapping in Africa An overview. *Progress in Physical Geography*, 36(4), 514-538.
- Dial, G., Bowen, H., Gerlach, F., Grodecki, J., & Oleszczuk, R. (2003). IKONOS satellite, imagery, and products. *Remote Sensing of Environment*, 88(1), 23-36.
- Diao, X., Hazell, P., & Thurlow, J. (2010). The role of agriculture in African development. *World development*, 38(10), 1375-1383.
- Ding, J., Wu, M., & Tashpolat, T. (2011). Study on Soil Salinization Information in Arid Region Using Remote Sensing Technique. *Agricultural Sciences in China*, 10(3), 404-411.
- Dixon, G. R. (2012). Climate change – impact on crop growth and food production, and plant pathogens. *Canadian Journal of Plant Pathology*, 34(3), 362-379. doi: 10.1080/07060661.2012.701233
- Djanibekov, N., van Assche, K., Bobojonov, I., & Lamers, J. P. A. (2012). Farm Restructuring and Land Consolidation in Uzbekistan: New Farms with Old Barriers. *Europe-Asia Studies*, 64(6), 1101-1126. doi: 10.1080/09668136.2012.691720
- Dong, G., Xu, E., & Zhang, H. (2015). Spatiotemporal variation of driving forces for settlement expansion in different types of counties. *Sustainability*, 8(1), 39.
- Douaik, A., Meirvenne, M., & Toth, T. (2008). Stochastic approaches for space–time modeling and interpolation of soil salinity. In G. Metternicht & J. A. Zinck (Eds.), *Remote sensing of soil salinization: impact on land management* (pp. 273-289). Boca Raton, United States of America: CRC Press
- Douaik, A., Van Meirvenne, M., Toth, T., & Serre, M. (2004). Space-time mapping of soil salinity using probabilistic bayesian maximum entropy. *Stochastic Environmental Research and Risk Assessment*, 18(4), 219-227.
- Douaoui, A. E. K., Nicolas, H., & Walter, C. (2006). Detecting salinity hazards within a semiarid context by means of combining soil and remote-sensing data. *Geoderma*, 134(1), 217-230.

- Drinnan, J. E., & Menzel, C. M. (1995). Temperature affects vegetative growth and flowering of coffee (*Coffea arabica* L.). *Journal of Horticultural Science*, 70(1), 25-34. doi: 10.1080/14620316.1995.11515269
- Dubovyk, O., Sliuzas, R., & Flacke, J. (2011). Spatio-temporal modelling of informal settlement development in Sancaktepe district, Istanbul, Turkey. *ISPRS journal of photogrammetry and remote sensing*, 66(2), 235-246.
- Dutkiewicz, A. (2006). *Evaluating hyperspectral imagery for mapping the surface symptoms of dryland salinity*. The University of Adelaide, Adelaide, Australia.
- Dwivedi, R. S. (2001). Soil resources mapping: A remote sensing perspective. *Remote Sensing Reviews*, 20(2), 89-122.
- Dwivedi, R. S., Kothapalli, R. V., Singh, A. N., Metternicht, G., & Zinck, J. (2008). Generation of farm-level information on salt-affected soils using IKONOS-II multispectral data. In G. metternicht & J. A. Zaid (Eds.), *Remote Sensing of Soil Salinization: Impact on Land Management* (pp. 73-89). New York: CRC Press, Taylor and Francis
- El-Khawaga, A. (2013). Effect of anti-salinity agents on growth and fruiting of different date palm cultivars. *Asian J Crop Sci*, 5(1), 65-80.
- El Harti, A., Lhissou, R., Chokmani, K., Ouzemou, J.-e., Hassouna, M., Bachaoui, E. M., & El Ghmari, A. (2016). Spatiotemporal monitoring of soil salinization in irrigated Tadla Plain (Morocco) using satellite spectral indices. *International Journal of Applied Earth Observation and Geoinformation*, 50, 64-73.
- Eldeiry, A. A., & Garcia, L. A. (2004). Spatial modeling using remote sensing, GIS, and field data to assess crop yield and soil salinity. *Hydrology Days*, 7, 55-66.
- Eldeiry, A. A., & Garcia, L. A. (2008). Detecting soil salinity in alfalfa fields using spatial modeling and remote sensing. *Soil Science Society of America Journal*, 72(1), 201-211.
- Eldeiry, A. A., & García, L. A. (2011). *Using deterministic and geostatistical techniques to estimate soil salinity at the sub-basin scale and the field scale*. Paper presented at the the 31th Annual Hydrology Days,, Fort Collins, CO.
- Elhaddad, A., & Garcia, L. (2005). *Detecting Soil Salinity Levels in Agricultural Lands Using Satellite Imagery*. Paper presented at the Esri International User Conference, San Diego.
- Elhag, M. (2016). Evaluation of Different Soil Salinity Mapping Using Remote Sensing Techniques in Arid Ecosystems, Saudi Arabia. *Journal of Sensors*, 2016, 8. doi: 10.1155/2016/7596175
- Elmetwalli, A. M. H., Tyler, A. N., Hunter, P. D., & Salt, C. A. (2012). Detecting and distinguishing moisture-and salinity-induced stress in wheat and maize through in situ spectroradiometry measurements. *Remote Sensing Letters*, 3(4), 363-372.
- Elnaggar, A., & Noller, J. (2010). Application of Remote-sensing Data and Decision-Tree Analysis to Mapping Salt-Affected Soils over Large Areas. *Remote Sensing*, 2(1), 151.
- Elprince, A. M. (1985). Model for the soil solution composition of an oasis. *Soil Science Society of America Journal*, 49(5), 1121-1128.
- Elprince, A. M., Makki, Y. M., Al-Barrak, S., & Tamim, M. (1982). *Use of computer graphics in developing densitiesmaps for the date culture of Al-Hassa oasis in Saudi Arabia*. Paper presented at the First Symposium on Date Palm Al-Hassa, Saudi Arabia.
- Erskine, W., Moustafa, A. T., Osman, A. E., Lashine, Z., Nejatian, A., Badawi, T., & Ragy, S. M. (2004). *Date palm in the GCC countries of the Arabian Peninsula*. Paper presented at the Proc. Regional Workshop on Date Palm Development in the Arabian Peninsula, Abu Dhabi, UAE.
- Everitt, J., Escobar, D., Gerbermann, A., & Alaniz, M. (1988). Detecting saline soils with video imagery. *Photogrammetric engineering and remote sensing*, 54(9), 1283-1287.

- Fallah Shamsi, S. R., Zare, S., & Abtahi, S. A. (2012). Soil salinity characteristics using moderate resolution imaging spectroradiometer (MODIS) images and statistical analysis. *Archives of Agronomy and Soil Science*, 59(4), 471-489. doi: 10.1080/03650340.2011.646996
- Fan, X., Pedroli, B., Liu, G., Liu, Q., Liu, H., & Shu, L. (2012). Soil salinity development in the yellow river delta in relation to groundwater dynamics. *Land Degradation & Development*, 23(2), 175-189.
- FAOSTAT. (2013). Food and Agriculture Organization of the United Nations. <http://faostat.fao.org/site/342/default.aspx>
- Farifteh, J. (2007). *Imaging spectroscopy of salt-affected soils: Model-based integrated method*. (PhD), International Institute Geo-information Science and Earth Observation (ITC) and Utrecht University, Netherlands.
- Farifteh, J., Farshad, A., & George, R. (2006). Assessing salt-affected soils using remote sensing, solute modelling, and geophysics. *Geoderma*, 130(3), 191-206.
- Farifteh, J., Van der Meer, F., Atzberger, C., & Carranza, E. (2007). Quantitative analysis of salt-affected soil reflectance spectra: A comparison of two adaptive methods (PLSR and ANN). *Remote sensing of Environment*, 110(1), 59-78.
- Fernandez-Buces, N., Siebe, C., Cram, S., & Palacio, J. (2006). Mapping soil salinity using a combined spectral response index for bare soil and vegetation: A case study in the former lake Texcoco, Mexico. *Journal of arid environments*, 65(4), 644-667.
- Fethi, B., Magnus, P., Ronny, B., & Akissa, B. (2010). Estimating soil salinity over a shallow saline water table in semiarid Tunisia. *The Open Hydrology Journal*, 4, 91-101.
- Field, A., Miles, J., & Field, Z. (2012a). *Discovering Statistics Using R*. London, United Kingdom: SAGE Publications.
- Field, C. B., Barros, V., Stocker, T. F., Qin, D., Dokken, D. J., Ebi, K. L., . . . Midgley, P. M. (2012b). *Managing the Risks of Extreme Events and Disasters to Advance Climate Change Adaptation: Special Report of the Intergovernmental Panel on Climate Change*. New York, USA: Cambridge University Press.
- Fourati, T. H., Bouaziz, M., Benzina, M., & Bouaziz, S. (2015). Modeling of soil salinity within a semi-arid region using spectral analysis. *Arabian J. Geosci*, 8(12), 11175-11182. doi: 10.1007/s12517-015-2004-3
- Fraser, D., & Joseph, S. (1998). *Mapping soil salinity in the Murray Valley (NSW) using satellite imagery*. Paper presented at the *In Proceeding of the 9th Australian Remote Sensing and Photogrammetry Conference*, Sydney, Australia
- Fung, T., & LeDrew, E. (1988). The determination of optimal threshold levels for change detection using various accuracy indices. *Photogrammetric engineering and remote sensing*, 54(10), 1449-1454.
- Furby, S., Australia, W., Mathematics, C. D. o., & Statistics. (1995). *Detecting and monitoring salt-affected land: A report from the LWRRDC project detecting and monitoring changes in land condition through time using remotely sensed data*: CSIRO Division of Mathematics & Statistics.
- Gao, J. (2008). *Digital Analysis of Remotely Sensed Imagery* (1st ed.). New York, United States of America: McGraw Hill
- Gardi, C. (2017). *Urban Expansion, Land Cover and Soil Ecosystem Services*. New York: Taylor & Francis.
- Ghabour, T., & Daels, L. (1993). Mapping and monitoring of soil salinity of ISSN. *Egyptian Journal of Soil Science*, 33(4), 355-370.

- Ghrefat, H. A., Goodell, P. C., Hubbard, B. E., Langford, R. P., & Aldouri, R. E. (2007). Modeling grain size variations of aeolian gypsum deposits at White Sands, New Mexico, using AVIRIS imagery. *Geomorphology*, 88(1), 57-68.
- Glenn, E. P., Brown, J. J., & Blumwald, E. (1999). Salt tolerance and crop potential of halophytes. *Critical Reviews in Plant Sciences*, 18(2), 227-255.
- Goldshleger, N., Ben-Dor, E., Benyamini, Y., & Agassi, M. (2004). Soil reflectance as a tool for assessing physical crust arrangement of four typical soils in Israel. *Soil Science*, 169(10), 677-687.
- Goldshleger, N., Chudnovsky, A., & Ben-Binyamin, R. (2013). Predicting salinity in tomato using soil reflectance spectra. *International Journal of Remote Sensing*, 34(17), 6079-6093. doi: 10.1080/01431161.2013.793859
- Goldshleger, N., Livne, I., Chudnovsky, A., & Ben-Dor, E. (2012). New results in integrating passive and active remote sensing methods to assess soil salinity: a case study from Jezre'el Valley, Israel. *Soil Science*, 177(6), 392-401.
- Goossens, R., Alavi Panah, S., De Dapper, M., & Kissyar, O. (1999). *The use of thermal band of Landsat TM for the study of soil salinity in Iran (Ardakan area) and Egypt (Ismailia Province)*.
- Goossens, R., El Badawi, M., Ghabour, T., & De Dapper, M. (1993). A simulation model to monitor the soil salinity in irrigated arable land in arid areas based upon remote sensing and GIS. *EARSeL. Advances in remote sensing*, 2(3), 165-171.
- Goto, K., Goto, T., Nmor, J. C., Minematsu, K., & Gotoh, K. (2015). Evaluating salinity damage to crops through satellite data analysis: application to typhoon affected areas of southern Japan. *Natural Hazards*, 75(3), 2815-2828. doi: 10.1007/s11069-014-1465-0
- Gupta, R. P. (2003). *Remote sensing geology*. New York: Springer Verlag.
- Hadrami, A. E., Daayf, F., & Hadrami, I. E. (2011). In Vitro Selection for Abiotic Stress in Date Palm. In M. S. Jain, M. J. Al-Khayri & V. D. Johnson (Eds.), *Date Palm Biotechnology* (pp. 237-252). Dordrecht: Springer Netherlands.
- Hall, F. G., Strebel, D. E., Nickeson, J. E., & Goetz, S. J. (1991). Radiometric rectification: Toward a common radiometric response among multitemporal, multisensor images. *Remote Sensing of Environment*, 35(1), 11-27. doi: 10.1016/0034-4257(91)90062-B
- Hampe, A. (2004). Bioclimate Envelope Models: What They Detect and What They Hide. *Global Ecology and Biogeography*, 13(5), 469-471.
- Hamzeh, S., Naseri, A. A., AlaviPanah, S. K., Mojaradi, B., Bartholomeus, H. M., Clevers, J., & Behzad, M. (2012a). Estimating salinity stress in sugarcane fields with spaceborne hyperspectral vegetation indices. *International Journal of Applied Earth Observation and Geoinformation*, 21, 282-290.
- Hamzeh, S., Naseria, A. A., Alavi Panah, S. K., Mojaradic, B., Bartholomeus, H. M., & Herold, M. (2012b). *Mapping salinity stress in sugarcane fields with hyperspectral satellite imagery*. Paper presented at the Proc. SPIE 8531, Remote Sensing for Agriculture, Ecosystems, and Hydrology XIV, Edinburgh, United Kingdom
- Hick, P., & Russell, W. (1987). *Remote sensing of agricultural salinity*: CSIRO, Division of Exploration Geoscience.
- Hillel, D. (1998). *Environmental soil physics: fundamentals, applications, and environmental considerations*. San Diego, California: Academic Press.
- Hillel, D. (2000). *Salinity management for sustainable irrigation: Integrating science, environment, and economics*: World Bank Publications.

- Hoffman, G. J., Evans, R. G., Jensen, M. E., Martin, D. L., & Elliott, R. L. (2007). *Design and operation of farm irrigation systems*: American Society of Agricultural and Biological Engineers St. Joseph, MI.
- Howari, F. (2003). The use of remote sensing data to extract information from agricultural land with emphasis on soil salinity. *Soil Research*, 41(7), 1243-1253.
- Howari, F., & Goodell, P. (2008). Characterization of Salt-Crust Build-Up and Soil Salinization in the United Arab Emirates by Means of Field and Remote Sensing Techniques. In G. Metternicht & A. Zinck (Eds.), *Remote Sensing of Soil Salinization: Impact on Land Management*: CRC Press.
- Howari, F., Goodell, P., & Miyamoto, S. (2002). Spectral properties of salt crusts formed on saline soils. *Journal of environmental quality*, 31(5), 1453-1461.
- Hu, Z., & Lo, C. (2007). Modeling urban growth in Atlanta using logistic regression. *Computers, Environment and Urban Systems*, 31(6), 667-688.
- Huang, C., Davis, L., & Townshend, J. (2002). An assessment of support vector machines for land cover classification. *International Journal of Remote Sensing*, 23(4), 725-749.
- Huang, S., Liu, Q., & Li, X. (2005). *Spectral model of soil salinity in Xinjiang of China*. Paper presented at the Geoscience and Remote Sensing Symposium, Seoul, Korea.
- Huete, A. R. (1988). A soil-adjusted vegetation index (SAVI). *Remote Sensing of Environment*, 25(3), 295-309.
- Hussain, G., Al-Zarah, A. I., & Latif, M. S. (2012). Influence of Groundwater Irrigation on Chemical Properties of Soils in the Vicinity of Wastewater Drainage Canals in Al-Alisa Oasis. *Research Journal of Environmental Toxicology (RJET)*, 7, 1-17. doi: 10.3923/rjet.2013.1.17
- Hussain, G., & Sadiq, M. (1991). Metal chemistry of irrigation and drainage waters of Al-Ahsa Oasis of Saudi Arabia and its effects on soil properties. *Water, Air, & Soil Pollution*, 57(1), 773-783.
- Hussain, N., Al-Rawahy, A. S., Rabee, J., & Al-Amri, M. (2006). Causes, origin, genesis and extent of soil salinity in the Sultanate of Oman. *Pakistan Journal of Agricultural Sciences* 43, 1-2.
- Hussain, Z. (1982). Problems of irrigated agriculture in Al-Hassa, Saudi Arabia. *Agricultural Water Management*, 5(4), 359-374.
- Hussein, A., El-Desouki, M., El-Kased, F., Nour, G., & Abd-El-Hamid, N. (1993). Effect of salinity on date palm seeds germination and early seedling growth. *Journal of Agricultural Sciences, Mansoura Univ.*, 18.
- Hyvönen, T., Luoto, M., & Uotila, P. (2012). Assessment of weed establishment risk in a changing European climate. *Agricultural and Food Science*, 21(4), 348-360.
- İlseven, M., & Ünsalan, C. (2012). Pixel-Based Change Detection Methods *Two-Dimensional Change Detection Methods* (pp. 7-21): Springer.
- IPCC. (2007). Climate Change 2007 - The Physical Science Basis. In S. Solomon, D. Qin, M. Manning, Z. Chen, M. Marquis, K. Averyt, M. M. Tignor & H. L. Miller (Eds.), *Contribution of Working Group I to the Fourth Assessment Report of the Intergovernmental Panel on Climate Change* (pp. 996). United Kingdom and New York: Cambridge University Press.
- Iqbal, F. (2011). Detection of salt affected soil in rice-wheat area using satellite image. *African Journal of Agricultural Research*, 6(21), 4973-4982.
- Irz, X., Lin, L., Thirtle, C., & Wiggins, S. (2001). Agricultural productivity growth and poverty alleviation. *Development policy review*, 19(4), 449-466.
- Ivushkin, K., Bartholomeus, H., Bregt, A. K., & Pulatov, A. (2017). Satellite thermography for soil salinity assessment of cropped areas in Uzbekistan. *Land Degradation & Development*, 28(3), 870-877.

- Izuchukwu, O. (2011). Analysis of the contribution of agricultural sector on the Nigerian economic development. *World review of business research*, 1(1), 191-200.
- Jabbar, M. T., & Chen, X. (2008). Land degradation due to salinization in arid and semi-arid regions with the aid of geo-information techniques. *Geo-spatial Information Science*, 11(2), 112-120.
- Jain, S. M. (2011). Prospects of in vitro conservation of date palm genetic diversity for sustainable production. *Emirates Journal of Food and Agriculture*, 23(2), 110-119.
- Jain, S. M., Al-Khayri, J. M., & Johnson, D. V. (2011). *Date palm biotechnology*: Springer Science & Business Media.
- Jaradat, A. A. (2016). Genetic Erosion of *Phoenix dactylifera* L.: Perceptible, Probable, or Possible. In M. R. Ahuja & M. S. Jain (Eds.), *Genetic Diversity and Erosion in Plants: Case Histories* (pp. 131-213). Cham: Springer International Publishing.
- Jardine, A., Speldewinde, P., Carver, S., & Weinstein, P. (2007). Dryland salinity and ecosystem distress syndrome: human health implications. *EcoHealth*, 4(1), 10-17.
- Jarvis, D. I., Hodgkin, T., Brown, A. H., Tuxill, J., Noriega, I. L., Smale, M., & Sthapit, B. (2016). *Crop Genetic Diversity in the Field and on the Farm: Principles and Applications in Research Practices*: Yale University Press.
- Jones, P. G., & Thornton, P. K. (2003). The potential impacts of climate change on maize production in Africa and Latin America in 2055. *Global Environmental Change*, 13(1), 51-59.
- Jordán, M., Navarro-Pedreño, J., García-Sánchez, E., Mateu, J., & Juan, P. (2004). Spatial dynamics of soil salinity under arid and semi-arid conditions: geological and environmental implications. *Environmental Geology*, 45(4), 448-456.
- Judkins, G., & Myint, S. (2012). Spatial variation of soil salinity in the Mexicali valley, Mexico: application of a practical method for agricultural monitoring. *Environmental management*, 50(3), 478-489
- Kaleita, A., Tian, L., & Hirschi, M. (2005). Relationship between soil moisture content and soil surface reflectance. *Transactions of the ASAE*, 48(5), 1979-1986.
- Kang, Y., Khan, S., & Ma, X. (2009). Climate change impacts on crop yield, crop water productivity and food security—A review. *Progress in Natural Science*, 19(12), 1665-1674.
- Karavanova, E. I., Shrestha, D. P., & Orlov, D. S. (2001). Application of remote sensing techniques for the study of soil salinity in semi-arid Uzbekistan. In E. M. Bridges, I. D. Hannam, L. R. Oldeman, F. T. P. de Vries, S. J. Scherr & S. Sombatpanit (Eds.), *Responses to Land Degradation*. (pp. 261-273). New Delhi: Oxford and IBH Publishing Co. Pvt. Ltd.
- Kassem, M. A. (2007). Water requirements and crop coefficient of date palm trees Sukariah CV. *Misr J. Ag. Eng*, 24(2), 339-359.
- Katawat, R., & Kotrapat, W. (2004). *Use of LANDSAT-7 ETM+ with ancillary data for soil salinity mapping in northeast Thailand*. Paper presented at the Third International Conference on Experimental Mechanics and Third Conference of the Asian
- Keddy, P. A. (2010). *Wetland ecology: principles and conservation*. Cambridge, United Kingdom Cambridge University Press.
- Kersten, G. E., Mikolajuk, Z., & Yeh, A. G.-O. (2000). *Decision support systems for sustainable development: a resource book of methods and applications*. Norwell, Massachusetts, USA: Kluwer Academic.
- Khan, N. M., Rastokuev, V. V., Sato, Y., & Shiozawa, S. (2005). Assessment of hydrosaline land degradation by using a simple approach of remote sensing indicators. *Agricultural Water Management*, 77(1), 96-109.
- Khorram, S., Nelson, S. A. C., & Koch, F. H. (2012). *Remote sensing*: Springer.

- Khuder, H., Danjon, F., Stokes, A., & Fourcaud, T. (2006). *Growth response and root architecture of black locust seedlings growing on slopes and subjected to mechanical perturbation*. Paper presented at the Proc. 5th Plant Biomechanics Conference–Stockholm, August.
- Kleinbaum, D. G., & Klein, M. (2010). *Logistic Regression: A Self-Learning Text*. New York, USA: Springer Verlag GmbH.
- Kleynhans, W., Olivier, J. C., Wessels, K. J., Salmon, B. P., Van den Bergh, F., & Steenkamp, K. (2011). Detecting Land Cover Change Using an Extended Kalman Filter on MODIS NDVI Time-Series Data. *IEEE Geoscience and Remote Sensing Letters*, 8(3), 507-511. doi: 10.1109/LGRS.2010.2089495
- Koohafkan, P. (2012). *Water and cereals in drylands*: The Food and Agriculture Organization of the United Nations and Earthscan.
- Koshal, A. K. (2010). *Indices based salinity areas detection through remote sensing and GIS In parts of south waste Punjab*. Paper presented at the 13th annual international conference and Exhibition on geospatial information technology and applications, Gurgaon, India.
- Koshal, A. K. (2012). Spectral characteristics of soil salinity areas in parts of South–West Punjab through Remote Sensing and GIS. *International Journal of Remote Sensing and GIS*, 1(2), 84-89.
- Kotak, S., Larkindale, J., Lee, U., von Koskull-Döring, P., Vierling, E., & Scharf, K.-D. (2007). Complexity of the heat stress response in plants. *Current Opinion in Plant Biology*, 10(3), 310-316. doi: 10.1016/j.pbi.2007.04.011
- Krannich, J. M. (2006). A Modern Disaster: Agricultural Land, Urban Growth, and the Need for a Federally Organized Comprehensive Land Use Planning Model. *Cornell JL & Pub. Pol'y*, 16, 57.
- Kriticos, D. J., Webber, B. L., Leriche, A., Ota, N., Macadam, I., Bathols, J., & Scott, J. K. (2012). CliMond: global high-resolution historical and future scenario climate surfaces for bioclimatic modelling. *Methods in Ecology and Evolution*, 3(1), 53-64. doi: 10.1111/j.2041-210X.2011.00134.x
- Kriticos, D. J., Yonow, T., & McFadyen, R. E. (2005). The potential distribution of *Chromolaena odorata* (Siam weed) in relation to climate. *Weed Research*, 45(4), 246-254. doi: 10.1111/j.1365-3180.2005.00458.x
- Kumar, L., Schmidt, K., Dury, S., & Skidmore, A. (2002). Imaging spectrometry and vegetation science. In F. v. d. Meer. & S. M. d. Jong. (Eds.), *Imaging spectrometry* (2 ed., pp. 111-156).
- Lasaponara, R., & Masini, N. (2012). *Satellite Remote Sensing: A New Tool for Archaeology* (Vol. 16): Springer.
- Laurance, W. F., Sayer, J., & Cassman, K. G. (2014). Agricultural expansion and its impacts on tropical nature. *Trends in ecology & evolution*, 29(2), 107-116.
- Lesch, S. M., Strauss, D. J., & Rhoades, J. D. (1995). Spatial prediction of soil salinity using electromagnetic induction techniques: 1. Statistical prediction models: A comparison of multiple linear regression and cokriging. *Water Resources Research*, 31(2), 373-386.
- Lhermitte, S., Verbesselt, J., Verstraeten, W. W., Veraverbeke, S., & Coppin, P. (2011). Assessing intra-annual vegetation regrowth after fire using the pixel based regeneration index. *J Photogramm Remote Sens*, 66(1), 17-27. doi: 10.1016/j.isprsjprs.2010.08.004
- Li, X., Zhou, W., & Ouyang, Z. (2013). Forty years of urban expansion in Beijing: What is the relative importance of physical, socioeconomic, and neighborhood factors? *Applied Geography*, 38, 1-10.
- Lillesand, T., Kiefer, R. W., & Chipman, J. (2014). *Remote Sensing and Image Interpretation*: John Wiley & Sons.

- Lim, T. K. (2012). *Edible Medicinal and Non-Medicinal Plants* (1 ed.): Springer Netherlands.
- Liu, H. Q., & Huete, A. (1995). A feedback based modification of the NDVI to minimize canopy background and atmospheric noise. *Geoscience and Remote Sensing, IEEE Transactions on*, 33(2), 457-465.
- Lobell, D. B., Lesch, S. M., Corwin, D. L., Ulmer, M. G., Anderson, K. A., Potts, D. J., . . . Baltes, M. J. (2010). Regional-scale assessment of soil salinity in the Red River Valley using multi-year MODIS EVI and NDVI. *Journal of environmental quality*, 39(1), 35-41.
- Lobell, D. B., Ortiz-Monasterio, J. I., Gurrola, F. C., & Valenzuela, L. (2007). Identification of saline soils with multiyear remote sensing of crop yields. *Soil Science Society of America Journal*, 71(3), 777-783.
- Lu, N., Zhang, Z., & Gao, Y. (2005). *Recognition and mapping of soil salinization in arid environment with hyperspectral data*. Paper presented at the Geoscience and Remote Sensing Symposium, 2005. IGARSS'05. Proceedings. , Seoul, Korea.
- Luleva, M. I. (2007). Identification of Soil Property Variation Using Spectral and Statistical Analyses on Field and ASTER Data. A Case Study of Tunisia. *International Institute for Geo-Information Science and Earth Observation, Enschede, The Netherlands*.
- Lunetta, R. S., Knight, J. F., Ediriwickrema, J., Lyon, J. G., & Worthy, L. D. (2006). Land-cover change detection using multi-temporal MODIS NDVI data. *Remote Sensing of Environment*, 105(2), 142-154. doi: 10.1016/j.rse.2006.06.018
- Luoto, M., Heikkinen, R. K., Pöyry, J., & Saarinen, K. (2006). Determinants of the biogeographical distribution of butterflies in boreal regions. *Journal of Biogeography*, 33(10), 1764-1778. doi: 10.1111/j.1365-2699.2005.01395.x
- Lyon, J. G., Yuan, D., Lunetta, R. S., & Elvidge, C. D. (1998). A change detection experiment using vegetation indices. *Photogrammetric engineering and remote sensing*, 64(2), 143-150.
- Madani, A. A. (2005). Soil salinity detection and monitoring using Landsat data: A case study from Siwa Oasis, Egypt. *GIsci Remote Sens*, 42(2), 171-181. doi: 10.2747/1548-1603.42.2.171
- Maeda, E. E., Clark, B. J., Pellikka, P., & Siljander, M. (2010). Modelling agricultural expansion in Kenya's Eastern Arc Mountains biodiversity hotspot. *Agricultural Systems*, 103(9), 609-620.
- Major, D., Baret, F., & Guyot, G. (1990). A ratio vegetation index adjusted for soil brightness. *International Journal of Remote Sensing*, 11(5), 727-740.
- Malash, N., Flowers, T., & Ragab, R. (2005). Effect of irrigation systems and water management practices using saline and non-saline water on tomato production. *Agricultural Water Management*, 78(1), 25-38. doi: 10.1016/j.agwat.2005.04.016
- Malins, D., & Metternicht, G. (2006). Assessing the spatial extent of dryland salinity through fuzzy modeling. *Ecological modelling*, 193(3), 387-411.
- Manchanda, M. (1984). Use of Remote Sensing Techniques in the Study of Distribution of Salt-Affected Soils in North-west India. *Journal of the Indian Society of Soil Science*, 32(4), 701-706.
- Mancino, G., Nolè, A., Ripullone, F., & Ferrara, A. (2014). Landsat TM imagery and NDVI differencing to detect vegetation change: assessing natural forest expansion in Basilicata, southern Italy. *iForest-Biogeosciences and Forestry*, 7(2), 75. doi: 10.3832/ifer0909-007
- Manickavasagan, A., Essa, M. M., & Sukumar, E. (2012). *Dates: Production, Processing, Food, and Medicinal Values*: CRC Press.
- Mariappan, V. E. N. (2010). Soil salinity assessment using geospatial technology, perspectives, approaches and strategies. *Indian Cartographer*, 30(30).

- Martínez, J.-M. Á., Suárez-Seoane, S., & Calabuig, E. D. L. (2011). Modelling the risk of land cover change from environmental and socio-economic drivers in heterogeneous and changing landscapes: The role of uncertainty. *Landscape and urban planning*, 101(2), 108-119.
- Mas, J.-F. (1999). Monitoring land-cover changes: a comparison of change detection techniques. *Int J Remote Sens*, 20(1), 139-152. doi: 10.1080/014311699213659
- Masoud, A., & Koike, K. (2006). Arid land salinization detected by remotely-sensed landcover changes: A case study in the Siwa region, NW Egypt. *Journal of Arid Environments*, 66(1), 151-167.
- Matinfar, H. R., Alavi Panah, S. K., Zand, F., & Khodaei, K. (2013). Detection of soil salinity changes and mapping land cover types based upon remotely sensed data. *Arabian Journal of Geosciences*, 6(3), 913-919. doi: 10.1007/s12517-011-0384-6
- McBratney, A., Mendonça Santos, M. d. L., & Minasny, B. (2003). On digital soil mapping. *Geoderma*, 117(1), 3-52.
- McFarlane, D. J., George, R., & Caccetta, P. (2004). *The extent and potential area of salt-affected land in Western Australia estimated using remote sensing and digital terrain models*. Paper presented at the Engineering Salinity Solutions: 1st National Salinity Engineering Conference 2004.
- Mehrjardi, R. T., Mahmoodi, S. H., Taze, M., & Sahebjalal, E. (2008). Accuracy assessment of soil salinity map in Yazd-Ardakan Plain, central Iran, based on Landsat ETM+ imagery. *American-Eurasian Journal of Agricultural & Environmental Sciences*, 3(5), 708-712.
- Menenti, M., Lorkeers, A., & Vissers, M. (1986). Application of thematic mapper data in Tunisia: estimation of daily amplitude in near-surface soil temperature and discrimination of hypersaline soils. *ICW technical bulletin new series*, 54.
- Meng, L., Zhou, S., Zhang, H., & Bi, X. (2016). Estimating soil salinity in different landscapes of the Yellow River Delta through Landsat OLI/TIRS and ETM+ Data. *Journal of coastal conservation*, 20(4), 271-279.
- Metternicht, G. (1998). Analyzing the relationship between ground based reflectance and environment indicators of salinity processes in the Cochabamba Valley (Bolivia). *International Journal of Ecology and Environmental Sciences*, 24, 359-370.
- Metternicht, G., & Zinck, J. A. (1997). Spatial discrimination of salt-and sodium-affected soil surfaces. *International Journal of Remote Sensing*, 18(12), 2571-2586.
- Metternicht, G., & Zinck, J. A. (2003). Remote sensing of soil salinity: potentials and constraints. *Remote Sensing of Environment*, 85(1), 1-20.
- Metternicht, G., & Zinck, J. A. (2008a). *Remote sensing of soil salinization: Impact on land management*. New York: CRC Press ,Taylor and Francis
- Metternicht, G., & Zinck, J. A. (2008b). Spectral behavior of salt types. In G. Metternicht & J. A. Zinck (Eds.), *Remote sensing of soil salinization: impact on land management* (pp. 21-36). Boca Raton, United States of America: CRC Press
- Mikki, M. S. (1998). *Present status and future prospects of dates and dates palm industries in Saudi Arabia*. Paper presented at the First International Conference on the Date Palm Al-Ain, UAE: United Arab Emirates University.
- Mitsuda, Y., & Ito, S. (2011). A review of spatial-explicit factors determining spatial distribution of land use/land-use change. *Landscape and Ecological Engineering*, 7(1), 117-125.
- Mohamed, A. M. O. (2006). *Arid Land Hydrogeology: In Search of a Solution to a Threatened Resource: Proceedings of the Third Joint UAE-Japan Symposium on Sustainable GCC Environment and Water Resources (EWR2006), 28 - 30 January 2006, Abu Dhabi, UAE (Volume IV in DARE series)*: CRC Press.

- Moriasi, D., Arnold, J., Van Liew, M., Bingner, R., Harmel, R., & Veith, T. (2007). Model evaluation guidelines for systematic quantification of accuracy in watershed simulations. *Transactions of the ASABE*, 50(3), 885-900.
- Morshed, M. M., Islam, M. T., & Jamil, R. (2016). Soil salinity detection from satellite image analysis: an integrated approach of salinity indices and field data. *Environmental monitoring and assessment*, 188(2), 119.
- Morton, J. F., & Dowling, C. F. (1987). *Fruits of Warm Climates*: J.F. Morton.
- Mostafazadeh-Fard, B., Heidarpour, M., Aghakhani, A., & Feizi, M. (2008). Effects of leaching on soil desalinization for wheat crop in an arid region. *Plant Soil Environ*, 54(1), 20.
- Mougenot, B., Pouget, M., & Epema, G. (1993). Remote sensing of salt affected soils. *Remote Sensing Reviews*, 7(3-4), 241-259.
- Mountrakis, G., Im, J., & Ogole, C. (2011). Support vector machines in remote sensing: A review. *ISPRS journal of photogrammetry and remote sensing*, 66(3), 247-259.
- Mulder, V., De Bruin, S., Schaepman, M., & Mayr, T. (2011). The use of remote sensing in soil and terrain mapping--A review. *Geoderma*, 162(1-2), 1-19.
- Naifer, A., Al-Rawahy, S. A., & Zekri, S. (2011). Economic Impact of Salinity: The Case of Al-Batinah in Oman. *International Journal of Agricultural Research*, 6(2), 134-142.
- Nakicenovic, N., Alcamo, J., Davis, G., de Vries, B., Fenhann, J., Gaffin, S., . . . Dadi, Z. (2000). *Special Report on Emissions Scenarios : a special report of Working Group III of the Intergovernmental Panel on Climate Change*.
- Nanni, M. R. D. (2006). Spectral reflectance methodology in comparison to traditional soil analysis. *Soil Science Society of America Journal*, 70(2), 393.
- Naumann, J. C., Young, D. R., & Anderson, J. E. (2009). Spatial variations in salinity stress across a coastal landscape using vegetation indices derived from hyperspectral imagery. *Plant Ecology*, 202(2), 285-297.
- Navulur, K. (2006). *Multispectral image analysis using the object-oriented paradigm*: CRC Press.
- Nawar, S., Buddenbaum, H., Hill, J., & Kozak, J. (2014). Modeling and mapping of soil salinity with reflectance spectroscopy and Landsat data using two quantitative methods (PLSR and MARS). *Remote Sensing*, 6(11), 10813-10834. doi: 10.3390/rs61110813
- Nazeri, M., Jusoff, K., Madani, N., Mahmud, A. R., Bahman, A. R., & Kumar, L. (2012). Predictive Modeling and Mapping of Malayan Sun Bear (*Helarctos malayanus*) Distribution Using Maximum Entropy. *PLoS ONE*, 7(10), e48104. doi: 10.1371/journal.pone.0048104
- Newman, M. E., McLaren, K. P., & Wilson, B. S. (2014). Long-term socio-economic and spatial pattern drivers of land cover change in a Caribbean tropical moist forest, the Cockpit Country, Jamaica. *Agriculture, Ecosystems & Environment*, 186, 185-200.
- Nield, S., Boettinger, J., & Ramsey, R. (2007). Digitally mapping gypsic and natric soil areas using Landsat ETM data. *Soil Science Society of America Journal*, 71(1), 245-252. doi: 10.2136/sssaj2006-0049
- Nong, Y., & Du, Q. (2011). Urban growth pattern modeling using logistic regression. *Geo-spatial Information Science*, 14(1), 62-67.
- Noroozi, A. A., Homaei, M., & Farshad, A. (2012). Integrated Application of Remote Sensing and Spatial Statistical Models to the Identification of Soil Salinity: A Case Study from Garmsar Plain, Iran. *Environmental Sciences*, 9(1), 59-74.
- Odeh, I. O., & Onus, A. (2008). Spatial analysis of soil salinity and soil structural stability in a semiarid region of New South Wales, Australia. *Environmental management*, 42(2), 265-278.

- Pakparvar, M., Gabriels, D., Aarabi, K., Edraki, M., Raes, D., & Cornelis, W. (2012). Incorporating legacy soil data to minimize errors in salinity change detection: a case study of Darab Plain, Iran. *International Journal of Remote Sensing*, 33(19), 6215-6238.
- Pal, M., & Mather, P. (2005). Support vector machines for classification in remote sensing. *International Journal of Remote Sensing*, 26(5), 1007-1011.
- Pallé, E., & Rodríguez, P. M. (2010). *The Earth as a Distant Planet: A Rosetta Stone for the Search of Earth-Like Worlds*: Springer Science & Business Media.
- Panah, S. K. A., Goossens, R., Matinfar, H. R., Mohamadi, H., Ghadiri, M., Irannegad, H., & Asl, M. A. (2008). The efficiency of Landsat TM and ETM⁺ thermal data for extracting soil information in arid regions. *Journal of Agricultural Science and Technology*, 10(5), 439-460.
- Patel, R., Prasher, S., God, P., & Bassi, R. (2002). Soil salinity prediction using artificial neural networks1. *Journal of the American Water Resources Association*, 38(1), 91-100.
- Paudel, B., Gao, J., Zhang, Y., Wu, X., Li, S., & Yan, J. (2016). Changes in cropland status and their driving factors in the Koshi River basin of the Central Himalayas, Nepal. *Sustainability*, 8(9), 933.
- Peñuelas, J., Isla, R., Filella, I., & Araus, J. L. (1997). Visible and near-infrared reflectance assessment of salinity effects on barley. *Crop Science*, 37(1), 198-202.
- Pérez González, M. E., García Rodríguez, M. P., González-Quiñones, V., & Jiménez Ballesta, R. (2006). Spatial variability of soil quality in the surroundings of a saline lake environment. *Environmental Geology*, 51(1), 143-149.
- Pitman, M. G., & Läuchli, A. (2002). Global impact of salinity and agricultural ecosystems. *Salinity: environment-plants-molecules* (pp. 3-20): Springer.
- Platonov, A., Noble, A., & Kuziev, R. (2013). Soil Salinity Mapping Using Multi-Temporal Satellite Images in Agricultural Fields of Syrdarya Province of Uzbekistan. In S. A. Shahid, M. A. Abdelfattah & F. K. Taha (Eds.), *Developments in Soil Salinity Assessment and Reclamation: Innovative Thinking and Use of Marginal Soil and Water Resources in Irrigated Agriculture* (pp. 87-98): Springer.
- Pontius, R. G., & Parmentier, B. (2014). Recommendations for using the relative operating characteristic (ROC). *Landscape ecology*, 29(3), 367-382.
- Porfirio, L. L., Harris, R. M. B., Lefroy, E. C., Hugh, S., Gould, S. F., Lee, G., . . . Mackey, B. (2014). Improving the Use of Species Distribution Models in Conservation Planning and Management under Climate Change. *PLoS ONE*, 9(11), e113749. doi: 10.1371/journal.pone.0113749
- Price, J. C. (1987). Calibration of satellite radiometers and the comparison of vegetation indices. *Remote Sensing of Environment*, 21(1), 15-27. doi: 10.1016/0034-4257(87)90003-4
- Radinger, J., Wolter, C., & Kail, J. (2015). Spatial Scaling of Environmental Variables Improves Species-Habitat Models of Fishes in a Small, Sand-Bed Lowland River. *PLoS ONE*, 10(11), e0142813. doi: 10.1371/journal.pone.0142813
- Raes, D., Smith, M., De Nys, E., Holvoet, K., & Makarau, A. (2002). *Charts with indicative irrigation intervals for various weather conditions*. Paper presented at the Proceedings of the Workshop FAO-ICID on Irrigation Advisory Services and Participatory Extension in Irrigation Management.
- Rahimi, S., Gholami Sefidkouhi, M. A., Raeini-Sarjaz, M., & Valipour, M. (2015). Estimation of actual evapotranspiration by using MODIS images (a case study: Tajan catchment). *Arch Agron Soil Sci*, 61(5), 695-709. doi: 10.1080/03650340.2014.944904
- Ramirez-Cabral, N. Y. Z., Kumar, L., & Taylor, S. (2016). Crop niche modeling projects major shifts in common bean growing areas. *Agricultural and Forest Meteorology*, 218-219, 102-113. doi: 10.1016/j.agrformet.2015.12.002

- Ramoliya, P. J., & Pandey, A. N. (2003). Soil salinity and water status affect growth of Phoenix dactylifera seedlings. *New Zealand journal of crop and horticultural science*, 31(4), 345-353. doi: 10.1080/01140671.2003.9514270
- Rao, B. R. M., Sharma, R. C., Ravi Sankar, T., Das, S. N., Dwivedi, R. S., Thammappa, S. S., & Venkataratnam, L. (1995). Spectral behaviour of salt-affected soils. *International Journal of Remote Sensing*, 16(12), 2125-2136. doi: 10.1080/01431169508954546
- Raza, S. A., Ali, Y., & Mehboob, F. (2012). Role of agriculture in economic growth of Pakistan.
- Rhoades, J., & Loveday, J. (1990). Salinity in irrigated agriculture. *Agronomy*(30), 1089-1142.
- Richards, L. A. (1954a). Determination of the properties of saline and alkali soils *Diagnosis and Improvement of Saline and Alkali Soils, Agriculture Handbook No. 60* (pp. 7-33). United States of America
- Richards, L. A. (1954b). Diagnosis and improvement of saline and alkali soils. *Soil Science*, 78(2), 154.
- Rienow, A., & Goetzke, R. (2015). Supporting SLEUTH–Enhancing a cellular automaton with support vector machines for urban growth modeling. *Computers, Environment and Urban Systems*, 49, 66-81.
- Rogers, E. D., & Benfey, P. N. (2015). Regulation of plant root system architecture: implications for crop advancement. *Current Opinion in Biotechnology*, 32, 93-98. doi: 10.1016/j.copbio.2014.11.015
- Royston, P., & Sauerbrei, W. (2008). *Multivariable model-building: a pragmatic approach to regression analysis based on fractional polynomials for modelling continuous variables*. Chichester, England: John Wiley & Sons.
- Sader, S. A., & Winne, J. C. (1992). RGB-NDVI colour composites for visualizing forest change dynamics. *Int J Remote Sens*, 13(16), 3055-3067. doi: 10.1080/01431169208904102
- Sakadevan, K., & Nguyen, M.-L. (2010). Extent, impact, and response to soil and water salinity in arid and semiarid regions. *Advances in agronomy*, 109, 55-74.
- Salah, A., Van Ranst, E., & Hisham, E. (2001). *Land suitability assessment for date palm cultivation in the Eastern Nile Delta, Egypt using an Automated Land Evaluation System and GIS*. Paper presented at the Proceedings of the Second International Conference on Date Palms, Al-Ain, United Arab Emirates.
- Satir, O., Berberoglu, S., Kapur, S., Nagano, T., Akça, E., Erdogan, M. A., . . . Tanaka, K. (2000). Soil salinity mapping using chris-proba hyperspectral data.
- Scherr, S. J., Neidecker-Gonzales, O., & Deutsche Stiftung für Internationale, E. (1997). *Agricultural growth, natural resource sustainability, and poverty alleviation in Latin America: the role of hillside regions*. Feldafing [Federal Republic of Germany]: Deutsche Stiftung für internationale Entwicklung, Zentralstelle für Ernährung und Landwirtschaft.
- Schlesinger, M. J. (1990). Heat shock proteins. *The Journal of Biological Chemistry*, 265(21), 12111-12114.
- Schmid, T., Koch, M., & Gumuzzio, J. (2008). Applications of hyperspectral imagery to soil salinity mapping. In G. Metternicht & J. A. Zaid (Eds.), *Remote Sensing of Soil Salinization: Impact on Land Management* (pp. 113-137). New York: CRC Press, Taylor and Francis.
- Schmugge, T. J., Kustas, W. P., Ritchie, J. C., Jackson, T. J., & Rango, A. (2002). Remote sensing in hydrology. *Advances in Water Resources*, 25(8-12), 1367-1385.
- Scull, P., Franklin, J., Chadwick, O., & McArthur, D. (2003). Predictive soil mapping: a review. *Progress in Physical Geography*, 27(2), 171-197.

- Seager, R., Ting, M., Held, I., Kushnir, Y., Lu, J., Vecchi, G., . . . Naik, N. (2007). Model Projections of an Imminent Transition to a More Arid Climate in Southwestern North America. *Science*, 316(5828), 1181-1184. doi: 10.1126/science.1139601
- Serneels, S., & Lambin, E. F. (2001). Proximate causes of land-use change in Narok District, Kenya: a spatial statistical model. *Agriculture, Ecosystems & Environment*, 85(1), 65-81.
- Sethi, M., Dasog, G., Van Lieshout, A., & Salimath, S. (2006). Salinity appraisal using IRS images in Shorapur Taluka, Upper Krishna Irrigation Project, Phase I, Gulbarga District, Karnataka, India. *International Journal of Remote Sensing*, 27(14), 2917-2926.
- Sethi, M., Lal, K., Kamra, S., Bundela, D., & Singh, G. (2010). Remote Sensing and Geographic Information System for Appraisal of Salt-Affected Soils in India. *Journal of environmental quality*, 39(1), 5-15.
- Setia, R., Lewis, M., Marschner, P., RAJA SEGARAN, R., Summers, D., & Chittleborough, D. (2011). Severity of salinity accurately detected and classified on a paddock scale with high resolution multispectral satellite imagery. *Land Degradation & Development*.
- Shabani, F., & Kumar, L. (2013). Risk Levels of Invasive *Fusarium oxysporum* f. sp. in Areas Suitable for Date Palm (*Phoenix dactylifera*) Cultivation under Various Climate Change Projections. *PLoS ONE*, 8(12), e83404. doi: 10.1371/journal.pone.0083404
- Shabani, F., & Kumar, L. (2014). Sensitivity Analysis of CLIMEX Parameters in Modeling Potential Distribution of *Phoenix dactylifera* L. *PLoS ONE*, 9(4), e94867. doi: 10.1371/journal.pone.0094867
- Shabani, F., Kumar, L., & Ahmadi, M. (2016). A comparison of absolute performance of different correlative and mechanistic species distribution models in an independent area. *Ecology and Evolution*, n/a-n/a. doi: 10.1002/ece3.2332
- Shabani, F., Kumar, L., & Esmaeili, A. (2014a). Future distributions of *Fusarium oxysporum* f. spp. in European, Middle Eastern and North African agricultural regions under climate change. *Agriculture, Ecosystems & Environment*, 197, 96-105. doi: 10.1016/j.agee.2014.08.005
- Shabani, F., Kumar, L., & Taylor, S. (2012). Climate Change Impacts on the Future Distribution of Date Palms: A Modeling Exercise Using CLIMEX. *PLoS ONE*, 7(10), e48021. doi: 10.1371/journal.pone.0048021
- Shabani, F., Kumar, L., & Taylor, S. (2014b). Projecting date palm distribution in Iran under climate change using topography, physicochemical soil properties, soil taxonomy, land use, and climate data. *Theoretical and Applied Climatology*, 118(3), 553-567. doi: 10.1007/s00704-013-1064-0
- Shabani, F., Kumar, L., & Taylor, S. (2014c). Suitable regions for date palm cultivation in Iran are predicted to increase substantially under future climate change scenarios. *The Journal of Agricultural Science*, 152(04), 543-557. doi: 10.1017/S0021859613000816
- Shaltout, K. H., & El-Halawany, E. F. (1992). Weed communities of date palm in eastern Arabia. *Qatar University Science Journal*, 12, 105-111.
- Shamsi, F. R. S., Sanaz, Z., & Abtahi, A. S. (2013). Soil salinity characteristics using moderate resolution imaging spectroradiometer (MODIS) images and statistical analysis. *Archives of Agronomy and Soil Science*, 59(4), 471-489.
- Shi, J., Wang, H., Xu, J., Wu, J., Liu, X., Zhu, H., & Yu, C. (2007). Spatial distribution of heavy metals in soils: a case study of Changxing, China. *Environmental Geology*, 52(1), 1-10.
- Shrestha, D., Margate, D., Meer, F., & Anh, H. (2005). Analysis and classification of hyperspectral data for mapping land degradation: An application in southern Spain. *International Journal of Applied Earth Observation and Geoinformation*, 7(2), 85-96.
- Shrestha, D. P., & Farshad, A. (2008). 13 Mapping Salinity Hazard: An Integrated Application of Remote Sensing and Modeling-Based Techniques. In G. Metternicht & J. A. Zinck (Eds.),

- Remote sensing of soil salinization: impact on land management* (pp. 257): CRC Press, Taylor and Francis Publisher.
- Shrestha, R. (2006). Relating soil electrical conductivity to remote sensing and other soil properties for assessing soil salinity in northeast Thailand. *Land Degradation & Development*, 17(6), 677-689.
- Silva, D. P., Vilela, B., De Marco, P., Jr., & Nemésio, A. (2014). Using Ecological Niche Models and Niche Analyses to Understand Speciation Patterns: The Case of Sister Neotropical Orchid Bees. *PLoS ONE*, 9(11), e113246. doi: 10.1371/journal.pone.0113246
- Singh, R. P., & Sirohi, A. (1994). Spectral reflectance properties of different types of soil surfaces. *ISPRS journal of photogrammetry and remote sensing*, 49(4), 34-40.
- Sinha, P., & Kumar, L. (2012). Binary images in seasonal land-cover change identification: a comparative study in parts of New South Wales, Australia. *Int J Remote Sens*, 34(6), 2162-2186. doi: 10.1080/01431161.2012.742214
- Sinha, P., & Kumar, L. (2013). Independent two-step thresholding of binary images in inter-annual land cover change/no-change identification. *ISPRS J Photogrammetry.ens*, 81, 31-43. doi: 10.1016/j.isprsjprs.2013.03.010
- Smits, P. C., Dellepiane, S. G., & Schowengerdt, R. A. (1999). Quality assessment of image classification algorithms for land-cover mapping: a review and a proposal for a cost-based approach. *Int J Remote Sens*, 20(8), 1461-1486. doi: 10.1080/014311699212560
- Somashekar, N. T. (2003). *Development and Environmental Economics*. New Delhi, India: New Age International.
- Song, W., Pijanowski, B. C., & Tayyebi, A. (2015). Urban expansion and its consumption of high-quality farmland in Beijing, China. *Ecological Indicators*, 54, 60-70.
- Sormunen, H., Virtanen, R., & Luoto, M. (2011). Inclusion of local environmental conditions alters high-latitude vegetation change predictions based on bioclimatic models. *Polar Biology*, 34(6), 883-897. doi: 10.1007/s00300-010-0945-2
- Sparks, D. L. (2003). *Environmental soil chemistry* (2 ed.). London, United Kingdom: Elsevier Science.
- Sperling, O., Lazarovitch, N., Schwartz, A., & Shapira, O. (2014). Effects of high salinity irrigation on growth, gas-exchange, and photoprotection in date palms (*Phoenix dactylifera* L., cv. Medjool). *Environmental and Experimental Botany*, 99, 100-109. doi: 10.1016/j.envexpbot.2013.10.014
- Spies, B., & Woodgate, P. (2005). Salinity mapping methods in the Australian context. *Department of the Environment and Heritage*.
- Statistics, A. A. B. o. (2002). *Salinity*. Canberra: Retrieved from [http://www.abs.gov.au/ausstats/abs@.nsf/Lookup/by%20Subject/1370.0~2010~Chapter~Salinity%20\(6.2.4.4\)](http://www.abs.gov.au/ausstats/abs@.nsf/Lookup/by%20Subject/1370.0~2010~Chapter~Salinity%20(6.2.4.4)).
- Suppiah, R., Hennessy, K., Whetton, P., McInnes, K., Macadam, I., Bathols, J., . . . Page, C. (2007). Australian climate change projections derived from simulations performed for the IPCC 4th Assessment Report. *Australian Meteorological Magazine*, 56(3), 131-152.
- Sutherst, R. W., & Maywald, G. (2005). A Climate Model of the Red Imported Fire Ant, *Solenopsis invicta* Buren (Hymenoptera: Formicidae): Implications for Invasion of New Regions, Particularly Oceania. *Environmental Entomology*, 34(2), 317-335. doi: 10.1603/0046-225x-34.2.317
- Sutherst, R. W., Maywald, G., & Kriticos, D. (2007). *CLIMEX version 3: user's guide*: Melbourne University.
- Sutherst, R. W., & Maywald, G. F. (1985). A computerised system for matching climates in ecology. *Agriculture, Ecosystems & Environment*, 13(3), 281-299. doi: 10.1016/0167-8809(85)90016-7

- Szabolcs, I. (1987). global problems of salt-affected soils. *Acta Agronomica Hungarica*, 36, 159–172.
- Taghizadeh-Mehrjardi, R., Minasny, B., Sarmadian, F., & Malone, B. (2014). Digital mapping of soil salinity in Ardakan region, central Iran. *Geoderma*, 213, 15-28.
- Tajgardan, T., Ayoubi, S., Shataee, S., Sahrawat, K. L., & Gorgan, I. (2010). Soil surface salinity prediction using ASTER data: Comparing statistical and geostatistical models. *Australian Journal of Basic and Applied Sciences*, 4(3), 457-467.
- Tajgardan, T., Shataee, S., & Ayoubi, S. (2007, 12-16 November). *Spatial prediction of soil salinity in the arid zones using ASTER data, Case study: North of Ag ghala, Golestan Province, Iran*. Paper presented at the Asian Conference on Remote Sensing (ACRS), Kuala Lumpur, Malaysia. .
- Tanji, K. (2004). Salinity in the soil environment. In A. Lauchli & U. Luttge. (Eds.), *Salinity: Environment-Plants-Molecules* (pp. 21-51). Netherlands, Dordrecht: Kluwer Academic Publisher.
- Tashi, Y., Chamard, P. C., Courel, M. F., Tiyp, T., Tuerxun, Y., & Drake, S. (2010). The Recent Evolution of the Oasis Environment in the Taklimakan Desert, China. *Water and Sustainability in Arid Regions*, 51-74.
- Taylor, G., Bennett, B., Mah, A., & Hewson, R. (1994). *Spectral properties of salinised land and implications for interpretation of 24 channel imaging spectrometry*.
- Taylor, S., Kumar, L., & Reid, N. (2012a). Impacts of climate change and land-use on the potential distribution of an invasive weed: a case study of *Lantana camara* in Australia. *Weed Research*, 52(5), 391-401. doi: 10.1111/j.1365-3180.2012.00930.x
- Taylor, S., Kumar, L., Reid, N., & Kriticos, D. J. (2012b). Climate Change and the Potential Distribution of an Invasive Shrub, *Lantana camara* L. *PLoS ONE*, 7(4), e35565. doi: 10.1371/journal.pone.0035565
- Tayyebi, A., Delavar, M. R., Yazdanpanah, M. J., Pijanowski, B. C., Saeedi, S., & Tayyebi, A. H. (2010). A spatial logistic regression model for simulating land use patterns: a case study of the Shiraz Metropolitan area of Iran *Advances in earth observation of global change* (pp. 27-42): Springer.
- Tayyebi, A., Perry, P. C., & Tayyebi, A. H. (2014). Predicting the expansion of an urban boundary using spatial logistic regression and hybrid raster–vector routines with remote sensing and GIS. *International Journal of Geographical Information Science*, 28(4), 639-659.
- Teggi, S., Costanzini, S., Despini, F., Chiodi, P., & Immordino, F. (2012). *SPOT 5 imagery for soil salinity assessment in Iraq*. Paper presented at the SPIE Remote Sensing.
- Thiruchelvam, S., & Pathmarajah, S. (1999). An economic analysis of salinity problems in the Mahaweli River System H Irrigation Scheme in Sri Lanka (pp. 39.). Ottawa, Canada: Economy and environment program for Southeast Asia (EEPSEA).
- Thomas, D. S. G. (2011). *Arid zone geomorphology: process, form and change in drylands*: John Wiley & Sons.
- Thung, M., & Rao, I. M. (1999). Integrated management of abiotic stresses *Common bean improvement in the twenty-first century* (pp. 331-370): Springer.
- Tilley, D. R., Ahmed, M., Son, J. H., & Badrinarayanan, H. (2007). Hyperspectral reflectance response of freshwater macrophytes to salinity in a brackish subtropical marsh. *Journal of environmental quality*, 36(3), 780-789.
- Tóth, T., Pasztor, L., Kabos, S., & Kuti, L. (2002). Statistical prediction of the presence of salt-affected soils by using digitalized hydrogeological maps. *Arid Land Research and Management*, 16(1), 55-68.

- Triantafyllidis, J., Odeh, I., & McBratney, A. (2001). Five geostatistical models to predict soil salinity from electromagnetic induction data across irrigated cotton. *Soil Science Society of America Journal*, 65(3), 869-878.
- Tripathi, N., Rai, B. K., & Dwivedi, P. (1997). *Spatial modelling of soil alkalinity in GIS environment using IRS data*. Paper presented at the 18th Asian Conference on Remote Sensing ACRS . Kuala Lumpur, Malaysia.
- Tripathi, R. (2009). *Alkali land reclamation*: Mittal Publications.
- Tripler, E., Ben-Gal, A., & Shani, U. (2007). Consequence of salinity and excess boron on growth, evapotranspiration and ion uptake in date palm (*Phoenix dactylifera* L., cv. Medjool). *Plant and Soil*, 297(1-2), 147-155. doi: 10.1007/s11104-007-9328-z
- Tucker, C. J. (1979). Red and photographic infrared linear combinations for monitoring vegetation. *Remote Sensing of Environment*, 8(2), 127-150. doi: 10.1016/0034-4257(79)90013-0
- Turhan, H., Genc, L., Smith, S., Bostanci, Y., & Turkmen, O. (2010). Assessment of the effect of salinity on the early growth stage of the common sunflower (Sanay cultivar) using spectral discrimination techniques. *Afr J Biotechnol*, 7(6).
- Valipour, M. (2014). Drainage, waterlogging, and salinity. *Archives of Agronomy and Soil Science*, 60(12), 1625-1640. doi: 10.1080/03650340.2014.905676
- Vergani, C., Schwarz, M., Cohen, D., Thormann, J. J., & Bischetti, G. B. (2014). Effects of root tensile force and diameter distribution variability on root reinforcement in the Swiss and Italian Alps. *Canadian Journal of Forest Research*, 44(11), 1426-1440. doi: 10.1139/cjfr-2014-0095
- Verma, K., Saxena, R., Barthwal, A., & Deshmukh, S. (1994). Remote sensing technique for mapping salt affected soils. *International Journal of Remote Sensing*, 15(9), 1901-1914.
- Vicente-Serrano, S. M., Pérez-Cabello, F., & Lasanta, T. (2008). Assessment of radiometric correction techniques in analyzing vegetation variability and change using time series of Landsat images. *Remote Sensing of Environment*, 112(10), 3916-3934. doi: 10.1016/j.rse.2008.06.011
- Vidal, A., Maure, P., Durand, H., & Strosser, P. (1996). *Remote sensing applied to irrigation system management: Example of Pakistan*.
- Vincent, B., Vidal, A., Tabbet, D., Baqri, A., & Kuper, M. (1996, 15-22 September). *Use of satellite remote sensing for the assessment of water logging or salinity as an indication of the performance of drained systems*. Paper presented at the 16th Congress on Irrigation and Drainage, Cairo, Cairo, Egypt.
- Vincenzi, S., Zucchetta, M., Franzoi, P., Pellizzato, M., Pranovi, F., De Leo, G. A., & Torricelli, P. (2011). Application of a Random Forest algorithm to predict spatial distribution of the potential yield of *Ruditapes philippinarum* in the Venice lagoon, Italy. *Ecological Modelling*, 222(8), 1471-1478. doi: 10.1016/j.ecolmodel.2011.02.007
- Wahid, A., Gelani, S., Ashraf, M., & Foolad, M. R. (2007). Heat tolerance in plants: An overview. *Environmental and Experimental Botany*, 61(3), 199-223. doi: 10.1016/j.envexpbot.2007.05.011
- Wang, D., Poss, J., Donovan, T., Shannon, M., & Lesch, S. (2002a). Biophysical properties and biomass production of elephant grass under saline conditions. *Journal of Arid Environments*, 52(4), 447-456.
- Wang, D., Wilson, C., & Shannon, M. (2002b). Interpretation of salinity and irrigation effects on soybean canopy reflectance in visible and near-infrared spectrum domain. *International Journal of Remote Sensing*, 23(5), 811-824.
- Wang, H., & Jia, G. (2012). Satellite-based monitoring of decadal soil salinization and climate effects in a semi-arid region of China. *Adv Atmos Sci*, 29(5), 1089-1099. doi: 10.1007/s00376-012-1150-8

- Wang, H., Wang, J., & Liu, G. (2007). *Spatial regression analysis on the variation of soil salinity in the Yellow River Delta*. Paper presented at the Proc. SPIE 6753, Geoinformatics 2007: Geospatial Information Science, Nanjing, China
- Wang, L., Chen, J., Gong, P., Shimazaki, H., & Tamura, M. (2009). Land cover change detection with a cross-correlogram spectral matching algorithm. *Int J Remote Sens*, 30(12), 3259-3273. doi: 10.1080/01431160802562164
- Wang, W., Vinocur, B., & Altman, A. (2003). Plant responses to drought, salinity and extreme temperatures: towards genetic engineering for stress tolerance. *Planta*, 218(1), 1-14.
- Weinhold, D., & Reis, E. (2008). Transportation costs and the spatial distribution of land use in the Brazilian Amazon. *Global Environmental Change*, 18(1), 54-68.
- Weiss, E., Marsh, S., & Pfirman, E. (2001). Application of NOAA-AVHRR NDVI time-series data to assess changes in Saudi Arabia's rangelands. *International Journal of Remote Sensing*, 22(6), 1005-1027.
- Weng, Y., Gong, P., & Zhu, Z. (2008a). Reflectance spectroscopy for the assessment of soil salt content in soils of the Yellow River Delta of China. *International Journal of Remote Sensing*, 29(19), 5511-5531.
- Weng, Y., Gong, P., & Zhu, Z. (2008b). Soil salt content estimation in the Yellow River delta with satellite hyperspectral data. *Canadian Journal of Remote Sensing*, 34(3), 259-270.
- Wharton, T. N., & Kriticos, D. J. (2004). The fundamental and realized niche of the Monterey Pine aphid, *Essigella californica* (Essig) (Hemiptera: Aphididae): implications for managing softwood plantations in Australia. *Diversity and Distributions*, 10(4), 253-262. doi: 10.1111/j.1366-9516.2004.00090.x
- Wheeler, T., & Von Braun, J. (2013). Climate change impacts on global food security. *Science*, 341(6145), 508-513.
- Wiegand, C., Anderson, G., Lingle, S., & Escobar, D. (1996). Soil salinity effects on crop growth and yield-Illustration of an analysis and mapping methodology for sugarcane. *Journal of Plant Physiology*, 148(3), 418-424.
- Wiegand, C., Rhoades, J., Escobar, D., & Everitt, J. (1994). Photographic and videographic observations for determining and mapping the response of cotton to soil salinity. *Remote Sensing of Environment*, 49(3), 212-223.
- Wolter, P. T., Mladenoff, D. J., Host, G. E., & Crow, T. R. (1995). Improved forest classification in the Northern Lake States using multi-temporal Landsat imagery. *Photogramm Eng Rem Sens*, 61(9), 1129-1144.
- Woodward, F. I. (1987). *Climate and Plant Distribution*: Cambridge University Press.
- Wu, J., Vincent, B., Yang, J., Bouarfa, S., & Vidal, A. (2008). Remote sensing monitoring of changes in soil salinity: a case study in Inner Mongolia, China. *Sensors*, 8(11), 7035-7049.
- Wu, W., Mhaimeed, A. S., Al-Shafie, W. M., Ziadat, F., Dhehibi, B., Nangia, V., & De Pauw, E. (2014). Mapping soil salinity changes using remote sensing in Central Iraq. *Geoderma Regional*, 2-3, 21-31. doi: 10.1016/j.geodrs.2014.09.002
- Yang, X., & Lo, C. (2000). Relative radiometric normalization performance for change detection from multi-date satellite images. *Photogrammetric engineering and remote sensing*, 66(8), 967-980.
- Yonghua, Q., Siongb, J., & Xudonga, L. (2008). *A partial least square regression method to quantitatively retrieve soil salinity using hyper-spectral reflectance data*. Paper presented at the Proc. SPIE 7147, Geoinformatics 2008 and Joint Conference on GIS and Built Environment: Classification of Remote Sensing Images, Guangzhou, China
- Yu, B., Zhu, T., Breisinger, C., & Hai, N. M. (2010a). Impacts of climate change on agriculture and policy options for adaptation. *International Food Policy Research Institute (IFPRI)*.

- Yu, R., Liu, T., Xu, Y., Zhu, C., Zhang, Q., Qu, Z., . . . Li, C. (2010b). Analysis of salinization dynamics by remote sensing in Hetao Irrigation District of North China. *Agricultural Water Management*, 97(12), 1952-1960. doi: 10.1016/j.agwat.2010.03.009
- Yuan, D., & Elvidge, C. D. (1996). Comparison of relative radiometric normalization techniques. *J Photogramm Remote Sens*, 51(3), 117-126. doi: 10.1016/0924-2716(96)00018-4
- Zaid, A., & Arias Jiménez, E. J. (1999). *Date palm cultivation*. Rome: Food and Agriculture Organization (FAO).
- Zakeri, H., Yamazaki, F., & Liu, W. (2017). Texture Analysis and Land Cover Classification of Tehran Using Polarimetric Synthetic Aperture Radar Imagery. *Applied Sciences*, 7(5), 452.
- Zatari, T. (2011). *Second National Communication: Kingdom of Saudi Arabia*. Paper presented at the A Report Prepared, Coordinated by the Presidency of Meteorology and Environment (PME), Riyadh, Saudi Arabia, and submitted to the United Nations Framework Convention on Climate Change [UNFCCC].
- Zhai, F., & Zhuang, J. (2012). Agricultural impact of climate change: A general equilibrium analysis with special reference to Southeast Asia. In V. Anbumozhi, M. Breiling, S. Pathmarajah & V. R. Reddy (Eds.), *Climate Change in Asia and the Pacific: How Can Countries Adapt?* India: SAGE Publications.
- Zhang, T. T., Zeng, S. L., Gao, Y., Ouyang, Z. T., Li, B., Fang, C. M., & Zhao, B. (2011). Using hyperspectral vegetation indices as a proxy to monitor soil salinity. *Ecological Indicators*, 11(6), 1552–1562.
- Zheng, Z., Zhang, F., Ma, F., Chai, X., Zhu, Z., Shi, J., & Zhang, S. (2009). Spatiotemporal changes in soil salinity in a drip-irrigated field. *Geoderma*, 149(3), 243-248.
- Zhu, J. K. (2001). Plant salt tolerance. *Trends in plant science*, 6(2), 66-71.